Searching for an HIV Vaccine: A Heterologous Prime-boost System using Replicating Vaccinia Virus and Plant-produced Virus-like Particles

by

Lydia Rebecca Meador

A Dissertation Presented in Partial Fulfillment
of the Requirements for the Degree
Doctor of Philosophy

Approved July 2016 by the
Graduate Supervisory Committee:

Tsafrir Leket-Mor, Co-Chair
Bertram Jacobs, Co-Chair
Joseph Blattman
Hugh Mason

ARIZONA STATE UNIVERSITY

August 2016

ABSTRACT

The HIV-1 pandemic continues to cause millions of new infections and AIDS-related deaths each year, and a majority of these occur in regions of the world with limited access to antiretroviral therapy. Therefore, an HIV-1 vaccine is still desperately needed. The most successful HIV-1 clinical trial to date used a non-replicating canarypox viral vector and protein boosting, yet its modest efficacy left room for improvement. Efforts to derive novel vectors which can be both safe and immunogenic, have spawned a new era of live, viral vectors. One such vaccinia virus vector, NYVAC-KC, was specifically designed to replicate in humans and had several immune modulators deleted to improve immunogenicity and reduce pathogenicity. Two NYVAC-KC vectors were generated: one expressing the Gag capsid, and one with deconstructed-gp41 (dgp41), which contains an important neutralizing antibody target, the membrane proximal external region (MPER). These vectors were combined with HIV-1 Gag/dgp41 virus-like particles (VLPs) produced in the tobacco-relative *Nicotiana benthamiana*. Different plant expression vectors were compared in an effort to improve yield. A Geminivirus-based vector was shown to increase the amount of MPER present in VLPs, thus potentially enhancing immunogenicity. Furthermore, these VLPs were shown to interact with the innate immune system through Toll-like receptor (TLR) signaling, which activated antigen presenting cells to induce a Th2-biased response in a TLR-dependent manner. Furthermore, expression of Gag and dgp41 in NYVAC-KC vectors resulted in activation of antiviral signaling pathways reliant on TBK1/IRF3, which necessitated the use of higher doses in mice to match the immunogenicity of wild-type viral vectors. VLPs and NYVAC-KC vectors were tested in mice, ultimately showing that the best antibody and Gag-specific T cell responses were generated when both components were administered simultaneously. Thus, plant-produced VLPs and poxvirus vectors represent a highly immunogenic HIV-1 vaccine candidate that warrants further study.

This document is dedicated to my family.

To my parents, who always pushed me to reach for the stars and follow my dreams.

To my sisters, who drove me to be my best self.

To my grandparents, who always believed in me, especially when I needed a reminder.

ACKNOWLEDGMENTS

I would like to acknowledge my advisors, Tsafrir Mor and Bert Jacobs, without whom the completion of this dissertation would not have been possible. Additionally, my committee members, Joe Blattman and Hugh Mason, who offered sound guidance that resulted in much higher quality experiments.

I would also like to acknowledge the members of each lab that were prominent in my training, and taught me the necessary skills to succeed in lab. Trung (Joe) Huynh, whose stark honesty was a constant reminder we can always improve, and there's always another way to complete a task. Karen Kibler, who always ensured experiments were carried out in the most ethical manner. I would like to thank Latha Kanna, who was always there for me to help me through those rough days. Sarah Kessans, who entrusted me with continuing on her work upon her graduation. Megan McAfee and Kavita Manhas, who helped me learn the essentials of immunological assays. Arpan Deb, whose antics in the lab kept me sane and always on my toes!

I would especially like to acknowledge Kathy Larrimore, an amazing friend and colleague throughout my time at Arizona State University. A friend who not only helped me through struggles with experiments, but was always there to listen when I needed someone. I would also like to acknowledge Hansa Done, though not a member of my lab, became one of my closest friends and made sure I always set aside time to relax and have fun. Additionally, I want to acknowledge my boyfriend, Adam Gushgari, who supported me and pushed me relentlessly through finishing up my dissertation. I could not have done this without him.

I have mentored many undergraduate students throughout my PhD, and I would like to thank all of them here for their efforts in data collection, dealing with all of my intense demands, and making me a better teacher/mentor: David Beaumont, Patrick Cervantes, Rebekah Dickey, Marissa Kaufman, Will Martelly, Carly Snyder, Siavosh Naji-Talakar, and Michelle Di Palma.

There are members of the ASU faculty and staff whom I would like to thank as well. Dave Lowry, for teaching me electron microscopy. Jacki Kilbourne, without whom my animal studies would not have been such a success! Jacki taught me everything I know about handling animal experiments, and without her wonderful stories the experiments would have been much more

dull. I would like to acknowledge the staff in the Biological Design program for their guidance and trying to maintain stability for us: Maria Hanlin, Laura Hawes, Joann Williams, and our director Tony Garcia. I would also like to thank Petra Fromme, though she did not serve on my PhD committee, her excellent questions in my comprehensive exam really taught me to be a better scientist.

Lastly, I would like to thank my funding sources. The Biological Design Graduate Program, the NSF Graduate Research Fellowship Program, the Philanthropic Education Organization Scholar Award, and the ASU Dissertation Fellowship supported me with a stipend and tuition throughout my doctoral studies. I also received travel awards from the Graduate College, the Graduate and Professional Student Association, the NSF GRFP, the Biological Design Graduate Program, and the International Society for Antiviral Research.

Thank you to everyone for their guidance and friendship throughout this process. I could not have completed my dissertation without any of these people.

TABLE OF CONTENTS

CHAPTER Page

CHAPTER Page

LIST OF TABLES

LIST OF FIGURES

Figure Page

Chapter 1

INTRODUCTION

The HIV-1 Pandemic and Treatment Options: Why a Vaccine is Necessary

Human immunodeficiency virus (HIV-1) was first discovered in 1983 as the causative agent of acquired immune deficiency syndrome [AIDS, (Barre-Sinoussi et al., 1983)]. Since then, HIV-1 has infected 78 million people and caused an estimated 35 million AIDS-related deaths (UNAIDS). Though antiretroviral therapy (ART) has greatly reduced the number of AIDS-related deaths, the overall number of HIV-1 infected individuals is still rising, with 2.1 million new infections globally in 2015 (Figure 1A). Furthermore, these infections are occurring disproportionately in undeveloped regions of the world with limited access to healthcare, and Africa accounts for over 66% of all new infections between 1990 and 2015 (Figure 1B). Furthermore, regional division of AIDS-related deaths shows a highly similar trend in which Africa accounts for 72% of deaths between 1990-2015, while North American and Europe only account for approximately 2% (Figure 1C). Comparison of new infections and AIDS-related deaths with ART coverage shows the importance of researching an HIV-1 vaccine, because those regions which have a majority of deaths and new infections do not receive proportionately higher ART coverage (Figure 1D). Over all regions listed, the average ART coverage is only 46% (UNAIDS). A recent study known as the strategic timing of antiretroviral treatment (START), highlighted the importance of beginning ART in HIV-1 positive patients whose CD4 count is above 500 cells/mL versus waiting until the CD4 count drops below 350 cells/mL, the current standard-of-care (Lundgren et al., 2015). Starting treatment immediately upon diagnosis reduced the risk of a serious AIDS-related event by approximately half. Therefore, this study suggests that pre-exposure prophylaxis (PrEP) would be extremely beneficial to highly afflicted regions, however, such a venture would require large funding efforts to achieve. An intriguing case in which this strategy was applied became known as the Mississippi baby, where an infant was placed on ART immediately after birth and treatment ceased around 18 months old (Persaud et al., 2013). The

child had undetectable HIV-1 viremia until two years after cessation of ART when a rebound occurred, thus dashing hopes that a functional cure for newborn infants had been discovered.

The rebound of viremia after cessation of ART or during treatment interruptions has routinely shown that targeting the viral reservoir is an essential component of any HIV-1 cure (Chun et al., 1997; Finzi et al., 1997; Wong et al., 1997). Simian immunodeficiency virus (SIV) infection has been shown to establish reservoirs within 72 hours of the initial infection (Whitney et al., 2014), emphasizing the need for either a prophylactic treatment (PrEP) or preventative vaccination. Reservoirs are a primary issue with therapeutic treatments because the latent virus avoids the immune responses due to limited replication. Certain ART drugs have been developed to combat reservoirs (Archin et al., 2012), however, the development of drug resistance often precludes use of one drug indefinitely (Clavel and Hance 2004). More advanced treatments directly target the HIV-1 latent provirus by disrupting the genome using CRISPR/Cas9 genomic editing technology (Ebina et al., 2013). Other strategies to render infected patients' cells resistant to viral entry and replication are based on the success of the "Berlin patient" who became the first person to be cured of HIV-1 after receiving a bone marrow transplant with a natural 32 bp deletion in the CCR5 co-receptor (Hütter et al., 2009). Following the success of the procedure, other less invasive strategies were explored to introduce genetic mutations in the CCR5 or CXCR4 co-receptor genes used technologies such as CRISPR/Cas9 (Hou et al., 2015; Ye et al., 2014), Zinc finger nucleases (Tebas et al., 2014), and TALENs (Ye et al., 2014). Though the technology is promising, it is still in its early phases, and will likely come with a large price tag. Thus, the limited access to treatment, drug resistance, rapid establishment of reservoirs, and the time and expense of the proposed genomic editing technologies makes the need for a prophylactic HIV-1 vaccine ever more apparent.

Vaccination Strategies and Correlates of Protection

Since the discovery of HIV-1 in 1983, only a handful of efficacy trials have been completed, and none have demonstrated success warranting widespread vaccination (Table 1). Strategies have primarily focused on eliciting either protective antibody (Ab) responses, or cell-

mediated immunity, a less well characterized part of vaccine immunology. Vaccines targeting Ab responses mainly target the HIV-1 envelope spike protein gp160/Env, the only protein exposed on the virion surface (Briggs and Krausslich, 2011; Engelman and Cherepanov, 2012). However, Env spikes are present at low density, and the immunodominant regions are often found in hypervariable loops that experience rapid turnover during immune escape, thus resulting in an evolutionary arms race with the immune system (Liao et al., 2013b). Furthermore, Ab responses to Env are faced with several difficult factors including occlusion of immunodominant regions by glycan shields or hypervariable loops and only transient exposure of the conserved neutralization sites (Labrijn et al., 2003; Moore et al., 2015; Moscoso et al., 2014; Munro et al., 2014; Pancera et al., 2014). Two phase III clinical trials, VAX003 and VAX004, were conducted using recombinant gp120 (rgp120) antigen in an effort to design a vaccine with Ab-mediated protection (Table 1). Both trials showed a lack of efficacy and an inability to reduce viral load or boost CD4 counts in vaccinees that subsequently became infected (Flynn et al., 2005; Pitisuttithum et al., 2006). The Ab responses which most closely correlated with decreased infection risk in vaccinated subjects were those that blocked CD4 binding (Gilbert et al., 2005).

The second major approach is based on T cell responses stemming from studies on elite controllers or long-term non-progressors (LTNPs), which have shown that the immune system is capable of naturally controlling HIV-1 infection and have provided insight into correlates of protection that vaccines should target (Betts et al., 2006; Deeks and Walker, 2007; Feinberg and Ahmed, 2012; Mudd et al., 2012). Additionally, these epitopes are known to have a strong HLA (human leukocyte antigen) genetic component, resulting control of replication only in the subsets of the population that express these alleles (Migueles et al., 2000). The Gag capsid protein contains many of these epitopes, and escape from cytotoxic T lymphocyte (CTL) control is almost always preceded by one or more mutations in these regions, but at a severe fitness cost to the virus (Boutwell et al., 2009; Kelleher et al., 2001; Prado et al., 2009; Schneidewind et al., 2007). Several of the protective epitopes were also shown to be isolated to structurally critical regions within the capsid protein, thus deterring viral escape mutations (Pereyra et al., 2014). Protective Gag epitopes are also presented earlier than those from other proteins, facilitating rapid CD8-

mediated killing of infected cells (Kloverpris et al., 2013). Therefore, there seems to be an advantage of a vaccine eliciting Gag-specific CD8 T cell responses.

The first clinical trial using a cell-mediated immunity approach was the Step Trial (HVTN502, Table 1). This study utilized a recombinant adenovirus (rAd5) expressing Gag-Pol-Nef (GPN) antigens and elicited robust CD4 T cell responses with exceedingly low CD8 T cell responses (< 1.0%), which were primarily directed at the Pol protein (Buchbinder et al., 2008; McElrath et al., 2008). Furthermore, in the vaccinated group, uncircumcised men that had preexisting Ad5 immunity had an increased risk of infection, resulting in no significant vaccine efficacy (Buchbinder et al., 2008). It has been hypothesized that this is due to the expansion of Ad5-specific CD4 T cells expressing mucosal homing markers, though there are conflicting reports on this (Benlahrech et al., 2009; Hutnick et al., 2009). Despite this disagreement, it is clear that preexisting Ad5 immunity does reduce the magnitude of the CD8 T cell response (Zak et al., 2012), thus Ad5 serostatus is an important factor influencing use of this vaccine. A second trial, HVTN505, attempted to improve the rAd5 immunity by first priming with a DNA vaccine (Hammer et al., 2013). Unfortunately, this trial was halted before completion due to lack of efficacy despite high response rates for CD4 and CD8 T cells and close to 100% Ab response rate. Though the T cell response rate was high and polyfunctional (> 60%), the T cell frequency was low for both CD4 (0.1%) and CD8 (0.2%). The CD4 response was primarily directed at Gag, while the CD8 response was dominated by Env-specific cells (Hammer et al., 2013). However, despite the lackluster results, the DNA/rAd5 regimen did not display the same increased risk of infection as the Step Trial (Huang et al., 2015), thus offering hope for future use of similar vectors.

One clinical trial sought to combine both strategies to elicit both T cell and Ab responses. The RV144 Thai Trial, enrolled 16,000 participants to test a non-replicating canarypox vector (ALVAC) followed by a combinatorial boost with AIDSVAX (B/E) used in the VAX003 trial, and was the first to show any clinical efficacy at approximately 31% (Rerks-Ngarm et al., 2009). The limited success of this vaccine regimen resulted in numerous follow-up studies to identify correlates of protection (listed in Table 1). T cell response rates were lower than for the rAd5 studies, at 19.7% versus > 70% in the Step Trial, though the responses in RV144 were primarily

CD8-dominated with a higher proportion of Env-specific than Gag-specific cells (Rerks-Ngarm et al., 2009). A later analysis identified a polyfunctional CD4-subset expressing CD40L, IL-2, IL-4, IFN-γ, and TNF-α, which were associated with reduced risk of infection (Lin et al., 2015). Poxvirus-specific CD4 T cells are not present at mucosal sites, and therefore this does not offer the same concern with enhancing infection risk as it did with the rAd5 vector (Perreau et al., 2011). Interestingly, Ab responses identified two correlates of risk: serum IgG for the V1-V2 loop of Env was inversely correlated with risk, while serum IgA to Env was directly correlated with infection risk (Haynes et al., 2012). It was later shown that V1-V2-specific IgG3 was the Ab isotype associated with reduced infection risk and these Abs demonstrated multiple effector functions, including antibody-dependent cell-mediated cytotoxicity [ADCC, (Chung et al., 2014; Yates et al., 2014)]. However, the IgG3 response was transient, thus accounting for the waning efficacy of the vaccine over time (Yates et al., 2014). An interesting note is that in the VAX003 trial, multiple boosting actually shifted from an IgG3 response toward IgG4, which interfered with IgG3 effector functions (Chung et al., 2014), suggesting that the canarypox prime used in RV144 may have actually improved the quality of the response though the magnitude was lower. Furthermore, a significant genetic component was found to be responsible for the induction of non-protective serum IgA over the protective V1-V2 IgG (Prentice et al., 2015). In the vaccinated population, individuals expressing HLA allele DPB1*13 had significantly higher V1-V2 IgG protection correlated with reduced risk of infection, and vaccine efficacy for this population subset was estimated at 71% (Prentice et al., 2015). Therefore, a successful HIV-1 vaccine must not only elicit both T cell and Ab responses, but also take into account subject genotype, quality of the Ab response, and proclivity for selectively eliciting responses to protective T cell epitopes.

In an effort to improve upon the results of the Thai Trial, other poxvirus-based vectors were pursued using attenuated vaccinia virus (VACV). The goal of the work presented here is to enhance immunogenicity of a similar HIV-1 vaccine by utilizing a replication-competent VACV vector in combination with plant-produced HIV-1 virus-like particles (VLPs), which more accurately display proteins in their native context for elicitation of broadly neutralizing Abs (bnAbs), to be further discussed below.

Vaccinia Virus as a Vaccine Vector

The moderate success of the RV144 trial enhanced interest in other poxvirus vectors that are attenuated for increased safety, yet display high immunogenicity. ALVAC was shown to be inherently safe due to its avian origin preventing replication in humans (Taylor and Paoletti, 1988; Taylor et al., 1988), and thus was chosen for the initial vaccine trials. However, in addition to ALVAC, two vaccine strains that have been widely studied for use as HIV-1 vaccine vectors are modified vaccinia virus Ankara (MVA) and New York vaccinia virus (NYVAC) [see these extensive reviews (Esteban, 2014; Gomez et al., 2012a; Jacobs et al., 2009; Pantaleo et al., 2010)]. MVA was generated by passaging in chicken embryonic fibroblasts, resulting in a non-replicating strain with demonstrated safety in animal models and humans (Garcia et al., 2011; Goepfert et al., 2011; Keefer et al., 2011; McCurdy et al., 2004), and even in immune-compromised individuals (Greenough et al., 2008). NYVAC was genetically engineered from the Copenhagen (Cop) strain to be replication incompetent in humans through specific deletion of 18 open reading frames (ORFs) thought to be associated with host-range and pathogenicity (Tartaglia et al., 1992b). NYVAC has a similar safety profile as described for MVA (Bart et al., 2008; Harari et al., 2012; McCormack et al., 2008). Furthermore, NYVAC is capable of generating similar, if not somewhat higher, responses when compared to ALVAC (Garcia-Arriaza et al., 2015; Hel et al., 2002), though ALVAC elicits a different cytokine profile than MVA and NYVAC upon immunization (Teigler et al., 2014), thus the vectors have distinct traits, which should be considered when choosing one for any given vaccine trial. Due to their demonstrated safety and high immunogenicity, multiple phase I/II clinical trials for both MVA and NYVAC expressing Gag-Pol-Nef (GPN) and gp120/Env have been conducted [reviewed in (Gomez et al., 2012a)]. While MVA has also demonstrated success, this study focuses on the use of NYVAC-based vectors, thus only these will be discussed further.

The phase I/II clinical trials involving NYVAC are summarized in Table 2. These trials were sponsored primarily by EuroVacc (www.eurovacc.org), an organization supporting studies of NYVAC and MVA expressing GPN/gp120 antigens. NYVAC is immunogenic on its own, though

the response rate and magnitude can be greatly improved when priming with DNA before a NYVAC antigen-matched boost, as demonstrated by the EV01 and EV02 safety and immunogenicity trials (Bart et al., 2008; McCormack et al., 2008). While Ab responses are improved when priming with DNA, the response rate does not quite reach 100% (Table 2). However, CD4 responses are robust (100% response rate with DNA prime) while CD8 responses are detectable, but have a less than 50% response rate (Table 2). Both T cell subsets are dominated by Env-specific cells with lesser responses to GPN. However, these responses have been shown to be polyfunctional, broad (recognizing 4 epitopes on average), and durable, with detectable circulating antigen-specific T cells almost one year after the final immunization (Harari et al., 2008). Furthermore, more recent studies with DNA/NYVAC regimens have shown the induction of HIV-specific T cells that express mucosal homing markers, and are found in the gut (Perreau et al., 2011). Studies in macaques revealed that NYVAC can also induce HIV-specific CD8 T cells and IgG Ab secretion in breast milk (Wilks et al., 2010), an important note for protection from mother-to-child transmission. All of these characteristics are important for HIV-1 vaccines because mucosal sites represent the primary mode of transmission for HIV-1, and broad, polyfunctional T cell responses are necessary to prevent viral escape.

NYVAC was recently assessed for immunogenicity and safety in a trial testing prime/boost schedules with NYVAC and rAd5 [HVTN078, (Bart et al., 2014)]. In this study, participants received three injections of viral vectors: two NYVAC followed by one rAd5, or one rAd5 (tested at three different doses) followed by two NYVAC. Interestingly, NYVAC served as a much better booster than as a priming vector, showing more robust Ab and T cell responses when used to boost rAd5 responses (Bart et al., 2014). Additionally, with increasing doses of rAd5 prime, CD8 T cell responses and Ab responses improved while CD4 responses declined (Bart et al., 2014), suggesting that the dosing of viral vectors can drastically alter the quality of the immune response, and must be optimized. Lastly, NYVAC was used in a therapeutic vaccination trial in HIV-1 infected patients undergoing ART, and showed the ability to safely generate *de novo* T cell responses in addition to boosting preexisting immunity (Harari et al., 2012). Therefore, NYVAC shows great promise as both a preventative and therapeutic vaccine, which can induce

robust, polyfunctional T cell responses, neutralizing Abs (nAbs), and is safe even in immune-compromised individuals, making it an excellent HIV-1 vaccine candidate. However, NYVAC is a non-replicating vector and a majority of the T cell responses were Env-specific CD4 T cells, which have not been protective through any of the HIV-1 efficacy trials (Table 1), and Gag-specific CD8 cells are known to be associated with control as discussed above. Thus, it was hypothesized that these immune responses could be improved by designing a replication competent, yet highly attenuated viral vector.

To achieve an attenuated, replicating VACV vector, Kibler et al. reinserted two host-range genes, K1L and C7L, into the NYVAC genome (NYVAC-KC), thus restoring replication in human tissue without compromising safety (Kibler et al., 2011). Both K1L and C7L are known to be antagonists of type I interferon (IFN) signaling, and loss of either of these genes significantly reduces host-range and virulence (Liu et al., 2013; Meng et al., 2009). K1L has specifically been shown to interfere with NFκB activation (Shisler and Jin, 2004), while C7L has been implicated as an inhibitor of apoptosis through an unidentified mechanism (Najera et al., 2006). Several studies have demonstrated the importance of C7L in the absence of K1L for NYVAC replication, ultimately enhancing immune responses (Najera et al., 2010; Sanchez-Sampedro et al., 2016). Furthermore, NYVAC-KC displayed improved antigen presentation, dendritic cell (DC) maturation, and increased CD8 T cell responses compared to NYVAC (Quakkelaar et al., 2011), thus reaffirming the use of a replication competent vector for enhanced immunogenicity. Additional modifications have been made to NYVAC-KC to further enhance immunogenicity, such as deletion of the soluble IFN-α/β receptor B19R (Symons et al., 1995), and the IFN-γ binding protein B8R (Verardi et al., 2001). Deletion of these genes also greatly increases the breadth of innate immune signaling, IFN production, and the magnitude of CD8 T cell responses (Delaloye et al., 2015; Gomez et al., 2012b; Quakkelaar et al., 2011). Deletion of A46R, an NFκB/IRF3 inhibitor of Toll-like receptor (TLR) signaling (Bowie et al., 2000), resulted in similar improvements in immunogenicity (Perdiguero et al., 2013).

Interestingly, during generation of viral vectors used in studies described here, severe toxicity to the cells and viral vector were noted when expressing HIV-1 antigens. It was

hypothesized that overexpression of recombinant protein may trigger ER stress and/or antiviral signaling pathways resulting in the observed toxicity. However, VACV encodes many immune modulators capable of inhibiting these pathways (Seet et al., 2003; Taylor and Barry, 2006). One such inhibitor is K3L, an eIF2α homolog, which prevents phosphorylation of eIF2α and the shutdown of protein translation in response to dsRNA activation of protein kinase R (PKR) or ER stress activation of PKR-like ER kinase [PERK, (Carroll et al., 1993)]. Multiple immune modulators of VACV are dedicated to the interference with IFN signaling (Smith et al., 2013), however, one of these inhibitors (C6L) is missing from NYVAC-KC. C6L is an inhibitor of TANK binding kinase 1 (TBK1), which is an upstream kinase of IRF3 (Unterholzner et al., 2011), thus its absence can result in activation of IRF3 antiviral signaling pathways and potentially cause the reduced viral titers. The importance of these pathways and the absence of C6L and many other immune modulators, in regard to NYVAC-KC HIV-1 vectors, is explored in Chapter 4.

Though all clinical trials for NYVAC involved virus alone or in combination with a DNA prime, the success of RV144 has been partially attributed to the combination of a viral vector with protein boosting. NYVAC was shown to elicit some Ab responses, but these are greatly improved when priming with rAd5 (Bart et al., 2014). Interestingly, poxviruses have been used to produce HIV-1 VLPs either with or without Env (gp140) spikes for elicitation of Ab responses *in vivo* (Bridge et al., 2011; Chen et al., 2005; Goepfert et al., 2011; Perdiguero et al., 2015). Additionally, vaccination with rgp120 in the absence of a viral vector in VAX003 and VAX004, resulted in non-protective, though robust, Ab responses (Table 1). Distinct differences in IgG isotypes were identified, noting that effector functions of IgG3 were important for the transient protection seen in RV144, and in VAX003 these responses were inhibited by IgG4 that was increased upon multiple protein boosts (Chung et al., 2014). Therefore, a combinatorial viral vector and protein boost is more protective than protein alone or a single viral vector administered alone. Recent studies assessed the use of NYVAC-GPN/gp140 VLP-producing vectors in combination with DNA prime/NYVAC+protein boost (Asbach et al., 2016) or NYVAC/NYVAC+protein regimen (Garcia-Arriaza et al., 2015). Results revealed significantly improved CD4 T cell responses with modest CD8 enhancement, and Abs with moderate ADCC

activity and low neutralization were induced. Additionally, no differences in T cell or Ab responses were detected when altering number or timing of prime/boosts (Asbach et al., 2016). Furthermore, the breadth of nAb responses and T cell responses to Env can be improved when using engineered mosaic gp120 sequences in a DNA/NYVAC/protein immunization scheme (Hulot et al., 2015). Overall, these studies suggest that utilizing VLP-producing viral vectors in combination with recombinant protein boosts can improve immune responses, however results can still be enhanced potentially through use of VLP boosting for more robust Ab production and a replication-competent viral vector in an effort to more drastically enhance CD8 T cell responses.

This study proposes the use of NYVAC-KC vectors expressing Gag and deconstructed-gp41 (dgp41) as a safe, immunogenic, replication competent vector for *in vivo* trials. Of note, in all studies listed above, when Env is included in the vector, the T cell response is dominated by Env-specific CD4 T cells, which only accounted for a small portion of the efficacy seen in RV144 (Lin et al., 2015). Therefore, vectors described here express Gag in an effort to elicit protective CD8 T cell responses known to be associated with control of viremia. The other vector expresses a deconstructed form of the gp41 (dgp41) transmembrane portion of gp160.

Dgp41 is truncated just outside of the membrane proximal external region (MPER), a portion of gp41 known to elicit broadly neutralizing Abs (bnAbs) such as 2F5, 4E10, and 10E8 (Huang et al., 2012; Purtscher et al., 1994; Zwick et al., 2001). The MPER is more highly conserved than Env [80% vs 66% conserved amino acids, respectively (Modrow et al., 1987)], and is largely immunodominant resulting in more potent neutralization (Jacob et al., 2015; Montero et al., 2008). However, in the context of gp160, the MPER also suffers from occlusion until binding to CD4 and a co-receptor results in its exposure (Montero et al., 2008; Moore et al., 2015; Pejchal et al., 2009). Therefore, the protein was truncated to better expose the MPER, and it has been suggested that in this context gp41 remains in a prefusion state (Gong et al., 2015). Furthermore, the MPER region fused to the B subunit of cholera toxin has been shown to elicit transcytosis blocking Abs (Matoba et al., 2008), an important mode of transmission for HIV-1. Similar results were seen when the MPER was displayed in the surface of a lipid virosome in a phase I clinical trial (Leroux-Roels et al., 2013), further supporting the use of HIV-1 VLPs.

Additionally, the soluble gp120 antigens used in HIV-1 clinical trials are now known to be incapable of interacting with bnAb germline B cell receptors (Hoot et al., 2013; McGuire et al., 2014). As a result, protein engineering developed germline-targeting antigens with the goal of vaccinating with a cascade of gp120 antigens with increasing affinity for the maturing B cells (Jardine et al., 2013; Jardine et al., 2015; Liao et al., 2013b). Other strategies involve more structurally accurate gp140 trimers, (Billington et al., 2007; Du et al., 2009; Sellhorn et al., 2012; Wan et al., 2009), but no clinical trials have been conducted with this antigen to date. It is also necessary to display the MPER in the context of a membrane because many of the bnAbs are partially autoreactive toward lipids, thus necessitating their close proximity to the MPER and a highly immunogenic antigen to overcome immune tolerance (Haynes et al., 2005; Haynes et al., 2016; Verkoczy et al., 2013; Verkoczy et al., 2010; Williams et al., 2015; Zhang et al., 2016). Thus, gp120 is not included in the viral vectors for elicitation of Ab or T cell responses in an effort to redirect the immune system towards more highly conserved, protective epitopes in Gag and gp41. For the protein component of the vaccine, it was hypothesized that antigen-matched VLPs would (i) provide a more structurally accurate context for the MPER for bnAb production, (ii) provide higher density of antigenic spikes on the VLP surface, and (iii) serve as a large immune complex for increased antigen presentation to induce more robust Ab and T cell responses through innate immune cell interactions.

Plant-produced VLPs

HIV-1 Gag VLPs have been produced in plants (Kessans et al., 2013; Meyers et al., 2008; Scotti et al., 2009), yeast (Sakuragi et al., 2002; Tsunetsugu-Yokota et al., 2003), and baculovirus insect cell cultures (Buonaguro et al., 2006; Deml et al., 2005). Plants are a desirable production platform for multiple reasons, including speed of production, attainable high yields (gram-level of protein in two weeks), ease of scale-up by regulatory standards, relative cost, and the lack of contaminating mammalian pathogens (Ma et al., 2005; Rybicki, 2009; Rybicki, 2014). Several plant-based products have been derived for both human and veterinary diseases, demonstrating their profound safety and immunogenicity [for extensive reviews see (Chen and

Lai, 2013; Daniell et al., 2009; Jacob et al., 2013; Liew and Hair-Bejo, 2015; Rybicki, 2010; Scotti and Rybicki, 2013)]. One plant-produced product is now an FDA approved treatment for Gaucher disease (Zimran et al., 2011). The primary deterrence for plant-made pharmaceuticals is the downstream purification costs, often accounting for approximately 80% of the total production expense (Wilken and Nikolov, 2012). One of the main reasons for this is difficulties in plant purification techniques for the separation of rubisco, which can account for 30-50% of the total soluble protein [TSP, (Feller et al., 2008; Spreitzer and Salvucci, 2002)], whereas recombinant protein oftentimes only accounts for 0.7-7% of the TSP (Egelkrout et al., 2012). Therefore, a primary goal of work described here was to both increase yield of plant-derived HIV-1 Gag/dgp41 VLPs and improve the purification strategy.

Many VLPs have been successfully produced in plants, and all display high immunogenicity (Chen and Lai, 2013; Scotti and Rybicki, 2013). Two successful VLP vaccines on the market are the human papillomavirus (HPV) vaccines (GlaxoSmithKline, 2014; Merck & Co., 2006). Though these are not plant-derived, they depict a bright future for VLP-based vaccines as safe, immunogenic alternatives to attenuated and/or subunit vaccines. As mentioned above, the hypothesis here is that the use of VLPs instead of a subunit vaccine in combination with a poxvirus vector will result in enhanced immunogenicity and more protective responses than seen with RV144 and other clinical trials.

The plant-derived VLPs used in studies reported here are made with Gag transgenic *Nicotiana benthamiana* supplemented with transient *Agrobacterium tumefaciens*-mediated expression of dgp41 using viral expression vectors (Kessans et al., 2013). These VLPs were shown to be immunogenic in mice as potent inducers of serum and mucosal Ab responses (Kessans et al., 2016). Others have demonstrated the proficiency of multiple VLPs for activating CD8 T cells through DC interactions (Barth et al., 2005; Buonaguro et al., 2006; Lacasse et al., 2008; Lenz et al., 2001; Tsunetsugu-Yokota et al., 2003), in addition to boosting T cell responses (Pillay et al., 2010). Furthermore, VLPs are capable of activating DCs to transport and present antigens to B cells more efficiently than subunit vaccines (Bessa et al., 2012; Link et al., 2012), thus demonstrating another advantage for MPER displayed in a VLP format versus the gp120

antigen used in RV144. While high yields are achievable in plants, VLPs are complex, large antigenic particles, and therefore often have poorer yields than other proteins. Gag VLPs seem to be more vulnerable to this than others, with yields for cytoplasmic expression reaching no more than 44 µg/kg FW (Meyers et al., 2008). For comparison, plant-derived HPV VLPs can obtain yields over 500 mg/kg FW (Maclean et al., 2007). The versatility of plant expression is demonstrated in that by switching the targeting of the Gag protein from cytoplasmic to chloroplast-based expression, Gag yield can be increased to 350 mg/kg FW (Scotti et al., 2009). In this study, an alternative approach of utilizing newly developed viral-based expression vectors for Gag and dgp41 expression was tested.

The most widely used commercially available viral-based expression vector for plant-based production is known as magnICON® (ICON), and is derived from tobacco mosaic virus [TMV, (Gleba et al., 2005; Marillonnet et al., 2004; Marillonnet et al., 2005)]. This expression system utilizes three plasmids delivered by *A. tumefaciens*: a 5' module containing a signal peptide and the TMV RNA-dependent RNA polymerase (RdRp) and movement protein (MP), a 3' module with the recombinant gene, and the integrase expression module which allows *in planta* recombination of the 5' and 3' T-DNA regions upon transfer to the nucleus [Figure 2A, (Marillonnet et al., 2004)]. The signal peptide can be chosen to target proteins through the secretory pathway to the apoplastic space, or alternatively use cytoplasmic expression, which is the natural site for Gag production. Upon recombination in the nucleus, mRNA is transported to the cytoplasm where it is amplified by the TMV RdRp and transferred to adjoining cells by the MP.

More recent development of a Geminivirus-based vector (Gemini) utilizes deconstructed bean yellow dwarf virus (BYDV) in a single-plasmid delivery system (Huang et al., 2009; Mor et al., 2003). Geminiviruses are ssDNA viruses which replicate via rolling-circle in the plant nucleus (Gutierrez, 1999), which requires Rep/RepA (C1/C2) present in the expression vector. However, the Gemini movement protein is not part of this expression system [Figure 2B, (Huang et al., 2009; Huang et al., 2008; Mor et al., 2003)], thus necessitating more efficient agroinfiltration. Geminiviruses are also known to induce gene silencing siRNAs targeting the origin of replication

and promoters preferentially (Aregger et al., 2012; Rodriguez-Negrete et al., 2009; Seemanpillai et al., 2003), thus p19, the silencing suppressor protein of tomato bushy stunt virus, can be included and substantially improves yield (Garabagi et al., 2012; Voinnet et al., 2003). The biology of these two viruses differs greatly, and thus the expression kinetics and yield could also be influence by vector choice. The direct comparison of these two vectors is discussed in Chapter 2 for enhancing Gag/dgp41 expression and yield.

VLPs and Innate Immunity

As noted above, plant-based expression requires the use of the gram-negative bacteria *A. tumefaciens*, and viral expression vectors. Both of these components offer a potential for natural adjuvancy if any pathogen associated molecular patterns (PAMPs) are remaining in the final VLP preparation. Mammalian innate immune systems are programmed to non-specifically recognize PAMPs and trigger a signal cascade ultimately leading to activation of antigen presenting cells (APCs), including DCs and macrophages, which then stimulate an adaptive response (Hoebe et al., 2004; Iwasaki and Medzhitov, 2015; Janeway and Medzhitov, 2002). Harnessing the innate immune system to generate robust adaptive immunity is an area of great interest for developing stronger, more durable responses with vaccines (Levitz and Golenbock, 2012; Pulendran and Ahmed, 2006; van Duin et al., 2006). In the case of plant-based VLPs, it was hypothesized in Chapter 3 that components of *A. tumefaciens* (e.g. LPS, flagellin) or the viral expression vector RNA could be incorporated into Gag VLPs upon agroinfiltration. Gag VLPs are known to encapsulate cellular RNA and can successfully deliver it to the cytoplasm of other cells (Valley-Omar et al., 2011). If these PAMPs are found in the VLP preparations, they could provide plant-derived VLPs with a unique adjuvant-like effect not found with other expression systems.

The specific PAMPs expected from plant-based production would primarily be recognized by the Toll-like receptors (TLRs, Table 3). TLRs are exposed at the cell surface for recognition of bacterial cell wall components, and are found in endosomes to respond to inappropriate localization of nucleic acids, often as a result of an intracellular pathogen invasion (Kawai and Akira, 2010; Takeda et al., 2003). Additionally, TLRs are linked to adaptive immunity through the

adaptor proteins MyD88 and TICAM (also known as TRIF), which control downstream activation of transcription factors NFκB and IRF3, resulting in up-regulation of IFN stimulated genes (ISGs), including cytokines, chemokines, and cell surface activation markers (Akira et al., 2001; Schnare et al., 2001). TLRs are known to help stimulate both Ab responses (Nemazee et al., 2006; Pasare and Medzhitov, 2005) and CD4 T cell help (Pasare and Medzhitov, 2004), thus making them a prime activation target for vaccines with the goal of inducing strong Ab responses. Indeed, many TLR ligand adjuvants have been explored for their utility in vaccination (Hjelm et al., 2014; Mata-Haro et al., 2007; Nagpal et al., 2015; Steinhagen et al., 2011; van Duin et al., 2006). Therefore, if the plant-produced VLPs contain inherent adjuvancy due to their production mechanism, they may be more immunogenic on their own than other protein subunit vaccines, thus requiring lower adjuvant doses, and can be strategically supplemented with a complementary adjuvant that stimulates separate pathways from those triggered by the VLPs without the need for multiple additives.

VLPs are known to be potent stimulators of the innate immune system (Raghunandan, 2011). One way of linking innate activation to an adaptive response is through CD4 T helper responses. CD4 helper T cells can be stimulated to be Th1 or Th2 based on the nature of signals received from the activating antigen (Mosmann and Coffman, 1989), and ultimately lead to differential responses in Ab isotype switching (Snapper and Paul, 1987). Ab isotypes are a critical factor of importance, as revealed by differences between the protective IgG3 in RV144 and the non-protective IgG4 in VAX003 clinical trials using the same rgp120 antigen (Table 1). Th1 CD4 T helper responses primarily result in IFN-γ secretion for potent CD8 T cell responses and IgG2a production (Fujieda et al., 1995; Snapper and Paul, 1987), a characteristic often attributed to VLP interactions with DCs (Lacasse et al., 2008; Tsunetsugu-Yokota et al., 2003). On the other hand, Th2 stimulation is often associated with allergic responses, but is a potent inducer of Abs through production of IL-4 stimulation of B cells to produce IgG1 (Fujieda et al., 1995). Th1 and Th2 responses can also be regulated by differential activation of macrophages, where classical macrophages activated by IFN-γ and LPS stimulate Th1, and alternatively activated macrophages triggered by immune complexes and TLR ligands preferentially induce Th2

responses (Gordon, 2003; Martinez and Gordon, 2014). Therefore, the type of activation in macrophages and DCs largely regulates the adaptive response for both T cell and B cell responses, thus the understanding of how vaccine components interact with these pathways will result in improved vaccine design.

HIV-1 Gag VLPs have been shown to be exceptionally robust stimulators of innate immunity (Deml et al., 2005). Interestingly, Gag VLPs produced in baculovirus were shown to stimulate DCs, monocytes, and PBMCs toward a Th2-biased CD4 helper response independently of TLR2 and TLR4 (Buonaguro et al., 2008; Buonaguro et al., 2006; Speth et al., 2008). However, adjuvanting a DNA/Gag VLP prime/boost vaccine with a stimulator of TLR4 was shown to induce a Th1 response (Poteet et al., 2015), resembling the responses of an HPV VLP vaccine (Pinto et al., 2005; Yan et al., 2005; Yang et al., 2004). Thus suggesting that the immune response can be tailored to suit the desired outcome of adaptive immune responses based on the natural biases induced by the antigen and adjuvant. In contrast, Gag VLPs produced in yeast were shown to stimulate a Th1 response that was dependent upon TLR2 (Tsunetsugu-Yokota et al., 2003). This indicates that the host production system may directly influence the pathways their respective VLPs can stimulate. Therefore, plant-derived VLPs have potential for stimulating adaptive responses through multiple innate pathways, inlcuding (i) interacting with DCs for CD8 T cell activation, as previously shown with other expression systems (Buonaguro et al., 2006; Deml et al., 2005; Tsunetsugu-Yokota et al., 2003), (ii) classical macrophage activation through LPS of *A. tumefaciens* for a Th1 response, and/or (iii) alternative activation of macrophages through TLR ligands being present on VLPs, a type of immune complex, for a Th2 response. The interaction between plant-derived VLPs and innate immune signaling pathways has yet to be explored and is the subject of Chapter 3.

Dissertation Overview

This dissertation will overall discuss the use of a replicating poxvirus vector, NYVAC-KC, for its use as an HIV-1 vaccine vector in combination with plant-produced VLPs for a more structurally accurate display of the important bnAb epitopes present in the MPER of gp41.

Chapter 2 describes the enhancement of Gag/dgp41 VLP production and yield in the tobacco-relative *Nicotiana benthamiana*, in addition to optimizing purification techniques in an effort to derive more enriched VLP preparations with minimal rubisco content. Interactions of HIV-1 VLPs with the innate immune system, particularly the Toll-like receptors, are assessed in Chapter 3, including the influence of these interactions on overall immunogenicity and potential vaccine formulations. Generation of recombinant NYVAC-KC vectors is described in Chapters 4 and 5. Chapter 4 will primarily focus on toxicity issues with Gag and dgp41 expression, in addition to the ER stress and innate immune signaling pathways potentially responsible for the observed toxicity, and the resulting effect on immunogenicity of the viral vectors. Lastly, Chapter 5 will describe the immunogenicity of NYVAC-KC and plant-derived VLPs in different prime/boost regimens and routes of immunization. The results of the studies described herein should improve future vaccine formulations involving plant-derived VLPs and NYVAC-KC viral vectors by (i) providing protocols for improving plant-based VLP production, (ii) enhancing knowledge of the natural innate immune biases induced by the VLPs, and how this might influence adaptive responses during vaccination, (iii) how to improve immunogenicity of NYVAC-KC by preventing toxicity of recombinant protein production, and (iv) provide data supporting the choice of prime/boost regimen based on desired vaccination outcomes.

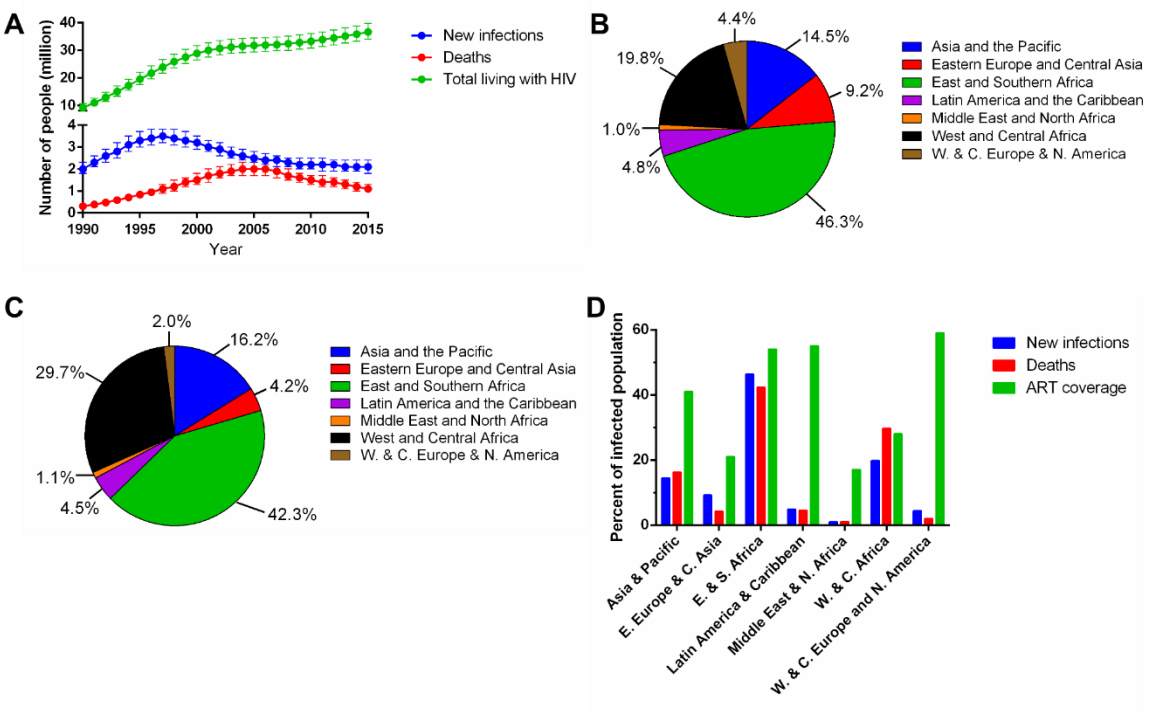

Figure 1 - Global Statistics for HIV-1

HIV-1 statistics gathered from UNAIDS (aidsinfo.unaids.org). (A) Plot over time of total people living with HIV-1 infection (green), number of AIDS-related deaths (red), and the number of new infections (blue) from 1990-2015. Error bars represent the upper and lower limits of the estimated counts. (B) Regional division of the number of new infections each year, showing that they occur disproportionately in undeveloped regions of the world. Percent of the global number of infections is shown. (C) The number of AIDS-related deaths is shown as a percentage of the total by region. (D) A combined plot to show percent of new infections (blue), AIDS-related deaths (red), and percent of infected population with access to antiretroviral therapy (ART, green). Data shows that regions accounting for a majority of HIV-1 infections and deaths do not have proportionately higher ART coverage. E – east; C – central; N – north; S – south

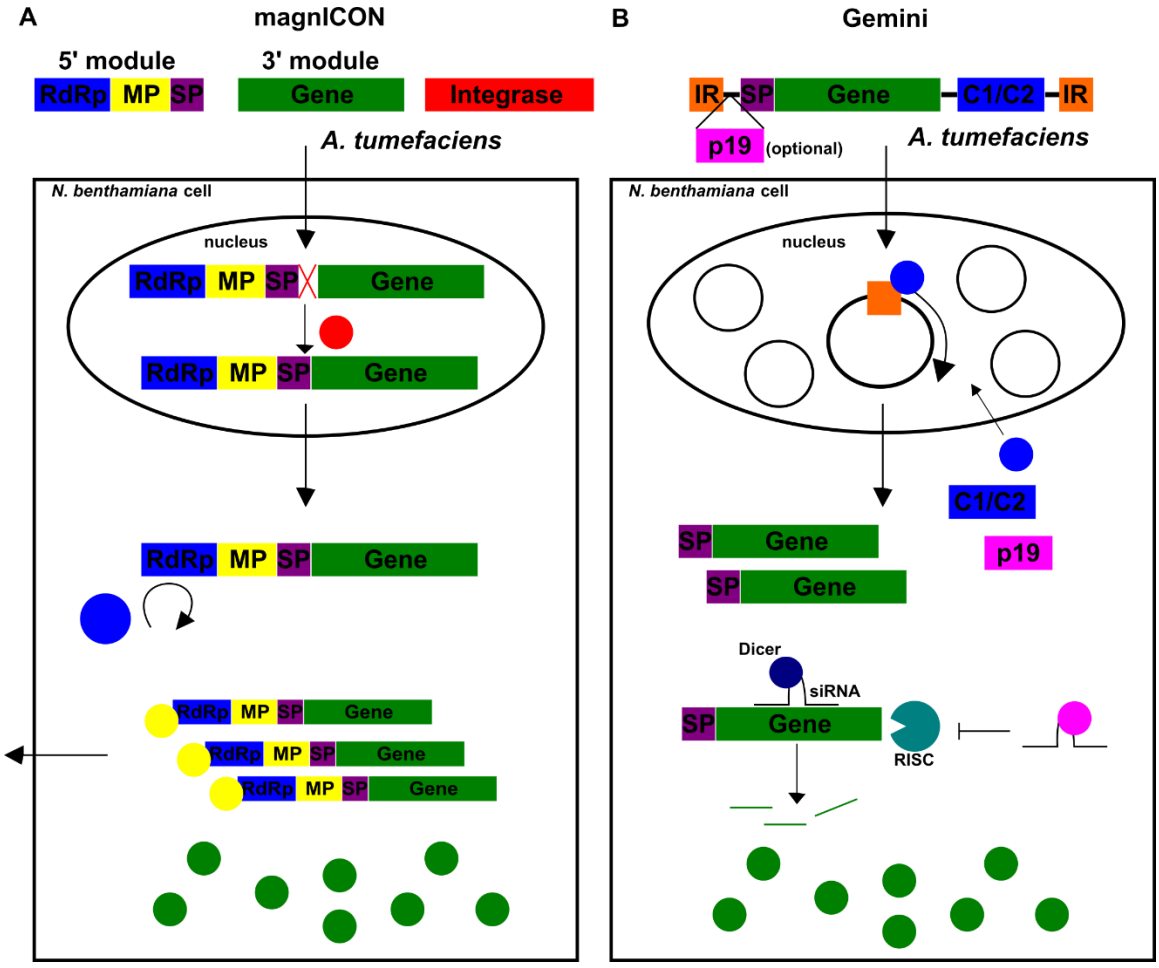

Figure 2 - Comparison of ICON and Gemini Plant Expression Vectors

The mechanism of plant-based expression for two deconstructed viral vectors based on tobacco mosaic virus (TMV) in the magnICON® system (A), or based on bean yellow dwarf virus (BYDV) in the Gemini expression vector (B). (A) ICON requires the use of three plasmid vectors harbored in individual *A. tumefaciens*, which transfers the T-DNA regions to the nucleus of infiltrated plant cells. Once in the nucleus, the integrase gene mediates recombination of the 5' and 3' modules to generate one DNA fragment. The mRNA is transported to the cytoplasm where the TMV RNA-dependent RNA polymerase (RdRp) amplifies the whole transcript, thus resulting in high expression levels of the recombinant gene product. The TMV movement protein (MP) transports mRNA to the adjacent cells to spread expression throughout leaf tissue. In this system the signal peptide (SP) for protein targeting is included in the 5' module and can be used for secretory or cytoplasmic expression pathways. (B) Geminivirus-based vectors are single plasmid delivery. *A. tumefaciens* mediates T-DNA transfer to the nucleus where expression of the replication proteins (C1/C2) amplify the ssDNA via rolling-circle replication by binding to the intergenic regions (IRs). This generates high mRNA levels resulting in accumulation of the gene product. Geminiviruses can induce gene silencing in which the plant generates siRNAs that are guided by Dicer proteins to bind mRNA and recruit the RNA-induced silencing complex (RISC), and result in degradation of the vector mRNA and reduced expression. To counteract this problem, the p19 silencing suppressor protein of tomato bushy stunt virus can be included. P19 binds the siRNA to prevent recognition by Dicer proteins, thereby enhancing expression.

Table 1 - HIV-1 Clinical Trials

Clinical Trial	Immunization	Efficacy	Primary immune responses & correlates of risk	References
VAX003	rgp120 (AIDSVAX, B/E)	0.1%	• Ab responses not protective • Boosting biased Abs to increase IgG4 and decrease IgG3 • IgG4 inhibits IgG3 Ab effector functions	(Pitisuttithum et al., 2006)
VAX004	rgp120 (AIDSVAX, B/B)	6.0%	• CD4 blocking Abs best predictor of infection risk	(Flynn et al., 2005; Gilbert et al., 2005)
Step (HVTN502)	rAd5 (GPN)	< 0%	• Preexisting Ad5 immunity increased infection risk in uncircumcised males & reduces CD8 responses • Polyfunctional CD4 T cell responses (Freq.: > 70%; RR: 41%) • Low CD8 responses (Freq.: < 1.0%; RR: 73%) • Transient increase in Ad5-specific CD4 cells expressing mucosal homing markers	(Benlahrech et al., 2009; Buchbinder et al., 2008; Hutnick et al., 2009; McElrath et al., 2008; Zak et al., 2012)
RV144	ALVAC (Gag-Pro, B/E; gp120 + gp41 membrane anchor, clade B) AIDSVAX rgp120 (B/E)	31.2%	• IgG to V1-V2 of Env decreased infection risk • IgA to Env increased infection risk • CD8/CD4 T cell responses (RR: 19.7%), primarily directed at Env • CD8-dominated responses • Transient IgG3 to V1-V2 associated with enhanced ADCC • Polyfunctional Env-CD4 decreased infection risk: CD40L, IL-2, IL-4, IFN-γ, TNF-α • HLA-controlled Ab responses	(Chung et al., 2014; Haynes et al., 2012; Lin et al., 2015; Prentice et al., 2015; Rerks-Ngarm et al., 2009; Yates et al., 2014)

HVTN505	DNA (GPN, Env)
	
	rAd5 (Gag-Pol, Env)
		< 0%	• Induced polyfunctional T cells
			  • CD4 freq.: 0.1%; RR: 61.5% (Gag > Env)
			  • CD8 freq.: 0.2%; RR: 64.1% (Env-dominant)
			• IgG to V1-V2 was low (RR: 20%)
			• IgA to Env: 43% RR
			• rAd5 after DNA prime did not result in increased infection risk, but study was halted early due to lack of efficacy
				(Hammer et al., 2013; Huang et al., 2015)

RR: response rate; HVTN: HIV Vaccine Trial Network; rgp120: recombinant gp120; rAd5: recombinant adenovirus 5; freq.: frequency; Ab: antibody; ADCC: antibody-dependent cell-mediated cytotoxicity; GPN: Gag-Pol-Nef

Table 2 - Phase I/II HIV-1 Vaccine Trials Involving NYVAC

Regimen	Antigens	Ab responses	T cell responses	References
EV01 NYVAC x 2	GPN, Env Clade C	RR: ~15% Mostly IgM to Env	• RR: 50% (60% of which is directed at Env) • Not durable	(Bart et al., 2008)
EV02 DNA x 2/ NYVAC x 2 or NYVAC x 2	GPN, Env Clade C	RR: 75% RR: 27% Transient & non-neutralizing for both regimens	• RR: 90% (Env > Gag) • CD4 – 100%, CD8 – 47% • Broad (4.2 epitopes) • Durable to 72 weeks (70%) • Polyfunctional (> 50%) • RR: 33% • Both regimens: 91% respond to Env, 48% to GPN	(Harari et al., 2008; McCormack et al., 2008)
EV03 DNA x 3/ NYVAC x 1	GPN, Env Clade C	ND	• RR: near 100% for blood and mucosal sites for CD4 and CD8 • 83% of CD4 express $\alpha_4\beta_7$ integrin • CD4 also have high CCR5 expression	(Perreau et al., 2011)
HVTN078 NYVAC x 2/ rAd5 x 1 or rAd5 x 2/ NYVAC x 1	NYVAC: GPN, gp120; rAd5: Gag-Pol (A/B/C), gp140 (B)	RR: 89.7% RR: 100% (up to 50% to V1/V2) nAbs: 69.3% RR to Tier 1 Transient (< 6 months)	• RR: CD4 – 42.9%, CD8 – 65.5% • RR: CD4 – 85.7%, CD8 – 85.7% • Increasing doses of rAd5 lowers CD4 response but increases CD8 • Both regimens induce polyfunctional CD4 and CD8	(Bart et al., 2014)
Theravac-01* NYVAC x 2	GPN, Env Clade B	ND	• Recall and expand preexisting HIV-specific CD4 and CD8 subsets • Generated 1-3 new peptide responses (mainly to Env) • CD4 significantly increased for Gag peptides • Optimal HLA-dependent Gag CD8 epitopes were preferentially expanded over other proteins	(Harari et al., 2012)

*Theravac-01 was conducted as a therapeutic vaccination trial in HIV-1 infected patients undergoing antiretroviral treatment

HVTN: HIV Vaccine Trial Network; EV: EuroVacc (www.eurovacc.org); RR: response rate; GPN: Gag-Pol-Nef; Env: envelope protein; rAd5: recombinant adenovirus; ND: not determined; Ab: antibody

Table 3 - Potential TLR Ligands from Plant-produced HIV-1 VLPs

Localization	TLR	Canonical PAMP	Adaptor Protein	Transcription Factor	Potential PAMP source in Plant VLPs
Cell surface	TLR2/6	Lipotechoic acids	MyD88	NFκB	Plant lipids/lipoproteins
	TLR4	LPS	MyD88/TICAM	NFκB/IRF3	*A. tumefaciens*
	TLR5	Flagellin	MyD88	NFκB	*A. tumefaciens*
Endosomal	TLR3	dsRNA	TICAM	IRF3	TMV vector
	TLR7	ssRNA	MyD88	NFκB	TMV vector
	TLR9	Unmethylated CpG motifs	MyD88	NFκB	Degraded plant DNA due to leaf necrosis

TLR: Toll-like receptor; LPS: lipopolysaccharide; PAMP: pathogen associated molecular pattern; TMV: tobacco mosaic virus; VLPs: virus-like particles

Chapter 2

ENHANCING EXPRESSION AND YIELD OF HIV-1 GAG/DGP41 VIRUS-LIKE PARTICLES PRODUCED IN *NICOTIANA BENTHAMIANA* WITH TRANSIENT, DECONSTRUCTED TMV AND GEMINIVIRUS-BASED VECTORS

Abstract

Virus-like particles (VLPs) are a safe and immunogenic vaccine platform. HIV-1 VLPs have been produced in a variety of expression systems. Plant production offers unique advantages based on scalability, safety from mammalian pathogen contamination, speed of expression, and platform flexibility. In an effort to increase yield of HIV-1 VLPs, a direct comparison was performed between a tobacco mosaic virus (TMV)-based magnICON vector and a Geminivirus-based expression vector. Gag yield was improved from previous reports of cytoplasmic expression (~44 µg p24/kg) to 1 mg p24/kg while transient dgp41 yields achieved levels above 5 mg MPER/kg. Interestingly, comparison of kinetics revealed that Gemini vectors express transient proteins earlier, often reaching peak levels 2-3 days post infiltration (dpi) and quickly lead to visible necrosis. However, the TMV vector does not express until 4 dpi and has much slower onset of necrosis. The silencing suppressor protein p19 was shown to delay necrosis and consistently increase expression and yield for Gemini vectors. However, Gemini vector yields were more variable than TMV, suggesting even with p19, gene silencing and severe necrosis may play drastically alter expression. Overall, simultaneous transient expression of Gag and dgp41 in wild-type *Nicotiana benthamiana* provided the highest VLP yield with a molar ratio of MPER:p24 of 1.7 up to 11.8, much higher than an HIV-1 virion. VLPs are immunogenic in mice and responses can be increased upon boosting. The higher density of gp41 spikes on Gemini-produced VLPs compared to TMV-based expression make these an interesting platform to pursue for HIV-1 vaccines with the goal of inducing neutralizing antibody responses to the MPER.

Introduction

Virus-like particles (VLPs) are a safe, immunogenic alternative to live or attenuated vaccines and more accurately represent the native structure of a virion than subunit vaccines, which is critical for eliciting neutralizing antibodies [nAbs, (Kushnir et al., 2012)]. Plant production of recombinant proteins and pharmaceuticals offers multiple advantages, including lack of contamination by mammalian pathogens, ease of scale-up by regulatory standards, speed of expression, and platform flexibility (Daniell et al., 2009; Egelkrout et al., 2012; Horn et al., 2003; Ma et al., 2005; Rybicki, 2009; Rybicki, 2010). Many different types of VLPs have been produced in plants, which has been thoroughly reviewed (Chen and Lai, 2013; Scotti and Rybicki, 2013). Several plant-made products have been tested in human clinical trials (Ma et al., 2005; Yusibov et al., 2014) with one product being approved by the FDA for treatment of Gaucher disease (Zimran et al., 2011). Economic viability of plant production relies heavily on oftentimes poor yields, and downstream processing costs to remove host proteins accounts for approximately 80% of production expenditures (Egelkrout et al., 2012; Wilken and Nikolov, 2012).

Several transient deconstructed viral-based vectors for rapid, high level protein expression in plants were developed in an effort to improve low protein yields. The tobacco mosaic virus (TMV)-based magnICON® system has been extensively used to express recombinant proteins in plants since its invention, and was the first to provide gram-levels of antigen per kilogram of leaf material (Gleba et al., 2005; Marillonnet et al., 2004; Marillonnet et al., 2005). However, newer expression systems such as Geminivirus [Gemini, (Huang et al., 2009; Mor et al., 2003)] and Cowpea mosaic virus (CPMV)-based pEAQ vectors (Peyret and Lomonossoff, 2013; Sainsbury et al., 2009) are less well characterized because they are not commercially available. The TMV system requires simultaneous delivery of three plasmids: a signal peptide module for targeting the secretory pathway or cytoplasmic expression, the vector containing a recombinant gene, and an integrase module for recombination *in planta* after *Agrobacterium tumefaciens* infiltration (agroinfiltration) mediates the transfer (T)-DNA transport to the nucleus (Marillonnet et al., 2004; Marillonnet et al., 2005). Once transcription occurs, the TMV RNA-dependent RNA polymerase (RdRp) amplifies mRNA in the cytoplasm and the movement

protein transfers the recombinant genes to surrounding cells (Marillonnet et al., 2004). However, Gemini vectors are a single plasmid delivery system offering simplicity for agroinfiltration culture preparation, yet Gemini vectors lack a movement protein and are known to induce gene silencing (Aregger et al., 2012; Rodriguez-Negrete et al., 2009; Seemanpillai et al., 2003), though this can be suppressed using the tomato bushy stunt virus p19 protein (Garabagi et al., 2012; Silhavy et al., 2002; Voinnet et al., 2003). Furthermore, multiple proteins can be delivered on the same plasmid and expressed in separate replicons established by short and long intergenic regions [SIR/LIR, (Huang et al., 2009)]. After transfer to the nucleus, Gemini vector T-DNA is amplified via rolling-circle mechanism by the C1/C2 (Rep/RepA) proteins (Gutierrez, 1999; Mor et al., 2003). Thus, due to differences in amplification stage, it was hypothesized that expression kinetics and time to peak expression would differ between the two expression systems.

HIV-1 VLPs have been produced in plants with low yield, particularly of full-length Gag capsid (Kessans et al., 2013; Meyers et al., 2008). Yield can be increased by expressing Gag in transgenic chloroplasts (Scotti et al., 2009). In this study, cytoplasmic expression of Gag in transgenic *Nicotiana benthamiana* and transient expression of deconstructed-gp41 (dgp41) was used to make enveloped VLPs (Kessans et al., 2013). The gp41 protein of HIV-1 is the transmembrane portion of the HIV-1 surface spike, and contains the highly immunogenic membrane proximal external region (MPER), a target of many broadly neutralizing antibodies [bnAbs, (Huang et al., 2012; Purtscher et al., 1994; Zwick et al., 2001)]. Previous studies have shown that VLPs displaying this region can elicit both systemic and mucosal MPER-specific Abs (Kessans et al., 2016), and transcytosis blocking Abs are also achievable (Matoba et al., 2008).

It is imperative to display the MPER in the context of a membrane because many of the bnAbs targeting this region are autoreactive for membrane components (Haynes et al., 2005; Haynes et al., 2016; Verkoczy et al., 2010; Williams et al., 2015; Zhang et al., 2016). Displaying the MPER in a virosome successfully elicited mucosal and systemic Abs in a phase I clinical trial (Leroux-Roels et al., 2013). Additionally, VLPs, but not subunit vaccines, properly induce antigen presenting cells and low affinity B cells to transport and display antigen for induction of Ab responses (Bessa et al., 2012; Link et al., 2012). Therefore, in an effort to improve yield and cost-

effectiveness of plant-produced HIV-1 Gag/dgp41 VLPs for structurally accurate display of the MPER in a membrane context, the TMV vector and newly developed Geminivirus vectors were compared for differences in expression kinetics and yield in addition to analysis of the amount of MPER co-localizing with Gag VLPs for enhanced immunogenicity.

Materials and Methods

Cloning Geminivirus-based Vectors

The TMV-based vector, pTM 602, was previously described (Kessans et al., 2013). Geminivirus-based vectors were generously provided by Dr. Hugh Mason (Arizona State University) for cloning dgp41 and Gag. Three vectors were generated: pTM 924 (Gemini), pTM 925 which contains p19 (Gemini +p19), and pTM 901 (Dual Gem. +p19), a dual-replicon vector for simultaneous expression of two genes from the same backbone, which also contains p19.

For cloning into pTM 924 and pTM 925, dgp41 was digested from pTM 602 using NcoI and SacI. The barley α-amylase (BAA) signal peptide was digested from pTM 796 using XbaI and SacI. The geminivirus backbone for pTM 924 is pTM 890 (formerly pBYR2fb) which was opened with XbaI and SacI. A triple ligation with dgp41, BAA, and the opened pTM 890 backbone using T4 DNA Ligase (Promega) yielded pTM 924. To derive pTM 925, the backbone pTM 800 was linearized using XbaI and SacI and the BAA-dgp41 insert was derived from pTM 924 by digesting with XbaI and SacI. The backbone and BAA-dgp41 fragment was ligated to yield pTM 925. Colonies were screened and sent for sequencing to confirm no mutations.

The dual-replicon vector, pTM 901, requires cloning into the XbaI/SacI cut site first due to the presence of a KpnI cut site in the multiple cloning site because the second cut site requires digestion with BsrGI and KpnI. BAA-dgp41 was excised from pTM 924 using XbaI and SacI while pTM 900 (formerly pBYR27p) was linearized using the same restriction sites. After confirming BAA-dgp41 insertion into the first cloning site, Gag was amplified from pTM 488 via PCR using AccuStart Taq DNA Polymerase HiFi (Quanta Biosciences) using oTM 776 (5’ – GAGA*TGTACA*ATGGGAGCTAGAGCCTCT – 3’) and oTM 777 (5’ – GAGA*GGTACC*TTATTGAGAGGAAGGGT – 3’) for addition of a 5’ BsrGI and 3’ KpnI cut site,

shown in italics, and ligated to a TOPO TA backbone (Invitrogen). The Gag gene contained a BsrGI cut site which was removed via mutagenesis using whole plasmid replication with the QuikChange II Site-Directed Mutagenesis Kit (Agilent Technologies) per manufacturer's protocol. The first reaction changed a TTG codon to CTG using primers oTM 827 (5' - GAGGAGCTTAGGTCTCTGTACAACACAGTGGCT – 3') and oTM 828 (5' - AGCCACTGTGTTGTACAGAGACCTAAGCTCCTC – 3'), where the mutated nucleotide is underlined. However, this introduces a non-synonymous codon, so an additional change from CTG to CTC was performed using oTM 829 (5' - GAGGAGCTTAGGTCTCTCTACAACACAGTGGCT – 3') and oTM 830 (5' - AGCCACTGTGTTGTAGAGAGACCTAAGCTCCTC – 3'). Upon sequence confirmation this plasmid was named pTM 923. From this point, pTM 923 and pTM 901 with BAA-dgp41 inserted were both digested using BsrGI and KpnI and then ligated together to derive the complete pTM 901. Sequences were confirmed for both Gag and dgp41 prior to use.

Each vector was transformed into GV3101 *A. tumefaciens* and colony-screened to confirm transformation. An isolated colony was grown and used to start infiltration cultures for each of the three Geminivirus-based vectors.

Kinetics Time Course

Six-week old *N. benthamiana* plants were vacuum infiltrated with an OD_{600} = 0.1 of *A. tumefaciens* resuspended in infiltration buffer (10 mM MES, 10 mM magnesium sulfate heptahydrate, pH 5.5). Bacteria harboring pTM 602, 924, or 925 were infiltrated into Gag transgenic plants, while pTM 901 was used in wild-type plants. Leaves were collected in triplicate every day for one week following infiltration. Collected leaves were scanned to monitor necrosis prior to flash-freezing 200 mg tissue samples in liquid nitrogen for expression analysis. Upon time-course completion, frozen tissue samples were homogenized in 1X SDS sample buffer without dye (60 mM Tris-HCl, 100 mM DTT, 1.6% SDS (w/v), 5% glycerol) using a ceramic bead in a Fast Prep-24 (MP Biomedicals, Solon, OH) machine twice for 30 s each. Homogenized samples were clarified by centrifugation at 14,000 x*g* for 10 min at 4° C. Supernatant was

collected and analyzed by Bradford assay (Bio-Rad) to determine total soluble protein (TSP) concentration. Equivalent TSP (20 µg) was loaded for each leaf sample into their respective lanes on a 12% polyacrylamide gel for SDS-PAGE followed by immunoblot as previously described (Kessans et al., 2013). Immunoblots for Gag were probed with primary polyclonal anti-p24 rabbit serum and goat anti-rabbit IgG-HRP (Santa Cruz), while dgp41 blots were probed with human anti-gp41 2F5 (AIDS Reagents Program) and goat anti-human IgG-HRP (Sigma). Coomassie staining was also performed to ensure equal protein loading for each lane.

To quantify expression over time, ImageJ software (Schneider et al., 2012) was used to measure band density. For each replicate, the peak day (highest density) for Gag and dgp41 was identified and each subsequent days' band densities are expressed as a percentage of the peak day.

Optimization of VLP Purification

Two strategies for removing rubisco from VLP preparations were tested. In the first experiment, flash-frozen leaf tissue harvested on peak expression day was homogenized in a blender in extraction buffer (25 mM sodium phosphate, 100 mM NaCl, 1 mM EDTA, 50 mM sodium ascorbate, 1 mM PMSF, pH 7.8), strained through miracloth, and insoluble protein was removed by centrifugation at 14,000 x*g* for 20 min at 4° C. The supernatant was collected and subjected to sequential ammonium sulfate precipitation at 20% followed by an increase to 40% with VLPs pelleted at 36,000 x*g* for 30 min at 4° C between precipitations. To remove rubisco using pH changes, after pelleting insoluble proteins, the supernatant was titrated to pH 5.5 to pellet rubisco, followed by adjustment to pH 5.0. After each pH change, protein was pelleted at 36,000 x*g* for 30 min at 4° C. The remaining pH 5.0 supernatant was subjected to a 40% ammonium sulfate precipitation to pellet all remaining VLPs and rubisco. All pellets were resuspended in 1X PBS (140 mM NaCl, 2 mM KCl, 10 mM Na_2HPO_4, 1 mM KH_2PO_4, pH 7.4). Samples were analyzed via Bradford assay and protein loaded equally into each lane for Coomassie and SDS-PAGE, as above.

Large-scale VLP Production and Purification

Six-week old *N. benthamiana* plants were infiltrated at OD_{600} = 0.1 with each of the four vectors. At peak expression day, as determined by the kinetics time course, leaf material was harvested in 20 g batches and flash frozen in liquid nitrogen and stored at -80° C until extraction. VLPs were purified using 20% ammonium sulfate precipitation, as described above. Following precipitation VLPs were resuspended in 1X PBS and separated via iodixanol density gradient as previously described (Kessans et al., 2013). Purification progress was monitored by immunoblot by loading 5 µg TSP per lane for each step of the extraction and density gradient. Gels were used for Coomassie staining, Gag expression, and dgp41 expression, as described above and in (Kessans et al., 2013).

VLP Quantification

VLP-containing fractions were concentrated on a 300 kDa molecular weight cut-off membrane (Sartorius), and quantified via immunoblot for total Gag and dgp41 content using bacterially-produced p24-CTA2 and CTB-MPER purified protein standards, respectively, as previously described (Kessans et al., 2016). Ammonium sulfate pellets were directly quantified prior to density gradients without concentrating each sample. Briefly, µg/mL amounts for both proteins were calculated by comparing serial dilutions of concentrated VLP gradient fractions and ammonium sulfate pellets to known concentrations of purified p24-CTA2 or CTB-MPER using ImageJ software to determine band density (Schneider et al., 2012). The total calculated p24 and MPER protein amount was then divided by kilograms of fresh leaf weight (FW) to determine µg/kg yield for Gag and dgp41. Molar ratio of MPER to p24 was determined by relative protein sizes (MPER = 15 kDa; p24 = 24 kDa) for a molecular weight ratio of 1.6 p24 to MPER.

Mouse Immunizations

All animal studies were conducted under the approval of the Arizona State University Institutional Animal Care and Use Committee.

Four to six-week old C57BL/6 mice (Jackson Laboratories; n = 3) were injected i.p. on days 0 and 45 with 2 µg p24 and 1.2 µg MPER gradient-purified VLPs mixed with Ribi adjuvant (Sigma) per manufacturer's protocol. Serum was collected every 2 weeks for analysis of p24 and MPER-specific IgG by ELISA as previously described (Kessans et al., 2016). Results are reported as OD 490 nm over time for the 1:50 dilution (lowest dilution tested).

Results

Construction of Transient Geminivirus Vectors

The commercial development of TMV-based vectors (MagnICON®) for transgene expression in plants has been extensively described (Gleba et al., 2005; Marillonnet et al., 2004; Marillonnet et al., 2005). A TMV vector for transiently expressing dgp41 for making HIV-1 VLPs was previously described [(Kessans et al., 2013), Figure 3A]. Two Geminivirus vectors were cloned to transiently express dgp41 with or without the silencing suppressor protein p19 (Figure 3B-C). Geminiviruses are known to induce gene silencing both during natural infection and with expression of transgenes, which primarily targets the replication origin and promoter regions (Aregger et al., 2012; Rodriguez-Negrete et al., 2009; Seemanpillai et al., 2003). The p19 protein has been shown to increase expression of recombinant proteins in plants by preventing gene silencing (Garabagi et al., 2012; Voinnet et al., 2003), thus co-expression of p19 in transient expression vectors is hypothesized to increase yield. A third Geminivirus vector was designed to co-express Gag and dgp41 from the same T-DNA fragment, but in separate Geminivirus replicons separated by LIR/SIRs (Figure 3D). These replicons are amplified by the replication proteins C1/C2 in the nucleus after *Agrobacterium*-mediated T-DNA transfer (Gutierrez, 1999; Huang et al., 2009; Mor et al., 2003). Expression in all Geminivirus vectors is under control of the Cauliflower mosaic virus (CMV) 35S promoter with two enhancer (2e) binding sites to improve transcription efficiency.

Geminivirus Vectors Display Accelerated Expression

After the three Geminivirus vectors were cloned into *A. tumefaciens*, expression kinetics was analyzed over the course of seven days in six-week old *N. benthamiana* plants. Three vectors (TMV, Gemini, and Gemini +p19) were infiltrated into Gag transgenic plants to transiently express dgp41 for VLP production while the fourth vector (Dual Gemini +p19) was infiltrated into wild-type (WT) plants for transient co-expression of Gag and dgp41. Triplicate leaf samples were collected and monitored for necrosis over seven days (Figure 4). All Geminivirus-based vectors display necrosis around 3-4 dpi, which is earlier than the TMV vector which shows visible necrosis around 6 dpi. The inclusion of p19 with Geminivirus vectors appears to delay the onset of necrosis by 1-2 days. However, all Geminivirus infiltrated plants had severe necrosis at 7 dpi that prevented further sampling.

Quantitation of western blot band densities was used to measure Gag and dgp41 expression and revealed distinct differences between TMV and Geminivirus vectors (Figure 5A-B). Gemini and Gemini +p19 vectors display a gradual decrease in transgenic Gag levels over the seven days, and including p19 increased expression levels by 26.5% on average after 2 dpi (Figure 5A & Figure 6B-C, compare red squares with green triangles). This could be a result of reduced gene silencing for both transient dgp41 and the Gag transgene leading to a decrease in necrosis. The TMV vector maintains steady levels in Gag expression with variability across plants and no clear peak day (Figure 5A & Figure 6A, blue circles), consistent with transgenic steady-state expression in the absence of gene silencing. Transient expression of Gag by the Dual Gemini +p19 vector shows a clear peak at 2 dpi followed by a steady decline with little to no expression after 4 dpi (Figure 5A & Figure 6D), correlating with onset of necrosis (Figure 4).

Transient expression of dgp41 in the TMV vector shows initial expression at 3 dpi with a steady increase over time, peaking at 7 dpi (Figure 5B & Figure 6A). The two Geminivirus vectors expressing dgp41 alone began expression much earlier at 2 dpi with peak expression between 2-4 dpi (Figure 5B & Figure 6B-C). Interestingly, there is a decrease in dgp41 expression in both vectors at 5 dpi despite equivalent protein loading into the gels (Figure 6), and this is far more drastic in the vector without p19. Dual Gemini +p19 initiates detectable expression at 2 dpi with a

steady decline similar to that seen with Gag expression by the same vector (Figure 5B & Figure 6D). Based on the combined necrosis and Gag/dgp41 expression levels during the time course, peak expression day was determined to be 4 dpi for TMV and 2-3 dpi for all Gemini vectors.

Removal of Rubisco in VLP Preparations

Two strategies were employed in an effort to reduce rubisco in VLP preparations. Rubisco bands were detected by Coomassie staining, with large bands around 50 and 25 kDa corresponding to the large and small subunits of rubisco, respectively. Gag (55 kDa) and dgp41 (23 kDa) were detected by western blot. A majority of VLPs were found to pellet with addition of 20% ammonium sulfate as determined by Gag and dgp41 presence (Figure 7B-C, 20% P), while the major rubisco band around 50 kDa remains in the 20% supernatant (SN, Figure 7A). The rubisco can be precipitated with further increase to 40% ammonium sulfate (Figure 7A, 40% P), along with any remaining Gag/dgp41 VLPs (Figure 7B-C). The second strategy utilized pH changes where a majority of the VLPs pellet at pH 5.5 and a further reduction to pH 5.0 did not result in detection of Gag or dgp41 (Figure 7B-C, pH 5.5 & 5.0 P). Ammonium sulfate was added to a concentration of 40% in the remaining pH 5.0 SN, and a large band around 50 kDa was visible after Coomassie staining with no detectable Gag and little dgp41, indicating this likely represents a majority of the rubisco (Figure 7, 5.0 – 40% P). Based on this data, the 20% ammonium sulfate precipitation appears cleaner with fewer protein contaminants, including rubisco, and was therefore chosen as the method of purification for subsequent experiments.

VLP Purification and Yield

Large-scale purifications were performed for each of the four vectors by harvesting at peak expression day and processing in 20 g batches. VLPs for all samples were primarily isolated to the 20% iodixanol fraction, with some large particles or aggregates accumulating in the 50% fraction (Figure 8). Comparison of Gag and dgp41 band intensity on equivalently loaded gels indicates that Gemini +p19 and Dual Gemini +p19 vectors qualitatively have the highest yield of both Gag and dgp41 (Figure 8C-D). After running density gradients, both the 20% ammonium

sulfate pellets and the 20% iodixanol gradient fractions were quantified by immunoblot as previously described (Kessans et al., 2016).

Total expression of Gag reached a maximum around 1 mg/kg fresh leaf weight for both Dual Gemini +p19 transient expression and with the TMV vector in stable transgenics (Table 4). Transient expression of Gag and dgp41 was lowest in the Gemini vector without p19 at 0.62 mg/kg and 0.82 mg/kg, respectively (Table 4). The highest transient dgp41 expression was seen with the Dual Gemini +p19 at 5.5 mg/kg (Table 4). Both Geminivirus vectors which include p19 had higher dgp41 expression than the TMV-based vector, however, the yields are less consistent. Interestingly, Gag yield in the VLP gradient fraction was similar for the TMV and Dual Gemini +p19, but the TMV vector had lower dgp41 yield (Table 5). A similar phenomenon was seen with the Gemini ± p19 vectors, where inclusion of p19 during expression resulted in an increase in dgp41 yield within the VLP fraction (Table 5). Furthermore, the higher dgp41 expression in both the Gemini +p19 and Dual Gemini +p19 vectors corresponds to a higher molar ratio of MPER:p24, with an average of 2.8 and 3.3, respectively (Table 5). This indicates more dgp41 per Gag in each VLP particle, thus presenting a potentially better immunogen with more neutralization targets.

VLPs Elicit Gag and Dgp41-specific Antibodies in Mice

C57BL/6 mice (n = 3) were immunized with Gag/dgp41 VLPs produced using the TMV-based vector at Day 0 and 45. Two weeks after the first dose, p24-specific IgG was detectable in the serum, wheras MPER-specific Abs were below detection limit (Figure 9). One week after the second immunization, a 100% response rate was observed for both p24- and MPER-specific serum IgG. This indicates the plant-produced VLPs are immunogenic in mice, generate memory responses which can be recalled upon boosting, and can elicit Abs specific to the MPER bnAb target in the dgp41 protein.

Discussion

The use of plants as vaccine antigen production platforms has been extensively reviewed (Chen and Lai, 2013; Daniell et al., 2009; Ma et al., 2005; Rybicki, 2009; Rybicki, 2010; Rybicki, 2014; Sala et al., 2003). The primary roadblocks to plant-produced pharmaceuticals revolve around both purification and low yield/expression levels (Wilken and Nikolov, 2012). Recombinant protein often accounts for only 0.7-7% of TSP (Egelkrout et al., 2012), whereas rubisco is the most prominent soluble protein, and the most abundant protein in the world, at 30-50% of the plant TSP (Feller et al., 2008; Spreitzer and Salvucci, 2002). Removal of rubisco has plagued the plant-produced pharmaceutical field, however, recent developments show great promise at removing rubisco with inexpensive chromatography and precipitation methods (Arfi et al., 2016; Buyel and Fischer, 2014; Buyel et al., 2013). One such study reports the ability to remove up to 92% of rubisco from plant extractions using polyethylene glycol (PEG) precipitation (Arfi et al., 2016). In this study, the removal of the primary large and small subunit bands of rubisco from VLP preparations was accomplished by a rapid, inexpensive method using 20% ammonium sulfate precipitation (Figure 7). These are critical advancements because the economic advantage of using plants over other expression systems is deterred by downstream processing accounting for up to 80% of production costs (Wilken and Nikolov, 2012).

VLPs are thought to be a safe alternative to live attenuated vaccines, yet highly immunogenic and more structurally accurate compared to subunit vaccines (Kushnir et al., 2012) and plants have been used to produce VLPs of multiple varieties (Chen and Lai, 2013; Scotti and Rybicki, 2013; Yildiz et al., 2011). The use of plants for HIV-1 vaccines has grown in interest as there is no current HIV-1 vaccine candidate and plants provide unique advantages (Horn et al., 2003; Rosales-Mendoza et al., 2012). HIV-1 VLPs and other antigens are successfully produced in plants (Kessans et al., 2013; Matoba et al., 2009; Meyers et al., 2008; Rosales-Mendoza et al., 2013; Scotti et al., 2009) and many of these have been shown to be immunogenic in animals (Kessans et al., 2016; Matoba et al., 2009; Meyers et al., 2008).

In particular, for HIV-1 VLPs, the low expression of full-length Gag has proven problematic (Meyers et al., 2008), and the highest yields are achieved with transplastomic

expression of Gag, reaching levels of 350 mg/kg FW (Scotti et al., 2009). Here improved expression was sought by comparing the TMV-based magnICON® system with more recently developed Geminivirus-based replicons. Previously, transient cytoplasmic expression of Gag yielded a maximum of 44 µg p24/kg FW (Meyers et al., 2008), while here, levels up to 1 mg p24/kg FW were reported using both the TMV and Dual Gemini +p19 vectors (Table 4). It is possible that this increase is due to transient co-expression of dgp41 as a similar phenomenon was previously reported using the TMV-based vector (Kessans et al., 2013). Furthermore, gradient-purified VLPs yielded an average up to 343 µg p24/kg FW (Table 5). Again, the Gag yield was similar between TMV and Dual Gemini +p19. Though this represents only a fraction of the total expression, yields are still far higher than previous reports, thus these vectors hold promise for larger-scale production. Additionally, transient genes were consistently expressed at higher levels with inclusion of p19 in Geminivirus replicons (Table 4 & Table 5), thus confirming the utility of the p19 protein for enhancing transient expression (Garabagi et al., 2012; Silhavy et al., 2002; Voinnet et al., 2003). Dual Gemini +p19 also produced the highest dgp41 levels with total average expression around 5.5 mg MPER/kg, and the highest yield in VLP fractions with a mean of 84 µg MPER/kg (Table 4 & Table 5). Overall, these results suggest transient expression of both Gag and dgp41 simultaneously results in the highest VLP yields.

It is interesting to note that analysis of peak expression for TMV and Gemini-based vectors show distinct differences (Figure 5 & Figure 6). All Gemini vectors have an early peak in transient dgp41 expression with or without p19, while the TMV vector may be delayed in detection of dgp41 but shows a gradual increase over time (Figure 5B). However, this contrasts sharply to the pattern seen with transgenic Gag expression (Figure 5A). Gemini and Gemini +p19 display an early peak in Gag levels corresponding to the peak in dgp41 levels, and Gag expression almost completely disappears around the time of severe necrosis (Figure 4 & Figure 6). What is intriguing is that the TMV vector shows no peak Gag expression with consistent variation across the entire time course (Figure 5A). It is likely that this difference is due to the gene silencing induced by Geminivirus vectors and not TMV vectors, thus the transgenic Gag and transient dgp41 disappear over time, though p19 makes this effect less severe. Additionally, it is

possible that gene silencing accounts for the larger variation seen with Gemini vectors, thus making harvesting prior to visible necrosis more critical. Therefore, Gemini vectors provide more rapid, though more variable, expression.

One of the major characteristics of HIV-1 responsible for the difficulty of neutralization is the low density of gp160 spikes on the virion, with approximately 10 envelope trimers per particle (Briggs and Krausslich, 2011). This corresponds to a molar ratio of 0.02 MPER:p24 on a native HIV-1 virion (2500 Gag proteins per 10 Env trimers at a molar ratio of 1.6 p24:MPER). The plant-produced VLPs range from molar ratios of 0.47 to 11.8 (Table 5) and are immunogenic in mice [Figure 9 and (Kessans et al., 2016)]. The prospect of increasing the frequency of the bnAb MPER target in the context of the enveloped, native Gag matrix is exciting because many bnAbs which recognize the MPER are autoreactive towards lipid membrane components (Haynes et al., 2005; Haynes et al., 2016; Verkoczy et al., 2010; Williams et al., 2015; Zhang et al., 2016), thus the MPER epitope must be in the context of a membrane in order to target bnAb lineages.

Here it was demonstrated that plant-made HIV-1 VLPs can be produced at high yields with maximum Gag expression around 1 mg/kg FW and dgp41 up to an average of 5.5 mg/kg, and transient Gemini-based vectors +p19 provided the highest yields (Table 4 & Table 5). The most exciting result is the consistently higher ratio of MPER on the surface of Gemini-produced VLPs compared to the TMV-produced VLPs, which are currently in immunization trials for heterologous prime-boosting to determine ability to elicit nAbs. Immunogenicity of the VLPs in this study revealed higher responses can be achieved upon boosting, with 100% response rates (Figure 9). Plant-produced vaccines and VLPs are gradually breaking through regulatory guidelines, thus vastly improving the chances of successful approval of a plant-produced product for human use (Fischer et al., 2012; Ma et al., 2005; Spok et al., 2008). The FDA-approved enzyme replacement therapy for Gaucher disease is a prime example of the potential for success of plant-produced pharmaceuticals (Zimran et al., 2011). Thus, results describe here show promise for plant-produced VLPs to be used alone or in combination with other prime-boost systems (see Chapter 5), as a cost-effective, scalable production system for an HIV-1 vaccine.

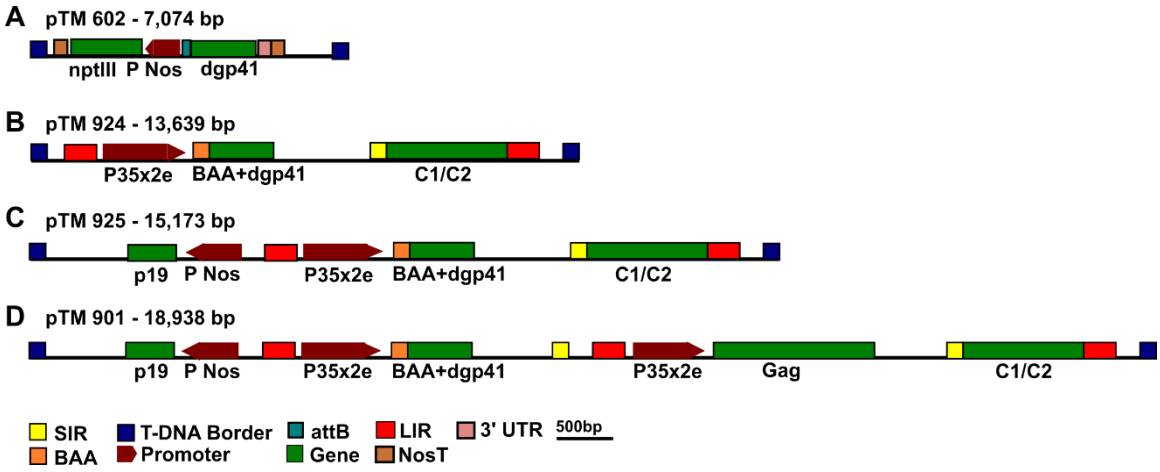

Figure 3 - T-DNA Regions of TMV and Geminivirus-based Transient Expression Vectors

Four transient deconstructed viral expression vectors were compared in this study. (A) A TMV-based vector, pTM 602, transiently expresses dgp41 after recombining with two other plasmids as part of the ICON expression system (Kessans et al., 2013; Marillonnet et al., 2004). (B-D) Vectors based on the Geminivirus bean yellow dwarf virus (BYDV) express dgp41 in a replicon, bordered by LIRs, in pTM 924 (B) and simultaneously with the silencing suppressor protein p19 in pTM 925 (C). These vectors contain the barley α-amylase signal peptide 5' of dgp41 for targeting to the secretory pathway which is under control of the cauliflower mosaic virus 35S promoter (P35) containing 2 transcription enhancer binding sites (2e). ICON systems recombine to add the signal peptide *in planta* and express dgp41 under the control of the TMV promoter in the *in planta* recombined construct. Additionally, the last Geminivirus vector contains two replicons separated by an SIR and LIR for simultaneous expression of Gag and dgp41 in addition to p19 in pTM 901 (D). The size of the full plasmid is indicated. For replicon amplification, Geminivirus-based systems also contain the viral replication proteins C1 and C2 (Rep and RepA, respectively). SIR – short intergenic region; BAA – barley α-amylase; T-DNA – transfer DNA; P – promoter, LIR – long intergenic region; 2e – 2 enhancer binding sites; NosT – nos terminator; 3' UTR – untranslated region; nptIII – kanamycin resistance gene

Figure 4 - Leaf Necrosis Over Seven-day Kinetics Time Course

Four transient expression constructs were analyzed for expression of dgp41 alone in Gag transgenic *N. benthamiana* (A-C) or simultaneously transient expression of Gag and dgp41 in WT plants (D). Leaf samples were collected in triplicate over seven days and images scanned to monitor leaf necrosis. (A) The TMV-based vector expressing dgp41 displays onset of necrosis around 5 dpi. Geminivirus-based transient expression of dgp41 in Gag plants displays necrosis more rapidly, around 3 dpi, without the silencing suppressor protein p19 (Gemini, B) than the Gemini vector which expresses dgp41 and p19 (Gemini +p19) from the same construct, which shows onset of necrosis around 4 dpi (C). WT plants infiltrated with the dual-replicon Gemini vector (Dual Gem. +p19) simultaneously express Gag, dgp41, and p19 from the same construct, and results in visible necrosis around 4 dpi (D). dpi - days post infiltration

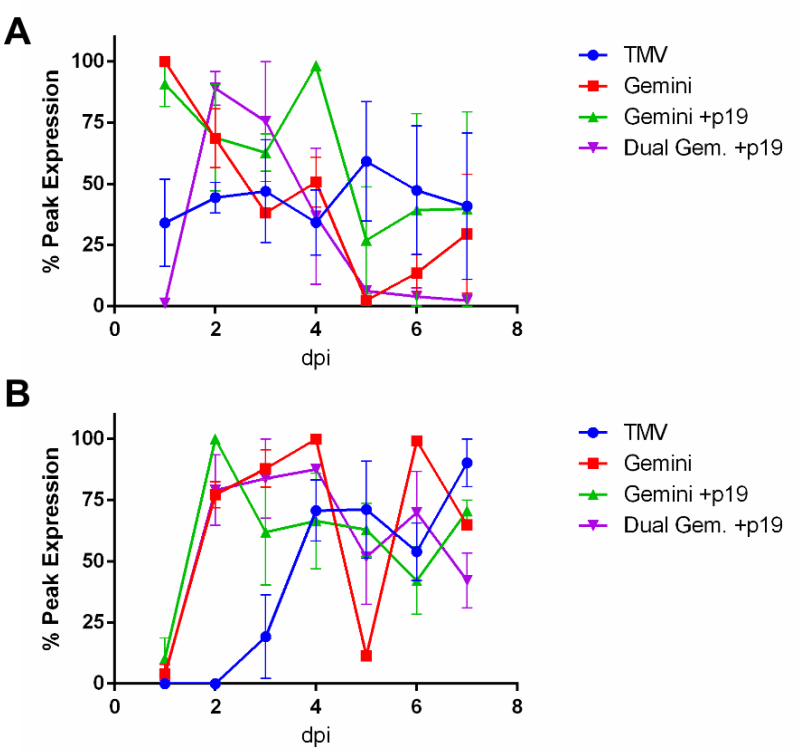

Figure 5 - Expression Kinetics of Gag and Dgp41 with TMV and Geminivirus-based Vectors

Homogenized leaf tissue was analyzed in triplicate for Gag (A) and dgp41 (B) expression by immunoblot over the seven-day time course and percent of peak expression day calculated through band intensity. For each replicate, the band with the highest intensity was set to 100% and every other day for that replicate calculated as a percent of the peak day. Peak day varied between replicates, and therefore some vectors do not have a consistent day for 100% between the replicates. Stable Gag expression and transient dgp41 expression was assessed for three vectors in Gag transgenic *N. benthamiana*: TMV, Gemini, and Gemini +p19. A fourth dual-replicon Gemini vector +p19 transiently expresses Gag, dgp41, and p19 simultaneously in wild-type plants. Peak expression day was determined for each vector as the day with highest Gag and dgp41 expression prior to severe necrosis. Data are the means of three replicates shown with standard error. dpi - days post infiltration

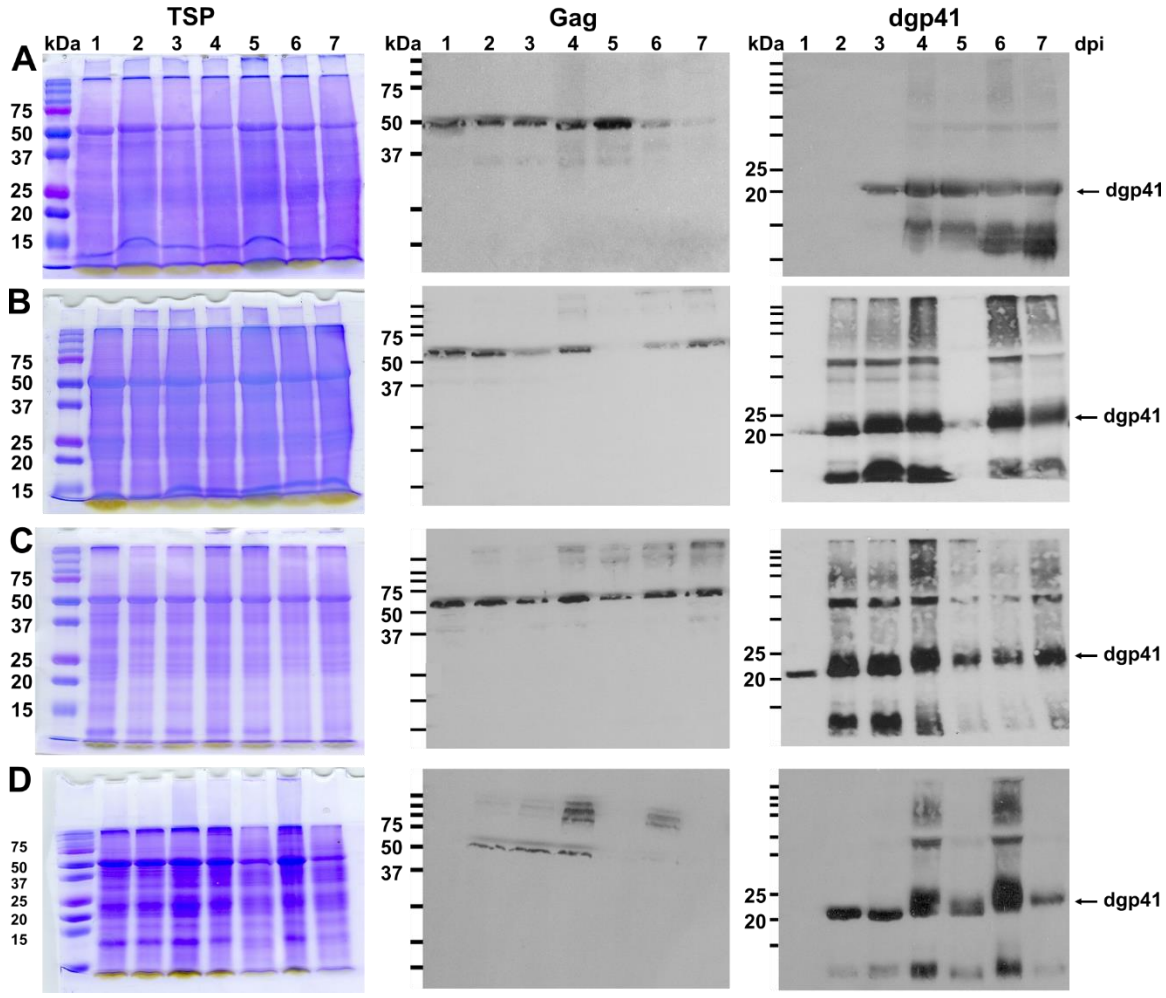

Figure 6 - Expression of Gag and Dgp41 with TMV and Geminivirus-based Vectors

Leaf samples pictured in Figure 4 were homogenized for each vector and 20 µg TSP was loaded in each lane (dpi 1-7). Three vectors were compared for dgp41 expression in Gag transgenic *N. benthamiana*: (A) TMV, (B) Gemini, and (C) Gemini +p19. A fourth dual replicon Gemini vector +p19 transiently expresses Gag, dgp41, and p19 simultaneously in WT plants (D). Coomassie-stained gels show equal TSP across lanes (left) and specific immunoblot for Gag (middle) and dgp41 (right) proteins was used to determine expression levels and identify peak expression day. Images shown are representative of triplicate leaf samples processed for each vector. dpi - days post infiltration; TSP – total soluble protein; WT – wild-type

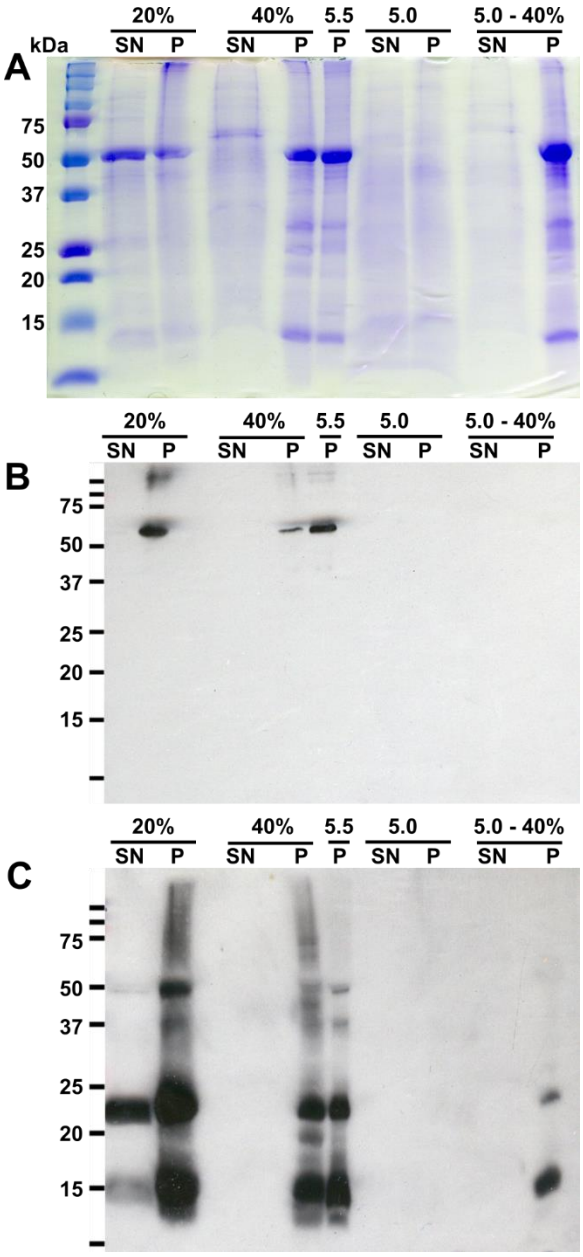

Figure 7 - Optimization of Purification Technique to Minimize Rubisco in VLP Extractions

Two strategies were tested for efficiency in extracting VLPs with minimal remaining rubisco in each sample. The first strategy utilized sequential ammonium sulfate precipitations at 20% (20% SN and P) and 40% (40% SN and P), where rubisco is expected to pellet around 25%. The second strategy employed pH changes to pH 5.5 (5.5 P) followed by pH 5.0 (5.0 SN and P) where rubisco is expected to pellet at pH 5.5. An additional 40% ammonium sulfate precipitation was performed on the pH 5.0 SN to pellet any remaining VLPs (5.0 – 40% SN and P). Lanes were loaded with equivalent TSP as shown by Coomassie staining (A). Expression of Gag (B) and dgp41 (C) in each fraction was analyzed by immunoblot. SN – supernatant; P – pellet; TSP – total soluble protein

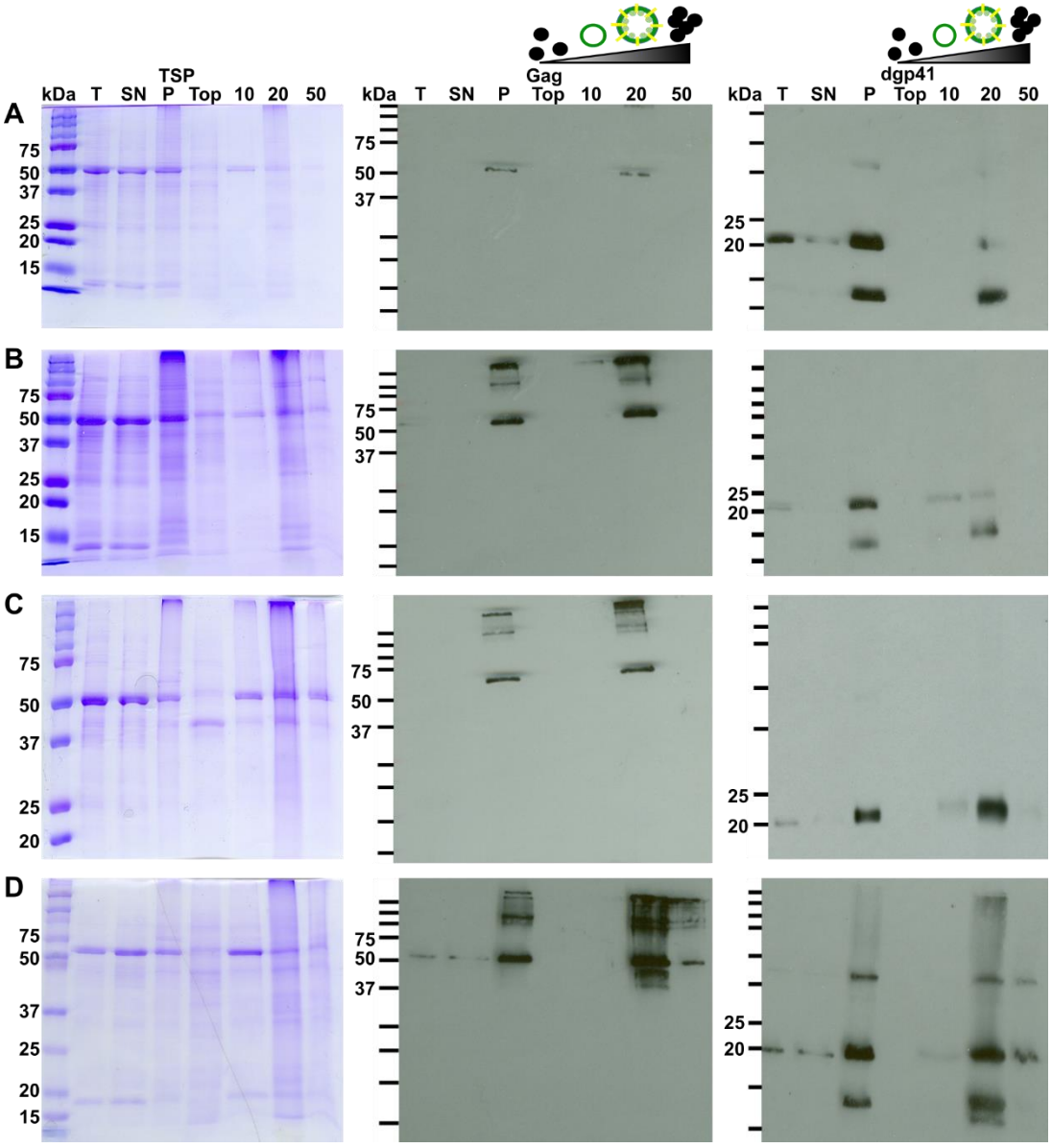

Figure 8 - Purification of HIV-1 VLPs Produced by TMV and Geminivirus-based Vectors

Six-week old *N. benthamiana* Gag transgenic plants were infiltrated to transiently express dgp41 with TMV (A), Gemini (B), or Gemini +p19 (C). (D) WT plants were infiltrated with a dual-replicon Gemini +p19 to transiently express Gag and dgp41. Leaf tissue was harvested on peak expression day and VLPs were extracted in 20 g batches (T – total extract) through 20% ammonium sulfate precipitation (SN – 20% ammonium sulfate supernatant; P – pellet) and density gradient centrifugation with step-wise 10-20-50% iodixanol layers (Top – sample after centrifugation; 10% iodixanol; 20% iodixanol; 50% iodixanol). 5 µg total soluble protein (TSP), as determined by Bradford assay, was loaded into each lane and analyzed by Coomassie staining (left), and for Gag (middle) and dgp41 (right) expression. VLPs are almost completely pelleted with 20% ammonium sulfate with little to no detectable protein remaining in the SN and isolate to the 20/50% barrier of the density gradient. Purifications representative of three independent extractions for each vector are shown.

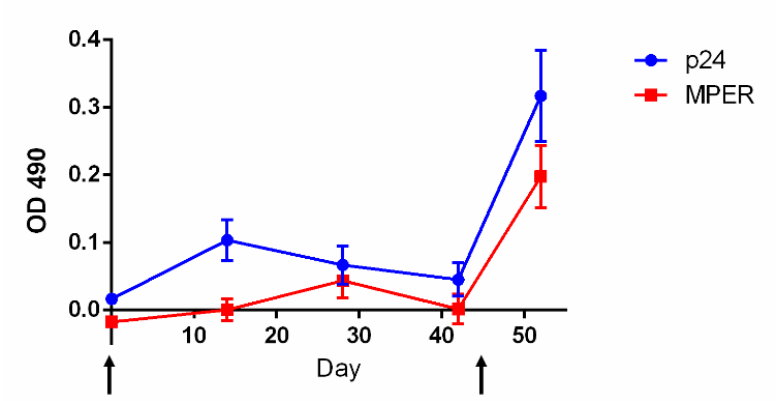

Figure 9 - VLP-induced Gag and Dgp41-specific Serum IgG

C57BL/6 mice (n = 3) were injected i.p. at Days 0 and 45 with VLPs, indicated by arrows. Anti-p24 (Gag) and anti-MPER (dgp41) serum IgG are shown over time as the ELISA OD 490 nm for the 1:50 dilution (lowest tested). At the Day 52 endpoint, all animals have detectable levels of both Gag and dgp41 specific antibodies. Data are the mean of two measurements for each sample for all time points.

Table 4 - Total Gag and Dgp41 Expression from Ammonium Sulfate Precipitation

Vector	Infiltrated Plant Line	Transient Expression	Gag Yield (mg p24/kg)[a]	dgp41 Yield (mg MPER/kg)[a]
TMV	Gag	dgp41	1.04 ± 0.59	3.45 ± 2.29
Gemini			0.62 ± 0.16	0.82 ± 0.52
Gemini (+p19)			0.85 ± 0.34	4.62 ± 1.52
Dual Gem. (+p19)	WT	Gag & dgp41	1.09 ± 0.38	5.46 ± 1.49

[a] Protein expression is expressed as mg of p24 or MPER per kg fresh leaf weight for Gag and dgp41, respectively. Triplicate samples were processed for each vector and reported here as mean with standard error.

Table 5 - HIV-1 VLP Yield with Transient Expression in *N. benthamiana*

Vector	Infiltrated Plant Line	Transient Expression	Gag Yield (µg p24/kg)[a]	dgp41 Yield (µg MPER/kg)[a]	Molar Ratio (MPER:p24)[b]
TMV	Gag	dgp41	343 ± 131	33 ± 16	0.74 – 5.2
Gemini			175 ± 68	11 ± 3	0.47 – 1.34
Gemini (+p19)			130 ± 30	57 ± 37	0.61 – 9.8
Dual Gem. (+p19)	WT	Gag & dgp41	322 ± 92	84 ± 38	1.7 – 11.8

[a] Levels of protein are expressed as µg p24 or MPER for Gag and dgp41, respectively, per kg fresh leaf weight. Gag and dgp41 yield were determined in triplicate by quantitative immunoblot from density gradient VLP-enriched fractions and reported here as mean with standard error.
[b] Molar ratio is calculated as amount of dgp41 MPER to p24 Gag based on a molecular weight ratio of 1.6 (p24 = 24 kDa/MPER = 15 kDa) and the lowest and highest ratios are shown as a range.

Chapter 3

PLANT-PRODUCED HIV-1 VLPS STIMULATE A TH2 RESPONSE THROUGH TOLL-LIKE RECEPTOR DEPENDENT ACTIVATION OF INNATE IMMUNE CELLS

Abstract

The innate immune system provides the pathway to activation of adaptive responses, and the Toll-like receptors (TLRs) represent one of the primary sensor groups that detect components of bacteria cell walls and endosomal nucleic acids. Plant-based production of virus-like particles (VLPs) inherently involves plant proteins, the gram-negative bacteria *Agrobacterium tumefaciens*, and viral-based expression vectors. Each of these offers a unique pathogen associated molecular pattern (PAMP), which could potentially lead to induction of the TLRs if present in the final VLP-enriched product. In this study, it was demonstrated that plant-produced HIV-1 Gag/dgp41 VLPs are capable of stimulating each TLR and do contain nucleic acids that could be delivered to the endosome. Furthermore, it was shown that VLPs induce a preferential up-regulation of the CD11b integrin and CD40 co-stimulatory factor in THP-1 cells and mouse splenocytes. Furthermore, the up-regulation of CD11b and cytokine production is dependent upon signaling through MyD88 and TICAM, but not IFN-α/β receptors, indicating a TLR-specific activation. It was further shown that the CD11b population represents alternatively activated M2b macrophages secreting primarily IL-10, thus resulting in Th2-biased responses characterized by IgG1 isotype switching and minimal IgG2a. Finally, the immunogenicity of the plant-produced VLPs was demonstrated to be dependent upon TICAM signaling. Results suggest that TLR4 is likely the primary receptor for VLP-induced activation, due the resemblance of responses to LPS exposure and the dependence on both TLR adaptor proteins. Based on these results, it is proposed that plant-based production of VLPs and other antigens represents a unique platform that introduces inherent adjuvancy, which could be complemented by specifically choosing a vaccine formulation to enhance the innate immune stimulatory effects described here.

Introduction

The innate immune system is the first defense against invading pathogens, and therefore provides key non-specific responses to pathogen associated molecular patterns (PAMPs) to initiate the adaptive response (Hoebe et al., 2004; Iwasaki and Medzhitov, 2015). These PAMP responses are often regulated through the Toll-like receptors (TLRs), which can sense both extracellular PAMPs primarily involving bacterial cell wall components [i.e. lipopolysaccharide (LPS), lipotechoic acids, flagellin] and intracellular nucleic acids in the endosomal compartment (Akira et al., 2006; Kawai and Akira, 2007; Kawai and Akira, 2010; O'Neill et al., 2013; Takeda et al., 2003). All TLRs, with the exception of TLR3, signal through the adaptor protein MyD88, to induce expression of cytokines primarily through the transcription factor NFκB (Janeway and Medzhitov, 2002; Takeda et al., 2003). TLR3 utilizes an alternative pathway through TICAM [Toll-IL-1 receptor homology domain (TIR)-containing adaptor molecule, also known as TRIF], while TLR4 is the only known TLR capable of signaling through both adaptor proteins, resulting in activation of NFκB and IRF3 transcription factors (Kawai and Akira, 2010).

Many antigen presenting cells (APCs), including dendritic cells (DCs) and macrophages, express TLRs, and stimulation through these pathways leads to up-regulation of co-stimulatory molecules, including CD40, CD80, and CD86 (Banchereau and Steinman, 1998; Hoebe et al., 2003; Kaisho et al., 2001; Schnare et al., 2001). These co-stimulatory molecules are involved in the immunological synapse between APCs and T cells, and are required for T cell activation (Friedl et al., 2005; Huppa and Davis, 2003; McHeyzer-Williams et al., 2000). TLR signaling is also required for efficient antibody (Ab) production through activation of B cell and CD4 T cell responses (Nemazee et al., 2006; Pasare and Medzhitov, 2004; Pasare and Medzhitov, 2005; Schnare et al., 2001), demonstrating the necessity of TLRs and other pattern recognition receptors (PRRs) in the initial responses which lead to mobilization of the adaptive response.

Activation of B cells not only requires stimulation by innate cells but also requires TLR expression and signaling within the B cells themselves (Pasare and Medzhitov, 2005). TLR2 and TLR4 signaling through MyD88 is required for the development of long-lived Ab responses (Komegae et al., 2013) while TLR4 and 9 induce memory B cells to differentiate into plasma cells

for Ab secretion (Richard et al., 2008). Furthermore, when TLR ligands are detected by antigen-stimulated B cells, a non-canonical NFκB pathway is triggered resulting in activation-induced cytidine deaminase (AID) up-regulation, which controls Ab class-switching (Pone et al., 2012). This leads to a T-independent class-switch towards IgG3 and IgG2a, which can occur in the absence of TLR signaling (Nemazee et al., 2006; Pasare and Medzhitov, 2005). However, TLR signaling is required for T-dependent antigens to produce IgM and IgG1, but not IgG3 (Pasare and Medzhitov, 2005). Such differences in class-switching can also be induced by differential stimulation of cytokines, such as IL-12 and IL-4, which respectively result in a bias toward either Th1 or Th2 CD4 responses (Snapper and Paul, 1987; Szabo et al., 2003), and TLRs have been implicated in at least partially regulating this outcome (Akira et al., 2001; Jankovic et al., 2002; Kaisho et al., 2002; Pasare and Medzhitov, 2005; Re and Strominger, 2001; Schnare et al., 2001). Therefore, the presence of antigen with or without TLR signaling can result in differential class-switching, ultimately resulting in two distinct types of immune responses. Understanding which pathways are activated by vaccine antigens is important when deciding vaccine formulations, including adjuvant choice, because alum, Freund's complete and incomplete adjuvant, and Ribi adjuvant, do not act through TLR pathways (Gavin et al., 2006; Nemazee et al., 2006).

Virus-like particles (VLPs) are immunogenic subunit vaccines which more accurately represent the structure of a native virion (Kushnir et al., 2012; Yildiz et al., 2011). VLPs are known stimulators of innate immunity (Raghunandan, 2011) and the role of TLRs in VLP immunogenicity is of great interest to determine their mode of activation. The interaction of VLPs, but not soluble, monomeric antigens, with naïve B cells and follicular DCs induces transport of antigen to draining lymph nodes where it initiates adaptive responses (Bessa et al., 2012; Link et al., 2012), making them an attractive vaccine component compared to other subunit vaccines. VLPs for several viruses, including HIV-1, human papillomavirus (HPV), and hepatitis C virus (HCV) have been shown to directly activate DCs (Barth et al., 2005; Buonaguro et al., 2006; Lacasse et al., 2008; Lenz et al., 2001; Tsunetsugu-Yokota et al., 2003; Yang et al., 2004). Baculovirus-produced HPV VLPs are known to stimulate through TLR4, and vaccination in mice or humans can induce a

mixed Th1/Th2 cytokine profile (Lenz et al., 2001; Pinto et al., 2005; Yan et al., 2005; Yang et al., 2004). Alternatively, baculovirus-produced HIV-1 Gag VLPs were shown to activate human PBMC monocytes resulting in a Th2-biased response (Buonaguro et al., 2008; Buonaguro et al., 2006; Speth et al., 2008), though this was shown to be independent of TLR2 and 4 (Buonaguro et al., 2006). Furthermore, HIV-1 Gag VLPs produced in a yeast system were shown to induce a Th1 response which requires TLR2 (Tsunetsugu-Yokota et al., 2003), suggesting that the VLPs are not only responsible for stimulating TLRs, but the host production system may also play a role in directing the specific cytokine activation due to differential PAMPs. To our knowledge, there is no data available on the interaction of TLRs with plant-produced antigens, despite the high safety profile and immunogenicity of plant-derived VLPs (Chen and Lai, 2013; Rybicki, 2009; Rybicki, 2010; Rybicki, 2014; Scotti and Rybicki, 2013; Yusibov et al., 2014).

HIV-1 Gag VLPs have been successfully produced in plants by several groups, and are known to be immunogenic in mice, inducing both B cell and CD8 T cell responses (Kessans et al., 2013; Kessans et al., 2016; Meyers et al., 2008; Pillay et al., 2010; Scotti et al., 2009). VLPs used in this study also contain the deconstructed-gp41 (dgp41) transmembrane protein (Kessans et al., 2013), which contains the highly conserved membrane proximal external region (MPER) targeted by several broadly neutralizing antibodies [bnAbs, (Huang et al., 2012; Purtscher et al., 1994; Zwick et al., 2001)]. Producing proteins in plants inherently involves the use of the gram-negative bacteria, *Agrobacterium tumefaciens*, and the widely used deconstructed viral expression vector based on tobacco mosaic virus (TMV), a positive-sense ssRNA virus (Gleba et al., 2005; Marillonnet et al., 2004; Marillonnet et al., 2005). *A. tumefaciens* contains potential TLR PAMPs, including LPS and flagellin (Chesnokova et al., 1997; Silipo et al., 2004). The TMV vector includes the viral RNA-dependent RNA polymerase, thus amplifying the recombinant gene's mRNA in the cytoplasm, resulting in abundant ssRNA which could be incorporated into VLPs (Marillonnet et al., 2004). Indeed, HIV-1 VLPs are known to incorporate cellular mRNAs and are capable of delivering them to other cells (Valley-Omar et al., 2011). Similar "RNA-loading" of bacteriophage Qβ VLPs can induce both systemic and mucosal IgA antibody responses through a TLR7-dependent mechanism (Bessa et al., 2009). Based on these

observations, it was hypothesized that plant-produced HIV-1 VLPs may incorporate some components which are known to be stimulators of the TLR pathways (Kawai and Akira, 2010; Takeda and Akira, 2004). This is proposed as an advantage of producing VLPs in plants, as many of the TLR ligands that could be artificially introduced during plant-based production have been explored as vaccine adjuvants (Hjelm et al., 2014; Mata-Haro et al., 2007; Nagpal et al., 2015; Steinhagen et al., 2011).

In this study, VLPs were specifically tested for their capacity to interact with the innate immune system through TLRs. HIV-1 VLPs can efficiently be produced in plants and have been shown to be immunogenic in mice (Kessans et al., 2013; Kessans et al., 2016; Meyers et al., 2008; Pillay et al., 2010; Scotti et al., 2009). It was shown here that plant-produced VLPs induce proliferation of $CD11b^+$ cell populations, up-regulating both CD11b itself and the co-stimulatory molecule CD40 in an *ex vivo* assay. This activation results in biased production of Th2 cytokines from alternatively activated macrophages, resulting in IgG1 Ab switching. The interaction with $CD11b^+$ innate cells is dependent upon both MyD88 and TICAM, and TLR signaling through TICAM is required for immunogenicity of the VLPs, indicating a potential TLR4-dominant adjuvant-like effect.

Materials and Methods

Plant Expression and Sample Purification

Wild-type (WT) or Gag transgenic six-week-old *Nicotiana benthamiana* plants were either left uninfiltrated (WT or Gag/uninfil), mock infiltrated with *A. tumefaciens* (OD_{600} = 0.1) harboring an empty vector (WT or Gag/mock) or a vector for expression of dgp41 (WT or Gag/dgp41; described previously Kessans et al., 2013). Leaf tissue was harvested at peak dgp41 expression (4 days post-infiltration, dpi) by flash freezing in liquid nitrogen. Expression vectors used here are based on the TMV magnICON® transient expression system (Gleba et al., 2005; Marillonnet et al., 2004; Marillonnet et al., 2005).

Sample purification was performed as previously described for plant-produced VLPs (Kessans et al., 2013). Briefly, leaf tissue was crushed in liquid nitrogen, solubilized in extraction

buffer (25 mM sodium phosphate, 100 mM NaCl, 1 mM EDTA, 50 mM sodium ascorbate, 1 mM PMSF, pH 7.8) for 1 hr, and protein precipitated with 40% ammonium sulfate. The 40% ammonium sulfate pellets were resuspended in 1X PBS and further purified by iodixanol density gradient. The 20% iodixanol fraction was collected for use in this study because this is the fraction in which VLPs are isolated (Kessans et al., 2013). Total soluble protein (TSP) was quantified by Bradford assay for the 20% gradient fraction to standardize amount of protein used in subsequent experiments. Equivalent TSP for each 20% gradient fraction was loaded in 12% polyacrylamide gels and assessed for expression of Gag and dgp41 as previously described (Kessans et al., 2013).

Toll-like Receptor Reporter Assay

HEK293T cells individually expressing TLR2/6, 3, 4, 5, 7, or 9 (Invivogen) were grown in DMEM (Corning Cellgro) with 10% heat-inactivated FBS and 10 µg/mL blasticidin (Invivogen). Null 293T cells lacking expression of any TLR were grown in the same manner, only without blasticidin. Cells were seeded in 6-well plates and transfected in a 3:1 ratio with Lipofectamine Reagent and 500 ng/well of the pNiFty2-SEAP reporter plasmid (Invivogen), which contains the SEAP gene under control of an NFκB promoter. After 24 hrs, wells were treated with 1 µg TSP of 20% gradient-purified plant samples: WT uninfiltrated (WT/uninfil), WT mock infiltrated (WT/mock), WT dgp41 infiltrated (WT/dgp41), Gag uninfiltrated (Gag/uninfil), Gag mock infiltrated (Gag/mock), or Gag/dgp41 (VLPs). Cells were allowed to incubate with plant samples for another 24 hrs, then growth medium was collected and 20 µL added to QUANTI-Blue™ (Invivogen) per manufacturer's protocol. Color change was monitored for up to 4 hrs, and upon reaching saturation (defined as no additional color change for 1 hr), samples were read at OD 630 nm. Positive controls for each TLR were included: TLR3 – 1 µg/mL poly(I:C) (Invivogen), TLR4 – 0.01-1 ng/mL LPS, TLR5 - *Escherichia coli* whole cell lysate (1 µg TSP), TLR7 – 1µg/mL imiquimod (Invivogen), and TLR9 – 10 µg/mL ODN2006 (Invivogen). A TLR2/6 positive control was not available.

Nuclease Digestion

WT or VLP 20% gradient fractions were treated with either DNase I (Fermentas) or RNase A/T1 mix (Thermo Scientific) per manufacturer's protocol. Samples were diluted to the same volume in PBS. Upon addition of the nuclease, samples were digested for 15 min at 37° C followed by addition of EDTA for enzyme inactivation at 65° C for 10 min. A control treatment was included in which all buffers and heating steps, including inactivation of the enzyme, were carried out in the absence of any nuclease. Another sample that was untreated was included in assays as a control for any alterations in signaling induced by buffer changes or heating cycles. Controls for proper digestion were included as plasmid DNA for DNase I and cellular mRNA extractions for RNase A/T1. These samples were either digested with their respective nucleases or subjected to all buffers and heat cycles in the absence of nucleases. After treatments were completed, all WT and VLP samples were incubated with TLR7 (RNase) or TLR9 (DNase) reporter cells as described above. All digested samples, control treatments, and TLR reporter samples were done in triplicate.

To assess the role of the VLP envelope in protecting nucleic acids from digestion, an additional assay was performed in which the above RNase treatments were done with or without 1% Triton X-100 detergent in order to disturb the VLP membranes. Samples were diluted into equal volumes of PBS, either with or without 1% Triton X-100, followed by addition of RNase A/T1 mix buffers and enzyme for the same incubations listed above. A control with all buffers and heat cycles in the absence of RNase was included. After nuclease treatment, RNA was extracted separately from DNA using TRIzol® reagent (Thermo Fisher) per manufacturer's protocol. Final RNA pellets were resuspended in 10 µL water and concentrations measured by OD 260 nm readings. RNA yield was calculated by setting the control (no RNase) samples to 100% yield and the samples containing RNase were then calculated as a percent of the control. All digests and controls were done in triplicate.

THP-1 Activation and Differentiation

THP-1 cells were grown in RPMI 1640 medium (Corning Cellgro) supplemented with 10% heat-inactivated FBS, 25 mM HEPES, 2 mM L-glutamine, penicillin (100 units/mL), and streptomycin (100 µg/mL). 4 x 10^5 cells were incubated with 5 µg TSP of WT or VLP 20% gradient fractions for 72 hrs. Cells were then stained with CD11b-PE (macrophage; BD Biosciences) or CD11c-V450 (DC; BD Biosciences) and activation marker antibodies CD40-APC, CD80-FITC, and CD86-PE (BD Biosciences). Surface expression was measured via flow cytometry on an LSR Fortessa. For analysis of up-regulation of activation markers on dendritic cells ($CD11c^+$), THP-1 cells were first differentiated into DCs by plating 2 x 10^5 cells/well and treating with 100 ng/mL of human IL-4 and GM-CSF (Gold Biotechnology, Inc.) for 5 days, refreshing cytokines and medium every 2 days and selecting for adhered cells only. After full differentiation, DCs were incubated with WT or VLP 20% gradient fractions for 72 hrs and analyzed via flow cytometry for expression of surface activation markers, as above.

Dendritic Cell VLP Attachment Assay

THP-1 cells were differentiated into DCs as described above, then incubated with 5 µg VLPs or Gag/uninfiltrated 20% gradient fractions for 2 hrs. After incubation was complete, cells were stained with CD11c-V450 (BD Biosciences) and human anti-gp41 antibody 2F5 (AIDS Reagents Program). Cells were fixed with Cytofix/Cytoperm™ Kit (BD Biosciences), then stained with anti-human Ig κ light chain-PE (BD Biosciences) for detection of 2F5. Cells were analyzed via flow cytometry.

Ex vivo VLP Stimulation of Mouse Splenocytes

Spleens were harvested from eight to ten-week-old C57BL/6 (n = 3), TICAM -/- (n = 5), MyD88 -/- (n = 3), or IFNAR -/- (n = 3) mice (Jackson Laboratories) in Hank's medium (Corning Cellgro), and cells strained through a 0.7 µm filter for resuspension in complete RPMI [cRPMI: 10% FBS, penicillin (100 units/mL), streptomycin (100 µg/mL), 2 mM L-glutamine]. Red blood cells were lysed with ACK Lysing Buffer (Gibco) and splenocytes resuspended in cRPMI at a

concentration of 2 x 10^7 cells/mL. Cells were plated at 1 x 10^6 cells/well and incubated with cRPMI (negative) or 5 µg TSP of WT or VLP 20% gradient fractions for 12 hrs and then a further 8 hrs after addition of GolgiPlug™ (BD Biosciences). After incubation, cells were stained with the indicated anti-mouse antibodies in each assay [including: CD11c-FITC (BD Biosciences), CD11b-APC (BD Biosciences) or CD11b-PerCP-Cy5.5 (BD Biosciences), F4/80-PE-Texas Red® (BD Biosciences)], fixed and permeabilized with Cytofix/Cytoperm™ Kit (BD Biosciences), and intracellularly stained with indicated antibodies for cytokines [including: TNFα-PE (BD Biosciences), IFNγ-eFluor® 450 (eBioscience), IL10-FITC (eBioscience), and IL12-PE (BD Biosciences)]. Cells were analyzed via flow cytometry.

Cell Proliferation Assay

Spleens were harvested and prepared from C57BL/6 mice (n = 3) as described above. After red blood cell lysis, cells were washed twice with 1X PBS (Corning Cellgro), labeled with 1 µM CFSE per manufacturer's protocol, and washed an additional three times in 1X PBS after labeling to remove excess dye. Cells were resuspended in cRPMI and plated 1 x 10^6 cells/well then incubated for 48 hrs with cRPMI (negative) or 5 µg WT or VLP 20% gradient fractions. Splenocytes were stained with CD11b and fluorescence intensity of CFSE was measured via flow cytometry.

Mouse Immunizations

All animal studies were done in accordance with the Arizona State University Institutional Care and Use Committee.

Six-week-old C57BL/6 (wild-type) or TICAM -/- mice (Jackson laboratories) were injected intraperitoneally (i.p.) with 2 µg p24 and 0.76 µg MPER, as quantified by immunoblot (described previously Kessans et al., 2016). Serum was collected after 14 days to analyze antigen-specific IgG Ab production.

ELISA and Antibody Isotyping

Serum samples were analyzed for antigen-specific IgG using either p24 (Gag) or MPER (dgp41) peptides, as previously described (Kessans et al., 2016). Total antigen-specific IgG was identified with rabbit anti-mouse IgG-HRP (Calbiochem). For Ab isotyping, isotype-specific antibodies were used: goat anti-mouse IgG1-HRP or goat anti-mouse IgG2a-HRP (Santa Cruz Biotechnology). Purified mouse IgG1 kappa chain or mouse IgG2a kappa chain primary antibodies (Sigma) were use as controls. ELISAs were developed using SIGMA*FAST*™ OPD (Sigma) per manufacturer's protocol with samples read at OD 450 nm.

Data Analysis

All flow cytometry was performed using an LSR Fortessa, and data analyzed using FlowJo Software (TreeStar Inc., San Carlos, CA). All statistical analyses were performed using ANOVA multiple comparisons one-way or two-way, depending on comparisons, in GraphPad Prism Software (GraphPad Prism Software Inc., La Jolla, CA). Significance cut-off was set as $p < 0.05$.

Results

VLP and Control Preparations for TLR Stimulation

HIV-1 Gag/dgp41 VLPs are of interest as an HIV-1 vaccine candidate (Kessans et al., 2016), and have potential for TLR stimulation due to their production mechanism. To assess these interactions, six control groups were devised: WT/uninfiltrated (plant protein only), WT/mock (plant + bacteria), WT/dgp41 (plant + dgp41 + bacteria), Gag/uninfiltrated (plant + Gag VLPs), Gag/mock (plant + Gag VLPs + bacteria), and Gag/dgp41 (plant + Gag/dgp41 VLPs + bacteria). Comparison of these controls will allow delineation of which VLP components are primarily responsible for any stimulation of innate pathways.

To generate these controls, six-week-old wild-type (WT) or Gag transgenic (Kessans et al., 2013) *N. benthamiana* plants were either left uninfiltrated, infiltrated with *A. tumefaciens* harboring an empty vector (mock infiltration), or with a TMV-based expression vector for dgp41

(Kessans et al., 2013). In an effort to fully mimic the VLP purification steps, whether or not Gag VLPs are present, all samples were passed through iodixanol density gradients. HIV-1 VLPs isolate to the 20% fraction (Kessans et al., 2013), therefore this is the only fraction used in immunological assays. The 20% fraction from each control was assessed for expression of Gag or dgp41, shown at 55 kDa and 23 kDa, respectively (Figure 10). All Gag transgenic extractions contain Gag VLPs, and infiltration appears to increase the yield of Gag in the 20% fraction when protein is loaded equally (Figure 10A). Furthermore, dgp41 was detectable in the Gag/dgp41 sample as expected, and interestingly, was also shown to be present in the WT/dgp41 sample in the absence of Gag VLPs (Figure 10B).

Plant-produced VLPs Stimulate TLRs

In order to determine which TLRs were activated by gradient-purified VLPs, HEK293T cell lines expressing each TLR independently were utilized for individual assessment. Upon transfection with a SEAP NFκB reporter plasmid, cells were treated with each of our six controls to identify which components (e.g. *A. tumefaciens* components, plant or recombinant HIV-1 proteins, or VLPs) are required for TLR stimulation.

Extracellular receptors, TLR2/6, 4 and 5 (Figure 11A), were all activated by the Gag transgenic plants that were mock infiltrated with an empty vector or with a dgp41-expressing vector. However, the matched WT plant controls did not show similar activation. For TLR4, a titration curve of purified LPS was used to quantify the endotoxin levels in the VLP sample, calculated at approximately 300 ng LPS/mL (data not shown). The TLR reporter cell treatment used 1 µg TSP of each sample which corresponds to a treatment of 0.27 ng of LPS, assuming a direct comparison between *E. coli* and *A. tumefaciens* LPS potency. Interestingly, a similar activation pattern was seen with the endosomal nucleic acid receptors, TLR3, 7 and 9 (Figure 11B), in which the Gag/mock and Gag/dgp41 VLP fractions activate NFκB reporter gene expression, but WT/mock and WT/dgp41 samples do not. Notably, the only exception to this was TLR2/6 stimulation by the WT/dgp41 sample, suggesting a non-canonical stimulator of TLR2/6 in this fraction (Figure 11A). These data indicate that VLPs are necessary for TLR-stimulating *A.*

tumefaciens components to co-purify to the 20% gradient fraction, because matching WT controls lacking VLPs do not induce a similar pattern of TLR activation.

VLP Stimulation of TLRs is Resistant to Nuclease Digestion

Activation of the nucleic acid sensors TLR3, 7 and 9 was surprising because they are endosomal, suggesting the VLPs must deliver nucleic acids to these compartments because the WT matched controls for these fractions do not mimic this interaction (Figure 11B). In order to first determine whether nucleic acids are detectable and encapsulated by the VLPs, we performed nuclease digestions on the WT/uninfiltrated and Gag/dgp41 VLP 20% gradient samples with and without membrane-disrupting detergent Triton X-100 (Figure 12A). The WT uninfiltrated sample showed clear loss of RNA when digested with RNase without Triton X-100, and this was not disrupted in the presence of 1% detergent. In sharp contrast to this, the VLP fraction had complete recovery of RNA when exposed to RNase in the absence of detergent. However, addition of 1% Triton X-100 allowed for the RNA to be digested in a similar manner to the WT sample. Therefore, the data suggest that VLPs protect nucleic acids from nuclease digestion and therefore, nuclease treatment should not affect their ability to stimulate the endosomal TLRs. To test this hypothesis, VLPs were left untreated, treated with nucleases, or exposed to nuclease buffer and heating cycles in the absence of any nuclease. Buffer and heating cycles alone did not alter signaling of VLP or WT samples (Figure 12B-C). While DNase treatment had no effect on TLR9 signaling (Figure 12C), RNase treatment of VLPs only slightly reduced TLR7 stimulation, though this is still significantly higher than WT samples (Figure 12B). Together, these data suggest that VLPs acquire nucleic acids from the plant cells during production, offer protection from nucleases through the membrane envelope to survive the purification process, and can successfully deliver them to the endosomal TLRs.

VLPs Induce THP-1 Differentiation

Many innate immune cells express TLRs, and undergo observable changes in expression of cell surface markers upon stimulation. Therefore, it was hypothesized that VLP interaction with

TLRs on human THP-1 monocytes could induce activation and/or differentiation. To this end, non-differentiated THP-1 cells were incubated with Gag uninfiltrated particles, VLPs, or medium alone (negative control), then stained for expression of CD11c (DC marker), CD11b (macrophage marker), and CD40 (activation marker). Unstimulated cells have a bias toward expression of CD11c, whereas VLPs shift the cell population to be primarily $CD11b^{+}$ (Figure 13A). Expression of the activation marker, CD40, is also up-regulated in VLP-treated wells for both the macrophage (Figure 13B) and DC (Figure 13C) populations. The Gag uninfiltrated VLPs display an intermediate phenotype in which the cell populations are more evenly split between DC and macrophage markers (Figure 13A); however, there is little up-regulation of CD40 by these particles (Figure 13B-C). This indicates the *A. tumefaciens* components are required for more potent activation of undifferentiated monocytes.

VLPs Directly Interact with and Activate DCs

If VLPs are capable of stimulating differentiation of THP-1 cells, it was reasoned that they could also activate fully differentiated cells derived from this cell line. THP-1 cells were differentiated into DCs and were then treated with Gag uninfiltrated particles or Gag/dgp41 VLPs for 2 hours to allow VLP attachment and then stained for flow cytometry (Figure 13D). Results clearly indicate VLPs are in association with DCs while Gag uninfiltrated particles, which lack expression of gp41, do not have significant detection of 2F5 similar to the negative control (Figure 13D), thus confirming the detection of 2F5 in this assay is specific to gp41.

In order to assess whether VLPs or WT plant material can induce activation of DCs, the THP-1-derived DCs were also incubated with WT uninfiltrated plant material or VLPs for 24 hrs and then analyzed by flow cytometry for expression of activation markers (Figure 13E-F). CD40 had the most significant up-regulation by VLPs (Figure 13E) and CD86 also displayed some minor up-regulation (Figure 13F). CD80 was also analyzed but did not display significant up-regulation by VLPs or WT gradient fractions (data not shown). Therefore, these data indicate that plant-produced VLPs are capable of inducing differentiation and activation of monocytes and DCs, likely through direct interaction by attachment to these cell types.

VLPs Activate CD11b$^+$ Cells in a TLR-dependent Manner

In order to test whether TLR stimulation has any significance in the activation of monocytes seen in cell culture, whole splenocytes were isolated from C57BL/6 mice strains: wild-type (B6), TICAM (TRIF) -/-, MyD88 -/-, and IFNAR -/- (Jackson laboratories). TICAM and MyD88 are the primary adaptor proteins for TLR signaling, where TLR3 is the only receptor solely dependent upon TICAM, and TLR4 is the only receptor which can signal through both TICAM and MyD88 (Kawai and Akira, 2010; Takeda and Akira, 2004). IFNAR knockout mice are deficient in their ability to respond to type I interferons (i.e. IFN-α/β), but TLR signaling is unaffected, and therefore they are included as a control.

Total splenocytes were incubated *ex vivo* for a total of 20 hrs in the presence of WT or VLP gradient fractions (5 µg TSP) then assessed for CD11b/c expression and production of IFN-γ and TNF-α cytokines (Figure 14). The negative control baseline expression was subtracted from all data unless it is shown in the graph. Down-regulation of CD11c was detected for both WT and VLP-treated samples in B6 mice, but only for VLP samples in all knockout mice (Figure 14A). The CD11c$^+$ population also showed up-regulation of CD80 when exposed to both WT and VLP gradient fractions, though this is not detectable in MyD88 -/- or IFNAR -/- mice, suggesting a non-specific, TLR-independent activation of the DC population (Figure 14B). WT plant material induces minor up-regulation of CD11b, which is significantly increased by VLPs in B6 mice (Figure 14C). Interestingly, both TICAM -/- and MyD88 -/- mice showed a similar loss of CD11b up-regulation induced by VLPs, while IFNAR -/- mice are unaffected (Figure 14C). Representative plots of CD11b and CD11c gates are shown in Figure 14E, noting the strong shift induced by VLPs towards a predominantly CD11b$^+$ population in B6 and IFNAR -/- mice. This up-regulation is reduced by approximately 50% in the TLR knockout mice. Interestingly, the CD11b$^+$ population in B6 and IFNAR -/- mice has increased IFN-γ single-positive and TNF-α/IFN-γ double positive cells when exposed to VLPs compared to WT plant material, and this activation is lost in both the TICAM -/- and MyD88 -/- mice (Figure 14D). No significant results were detected for TNF-α single-positive cells.

Furthermore, nuclease treatment of VLPs did not largely effect up-regulation of CD11b or cytokine expression in B6 mice (Figure 15A-B). Only a slight reduction in the CD11b up-regulation was seen with DNase treatment of VLPs, though this did not alter cytokine expression (Figure 15A). WT plant material actually showed an increase in cytokine expression when exposed to DNase treatment (Figure 15B), potentially indicating some off-target effect by the presence of the enzyme during the assay, even though it was inactivated prior to incubation. Overall, this data suggests that VLPs uniquely induce a shift toward a $CD11b^+$ population that expresses IFN-γ and TNF-α cytokines in a TLR-dependent manner, matching the biased activation seen in THP-1 monocytes (Figure 13A-C).

VLPs Induce Macrophage Proliferation

It was noted during the *ex vivo* splenocyte stimulation (described above) that there was a vast expansion of the $CD11b^+$ population in VLP-treated samples (Figure 13A). A likely explanation for this would be proliferation and expansion of this population upon VLP treatment, which could also be dependent upon the presence of *A. tumefaciens* components from the infiltration process. To address this question, splenocytes from B6 mice were stained with CFSE, then incubated with medium alone or 5 µg TSP of WT, Gag uninfiltrated (Gag), or VLP gradient fractions for a total of 20 hrs. The $CD11b^+$ population is clearly up-regulated in the VLP-treated samples, with somewhat intermediate phenotypes for Gag and WT samples (representative plots shown in Figure 16A). Proliferation was measured for the $CD11b^+$ population by analyzing reduction in CFSE fluorescence, represented by the gate in Figure 16A. The negative control and WT samples show no detectable proliferation of the $CD11b^+$ population (Figure 16A), which is also expressed as a percentage of total live cells in Figure 16B. However, Gag uninfiltrated and VLP samples both induced a significant reduction in CFSE fluorescence intensity in the $CD11b^+$ population that is much more profound in the VLP sample (Figure 16B). The significant difference between the Gag and VLP samples indicate that infiltration with *A. tumefaciens* contributes toward the VLP-induced proliferation, though Gag particles are capable of some stimulation on their own.

VLPs Stimulate a TLR-dependent, Th2 Immune Response

CD11b can be expressed by multiple cell types, and due to the non-specific interaction between VLPs and $CD11c^+$ DCs, further analysis of the specific macrophage population was pursued. Therefore, to better characterize the macrophage cytokine profile of this population, a secondary marker for splenic macrophages (F4/80) was included in assays below.

Macrophages can differentiate into a multitude of classes, each activated by different signals and each possessing unique immunological functions (Gordon, 2003; Martinez and Gordon, 2014; Mosser and Edwards, 2008). Based on the characteristics of plant-produced VLPs, two potential macrophage subsets were candidate targets: M1 and M2b (Martinez and Gordon, 2014; Mosser and Edwards, 2008). M1, or classically activated macrophages, are triggered by a combination of LPS and IFN-γ, while M2b macrophages are stimulated by immune complexes and TLR ligands, thus making either subset a potential target of the VLPs. These subsets can be distinguished by their cytokine profiles: M1 macrophages produce more IL-12 than IL-10, while M2b macrophage cytokine profile is precisely the opposite. Therefore, VLP and WT-stimulated B6 mouse splenocytes were analyzed for IL-10 and IL-12 expression. WT plant material elicited no detectable levels of either cytokine while VLPs stimulated primarily IL-10, though IL-12 expression was still significantly higher than in the WT sample (Figure 17A). This is indicative of M2b macrophage activation.

Macrophage cytokine production is known to skew CD4 responses toward either Th1 or Th2, which ultimately results in differential Ab isotype switching by B cells. Production of IL-10 by M2b macrophages is associated with a Th2 immune response, which predominantly elicits IgG1 Ab isotype switching, while IL-12 and M1 macrophages induce a Th1-dominanted response characterized by production of IgG2a (Martinez and Gordon, 2014; Snapper and Paul, 1987). To assess whether the M2b cytokine profile induces the expected IgG1 isotype switching, four to six-week-old wild-type C57BL/6 mice (n = 5) were immunized i.p. with VLPs and serum collected 14 dpi for analysis of serum IgG isotypes. Antigen-specific ELISA for the p24 subunit of Gag (Figure 17B) and the MPER peptide of dgp41 (Figure 17C) detected primarily IgG1 isotypes with minimal

IgG2a production. Therefore, the Ab isotype switching directly correlates with the M2b macrophage activation indicative of a Th2 biased immune response through production of IL-10.

TLR Signaling is Required for VLP Immunogenicity

In order to assess whether the TLR-dependent stimulation of M2b macrophages *ex vivo* translates to enhanced immunogenicity *in vivo*, wild-type C57BL/6 (B6) and TICAM -/- mice were immunized with VLPs or a mock injection of PBS via the i.p. route, and analyzed for antigen-specific serum IgG 14 dpi. Gag-specific responses to the p24 subunit are detectable in B6 mice but not TICAM -/- mice, resulting in a significant difference in Ab production (Figure 18A). Responses to the MPER peptide of dgp41 indicate a similar trend, though the Ab levels did not reach significance in any group after a single injection (Figure 18B). Therefore, it is clear that plant-produced HIV-1 VLPs induce antigen-specific Ab responses that are dependent upon TLR signaling through TICAM.

Discussion

VLPs are an attractive alternative to subunit vaccines and are considered to be a safer choice than live or attenuated viral vectors (Kushnir et al., 2012; Noad and Roy, 2003). In addition to a high safety profile, VLPs are highly immunogenic and plant-based production has successfully produced VLPs from a variety of human and veterinary infectious diseases [for extensive reviews see (Chen and Lai, 2013; Rybicki, 2009; Rybicki, 2010; Rybicki, 2014; Scotti and Rybicki, 2013; Yusibov et al., 2014)]. Plants offer some unique advantages over other production systems, including: speed to production, versatility of expression vectors, ease of scale, and most importantly, a lack for potential contaminating human pathogens (Egelkrout et al., 2012; Rybicki, 2009). A variety of HIV-1 antigens have been produced in plants (Horn et al., 2003; Matoba et al., 2009; Meyers et al., 2008; Rosales-Mendoza et al., 2012; Rosales-Mendoza et al., 2013; Scotti et al., 2009), including Gag/dgp41 VLPs used here (Kessans et al., 2013), which were shown to be immunogenic in mice (Kessans et al., 2016). The nature of plant-based protein expression involves the gram-negative *A. tumefaciens*, which delivers T-DNA to the plant

nuclei where a deconstructed TMV viral expression vector is utilized to amplify mRNA in the cytoplasm (Gleba et al., 2005; Marillonnet et al., 2004; Marillonnet et al., 2005). Therefore, this system offers a range of potential TLR ligands for activating the innate immune system (Kawai and Akira, 2007; Kawai and Akira, 2010; Takeda et al., 2003). While there is data collected on VLPs produced in baculovirus (Buonaguro et al., 2008; Buonaguro et al., 2006; Petrizzo et al., 2012; Pinto et al., 2005; Yan et al., 2005; Yang et al., 2004) and yeast (Tsunetsugu-Yokota et al., 2003) for innate immune activation, there was no available information on plant-produced VLPs or other antigens. Here it was demonstrated that plant-produced HIV-1 VLPs stimulate the innate immune system to activate a Th2 response in a TLR-dependent manner, and this signaling is necessary for immunogenicity. Thus, this finding promotes the use of plants for vaccine antigen production due to their natural adjuvancy through the TLR sensors.

Surprisingly, plant-produced VLPs infiltrated with mock or dgp41 expression vectors both stimulated all extracellular and endosomal TLRs while the Gag and WT/uninfiltrated, WT/mock, and WT/dgp41 samples did not induce a similar pattern (Figure 11). This suggests that both Gag VLPs and *A. tumefaciens*/TMV must be present in order for the PAMPs to localize to the 20% gradient fraction. Additionally, TLR2/6 was stimulated by WT/dgp41 in the absence of Gag VLPs (Figure 11A), and dgp41 is detectable in the gradient fraction (Figure 10). It is likely that dgp41 formed large aggregates or was incorporated into liposomes during the extraction process due to its hydrophobicity, thus allowing the protein to pass through the density gradient. Though the presence of flagellin (TLR5) and LPS (TLR4) was anticipated in the VLP preparations due to *A. tumefaciens*, and dsRNA (TLR3) and ssRNA (TLR7) due to the replication of the TMV vector, the stimulation of the remaining TLRs was unexpected. Nonetheless, it is possible for each of the remaining PAMPs to be present in the plant tissue. For instance, TLR2 and TLR4 ligands have been found in minimally processed vegetables (Erridge, 2011a; Erridge, 2011b), suggesting *N. benthamiana* may also have similar contaminating byproducts. Additionally, after infiltration, the plants undergo varying stages of necrosis until the tissue dies. During this process, it is possible that some damaged plant DNA may end up in the cytoplasm, thus also allowing incorporation into budding Gag virions leading to activation of TLR9. Thus, it can be concluded that due to the lack

of stimulation by Gag VLPs in the absence of *A. tumefaciens* infiltration, this stimulation pattern is not an inherent property of HIV-1 VLPs. This is consistent with the TLR2/TLR4-independent innate response by baculovirus-produced HIV-1 Gag VLPs (Buonaguro et al., 2006) and the TLR2-dependent response from yeast-produced Gag VLPs, indicating a strong influence by the production method in determining the immune activation pathways.

Furthermore, data revealed that the enveloped VLPs are harboring RNA and inadvertently protecting it from nuclease digestion (Figure 12). This characteristic is unique to the VLPs because a WT extract lacking Gag contains RNA which is not resistant to nuclease digestion (Figure 12A). One of the functions of the Gag protein is to incorporate HIV-1 genomic ssRNA (Parent and Gudleski, 2011), and Gag VLPs are not only capable of incorporating cellular RNA species, but can also deliver functional mRNA to cells (Valley-Omar et al., 2011). However, future studies should address the functionality, if any, of the mRNA found in these VLPs. Stimulation of TLR3, 7 and 9 suggests that Gag/dgp41 VLPs can successfully deliver nucleic acids to the endosomal compartment (Figure 11B), despite the lack of a functional gp120, potentially implicating the VLPs are endocytosed non-specifically. The absence of activation by any of the WT samples, further supports the premise that VLPs must be present in order to encapsulate and deliver nucleic acids to the endosome, and infiltration with *A. tumefaciens* carrying a TMV vector can greatly enhance the level of mRNA incorporated, because Gag/uninfiltrated VLPs did not activate the nucleic acid sensors.

Stimulation of multiple TLR pathways indicates that the VLPs could be potent activators of innate immune cells, and many types of VLPs are known to induce innate responses through TLR-dependent mechanisms (Buonaguro et al., 2006; Deml et al., 2005; Lacasse et al., 2008; Lenz et al., 2001; Yan et al., 2005; Yang et al., 2004). Therefore, VLP were first tested for induction of differentiation of the human THP-1 monocytic cell line. THP-1 cells can be induced to differentiate into macrophages (Daigneault et al., 2010; Tsuchiya et al., 1982) and DCs (Berges et al., 2005), which are capable of antigen presentation (Sallusto and Lanzavecchia, 1994). Such differentiation can be assessed by expression of surface markers CD11b (macrophage) and CD11c [DC, (Rosmarin et al., 1989)]. Incubation of THP-1 cells with Gag/dgp41 VLPs induced a

preferential up-regulation of macrophage marker CD11b (Figure 13A), which is also accompanied by increased expression of the co-stimulatory factor CD40 (Figure 13B-C). Even though Gag/uninfiltrated VLPs do not activate any of the TLRs based on reporter assays, they do induce an intermediate phenotype for maturation of CD11b monocytes. Therefore, the Gag VLPs can induce an activation state in the absence of detectable TLR NFκB activity, though infiltration with *A. tumefaciens* greatly enhances this functionality. Additionally, THP-1 derived DCs can be detected in direct association with VLPs (Figure 13D) in addition to up-regulation of CD40 (Figure 13E) and CD86 (Figure 13F), but not CD80 (data not shown). Thus, VLPs can also induce DC maturation despite the biased induction of CD11b macrophages from immature monocytes. Additionally, VLP-treated THP-1 cells show increased phosphorylation of p38 MAP kinase within 24-48 hours (data not shown), which is known to be triggered by TLR pathways (Feng et al., 1999; Park et al., 2004). The CD11b bias resembles other stimulatory molecules, including all-trans retinoic acid [ATRA, (Cho et al., 2011)] and similar flavonoids from *Morus alba* (Kollar et al., 2015), both of which trigger a similar CD11b differentiation, which has also been at least partially attributed to stimulation of p38 kinase pathways (Kollar et al., 2015). The resemblance in differentiation of THP-1 towards CD11b monocytes by our plant-produced VLPs could indicate incorporation of a similarly acting compound(s) from *N. benthamiana*.

Interestingly, *ex vivo* stimulation of B6 splenocytes mirrors the activation phenotype seen with THP-1 cells (Figure 14C) with a shift towards a CD11b-dominant population and this stark increase in numbers was shown to be attributable to VLP-induced proliferation of these cells (Figure 16). The $CD11c^+$ DC population showed down-regulation of CD11c (Figure 14A), which is an indicator of DC activation (Winzler et al., 1997), in addition to the up-regulation of CD80 (Figure 14B). However, the activation of DCs was not specific to the VLPs, as WT/uninfiltrated samples induced a similar activation state, which is no dependent upon TLR signaling. Thus, potentially suggesting an alternative pathway is responsible for this phenotype. Others have shown that endotoxin-induced down-regulation of CD11c does not require MyD88, but is dependent upon TLR4 (Winzler et al., 1997), however, MyD88 -/- mice still have an impaired

ability to respond to endotoxin (Kawai et al., 1999). Therefore, future studies should address the role specifically of TLR4 in the DC activation shown in this study.

The up-regulation of CD11b is significant to note due to its stimulatory role in the response to sensing endotoxin (Ling et al., 2014; Perera et al., 2001), it is even implicated in direct binding to bacterial LPS (Wright et al., 1989). CD11b has been shown to be a key regulator in TLR responses (Han et al., 2010), and often displays distinct roles depending upon cell type. For instance, in DCs CD11b enhances TLR4-induced innate stimulation (Ling et al., 2014), but negatively regulates TLR9 (Bai et al., 2012). In contrast, CD11b is secreted by macrophages which sense a TLR9 PAMP (Kim et al., 2016), can act as a co-stimulatory molecule to enhance certain macrophage functions in response to LPS stimulation (Fan and Edgington, 1991), and is an important marker for phagocytosis (Aderem, 2003). Peritoneal $CD11b^+$ macrophages infiltrate the peritoneum in response to multiple exposures to LPS (Kim et al., 2009), and are capable of facilitating more rapid antigen clearance (Kataru et al., 2009). Therefore, CD11b could play a role in regulating the innate response to the VLPs, potentially enhancing phagocytosis and antigen presentation.

In this study, data showed that VLP-triggered activation of $CD11b^+$ cells is dependent upon both of the TLR adaptor proteins, TICAM and MyD88, but independent of the IFN-α/β receptor (Figure 14). The loss of CD11b up-regulation and cytokine expression when either TLR signaling adaptor protein is lost suggests that the VLPs are likely primarily stimulating TLR4 due to its ability to signal through both adaptors. It would be interesting to test whether TLR4 knockout mice have a similar loss in signaling comparable to the MyD88 and TICAM knockouts to further validate this hypothesis. Additionally, no loss in activation by the IFNAR -/- mice correlates well with unpublished data in which VLP treatment of THP-1 cells did not lead to production of detectable IFN-β mRNA when analyzed via quantitative RT-PCR (data not shown). Based on these findings, the VLP-induced CD11b up-regulation (Figure 13A & Figure 14C) and proliferation (Figure 16) is characteristic of described responses due to LPS exposure, and future studies would benefit from LPS removal assays to determine the significance of this correlation.

When taken together, the bias towards CD11b and CD40 up-regulation in the THP-1 cells and splenocytes should induce Th2 responses which result in B cell isotype switching to IgG1, 3, or 4 but not IgG2 (Fujieda et al., 1995; Hasbold et al., 1999; Pasare and Medzhitov, 2005). In the absence of CD40 signaling, Th2 responses are specifically impaired (Gardby et al., 2000). Additionally, CD40 is required to induce class switching (Jabara et al., 2009), and TLR signaling can up-regulate AID to initiate class switching in B cells (Pone et al., 2012). In support of this hypothesis, the $CD11b^{+}$ $F4/80^{+}$ macrophage population displayed a cytokine profile characterized by VLP-induced IL-10 Th2 cytokine production with lower, though detectable amounts of the Th1 cytokine IL-12 (Figure 17A). Thus, this data matches an alternative activation phenotype for M2b macrophages, which primarily recognize TLR ligands and immune complexes (Gordon, 2003; Martinez and Gordon, 2014; Mosser, 2003; Mosser and Edwards, 2008). Other types immune complexes have also been shown to elicit IL-10 through alternative activation of macrophages (Ronnelid et al., 2003; Tripp et al., 1995). The Th2 cytokine bias should result in class switching towards IgG1 and not IgG2 (Fujieda et al., 1995). Indeed, isotyping of VLP-injected mice showed a strong bias towards IgG1 with minimal, though detectable, antigen-specific IgG2a (Figure 17B-C), thus suggesting that the CD40-induced isotype switching may be relevant to VLP immune activation. LPS is known to be a potent inducer of CD40 expression in splenic DCs (Kaisho et al., 2002; Kaisho et al., 2001) and peritoneal macrophages (Hoebe et al., 2003). Therefore, it is possible that incorporation of LPS into the VLP envelope during plant infiltration is primarily responsible for the activation of innate immunity. The lack of Ab production in TICAM -/- mice further indicates TLR signaling through TLR3 or TLR4 is likely the primary target of VLP innate activation (Figure 18). Endotoxin induction of a Th2 response can occur through both MyD88 and TICAM pathways (Hoebe et al., 2003; Kaisho et al., 2002; Kaisho et al., 2001; Kawai et al., 1999). Indeed, it would be interesting in future work to address the requirement for CD40 and TLR4 in VLP-induced innate immune activation and Ab responses. Additionally, it is interesting to note that Th2 responses are not regulated by IFN (Mosmann and Coffman, 1989; Snapper and Paul, 1987), thus the data showing no loss of activation in the IFNAR -/- mice further substantiates the Th2-bias.

Furthermore, it is known that T-independent antigens activate B cells directly and do not require TLR signaling (Nemazee et al., 2006), while T-dependent antigens do require TLRs for Ab production (Pasare and Medzhitov, 2005). Long-lived Ab responses require TLR4 and TLR2 signaling and memory cell differentiation (Nemazee et al., 2006). Furthermore, T-dependent antigens not only require TLR signaling in DCs to induce maturation and activate T helper cell responses, primarily controlled through CD40/CD40L interactions (Fujieda et al., 1995; Gardby et al., 2000; Grewal and Flavell, 1998; Hasbold et al., 1999; Schonbeck and Libby, 2001), but B cells must also have functional TLR signaling to initiate Ab production (Pasare and Medzhitov, 2005). Therefore, the lack of Ab production in the TICAM -/- mice may not only be due to the reduced innate immune activation seen in Figure 14, but may also be a result of dysfunctional B cell TLR signals. It is important to determine if plant-produced VLPs are T-independent or T-dependent antigens, because many immune complexes are T-independent, meaning they can stimulate B cell receptors (BCRs) and TLRs simultaneously, thus bypassing the need for CD4 T cell help (Medzhitov, 2007). However, the up-regulation of CD40 and the Th2 cytokine profile of the macrophage population indicates that CD4 T cell help may be critical for these particular VLPs (Figure 17A).

In this study, a TLR-dependent activation of macrophages was shown to result in a Th2 cytokine response which affects B cell isotype switching in response to plant-produced HIV-1 VLPs. This proposes that plants offer a unique platform for protein production due to the inherent adjuvancy provided by plant proteins, *A. tumefaciens*, and viral-based expression vectors. Overall, the TLR-dependent immune activation here could be supplemented by choosing specific adjuvants for vaccine formulation to either enhance the VLP effects using TLR4-dependent adjuvants such as monophosphoryl lipid A (Mata-Haro et al., 2007), or complement the VLP responses by using TLR-independent adjuvants such as Freund's, alum, or Ribi (Gavin et al., 2006; Nemazee et al., 2006). The results shown in this study, combined with the known ability of plant-produced VLPs to induce systemic and mucosal Ab responses (Kessans et al., 2016; Meyers et al., 2008) and their ability to boost T cell responses (Pillay et al., 2010), make plant-based vaccine production of HIV-1 VLPs an attractive platform.

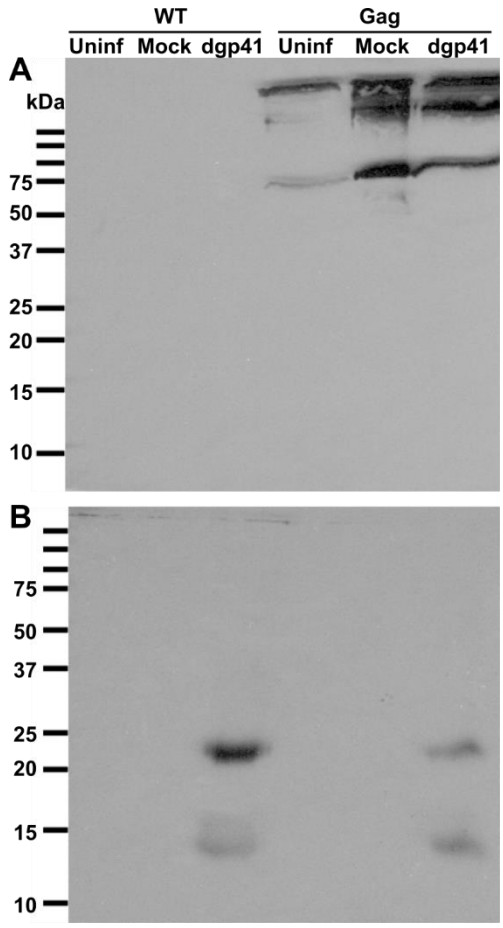

Figure 10 - Expression of Gag and Dgp41 in Gradient-purified Plant Extractions

N. benthamiana wild-type (WT) or Gag transgenics (Gag) were either left uninfiltrated or infiltrated with *A. tumefaciens* harboring an empty plasmid vector (mock) or a dgp41 expression vector (dgp41). The 20% Optiprep gradient fractions were analyzed for presence of Gag (A) or dgp41 (B) via immunoblot.

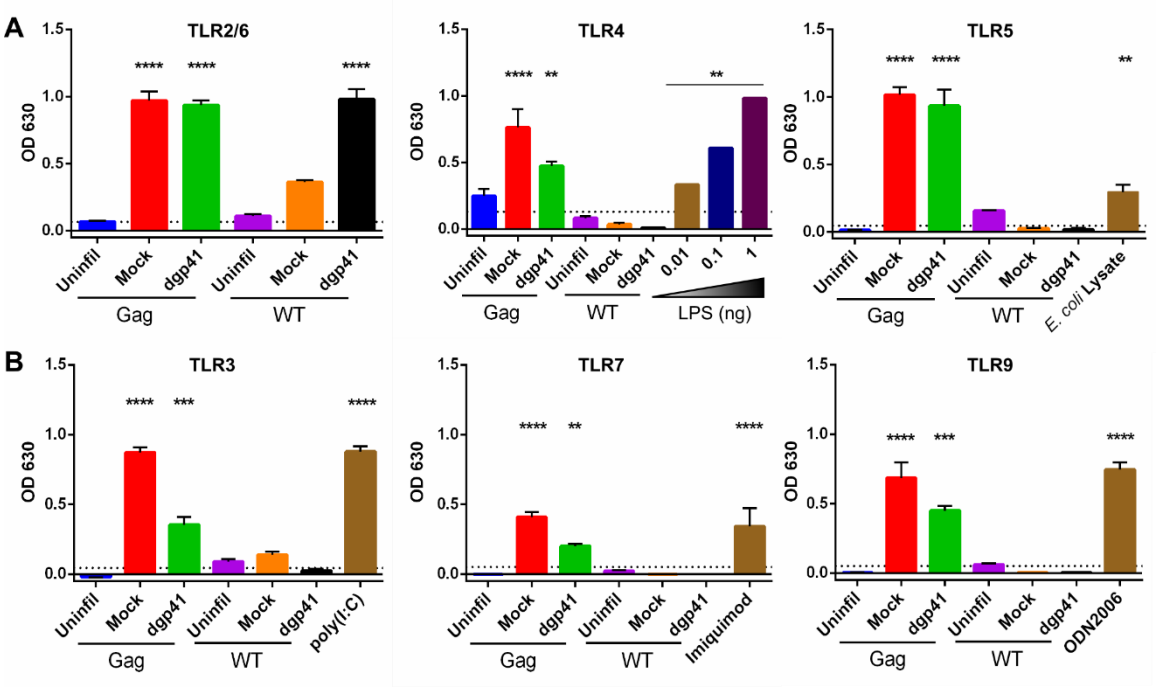

Figure 11 - 293T TLR Reporter Cell Stimulation with VLPs

Gag transgenic or wild-type (WT) *N. benthamiana* plants were either left uninfiltrated (uninfil), mock infiltrated (mock), or infiltrated with *A. tumefaciens* harboring an expression vector for the dgp41 protein (dgp41). Both cell surface (A) and endosomal (B) TLRs were treated for 24 hrs with 1 µg total soluble protein (TSP) from density gradient-purified VLPs or controls. SEAP reporter expression, under control of an NFκB promoter, was read as a colormetric output at OD 630 nm until saturation. Background levels from untreated negative controls was subtracted from reported values for each TLR cell line. 293T null cells lacking expression of any TLR were used as a negative control for non-specific activation. The average OD for null cells is represented by a dotted line in each graph. Data are means of three replicates shown with standard error. Statistical significance when compared to the WT uninfiltrated sample is indicated with an asterisk. (** $p < 0.01$; *** $p < 0.001$; **** $p < 0.0001$)

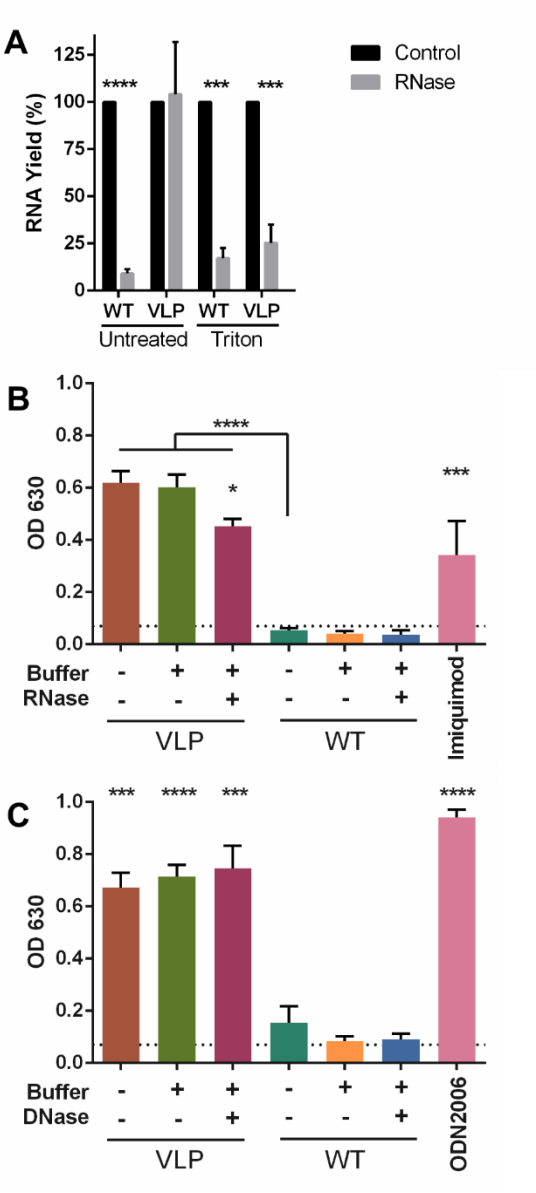

Figure 12 - Nuclease Treatment of VLP and WT Gradient Fractions

(A) VLP and WT 20% gradient fractions were treated with RNase A/T1 mix, with or without 1% Triton X-100, followed by TRIzol® extraction. The OD 260 nm was measured for RNA-containing TRIzol® fractions. Untreated controls were set to have 100% yield and the percent of RNA in the nuclease treated sample was calculated as percent of untreated samples. Data shown is from three independent replicates and asterisks indicate significant differences between control and RNase samples. (B-C) VLP or WT 20% gradient fractions were left untreated, treated with digestion buffers and heating cycles (Buffer group), or complete treatment with buffers and nuclease (RNase or DNase). RNase samples were incubated with TLR7 (B) and DNase samples with TLR9 (C) in a 293T cell SEAP reporter assay for NFκB activation. The dotted line represents background OD 630 nm of null 293T cells, which do not express any TLR. Asterisks over VLP samples indicate significance compared to WT uninfiltrated sample. The asterisk over VLP +RNase indicates significant difference from VLP untreated. Data are means of three replicates shown with standard error. (* $p < 0.05$; *** $p < 0.001$; **** $p < 0.0001$)

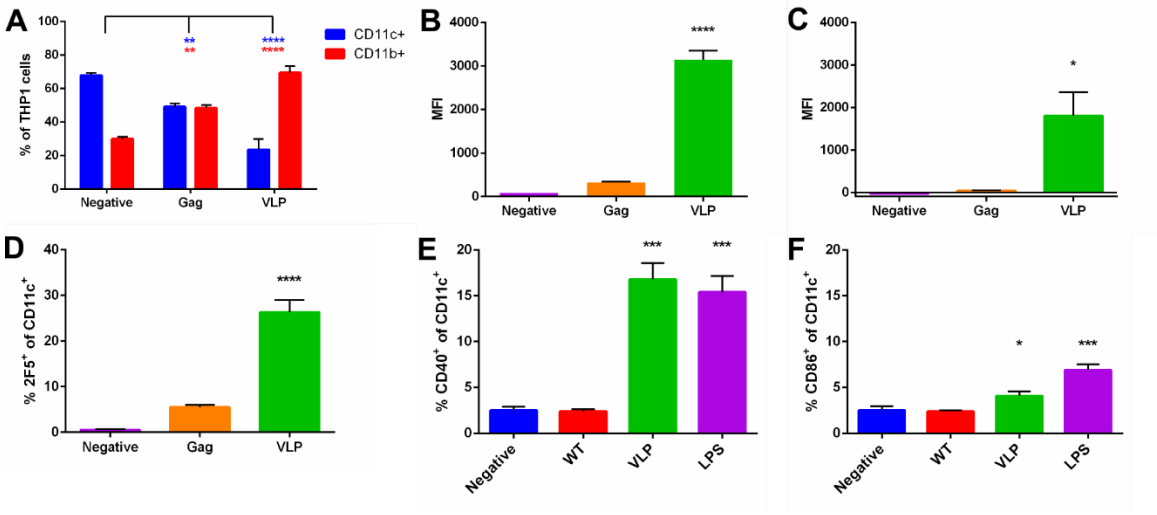

Figure 13 - Interaction Between THP-1 Cells and Plant-produced VLPs

(A) Expression of CD11c and CD11b surface markers on THP-1 cells exposed to gradient-purified Gag uninfiltrated (Gag) or Gag/dgp41 VLPs (VLP). Statistically significant differences between negative and treated samples are indicated by asterisks, which are color-coded to their respective cell surface marker. CD40 up-regulation on $CD11b^+$ (B) and $CD11c^+$ (C) cells is shown as mean fluorescence intensity (MFI) of CD40. (D) VLP attachment to THP-1-derived DCs was determined by flow cytometry after 2 hrs of exposure to splenocyte medium (Negative), Gag uninfiltrated (Gag), or Gag/dgp41 (VLP) 20% gradient fractions. 2F5 and a fluorescent anti-human IgG secondary were used to detect Gag/dgp41 VLPs on $CD11c^+$ cells and the Gag sample (i.e. no dgp41) is included as a negative control for 2F5 and anti-human IgG staining. (E-F) THP-1 cells were differentiated into DCs and exposed to either wild-type (WT) or VLP gradient fractions or an LPS control. Surface expression of CD40 (E) and CD86 (F), as measured by flow cytometry, is shown as percent of the $CD11c^+$ population. Data show the means for three independent measurements with standard error. Statistical significance from the negative control is indicated by an asterisk. (* $p < 0.05$; ** $p < 0.01$; *** $p < 0.001$; **** $p < 0.0001$)

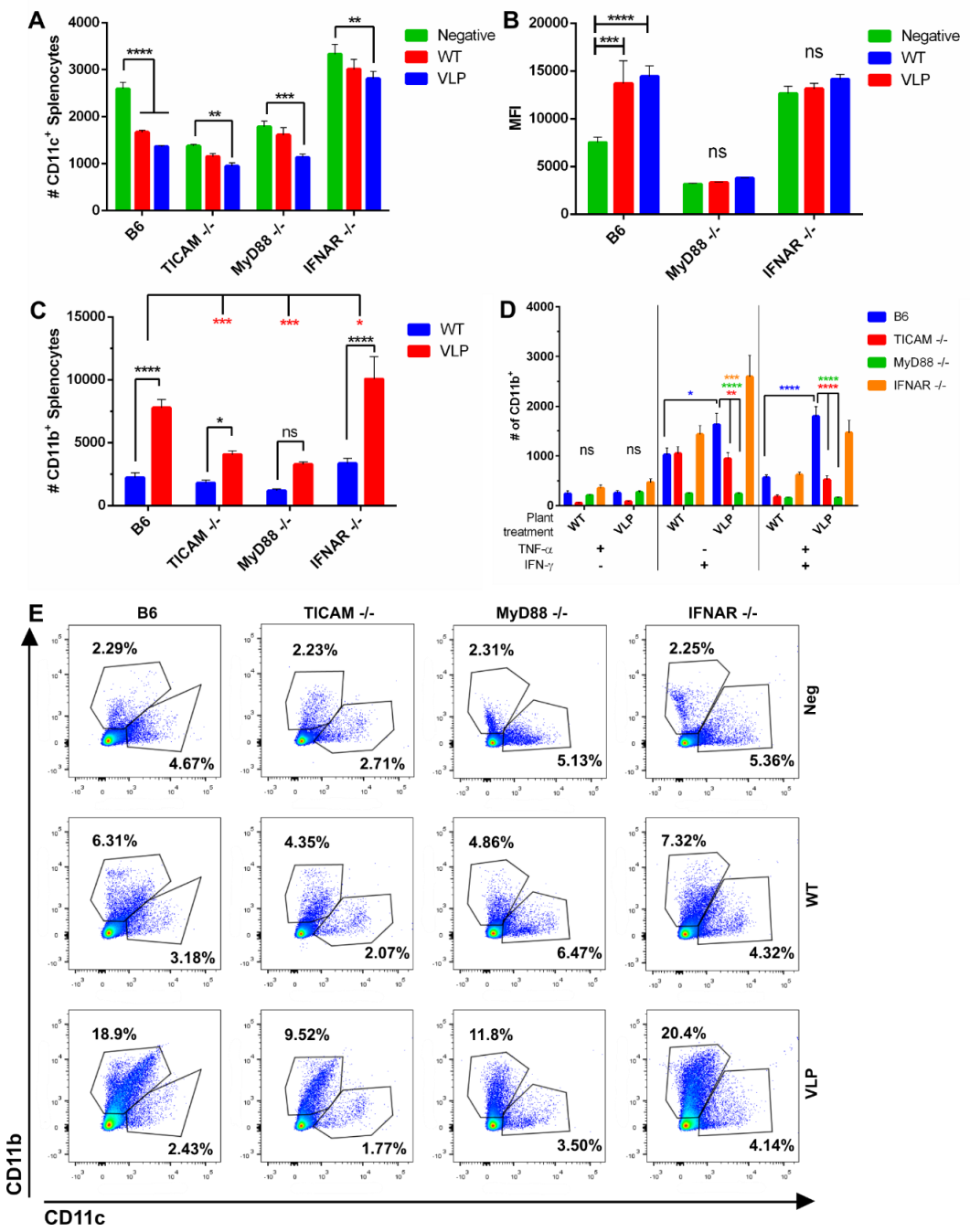

Figure 14 - DC and Macrophage Activation in Knockout Mice

Mouse splenocytes from wild-type C57BL/6 (B6, n = 4), TICAM -/- (n = 5), MyD88 -/- (n = 3), or IFNAR -/- (n = 3) were treated with either cell growth medium (negative), gradient-purified wild-type (WT) or VLP plant samples and analyzed by flow cytometry for expression of CD11c (A) and CD80 (B) to measure DC activation. Macrophage activation was measured by up-regulation of CD11b (C) and expression of TNF-α and IFN-γ cytokines (D). Representative flow cytometry plots for CD11b and CD11c populations are shown. Percent of total live splenocytes population is indicated for both CD11b and CD11c (E). (* $p < 0.05$; ** $p < 0.01$; *** $p < 0.001$; **** $p < 0.0001$)

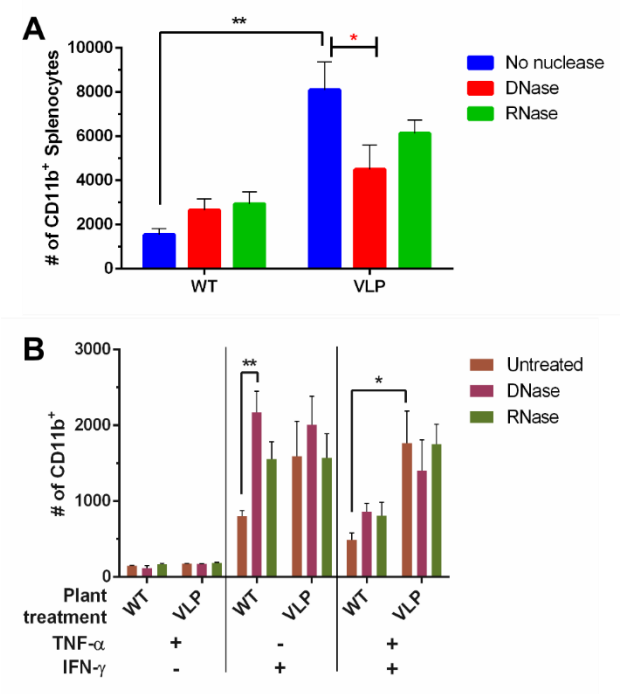

Figure 15 - Effect of Nuclease Treatment on VLP Stimulation of Macrophages

Gradient-purified wild-type (WT) or VLP plant material was either left untreated or exposed to DNase I or RNase A/T1 mix. Samples were then used to stimulate splenocytes from wild-type C57BL/6 mice (n = 3). Cells were analyzed by flow cytometry for up-regulation of CD11b (A). The $CD11b^+$ population was assessed for expression of TNF-α and IFN-γ (B). Statistical significance is indicated by asterisks. (* $p < 0.05$; ** $p < 0.01$)

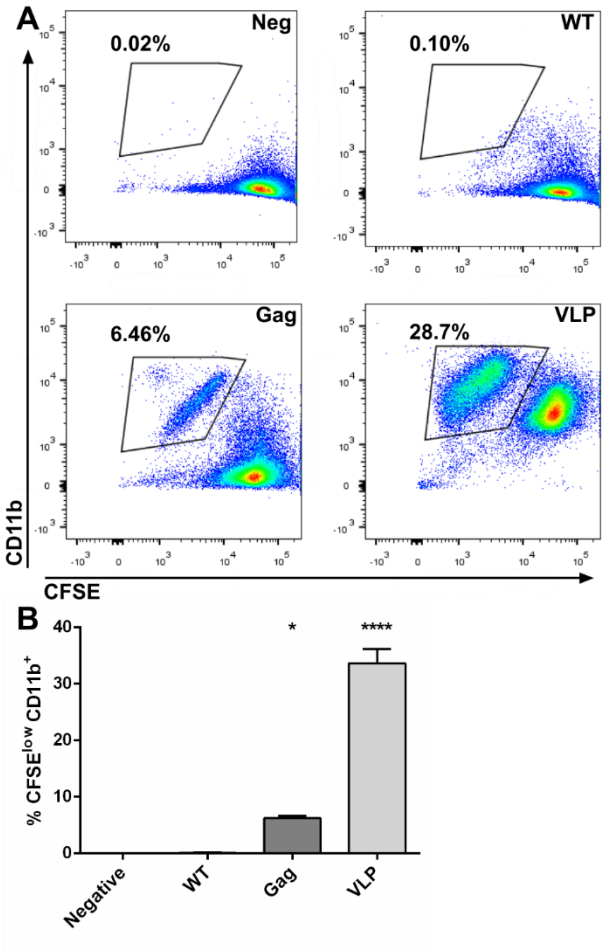

Figure 16 - Macrophage Proliferation Induced by VLP Stimulation

Mouse splenocytes from wild-type C57BL/6 mice (n = 3) were labeled with CFSE and exposed to medium (Negative/Neg), gradient-purified wild-type (WT), Gag uninfiltrated (Gag), or Gag/dgp41 VLP (VLP) plant material for 48 hrs. Surface expression of CD11b and fluorescence intensity of CFSE was analyzed by flow cytometry (A). A reduction in CFSE intensity was interpreted as cellular proliferation. The mean percentage of live cells which are $CFSE^{low}$ $CD11b^{+}$ (population indicated by the gate in A) is shown with statistical significance indicated by asterisks (B). (* $p < 0.05$; **** $p < 0.0001$)

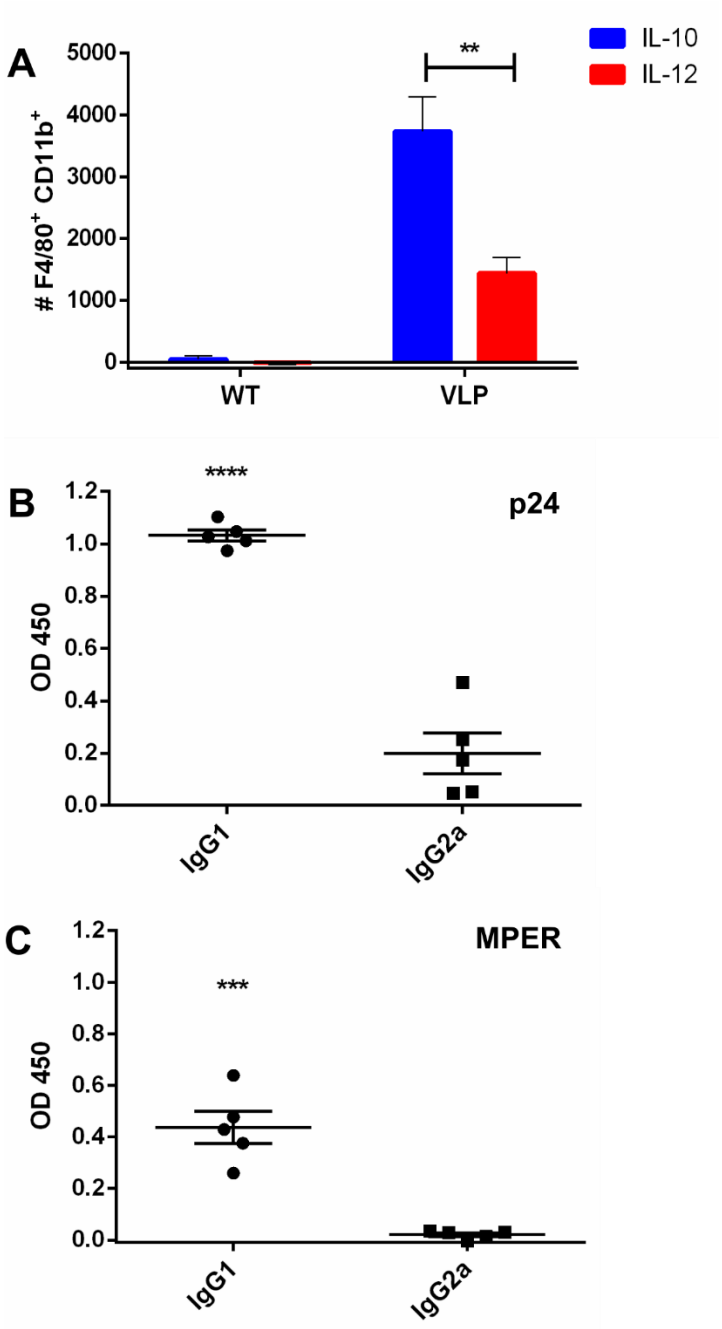

Figure 17 - Characterization of Macrophage Cytokine Profile and Antibody Isotypes

(A) Splenocytes from wild-type C57BL/6 mice (n = 3) were stimulated with gradient-purified wild-type (WT) or VLP samples and analyzed by flow cytometry. F4/80+ CD11b+ cells were selected by gating and assessed for expression of IL-10 or IL-12. (B-C) Mice immunized with VLP samples were tested by isotype-specific ELISA for presence of p24- (B) or MPER-specific (C) IgG1 or IgG2a. OD 450 nm values are shown for the lowest dilution (1:50) tested, and statistical significance is indicated by asterisks. (** $p < 0.01$; *** $p < 0.001$; *** $p < 0.0001$)

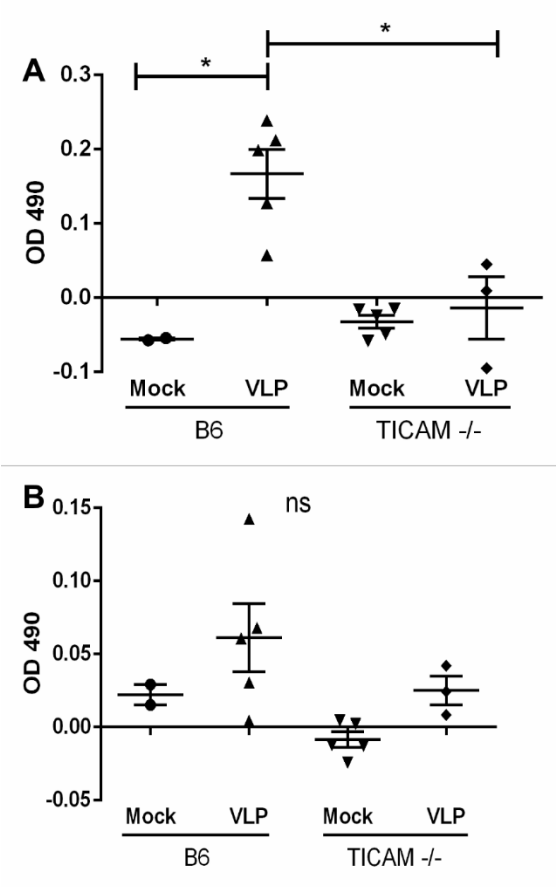

Figure 18 - TLR Signaling is Required for VLP Immunogenicity

Wild-type C57BL/6 (B6) or TICAM -/- mice were injected with 2 µg p24 and 0.75 µg MPER intraperitoneally without adjuvant (B6, n = 5; TICAM -/-, n = 3). Mock injections consisted of PBS for wild-type B6 (n = 2) and TICAM -/- mice (n = 5). Serum samples were collected 14 dpi and analyzed by ELISA to determine Ab responses specific for Gag (p24, A) or dgp41 (MPER, B). Raw OD 490 nm values are shown for the 1:50 dilution (lowest tested), and statistical significance is indicated by asterisks. (* $p < 0.05$)

Chapter 4

ACTIVATION OF ANTIVIRAL AND ER STRESS PATHWAYS BY NYVAC-KC VACCINIA VIRUS VECTORS EXPRESSING HIV-1 ANTIGENS GAG AND DGP41

Abstract

Due to the most successful HIV-1 clinical trial (RV144) utilizing a non-replicating canarypox vector (ALVAC) and a protein boosting system, much interest has been generated in the use of poxviral vectors to improve the modest 30% efficacy obtained in the RV144 trial. One such vector was generated by re-inserting two host-range genes, K1L and C7L, into the highly attenuated NYVAC vector to create NYVAC-KC, thus maintaining attenuation while restoring replication in human tissues. Here, we describe expression of HIV-1 Gag and deconstructed-gp41 (dgp41) in NYVAC-KC vectors resulting in cytotoxic effects and reduced growth of the viral vector. This phenotype is linked to activation of IRF3 and IFN-β through a TBK1-dependent pathway and the stimulation of the unfolded protein response (UPR) through PERK/eIF2α phosphorylation. Though the TBK1 inhibitor MRT67307 could abrogate IRF3 signaling and PERK phosphorylation, it could not prevent eIF2α activation or rescue viral growth. The activation of eIF2α is PKR-independent, suggesting an alternative upstream kinase is stimulated. Furthermore, re-insertion of 12 immune modulators in NYVAC+12-ZM96 and Cop-Gag vectors neither prevented IRF3 signaling nor rescued growth. However, when immunogenicity was compared in C57BL/6 mice, wild-type Cop-Gag induced higher Gag-specific CD8 T cell responses at lower doses than NYVAC-KC-Gag, suggesting that while the *in vitro* system indicates similar toxicity and IRF3 activation, there is an unidentified factor in the Cop genome which is compensating *in vivo*. Future studies will focus on identifying the gene(s) responsible for the enhanced immunogenicity and further characterize the IRF3/TBK1 signaling pathway. Such characterization would allow for the strategic development of poxvirus HIV-1 vaccine vectors and could be applied for use in other vaccines.

Introduction

Poxviruses have been of interest as vaccine vectors since their use in the eradication of smallpox (Wehrle, 1980). Many strains of VACV have been engineered primarily for enhanced immunogenicity while maintaining high safety profiles (Jacobs et al., 2009; Tartaglia et al., 1992a; Verardi et al., 2012). The canarypox vector, ALVAC, has been a major focus of HIV-1 vaccine research due to the modest success of the RV144 phase III clinical trial [Thai Trial, (Rerks-Ngarm et al., 2009)]. Avipoxviruses are naturally attenuated in human hosts, due to their evolution in avian systems, thus accounting for the high safety of this vector (Taylor and Paoletti, 1988; Taylor et al., 1988). In an effort to improve immunogenicity of the ALVAC vector, many variations of other VACV vaccine strains, namely modified vaccinia Ankara (MVA) and NYVAC, were tested for efficacy as HIV-1 vaccines (Esteban, 2014; Gomez et al., 2012a; Pantaleo et al., 2010). MVA is a non-replicating strain derived by passaging in chick embryo fibroblasts (CEFs) which resulted in a highly restricted host-range (McCurdy et al., 2004). NYVAC was derived from Copenhagen (Cop) by specifically deleting 18 ORFs and, similarly to MVA, lacks the ability to replicate in human cells (Tartaglia et al., 1992b). However, a now more widely accepted regime is the design replication-competent, highly attenuated HIV-1 viral vectors that cause little to no adverse side effects (Parks et al., 2013). It was recently shown that a replicating cytomegalovirus (CMV) vector was capable of clearing SIV infection through a mechanism involving non-canonical CD8 T cell responses recognizing antigen presented on MHC II (Hansen et al., 2013a; Hansen et al., 2013b). Replication competence was achieved for NYVAC by reintroducing two host-range genes, K1L and C7L, thereby generating NYVAC-KC which permits replication in humans while maintaining a high safety profile (Kibler et al., 2011; Quakkelaar et al., 2011). Therefore, this study proposes the use of NYVAC-KC as a replicating, yet attenuated, HIV-1 vaccine candidate. To this end, NYVAC-KC-Gag and NYVAC-KC-dgp41 were generated.

Gag contains many important CD8 T cell epitopes which are correlated with reduced viral load in HIV-infected patients (Jiao et al., 2006; Kiepiela et al., 2007; Ogg et al., 1998; Stephenson et al., 2012). The HIV-1 membrane protein gp41 contains the highly conserved membrane proximal external region (MPER), which is the target of the difficult-to-elicit broadly neutralizing

antibodies (bnAbs) such as 2F5, 4E10, and 10E8 (Huang et al., 2012; Purtscher et al., 1994; Zwick et al., 2001). Therefore, the use of these two vectors for an HIV-1 vaccine would effectively target both critical T cell epitopes and potentially protective Ab responses. However, during generation of the recombinant NYVAC-KC vectors, it was observed that the viruses grew to reduced titers, and in the case of NYVAC-KC-dgp41, had greatly reduced plaque sizes, suggesting toxicity to the VACV vector. Analysis of NYVAC-KC-Gag or NYVAC-KC-dgp41 infected cells using transmission electron microscopy (TEM) revealed large protein aggregates in the cytoplasm amongst visible signs of apoptosis. Therefore, it was hypothesized that the UPR may be triggered when VACV is expressing recombinant proteins.

The UPR is a critical regulator of protein expression and cell stress response mechanisms in a variety of eukaryotic organisms (Chakrabarti et al., 2011; Hetz, 2012; Schroder, 2006; Schroder and Kaufman, 2005). Recombinant protein expression is known to trigger the UPR in multiple expression systems, including mammalian cells (Du et al., 2013; Pybus et al., 2014), yeast (Čiplys et al., 2011; Mattanovich et al., 2004), and fungi (Ohno et al., 2011). Furthermore, the UPR has an increasingly understood role in immunity due to induction by viral infection in both mammalian (Bettigole and Glimcher, 2015; Janssens et al., 2014; Smith, 2014) and plant systems (Zhang et al., 2015; Zhang and Wang, 2012). In the event of non-recovery by the cell, integration of UPR signals results in apoptosis, generally through mitochondria-regulated pathways (Boyce and Yuan, 2006; Hetz, 2012; Holcik and Sonenberg, 2005; Li and Dewson, 2015; Marchi et al., 2014; Rainbolt et al., 2014) and will activate autophagy to clear the effected organelles or protein aggregates (Marchi et al., 2014; Ogata et al., 2006; Ron and Walter, 2007). There are two predominant branches of the UPR, one regulated through ATF6 and IRE-1, which are ER-stress specific, and the other controlled by PERK, which converges with multiple pathways at the phosphorylation of eIF2α for an integrated stress response (ISR), resulting in shutdown of translation (Donnelly et al., 2013; Harding et al., 2000; Okada et al., 2002). PERK serves multiple roles, including increasing ER/mitochondria connections to facilitate cross-talk and calcium transfer, and directly links eIF2α phosphorylation to stimulation of other transcription factors and induction of autophagy (Kouroku et al., 2007; Rainbolt et al., 2014). VACV encodes

an eIF2α homolog, K3L, which interferes with the activation of eIF2α (Carroll et al., 1993). Though K3L is present in NYVAC, the vector is known to induce apoptosis when expressing HIV-1 antigens Gag-Pol-Nef (GPN), a phenotype not characteristic of MVA expressing GPN (Gomez et al., 2007; Guerra et al., 2006; Najera et al., 2006). Many of the genes which were deleted from NYVAC are known immune modulators (Tartaglia et al., 1992b), including several inhibitors of apoptosis (Taylor and Barry, 2006). However, NYVAC-induced apoptosis was shown to be inhibited by re-insertion of C7L (Najera et al., 2006), suggesting an important, non-redundant function for inhibiting apoptosis by one or more of the other missing genes in NYVAC-KC expressing HIV-1 antigens.

Furthermore, multiple inhibitors of IFN signaling are absent in the NYVAC-KC genome (Smith et al., 2013), and signaling by vectors described here persists despite the antagonism provided by K1L and C7L (Meng et al., 2009), suggesting non-redundant mechanisms by one or more of the other deleted genes. Notably, a TBK1 inhibitor C6L is among the deleted genes in NYVAC-KC (Unterholzner et al., 2011), and is expressed by MVA (McCurdy et al., 2004). TBK1 is a downstream kinase of multiple antiviral signaling pathways (Zhao, 2013), but of significance here is its role in the downstream regulation of the stimulator of interferon genes (STING, also known as MPYS, MITA, and ERIS), whereby the activation of STING/TBK1 results in phosphorylation of the transcription factor IRF3 (Tanaka and Chen, 2012; Zhong et al., 2008). STING is an ER-resident transmembrane protein primarily known for its role in cytoplasmic DNA sensing, resulting in upregulation of type I interferons (IFNs) due to the ultimate activation of IRF3 (Abe et al., 2013; Burdette and Vance, 2013; Ishikawa and Barber, 2008; Ishikawa et al., 2009; Sun et al., 2009). Interestingly, MVA was shown to signal through cyclic GMP/AMP synthase (cGAS) production of cyclic di-nucleotides (diNTs) that interact with STING (Dai et al., 2014). STING also has a less well characterized role in the UPR that was recently shown to activate IRF3 through calcium signaling, and trigger autophagy as a negative regulation for STING activation (Liu et al., 2012; Mitzel et al., 2014; Petrasek et al., 2013; Rasmussen et al., 2011; Saitoh et al., 2009). The lack of C6L and the known induction of apoptosis by NYVAC-based HIV-

1 vectors thereby presents a potential mechanism for the toxicity and reduced titers seen with recombinant NYVAC-KC vectors, and is the subject of this study.

NYVAC-KC-dgp41 notably also had reduced plaque sizes, and the protein aggregates visualized with TEM are subjectively more predominant than infection with NYVAC-KC-Gag. The cytoplasmic tail (CTT) of gp41 contains lentiviral lytic peptides (LLPs), which are amphipathic helices that can disrupt membrane integrity, and are implicated in virally-induced apoptosis (Postler and Desrosiers, 2013). During HIV-1 infection, the CTT interacts with many host proteins, such as calmodulin (CaM), to enhance replication efficiency and minimize Env exposure at the cell surface to avoid immune detection (Santos da Silva et al., 2013). HIV-1 induced apoptosis is CaM-dependent and can be disrupted by specific mutations or deletions in the C-terminus of the cytoplasmic tail (Micoli et al., 2006; Newman et al., 2007; Sasaki et al., 1996). Calcium release from the ER during times of ER stress can result in the uptake of calcium by the mitochondria and activate pro-apoptotic proteins such as Bak and Bax resulting in cytochrome *c* release and inflammasome formation for caspase-dependent cell death (Marchi et al., 2014). STING also interacts with RIG-I and MAVS (mitochondria antiviral signaling protein), the primary site of NLRP3 (NOD-like receptor protein) inflammasome formation, and is also involved in the ER translocon for protein secretion through the Golgi (Ishikawa and Barber, 2008; Marchi et al., 2014). Activation of the NLRP3 inflammasome results in proteolytic cleavage of proIL-1β and proIL-18 for secretion and antiviral signaling (Marchi et al., 2014), and VACV encodes respective soluble receptors B15R (Spriggs et al., 1992) and C12L (Smith et al., 2000) to disrupt this signaling, both of which are present in NYVAC-KC and MVA. However, MVA was recently shown to activate the NLRP3 inflammasome through TLR2/6 and MDA-5 (Delaloye et al., 2009), implicating other poxvirus genes in the upstream prevention of inflammasome formation by MVA and NYVAC vectors. Thus, the induction of calcium signaling by expression of full-length CTT of gp41 in NYVAC-KC vectors could activate the STING-dependent ER stress pathway resulting in caspase-dependent cell death and inflammasome formation mediated by the mitochondria.

Truncation of the gp41 CTT is not a viable option to rescue cytotoxicity because such alterations change the conformation of the gp120 spike and induce differing neutralizing antibody

(nAb) profiles (Durham et al., 2012; Kalia et al., 2005; Kuwata et al., 2013; Vzorov et al., 2016), in addition to the requirement for full-length CTT for efficient virion incorporation (Murakami and Freed, 2000). Thus, full-length CTT is essential for the production of structurally accurate HIV-1 VLPs and understanding its interaction with the host system in viral vectors is an important avenue of study. This chapter describes the induction of toxic effects to both the cell and viral vector by NYVAC-KC-Gag and dgp41 vectors resulting in activation of the UPR and IRF3 through a TBK1-dependent mechanism. The activation of the UPR results in reduced immunogenicity *in vivo* compared to Cop vectors which contain all 18 deleted ORFs from NYVAC. However, expression of the TBK1 inhibitor C6L was not sufficient to rescue IRF3 activation. Therefore, it is likely there are redundant mechanisms by which the host senses NYVAC-KC vectors and further identification of the genes involved in abrogating this signaling should be pursued to enhance immunogenicity.

Materials and Methods

Plasmid Cloning

Gag and deconstructed-gp41 genes were derived from pTM 813 and pTM 816, respectively (described in Chapter 5), for insertion into the pTK-MCS plasmid under the synthetic early/late promoter. The Gag gene was amplified using primers oTM 864 (5'-TATA*CTCGAG*ATGGGAGCTAGAGC-3') and 865 (5'- TACA*CCCGGG*TTATTGAGAGGAAG-3') with AccuStart Taq DNA polymerase HiFi PCR kit (Quanta Biosciences) and ligated into TOPO pCR-2.1 vector (Invitrogen) and screened in DH5α *Escherichia coli*. Sequence was confirmed with M13F and M13R primers and the plasmid was denoted pTM 936. The added XhoI and XmaI sites (shown in italics) were then used to ligate Gag into pTK-MCS under the synthetic early/late promoter already present in the backbone. For addition of the dgp41 gene, primers oTM 866 (5'-TATA*GTCGAC*GGATCCGGTCGACC-3') and 867 (5'- TATA*GCGGCCGC*TTATTGCAAAGCAG-3') were used to amplify the gene plus the synthetic early/late promoter from pTM 816 for ligation into the TOPO vector, subsequently named pTM 926, and screened using DH5α *E. coli*. The added NotI and SalI sites (shown in italics) were used to ligate the synthetic early/late promoter

and dgp41 into the pTK-Gag plasmid with the promoters facing opposite directions. This plasmid was named pTK-Gag/dgp41 and further used for generating recombinant viruses.

In vivo Recombination

BSC-40 cells were maintained in DMEM (Corning Cellgro) with 5% FBS, gentamycin, and 2 mM L-glutamine. Simultaneous transfection/infection [*in vivo* recombination, IVR (Brandt and Jacobs, 2001; Kibler et al., 1997)] was performed with pTM 815 (Gag) and pTK-Gag/dgp41 and Cop-PGNR (Gyrase-PKR, GFP, neomycin resistance) to insert Gag and dgp41 into the vaccinia virus TK locus for negative selection using coumermycin (Cmr) sensitivity (White et al., 2011). 500 ng of plasmid DNA was transfected using Lipofectamine and Plus™ Reagent (Invitrogen) per manufacturer's protocol. This was immediately followed by infection with Cop-PGNR at an MOI = 0.01 in 35 mm^2 dishes of BSC-40 cells. Recombination was allowed to proceed for 24 hrs followed by addition of Cmr antibiotic (100 ng/mL). Cells were harvested and lysed at 48 hours post infection (hpi). The IVR was used to infect 100 mm^2 dishes of BSC-40 cells for selection of individual antibiotic-resistant plaques for subsequent expression screening. This process was repeated for multiple rounds of antibiotic selection before a >98% pure virus was isolated as measured by immunoplaque assay.

Generation of NYVAC-KC-Gag and NYVAC-KC-dgp41 is described in Chapter 5. NYVAC-C-KC (referred to as ZM96 in all figures and text) was previously described (Kibler et al., 2011) as a vector that expresses HIV-1 Gag-Pol-Nef (GPN) and gp120. NYVAC+12-C (referred to as +12-ZM96 throughout) also expresses GPN/gp120 in addition to containing the re-insertion of 12 genes between K1L and C7L and was a kind gift of Karen Kibler (Arizona State University). ZM96 refers to the HIV-1 isolate that matches the Gag gene present in the viral vectors.

Expression Screening

Individual antibiotic-resistant plaques were grown in 60 mm^2 dishes of BSC-40 cells to CPE and lysed with RIPA lysis buffer [1% NP40, 0.1% SDS, 0.5% sodium deoxycholate, 1X protease inhibitor cocktail III (Research Products International Corp., Prospect, IL), in 1X PBS

without calcium or magnesium (Corning)]. RIPA lysates were mixed with an equal volume of 2X SDS sample buffer (1X concentrations: 50 mM Tris-Cl pH 6.8, 2% SDS, 0.1% bromophenol blue, 10% glycerol, 100 mM β-mercaptoethanol). Cell lysates were screened using SDS-PAGE as previously described (Kessans et al., 2013). Briefly, boiled samples were run on 12% polyacrylamide gels under denaturing conditions, transferred to nitrocellulose membranes (Bio-Rad) and probed with either Gag or dgp41 antibodies and anti-rabbit or anti-human IgG-HRP secondaries, respectively. Proteins were detected via chemiluminescence (ImmunoCruz Luminol Reagent, Santa Cruz).

Immunoplaque Assays

Immunoplaque assays were performed in 6-well dishes by infecting BSC-40s with 50 pfu of individual plaques. Once plaques were visible the cells were fixed with 1:1 acetone:methanol for 30 min at -20° C, washed with PBS, then incubated with anti-p24 Gag polyclonal rabbit serum or 2F5 (obtained through the NIH AIDS Reagent Program, Division of AIDS, NIAID, NIH: from Dr. Hermann Katinger) at 1:1000 in 3% FBS-PBS. Secondary biotinylated antibodies for anti-rabbit IgG or anti-human IgG from Vectastain ABC Kits (Vector Laboratories, Inc.) were used for detection with DAB peroxidase substrate (Vector Laboratories, Inc.) per manufacturer's protocol. After counting positive plaques, cells were stained with Coomassie blue dye to count the number of negative plaques. Percentages were calculated by dividing positive plaques by total plaques per well. The plaque with the highest percentage of positives was used for further purification until a plaque with >98% purity was identified and used to grow stocks.

Virus Stocks

BHK-21 cells were maintained in MEM (Corning Cellgro) with 5% FBS, gentamycin, and 2 mM L-glutamine. The final Cop-Gag and Cop-VLP (Gag/dgp41) plaques with >98% purity determined by immunoplaque assay were grown to CPE in BHK-21 cells in a 60 mm^2 dish for the first passage (P1) stock. The P1 stock was titered in BSC-40s and used to infect five T150 flasks

of BHK-21 cells at an MOI = 0.01 for the P2 stock. Cells were harvested at CPE, subjected to freeze-thaw and sonication, then cell lysates were placed on a 36% sucrose pad and centrifuged at 22,000 rpm for 80 min at 4° C with an SW28 rotor to pellet virions. Purified virions were resuspended in 10 mM Tris-HCl pH 9.0, their titer determined in BSC-40s, and were stored in aliquots at -80° C until further use.

Antibodies

The following antibodies were used for protein detection where indicated: anti-p24 Gag polyclonal rabbit serum (Kessans et al., 2013); human anti-MPER 2F5 (AIDS Reagent Program and the kind gift of Morgane Bomsel); goat anti-human IgG-HRP (Sigma) for immunoblot; goat anti-rabbit IgG-HRP (Santa Cruz Biotechnology) for immunoblot; rabbit anti-IRF3-P S386 (Abcam); rabbit anti-eIF2α-P S51 (Abcam); rabbit anti-PKR-P T446 (Abcam); rabbit anti-PERK-P Y980 (Cell Signaling Technology); rabbit anti-TBK1/NAK-P S172 (Cell Signaling Technology); anti-E3L polyclonal rabbit serum (#1675, generated in the laboratory of Bertram Jacobs, Arizona State University); mouse anti-GAPDH (Santa Cruz Technology).

Transmission Electron Microscopy (TEM)

BSC-40 cells grown in T75 flasks were infected at an MOI = 5 and harvested by trypsinization 24 hpi. Cells were pelleted between all wash steps at 700 x*g* for 5 min at 4° C until embedded in agarose prior to secondary fixation. Pelleted cells were washed twice in 1X PBS (140 mM NaCl, 2 mM KCl, 10 mM Na_2HPO_4, 1 mM KH_2PO_4, pH 7.4). For primary fixation, cells were placed in 2% glutaraldehyde in PBS for 15 min at room temperature followed by a second incubation with fresh fixative for 1 hour at 4° C. Fixed cells were resuspended in 1% agarose and washed three times in PBS for 30 min each at room temperature. Cells were then fixed with 1% osmium tetroxide in PBS for 1 hour at room temperature followed by four 15-minute washes in water. A 0.2% uranyl acetate solution in water was used to stain en bloc overnight at 4° C followed by three 15-minute washes in water. An ethanol series from 20% to 100% (anhydrous)

was used for dehydration, increasing the ethanol concentration by 20% every 10 min with three incubations in anhydrous ethanol. Spurr's resin was gradually introduced through 4- to 8-hour incubations with 1:3, 1:1, and 3:1 ratios of resin:100% ethanol followed by three incubations in 100% resin. Cells were divided into several blocks of Spurr's resin and polymerized at 60° C for 36 hours. 70 nm sections were placed on formvar-coated copper slot grids and post-stained with 2% uranyl acetate and 3% Sato's lead citrate before imaging.

Viral Growth Curves

Single-step growth curves were performed in 35 mm^2 dishes of BSC-40 cells infected at an MOI = 5 and rocked for 1 hour at 37° C to allow viral entry. Cells were then washed three times with 1X PBS prior to adding growth medium. The 0 hpi well was harvested immediately and 24 hpi wells harvested in duplicate. Cells were scraped into medium and subjected to three rounds of freezing and thawing. For those analyses where intracellular and extracellular virions are titered separately, cells were pelleted at 1000 x*g* for 3 min and medium removed. Fresh medium was added to resuspend cells prior to freeze/thaw cycles to release virions. Virus was titered in BSC-40s for all growth curves. Multi-step growth curves were performed in the same manner as single-step curves, except that the beginning MOI = 0.01.

Chemical inhibitors were added directly to growth medium (where indicated) immediately after PBS washes at the following final concentrations: 2 μM MRT67307 (Sigma) or 10 μM W-7 (Santa Cruz Biotechnology). For experiments involving Vpu, 500 ng of the expression vector pTM 808 [obtained through the NIH AIDS Reagent Program, Division of AIDS, NIAID, NIH: pcDNA-Vphu from Dr. Stephan Bour and Dr. Klaus Strebel; (Nguyen et al., 2004)] was transfected into BSC-40 cells using X-tremeGENE 9 DNA Transfection Reagent (Roche Diagnostics) per manufacturer's protocol. Expression was allowed to proceed for 24 hrs before infection with VACV vectors and addition of fresh media, with inhibitors where indicated.

Detection of Phosphorylated Proteins via SDS-PAGE

THP-1 cells (4 x 10^5) were infected at the indicated MOIs by pelleting cells at 500 x*g* for 3 min at 4° C and resuspended in 100 µL cell growth medium with the indicated virus(es). Cells were incubated for 30 min at 37° C prior to addition to 1 mL of growth medium either with inhibitors where indicated at the following concentrations: 2 µM MRT67307 (Sigma), 10 µM W-7 (Santa Cruz Biotechnology), or 100 µg/mL rifampicin (Gold Biotechnology). AraC was added at 200 µg/mL 30 min prior to addition of virus for infection, then added fresh to growth medium after 30 min of incubation with virus. Experiments involving Vpu were transfected and infected as described above for growth curves.

Cells were harvested 18 hpi in RIPA lysis buffer with HALT™ Protease and Phosphatase Inhibitor Cocktail with 5 mM EDTA (Thermo Fisher Scientific) and mixed with equal volume of 2X SDS sample buffer as described above. Fresh BSC-40 cells were seeded in 35 mm^2 dishes upon first split and infected at the indicated MOIs for each experiment and harvested the same as THP-1 cells at 18 hpi. For THP-1 time courses, infection proceeded as above only in the presence of rifampicin, and samples were harvested as described at each indicated time point.

Cell lysates were analyzed via SDS-PAGE on 10% polyacrylamide gels transferred to nitrocellulose membranes and probed with antibodies in 3% BSA-TBST overnight at 4° C for phosphorylated IRF3, TBK1, and PKR or 1 hour at room temperature for phosphorylated PERK and eIF2α. E3L expression was used to ensure equal viral infectivity and also monitor viral replication stages in time courses. GAPDH expression is used as a total cell loading control for all experiments. Phosphorylated proteins were developed with SuperSignal™ West Dura Extended Duration Substrate (Thermo Fisher Scientific) and E3L and GAPDH were detected with Pierce™ ECL Western Blotting Substrate (Thermo Fisher Scientific).

Quantitative RT-PCR

THP-1 cells (4 x 10^5) were infected at an MOI = 5 with or without inhibitors as described above and harvested 18 hpi in NP-40 lysis buffer (20 mM HEPES pH 7.5, 120 mM KCl, 5 mM magnesium acetate, 1 mM DTT, 10% glycerol, 0.5% Nonidet P-40). RNA was extracted from cell

lysates using the RNeasy® Mini Kit (Qiagen). The cDNA conversion was performed using PrimeScript™ RT reagent Kit (TaKaRa Bio, Inc.) per manufacturer's protocol. The cDNA was analyzed for IFN-β and GAPDH mRNA levels using the PerfeCTa® SYBR® Green FastMix® for iQ™ (Quanta Biosciences) per manufacturer's protocol on a Bio-Rad CFX Connect™ Real-Time PCR Detection System. Human IFN-β primers: forward 5'- AAACTCATGAGCAGTCTGCA-3' and reverse 5'-AGGAGATCTTCAGTTTCGGAGG-3'. Human GAPDH primers: forward 5'-GCCTTCCGTGTCCCCACTG-3' and reverse 5'- CGCCTGCTTCACCACCTTC-3'. Results were normalized to GAPDH.

Mouse Immunization

All experiments were done with approval from the Arizona State University Institutional Care and Use Committee.

Four- to six-week-old C57BL/6 mice (bred at Arizona State University), were injected intraperitoneally (i.p.) or scarified at the base of the tail with indicated doses of NYVAC-KC-Gag (n = 3/dose), Cop-Gag (n = 4/dose), or Cop-VLP (n = 4/dose) diluted in 1X PBS, pH 7.4 (Corning Cellgro). Mock mice (n = 3 for scarification; n = 5 for i.p.) received equivalent volumes of 1X PBS via the same route. Mice were monitored for weight loss and other signs of illness to ensure vector safety. Spleens were collected 7-10 dpi for analysis of antigen-specific CD8 T cell responses.

Intracellular Cytokine Staining and Flow Cytometry

Spleens were harvested in Hank's medium (Corning Cellgro) and cells strained through a 0.7 µm filter for resuspension in complete RPMI [cRPMI: 10% FBS, penicillin (100 units/mL), streptomycin (100 µg/mL), 2 mM L-glutamine]. Red blood cells were lysed with ACK Lysing Buffer (Gibco) and splenocytes resuspended in cRPMI at a concentration of 2 x 10^7 cells/mL. Cells were plated at 1 x 10^6 cells/well and incubated for 5 hours in the presence of GolgiPlug™ (BD Biosciences) and 1 µg/mL of each of five different immunodominant ZM96 Gag CD8 epitopes (5 µg/mL total): LRSLYNTV (LRS8), VIPMFTAL (VIP8), AMQMLKDT (AMQ8), YSPVSILDI (YSP9),

EVKNWMTDTL (EVK10) (synthesized by GenScript and resuspended according to manufacturer's protocol). Cells were stained with fluorescently conjugated antibodies: CD3-APC (BD Biosciences), CD8-APC-Cy7 (BD Biosciences), TNFα-PE (BD Biosciences), and IFNγ-eFlour 450 (eBioscience). Fixation and permeabilization was performed with a Cytofix/Cytoperm™ Kit (BD Biosciences) with final resuspension in FACS Buffer (1% FBS in 1X PBS). Samples were analyzed by flow cytometry on an LSR Fortessa. Data was analyzed using FlowJo Data Analysis Software (FlowJo, LLC; Ashland, OR).

Statistics

All statistical analyses were performed in GraphPad Prism Software (GraphPad Prism Software Inc.; La Jolla, CA). All data were analyzed using a one-way or two-way ANOVA with correction for multiple comparisons. Significance cut-off was defined as $p < 0.05$.

Results

NYVAC-KC HIV-1 Vectors Display Cytotoxic Effects that Deter Viral Growth

During the generation of recombinant NYVAC-KC vectors, it was noted that NYVAC-KC-dgp41 plaques displayed reduced plaque size and grew to lower titers during virus stock preparations. Visualization with a transmission electron microscope (TEM) revealed what appear to be large protein aggregates or precipitates in the cytoplasm of NYVAC-KC-Gag or NYVAC-KC-dgp41 single and co-infected BSC-40 cells (Figure 19). In contrast, NYVAC-KC (Figure 19A), showed organized viral factories with characteristic intracellular mature virions (IVs, white arrows), immature virions with (white triangles) and without (black triangles) genome incorporated. However, upon infection with NYVAC-KC-Gag or dgp41-expressing vectors or co-infected cells (Figure 19B-D), few mature virions were visible, and factories are dominated by presumably "empty" shell virions ("E") and early crescent formations (black arrows). Overall the viral factories appear disorganized and are surrounded by large, dense areas of protein denoted here as cytoplasmic "junk" ("J") and malformed mitochondria ("M"). Mitochondria are a key regulator of apoptotic cell death (Li and Dewson, 2015), and their malformation visualized with

TEM potentially indicates that infection with the NYVAC-KC-Gag and dgp41 vectors trigger mitochondrial stress leading to apoptosis. Intense vacuolization of the cytoplasm is also apparent in the micrographs, which could be indicative of autophagy. Autophagy can be induced in an effort to recover from ER stress, but can also be associated with cell death (Marchi et al., 2014; Ogata et al., 2006). Furthermore, NYVAC-KC-dgp41 infected cells display other hallmarks of apoptosis, notably nuclear condensation (see Chapter 5).

Upon discovery of the severe toxicity seen with TEM in NYVAC-KC vectors expressing Gag and dgp41, it was questioned whether this had a direct impact on viral growth in cell culture. To this end, BSC-40 cells were infected with NYVAC-KC-wild-type (WT, i.e. empty TK locus), -Gag, -dgp41, or co-infected with Gag/dgp41 vectors at an MOI = 5 per virus for a 24-hour single-step growth curve. Cells and growth medium were harvested separately to titer intracellular mature virions (IVs) and extracellular enveloped virions (EVs) separately. After a single round of growth, the Gag and dgp41 single or co-infections grew to significantly reduced titers for both IVs (Figure 20A) and EVs (Figure 20B). NYVAC-KC-Gag growth was reduced by approximately 1 log compared to WT while expression of dgp41 reduced growth by 2-3 logs. The extreme reduction in EVs suggests that viral spread may also be affected as this is the primary virion form responsible for spread in animals, though it accounts for less than 1% of the total virus production (Payne, 1980; Smith and Law, 2004). To assess any effect on viral spread, BSC-40 cells were infected with NYVAC-KC-WT, Gag, or dgp41 at an MOI = 0.01 and harvested 72 hpi. For this assay, medium and cells were harvested and titered together for total virion yield. Both NYVAC-KC-Gag and dgp41 vectors displayed significantly reduced viral spread by 1 log and 2 logs, respectively (**Figure 2C**). As these vectors are candidates for HIV-1 vaccine development, a reduction in viral spread, while enhancing safety, may also reduce vector immunogenicity. In order to prevent this phenotype *in vivo*, the signaling pathways involved in the observed toxicity must be identified.

NYVAC-KC HIV-1 Vectors Activate IRF3 and IFN-β Production

NYVAC-KC was specifically developed to replicate in human cells (Kibler et al., 2011), therefore, the human monocytic cell line, THP-1, was chosen for signaling assays. THP-1 cells

were infected at an MOI = 10 with NYVAC-KC-WT, Gag, dgp41, or an MOI = 5 of each of the Gag and dgp41 vectors in co-infections. Cell lysates were harvested at a late time post-infection (18 hours) due to the TEM images being taken at 24 hpi. All HIV-1 protein-expression vectors induced IRF3 phosphorylation (IRF3-P) while the WT vector did not (Figure 21A). E3L expression shows equal infectivity of each viral vector, suggesting the lack of IRF3 in the WT vector is not due to reduced growth. IRF3 is a primary transcription factor for type I interferons (IFNs), therefore the levels of mRNA for IFN-β in THP-1 virally-infected cells was assessed, and WR-ΔE3L served as a positive control for the assay. Infection with both the Gag and dgp41 vectors induced significantly higher IFN-β mRNA than the WT vector (Figure 21B). Interestingly, infection in the human HeLa cell line does not induce IRF3 activation (data not shown), suggesting an inherent difference in pathway components between these two cell lines.

IRF3 Activation Initiates Early and Persists Throughout Viral Infection

The phenotype visualized in the TEM closely resembled a known issue in VACV morphogenesis associated with palmitate deficiency for *de novo* fatty acid synthesis in the mitochondria (Greseth and Traktman, 2014), and the general malformation of the mitochondria suggested stress induced on this particular organelle may play a role. Therefore, in order to better characterize the stage of replication during which activation of IRF3 occurs, two inhibitors were utilized, to target different stages. AraC is a nucleotide analog inhibitor of DNA replication (Furth and Cohen, 1968), and the antibiotic rifampicin (Rif) is an inhibitor of VACV morphogenesis (Moss et al., 1969). By comparing results between these two extremes it is possible to delineate whether the stress occurs during entry, morphogenesis, or between these stages. Inhibition by AraC effectively prevented IRF3 phosphorylation and activation of a known up-stream kinase TBK1 (Figure 22A), however, Rif did not completely eliminate IRF3 activation (Figure 22B). Thus, DNA replication must occur, but the toxicity is not necessarily due to a hindrance of morphogenesis induced by Gag or dgp41 expression. In agreement with these results, supplementing fatty acid free BSA conjugated to palmitate in the cell growth medium did not inhibit IRF3 or increase viral growth (data not shown). This implicates a unique phenotype

associated with cytotoxic effects induced by expression of Gag and dgp41 during VACV growth, which is unrelated to fatty acid synthesis in the mitochondria.

The inhibition by AraC suggests that the activator of IRF3 does not inherently enter the cell with the virion, but must be produced *de novo*. To narrow down the stage of replication, THP-1 cells were harvested at multiple times post infection to individually assess each transition in replication: entry, uncoating, early/middle/late gene expression, morphogenesis/assembly, and viral release (0, 1, 3, 6, 9, 12, and 24 hpi, respectively). Infections were done in the presence of Rif to prevent virion spread to other cells, which would induce another round of gene expression and antiviral pathway stimulation. NYVAC-KC-dgp41 shows early TBK1 phosphorylation followed immediately by IRF3 phosphorylation which persists until the last time point (Figure 22C). Interestingly, expression kinetics for an early gene (E3L) is delayed in both NYVAC-KC-dgp41 (Figure 22C) and NYVAC-KC (Figure 22D), suggesting a natural attenuation for both viruses in this cell type, which may not be related to dgp41 expression, but perhaps to one or several of the 16 ORFs deleted during the generation of NYVAC.

Signaling Occurs Through PERK and TBK1

Due to the large protein aggregates/precipitates seen with TEM during NYVAC-KC-Gag and dgp41 infections, it was hypothesized that these could be due to ER stress. One canonical ER stress occurs through membrane proteins such as PERK, which results in phosphorylation of eIF2α and the shut-down of translation as an antiviral defense mechanism (Boyce and Yuan, 2006; Donnelly et al., 2013; Ron and Walter, 2007). Protein kinase R (PKR) can also act to phosphorylate eIF2α during sensing of dsRNA (Donnelly et al., 2013) and this is known to occur during VACV infection (Kibler et al., 1997), and is inhibited by the VACV E3L gene (Langland and Jacobs, 2004; Langland et al., 2006). VACV also encodes a homolog of eIF2α known as K3L, which re-directs phosphorylation away from eIF2α to prevent translational shutdown (Beattie et al., 1991; Carroll et al., 1993). Both K3L and E3L are present in NYVAC-KC. Therefore, BSC-40 cell lysates were analyzed for phosphorylation of PERK, PKR, and eIF2α at 18 hpi to assess activation of antiviral signaling and ER stress pathways. Infection with NYVAC-KC-Gag, dgp41, or

co-infection with Gag/dgp41 displayed increased eIF2α phosphorylation, which was not evident in WT infection (Figure 23A). Analysis of up-stream kinases PKR and PERK revealed that PKR was not activated in the NYVAC-KC vectors but was detectable in our positive control (Cmr-treated WR-GyrPKR). However, PERK was constitutively phosphorylated in BSC-40s, and was down-regulated by NYVAC-KC but not the Gag or dgp41-expressing vectors. This suggests that during recombinant gene expression, K3L is not sufficient to prevent activation of ER stress while E3L remains fully capable of preventing dsRNA-stimulated antiviral pathways.

Interestingly, ER stress can lead to IRF3 activation in cases involving calcium flux through a STING/TBK1-dependent pathway (Liu et al., 2012; Mitzel et al., 2014; Petrasek et al., 2013). Additionally, HeLa cells do not express STING while THP-1 cells do (Sun et al., 2009), thus we hypothesized that this difference may account for the lack of IRF3 signaling in HeLa cells by the NYVAC-KC-Gag and dgp41 vectors. Therefore, to determine whether the IRF3 activation was TBK1-dependent, a specific inhibitor of TBK1, MRT67307 (MRT), was used (Clark et al., 2011). THP-1 cells were infected with NYVAC-KC vectors with or without 2 μM MRT, then assessed 18 hpi for activation of IRF3, TBK1, and PERK (Figure 23B). MRT did not prevent TBK1 phosphorylation, but was capable of preventing downstream activation of IRF3 in both Gag and dgp41-infected cells. It also effectively prevented the activation of PERK in all infections. This suggests that in NYVAC-KC-Gag or dgp41 infections, ER stress and IRF3 activation are linked through the phosphorylation of TBK1.

Inhibition of TBK1, but not Calmodulin, can Prevent IRF3 Activation

As mentioned above, there is a known ER stress pathway which is dependent upon STING/TBK1 and is known to be activated during stressors involving calcium flux (Liu et al., 2012). HIV-1 infection is known to induce calcium flux through a CaM-dependent pathway (Sasaki et al., 1996), and this has, at least in part, been linked to the CTT of gp41 (Newman et al., 2007). Therefore, this led to the hypothesis that this pathway may be triggered by infection with a dgp41-expressing virus, which contains the full-length CTT. In order to determine if inhibition of either TBK1 or CaM can prevent IRF3 signaling and IFN-β production, THP-1 cells

were infected with NYVAC-KC-dgp41 with or without the TBK1 inhibitor, MRT, and the CaM antagonist, W-7, or the two in combination. Interestingly, MRT but not W-7 was capable of inhibiting IRF3 phosphorylation (Figure 24A) and significantly reducing IFN-β production (Figure 24B). The combination of MRT and W-7 resembled MRT alone. Furthermore, it is interesting to note that in the presence of W-7, IRF3-P and IFN-β appear to be up-regulated, suggesting an additional stress on the cells in the absence of CaM signaling.

HIV-1 Vpu cannot Inhibit ER Stress Pathways, but Increases VACV Protein Expression

To assess whether inhibition of IRF3 in THP-1 cells correlates with reduced ER stress signs, the same inhibitors were tested in BSC-40 cells for their ability to prevent activation of eIF2α and PERK. Surprisingly, neither MRT nor W-7 were able to inhibit eIF2α-P and may have even caused an increase in phosphorylation (Figure 25A). However, in the presence of MRT, with or without W-7, PERK phosphorylation was undetectable and the kinase source for eIF2α activation was not a result of PKR stimulation. HIV-1 Vpu protein is a potential inhibitor of IRF3, though there are conflicting reports of the true functionality of this role (Doehle et al., 2012a; Doehle et al., 2012b; Hotter et al., 2013; Manganaro et al., 2015; Park et al., 2014). Despite the few negative reports, the ability of Vpu to abrogate ER stress signaling by our VACV vectors was analyzed in BSC-40s. 24 hours prior to infection with NYVAC-KC-dgp41, Vpu was transfected into BSC-40s. Chemical inhibitors MRT, W-7, or both MRT/W-7 were added to growth medium upon infection, and cell lysates were analyzed 18 hpi for signs of ER stress activation. Vpu expression was not able to inhibit eIF2α or PERK phosphorylation. Additionally, the presence of MRT, with or without W-7, induced a noticeable increase in activation of eIF2α, while the PERK-P seemed to be a result of Vpu expression (Figure 25B). Despite the increased PERK activation, the presence of Vpu substantially increased VACV E3L expression from the untreated sample, potentially indicating that enhanced viral replication may be a side effect of Vpu co-expression. Viral vectors expressing Vpu are being pursued for co-expression with HIV-1 proteins for inhibition of IRF3.

TBK1 Inhibition can Partially Rescue Replication Kinetics, but not Growth

Due to the inhibition of IRF3-P and IFN-β production seen with the TBK1 inhibitor MRT, it was hypothesized that MRT might rescue viral kinetics and growth. THP-1 cells were infected with NYVAC-KC-dgp41 at an MOI = 5 and lysates harvested at the indicated time points to determine the stage at which E3L, an early VACV gene, is expressed. In the absence of MRT, E3L expression is not substantial until 12-24 hpi for either NYVAC-KC or NYVAC-KC-dgp41 (Figure 22C-D). However, in the presence of MRT, detectable E3L expression begins around 6 hpi (Figure 26A), indicating a marginal rescue of kinetics more closely resembling what would be expected of a wild-type VACV. In contrast, inhibition of TBK1 by MRT did not rescue growth to WT NYVAC-KC levels (Figure 26B). Quite surprisingly, W-7 was the only inhibitor to display a marginal enhancement of growth for NYVAC-KC-dgp41, though this is not statistically significant (Figure 26B). The results for W-7 contradict its inability to inhibit IRF3, eIF2α, or PERK phosphorylation or IFN-β production (Figure 24 & Figure 25). These contrasting results indicate there may be a more complex pathway involved in the cytotoxicity of HIV-1 Gag and dgp41 proteins.

Inhibition of IRF3 by VACV Immune Modulators

The NYVAC strain was originally derived from Cop by specifically deleting 18 open reading frames (ORFs), many of which are known immune modulators (Tartaglia et al., 1992b). NYVAC was subsequently engineered to replicate in human cells by re-introducing two host-range genes, K1L and C7L (Kibler et al., 2011). Thus, NYVAC-KC is still missing 16 ORFs, including C6L, a known TBK1 inhibitor (Unterholzner et al., 2011) and multiple genes responsible for inhibition of NFκB (Smith et al., 2013), another transcription factor involved in ER stress signal transduction. To broadly assess the ability of these genes to prevent IRF3 activation, two viruses were utilized, NYVAC-KC-ZM96-Gag and NYVAC+12-ZM96-Gag (kind gift of Karen Kibler), which has a re-insertion of a large genome fragment with the 12 genes between K1L and C7L that includes C6L and other inhibitors of NFκB activation (N1L, N2L, M2L, and C4L). Expression of these genes in NYVAC+12 was not sufficient to prevent IRF3 activation (Figure 27A), and did

not rescue growth to WT NYVAC-KC levels (Figure 27C). However, IRF3 activation can still be prevented by TBK1 inhibitor MRT with the NYVAC+12 vector, suggesting that C6L's interference with TBK1 does not preclude activation of this particular antiviral signaling pathway (Figure 27B). Furthermore, Cop-Gag infection results in IRF3 signaling (Figure 27A), despite the inclusion of all gene products deleted from NYVAC. Additionally, both Cop-Gag and Cop-VLP (Gag/dgp41 co-expressing vector) show reduced replication compared to WT Cop (Figure 27C). These results suggest that no Cop gene product is fully capable of interfering with the pathway *in vitro*. However, when Gag is co-expressed with dgp41 in the same vector, no IRF3 activation is evident but the virus still grows to reduced titers (Figure 27A & C). This implies co-expression of Gag and dgp41 can prevent the stimulation of the IRF3 antiviral pathway but may still result in ER stress, thus reducing growth. Additionally, NYVAC-KC-PGNR (Gyrase-PKR, neomycin resistance) does not result IRF3 activation, indicating that the stimulation of the pathway is not a result of merely any gene expression from the TK locus, but is specific to the HIV-1 antigen-expressing constructs (Figure 27A).

Toxicity by NYVAC-KC Vectors Reduces Immunogenicity in Mice

Due to IRF3 activation and reduced replication seen with Cop and NYVAC-KC vectors, immunogenicity was assessed in C57BL/6 mice in dose curves with Cop-Gag (n = 4/dose), Cop-VLP (n = 4/dose), and NYVAC-KC-Gag (n = 3/dose) vectors. Peak CD8 T cell response were analyzed 7-10 dpi for specificity to 5 immunodominant ZM96 Gag epitopes. Mice receiving NYVAC-KC-Gag displayed low CD8 responses, which did not reach significance even amongst the highest dose when administered intraperitoneally (Figure 28A). However, Cop-Gag and Cop-VLP were able to elicit an average Gag-specific response of 2.9% and 3.3% IFN-γ expressing CD8 T cells, respectively, after a single dose of 10^5 pfu. Increasing the dose to 10^7 pfu induced a higher peak CD8 T cell response to 5.0% (Cop-Gag) and 4.8% (Cop-VLP) IFN-γ^+ $CD8^+$ T cells in the spleen (Figure 28A). Despite the activation of IRF3 by Cop-Gag but not Cop-VLP, no large differences were detectable in their CD8 T cell responses, suggesting that this difference is not significant *in vivo*.

NYVAC-KC-Gag was also tested via scarification immunization route, as it is the primary method used in practice for VACV, and mice can tolerate higher doses of VACV via this route. C57BL/6 mice (n = 3/dose) were scarified at the base of the tail after hair removal with increasing doses of NYVAC-KC-Gag, and peak CD8 T cell responses in the spleen were analyzed 7-10 dpi. Responses were much higher using this route of immunization, with both 10^8 and 10^9 pfu eliciting 8.0% IFN-γ secreting, Gag-specific $CD8^+$ T cells (Figure 28B). Though these results are higher than Cop vectors administered i.p., NYVAC-KC-Gag required several log higher doses to achieve significant responses. However, despite the similarities with IRF3 activation and reduced growth *in vitro* between NYVAC-KC-Gag and Cop-Gag, the lower responses in NYVAC-KC-Gag infected mice indicates that one or more of the additional gene products in Cop, including C6L, may have a significant impact *in vivo*.

Discussion

The modest success of the RV144 clinical trial utilizing a non-replicating canarypox vector (ALVAC) generated interest in improving immunogenicity of the vaccine strategy by exploring different strains and modifications of poxvirus vectors. Many variations to the vaccine strains MVA and NYVAC have been tested for efficacy in animal models and a few human safety trials (Esteban, 2014; Garcia et al., 2011; Goepfert et al., 2011; Gomez et al., 2012a; Greenough et al., 2008). Though MVA and NYVAC are both non-replicating in human cells (McCurdy et al., 2004; Tartaglia et al., 1992b), they can induce robust T cell responses (Gomez et al., 2007; Mooij et al., 2008) which are polyfunctional (Harari et al., 2008; Harari et al., 2012; Precopio et al., 2007) and even detectable at mucosal sites (Perreau et al., 2011). However, the only known case of a viral vector capable of clearing an established SIV infection utilized a replicating cytomegalovirus (CMV) vector (Hansen et al., 2013a), thus emphasizing the important role that safe, yet replicating vectors could play in the pursuit of a more immunogenic and protective HIV-1 vaccine. Re-insertion of the K1L and C7L genes to NYVAC restored the ability to replicate in human cells while remaining heavily attenuated (Kibler et al., 2011), yet displaying improved

immunogenicity (Quakkelaar et al., 2011). Therefore, NYVAC-KC is of interest as a safe, immunogenic, and replicating HIV-1 vaccine candidate.

The generation of NYVAC-KC-Gag and NYVAC-KC-dgp41 revealed severe toxicity to the cells (Figure 19) and the viral vector itself (Figure 20). Signs of apoptosis and autophagy were apparent, especially in NYVAC-KC-dgp41 infected cells (Figure 20C). While NYVAC is known to induce apoptosis when expressing GPN (Gomez et al., 2007), inclusion of K1L and C7L was shown to reduce this by 2-fold (Kibler et al., 2011). Further direct measures of apoptosis are necessary in order to assess whether expression of dgp41 significantly increases cell death induced by NYVAC-KC. Not only does this affect vector growth *in vitro*, but the 1-2 log reduction in EV formation and lesser ability to spread could have a substantial impact on animal immunogenicity (Figure 20B-C). Indeed, NYVAC-KC-ZM96 (C-KC) is known to have limited spread compared to the mouse adapted VACV strain, WR (Kibler et al., 2011). Furthermore, the inclusion of GPN/gp120 in Cop, the parental strain of NYVAC, attenuates the virus by 1 log in a mouse model of pathogenicity (Kibler et al., 2011). This suggests one or more of the HIV-1 proteins expressed in those vectors is contributing to the attenuation, potentially through vector or cellular toxicity as seen with the vectors described in this study.

It was shown here that expression of Gag or dgp41 results in IRF3-P in THP-1 cells (Figure 21A), which led to significant up-regulation of IFN-β (Figure 21B). IRF3 activation corresponds exactly with the phenotype visualized under TEM (Figure 19), thus cellular stress pathways related to protein expression were assessed, as the additional HIV-1 antigen gene is the only difference between NYVAC-KC and the vaccine vectors.

ER stress can be triggered by PERK, ATF6, or IRE-1 activation as part of the UPR, which can ultimately lead to apoptosis (Boyce and Yuan, 2006; Chakrabarti et al., 2011; Hetz, 2012; Hussain et al., 2014; Ron and Walter, 2007). It is known that VACV-encoded K3L is an eIF2α homolog which is the downstream target of PERK (Carroll et al., 1993). However, another upstream sensor known as PKR can sense VACV-produced dsRNA, which is abrogated by expression of E3L (Kibler et al., 1997; Langland and Jacobs, 2004; Langland et al., 2006). Therefore, the phosphorylation of all three signaling components was assessed, and it was clear

that even though NYVAC-KC contains K3L, this is insufficient to prevent activation of PERK when recombinant HIV-1 proteins Gag and dgp41 are being expressed, though E3L expression is sufficient to preclude PKR activation (Figure 23A). Intriguingly, an ALVAC HIV-1 vaccine vector engineered to express VACV K3L and E3L displayed increased VLP production and reduced apoptosis in HeLa cells, though the vector was shown to signal through PKR (Fang et al., 2001). Thus, stimulation of an IRF3 pathway correlates exactly with the inability to prevent phosphorylation of the ER/cell stress regulator PERK and eIF2α (Figure 23A), and thereby offers an explanation for the large protein aggregates in the electron micrographs being indicative of UPR activation (Figure 19).

Another interesting point is that the TBK1 inhibitor could rescue PERK-P but did not prevent eIF2α-P, however, the activation was PKR-independent (Figure 25A). There are other upstream kinases for eIF2α which could be analyzed (de Haro et al., 1996; Donnelly et al., 2013), and it would be key to show that in PKR -/- cell lines or mice that antiviral signaling and growth cannot be rescued. Furthermore, inhibition of PERK-P did not rescue growth when using the TBK1 inhibitor, suggesting that multiple ER stress pathways are likely triggered. Namely, IRE-1 activation is known to trigger multiple signaling pathways, including mitogen-activated protein kinases (MAPK), caspases, and its primary target XBP1 can even act as an enhancer for IRF3 (Bettigole and Glimcher, 2015; Ron and Walter, 2007). It would be interesting to assess IRE-1 and its downstream effectors in the presence of the different inhibitors used in this study. Overall, this data implicates an ER stress pathway in the attenuation, reduced growth, and IFN sensitivity of NYVAC-KC vectors expressing GPN, Gag, or dgp41 antigens.

ER stress has also been linked to STING/IRF3 activation in several systems (Liu et al., 2012; Mitzel et al., 2014; Petrasek et al., 2013), including a calcium flux-dependent pathway (Liu et al., 2012). STING is an ER-resident cytoplasmic DNA sensor which signals through TBK1 to stimulate IRF3 resulting in IFN-stimulated gene (ISG) expression, including IFN-β (Burdette and Vance, 2013; Ishikawa and Barber, 2008; Ishikawa et al., 2009; Sun et al., 2009; Tanaka and Chen, 2012; Zhong et al., 2008). Interestingly, the CTT of dgp41 contains LLPs which have been linked to CaM-dependent calcium flux during HIV-1 infection, and can be prevented by specific

point mutations in the LLPs or the CaM antagonist W-7 (Micoli et al., 2006; Sasaki et al., 1996). HIV-1 also evolved to inhibit the activity of IRF3 with the Vpu, which is known to interfere with IRF3, potentially through targeting it for degradation (Doehle et al., 2012a; Doehle et al., 2012b; Park et al., 2014), thus suggesting that *in vivo* this pathway can have adverse antiviral effects for HIV-1 replication.

Activation of IRF3 by NYVAC-KC-Gag and -dgp41 was inhibited by a TBK1-specific inhibitor, MRT67307 (Figure 23B & Figure 24A), which effectively prevented IFN-β production (Figure 24B). However, this could not be linked to CaM signaling because the CaM antagonist W-7 did not prevent IRF3 or PERK activation (Figure 24A). This suggests that while the pathway utilizes the TBK1 adaptor protein for IRF3 activation and could still be linked to STING and calcium flux, the CaM-dependent apoptosis known to be induced by the CTT of gp41 may not be responsible for the phenotype of these vectors. Consistent with this hypothesis, co-expression of Vpu in NYVAC-KC-dgp41 infected cells did not substantially impact eIF2α-P and actually increased PERK-P (Figure 25B), likely due to the added protein production stress on the ER from transfection of an expression vector. However, expression of Vpu seemingly increases VACV E3L expression, implying that this protein has beneficial effects to the viral vector, despite the PERK phosphorylation (Figure 25B). It would be interesting to express Vpu in a viral vector with Gag or dgp41 to assess the ability to preclude IRF3 activity in THP-1 cells and the effect on immunogenicity *in vivo*. Furthermore, none of the inhibitors were capable of rescuing growth (Figure 26B) regardless of their interaction with IRF3 and PERK, suggesting alternative pathways are also activated. Future studies would benefit from genetic knockouts for TBK1, IRF3, and STING to more stringently identify the reliance of IRF3 activation on this pathway.

Intriguingly, none of the 12 genes inserted to generate NYVAC+12-ZM96 were capable of abrogating signaling (Figure 27A). This implies that inhibition of TBK1 by C6L and N1L, NFκB by K1L, IRF3 by N2L, MAPK/ERK by M2L, and apoptosis by C7L and N1L was insufficient to rescue the phenotype, implying non-redundant mechanisms of inhibition by other proteins outside this region (see Figure 29 for an overview of the proteins and pathway interactions). Of interest are two genes which are deleted from both MVA and NYVAC, B13R and B14R. B13R is a viral

serine protease inhibitor (serpin) that serves as a pan-caspase inhibitor (Dobbelstein and Shenk, 1996; Kettle et al., 1997; Macen et al., 1996), and has been suggested as the most potent of the poxvirus anti-apoptotic proteins (Veyer et al., 2014). Caspase cascades can be a result of both intrinsic and extrinsinc death receptor stimuli and are critical executors for inflammasomes and the mitochondria-regulated cell death pathway (Duprez et al., 2009). MVA was shown to stimulate the inflammasome through a TLR2/6-dependent pathway (Delaloye et al., 2009), however, the induction of apoptosis by MVA is cell-specific. MVA and NYVAC both induce apoptosis in monocyte-derived dendritic cells (MDDCs), similar to the THP-1 cell line, but only NYVAC results in apoptosis in HeLa cells (Guerra et al., 2006), a phenotype prevented by expression of C7L (Najera et al., 2006). However, C7L is present in NYVAC-KC, and N1L was introduced in NYVAC+12, and thus neither can account for the results shown here. In support of this, analysis of MDDCs revealed differential up-regulation of genes when compared to HeLa cells (Guerra et al., 2007), suggesting cell-specific pathways are involved. Many of the up-regulated genes implicate inflammasome formation and TNF/Fas-mediated apoptosis, which relies on caspases (Duprez et al., 2009), and is the primary apoptotic pathway induced by HIV-1 (Micoli et al., 2006; Sasaki et al., 1996). The soluble IL-1 receptors B15R and C12L act downstream of the inflammasome, thus would not rescue an infected cell from apoptosis, but merely prevent signaling to surrounding cells, thus accounting for their inability to rescue signaling in these assays. Taken together, this data suggests a role for B13R in the inhibition of apoptosis and inflammasome production of IL-1β and IL-18 in caspase-dependent cell death (Figure 29). If the cell death is indeed caspase-dependent, then this implies an alternative apoptotic pathway than the CaM-dependent apoptosis induced by gp41, and thus explains why W-7 could not rescue growth (Figure 27B). To confirm this hypothesis, re-insertion of B13R to NYVAC-KC vectors and/or the use of a pan-caspase inhibitor should be pursued to determine the importance of this pathway in the phenotype presented here.

The absence of IRF3 signaling in HeLa cells contrasted by potent stimulation in MDDCs described above and in agreement with data presented here, is best explained by the difference in STING expression (Sun et al., 2009). Indeed, MVA infection results in activation of a

cGAS/STING-dependent pathway (Dai et al., 2014), thus analysis of NYVAC-KC vectors in STING knockout cell lines is being pursued in an effort to confirm a similar pathway. The activation of STING is known to activate both NFκB and IRF3 pathways (Ishikawa and Barber, 2008), and in cases of ER stress involving calcium flux, STING was shown to regulate the activation of IRF3 in response to these stressors (Liu et al., 2012). STING is also implicated in regulation of the exocytosis pathway from the ER due to its association with the translocon (Ishikawa and Barber, 2008), thus providing a potential physical link in regulation of ER stress pathways, though this has not yet been fully delineated. STING's activation of NFκB is prudent to data shown here because abrogating TBK1/IRF3 signaling does not rescue growth (Figure 26B), and NYVAC+12-ZM96 still induced IRF3 signaling (Figure 27A), despite the inclusion of C6L and N1L, which inhibit TBK1 (DiPerna et al., 2004; Unterholzner et al., 2011), and N2L, a nuclear inhibitor of IRF3 (Ferguson et al., 2013). This is further substantiated by MVA's activation of STING/cGAS (Dai et al., 2014), because MVA also expresses C6L and N2L, suggesting neither of these proteins are sufficient to inhibit this pathway. B14R is the most likely protein outside of the region re-inserted into NYVAC+12 to be necessary to inhibit STING downstream effector functions (Figure 29).

B14R is a specific inhibitor of the IKKα/β complex responsible for degradation of IκBα to activate NFκB (Chen et al., 2008; Graham et al., 2008), and this complex has also been shown to stimulate TBK1 through TLR and TNF receptor signal cascades (Clark et al., 2011). Thus, in the presence of MRT, TBK1 phosphorylation can still occur through the IKK complex, but downstream activation of IRF3 would be inhibited, in agreement with Figure 24. Furthermore, MRT and C6L/N1L/N2L expression would have no effect on NFκB activation, thus potentially explaining the inability to rescue growth. Interestingly, MRT can still prevent activation of IRF3 in NYVAC+12-ZM96 (Figure 27B), suggesting that the pathway is still reliant on TBK1 and perhaps the VACV-encoded inhibitors are insufficient to prevent it, or there is a novel role for B14R in the cross-talk with the IKK complex and IRF3.

Furthermore, STING induces autophagy as a negative regulation mechanism to prevent prolonged signaling (Mitzel et al., 2014; Saitoh et al., 2009). When considered along with the

ability for PERK/eIF2α to induce autophagy (Kouroku et al., 2007), and the inhibition of PERK phosphorylation by MRT treatment (Figure 24A), this provides a mechanism linking STING and PERK activation to the visible signs of autophagy and apoptosis seen with TEM (Figure 19). Additionally, STING is known to interact with RIG-I at the ER-mitochondria interface (Ishikawa and Barber, 2008), where assembly with MAVS provides a plausible platform for inflammasome formation (Marchi et al., 2014). It would be interesting to assess inflammasome activation by NYVAC-KC HIV-1 vectors and determine whether they show a similar reliance on TLR2/6 as shown for MVA (Delaloye et al., 2009), because both viruses have deleted B13R and B14R genes. Therefore, B14R should be assessed alongside B13R for independent or cooperative inhibition of STING and caspase-dependent apoptosis/inflammasome formation.

Surprisingly, even expression of all NYVAC-deleted genes in Cop-Gag did not preclude IRF3 signaling (Figure 27A). There is a little characterized pathway involving cyclophilin A (CYPA) in which newly synthesized p55 capsid protein engages CYPA to activate IRF3 in dendritic cells (Manel et al., 2010), though this pathway has been suggested to be an evasion mechanism to avoid detection by cGAS during HIV-1 entry and replication and the subsequent activation of STING (Lahaye et al., 2013; Rasaiyaah et al., 2013). Interestingly, co-expression of Gag and dgp41 in Cop-VLP does not display the same IRF3 activation though it has limited growth compared to WT (Figure 27), thereby implicating that interaction between gp41 and the newly synthesized Gag protein may abrogate its interaction with CYPA and prevent activation of IRF3. Thus, it is possible that even in the presence of VACV-encoded inhibitors, these vectors could trigger an alternative antiviral pathway through CYPA, thus activating IRF3 independently of TBK1 resulting in antiviral signaling and reduced growth. Therefore, it is necessary to generate knockout cell lines of STING, cGAS, and CYPA to assess the individual contributions to IRF3 activation in the NYVAC-KC HIV-1 vectors.

Interestingly, Cop-Gag and Cop-VLP induced higher Gag-specific CD8 T cell responses at lower doses than NYVAC-KC-Gag (Figure 28A). This suggests that while Cop-Gag, Cop-VLP, and NYVAC-KC-Gag all display reduced growth in BSC-40s (Figure 27C), Cop vectors have an advantage *in vivo* which allows them to compensate and generate higher responses, despite the

similar activation of IRF3 seen *in vitro*. Furthermore, this offers a unique opportunity to analyze the effect of these pathways on immunogenicity of the viral vectors by directly comparing CD8 T cell responses to Gag in knockout mouse strains for STING, cGAS, and CYPA. It would be hypothesized that if this pathway is responsible for vector toxicity, then removal of this signaling would increase replication and antigen load for enhanced immunogenicity. Such studies will directly compare *in vivo* pathogenicity and immunogenicity of NYVAC-KC-Gag, NYVAC+12-ZM96, NYVAC-KC-B13/B14R-Gag, and Cop-Gag. Additionally, due to the IFN-β production by these vectors, similar experiments in IFN-α/β receptor (IFNAR) -/- mice would also determine whether or not the *in vivo* attenuation and reduced immunogenicity/spread is IFN-dependent.

A balance between immunogenicity and safety can be difficult to strike, therefore it would be beneficial to identify for NYVAC-KC which of the deleted genes from Cop or NYVAC+12 are necessary to improve immunogenicity (i.e. higher responses at lower doses) by inhibiting the IRF3 activation pathway described here. Many vectors have been studied by individually deleting genes in an effort to enhance immunogenicity. For instance, deletion of C6L from MVA results in an enhancement of immunogenicity for HIV-1 antigens, which is likely due to the activation of IRF3 and other signaling pathways regulated by TBK1 (Garcia-Arriaza et al., 2013; Garcia-Arriaza et al., 2011). In addition to C6L, other immune modulators have been deleted in NYVAC and MVA vectors, such as the soluble IFN receptors B19R and B8R (Kibler et al., 2011; Quakkelaar et al., 2011), a TLR inhibitor A46R (Perdiguero et al., 2013), and an NFκB/IRF3 inhibitor K7R (Garcia-Arriaza et al., 2013). In each case, immunogenicity of the viral vector was enhanced, allowing the presumption that these genes are not essential for *in vivo* efficacy of VACV vaccine vectors. It is plausible that in the case of NYVAC-KC, re-insertion of B14R could abrogate IRF3 signaling, and B13R could serve to prevent caspase activation and apoptosis, thus making a strategically engineered HIV-1 vaccine vector for enhanced immunogenicity, specifically for these antigens. Similar strategies could be employed for other viral vectors which may express proteins that result in toxicity to both the host cells and viral vector itself.

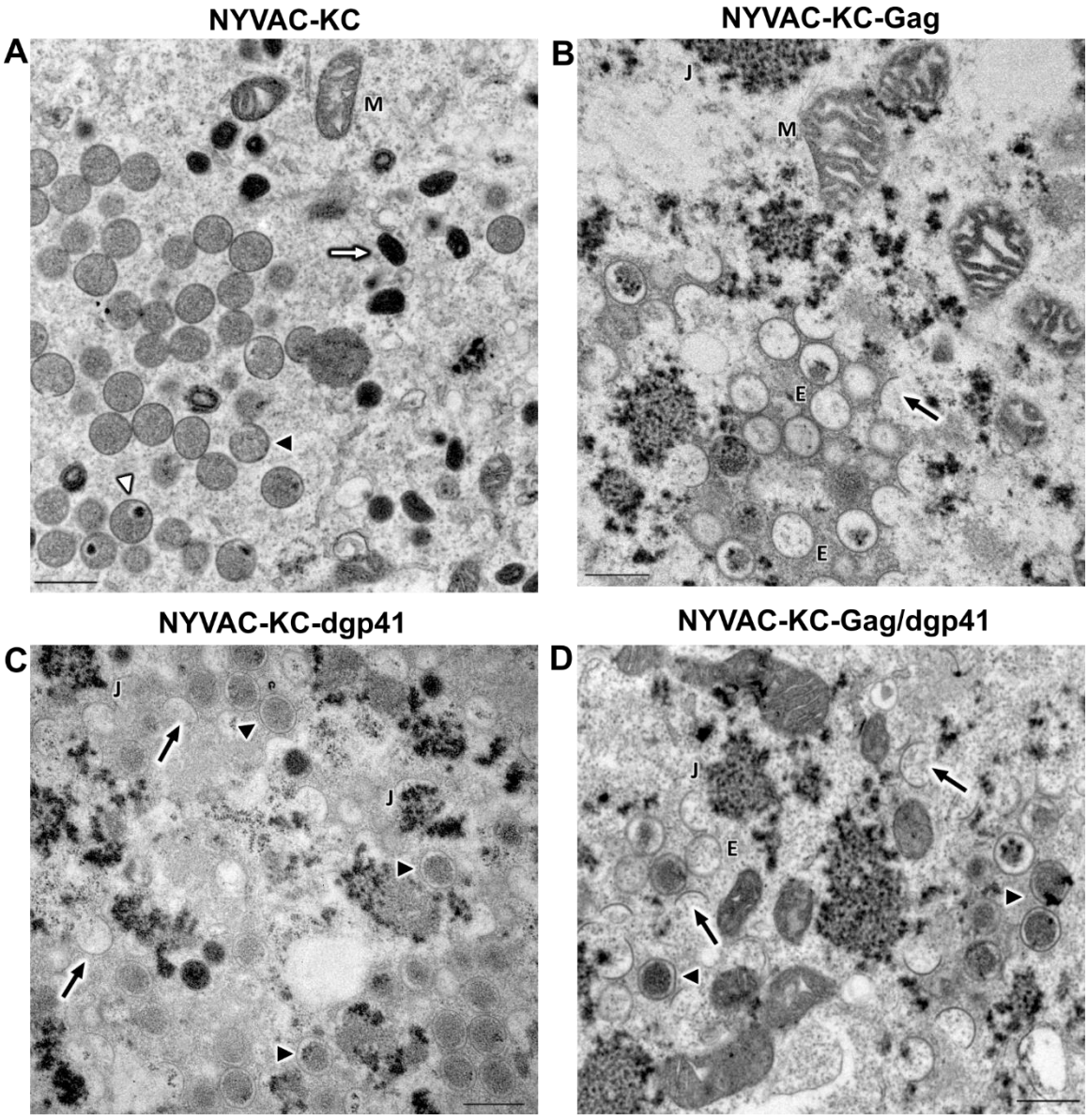

Figure 19 - TEM with NYVAC-KC HIV-1 Vectors Show Signs of Cytotoxicity

BSC-40 cells were infected at an MOI = 5 with NYVAC-KC (A), NYVAC-KC-Gag (B), NYVAC-KC-dgp41 (C), or co-infected with NYVAC-KC-Gag and dgp41 (D). Representative images of viral factories are shown, revealing disorganization in the HIV-1 vectors with few, if any, mature virions and accumulation of protein precipitates. Mitochondria also appear to be malformed. Scale bars: 500 nm. Mature virions, white arrows; white triangles, immature virions with genome incorporated; crescents, black arrows; immature virions, black triangles; cytoplasmic junk, “J”; empty virions, “E”; mitochondria, “M”.

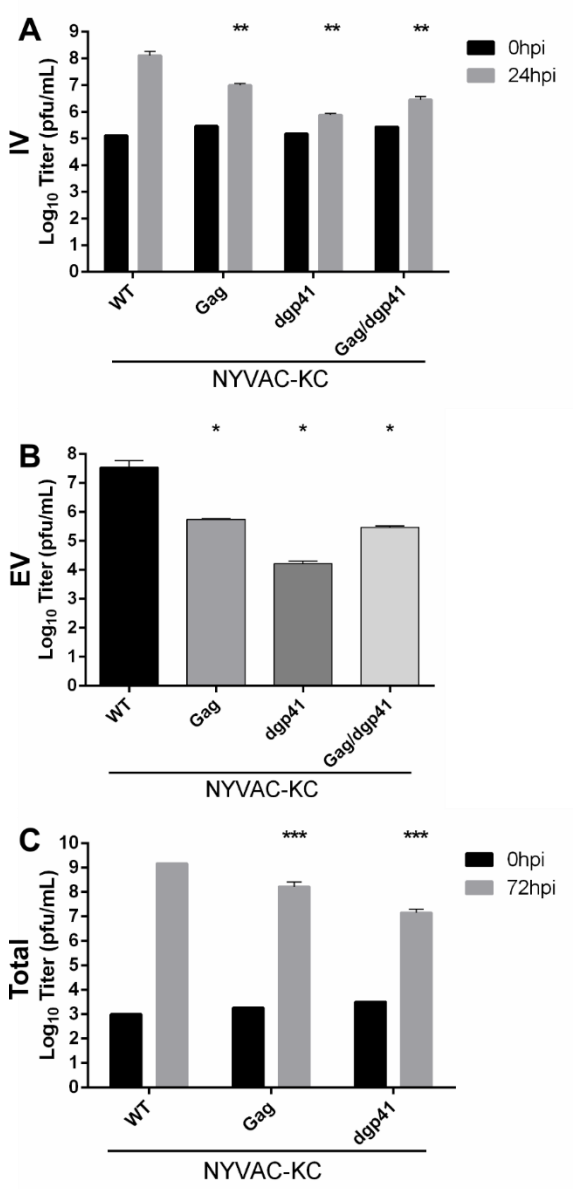

Figure 20 - NYVAC-KC Vectors have Impaired Growth in BSC-40s

(A-B) BSC-40 cells were infected for single-step growth curves at an MOI = 5 with each of the indicated viruses (co-infection total MOI = 10), then medium and cells were harvested at 0 or 24 hpi. Cell lysates were titered in BSC-40s for intracellular mature virions (IVs) for input at 0 hpi and growth at 24 hpi (A). Infection medium was titered in BSC-40s at 24 hpi for release of extracellular mature virions (EVs, B). A multi-step growth curve was also performed in BSC-40s harvesting medium and cells together at 72 hpi for titering total virion production (C). Statistical significance from wild-type (WT) NYVAC-KC titer is indicated by asterisks. (* $p < 0.05$; ** $p < 0.01$; *** $p < 0.001$)

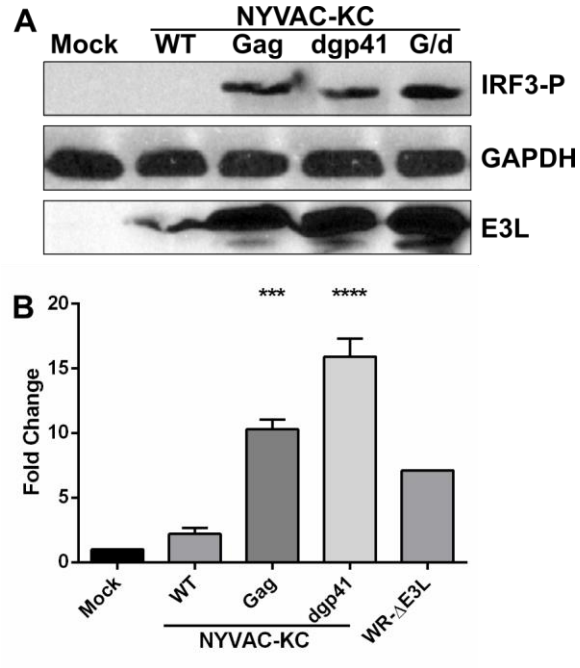

Figure 21 - NYVAC-KC Vectors Activate Antiviral Signaling Pathway Through IRF3

THP-1 cells were infected at an MOI = 10 [MOI = 5 of each virus in the Gag/dgp41 (G/d) co-infection]. Cells were harvested 18 hpi and tested for IRF3 phosphorylation by western blot (A) and IFN-β production via quantitative RT-PCR (B). GAPDH serves as a total cell loading control while E3L expression determines equivalent infectivity of viruses. RT-PCR results are normalized to GAPDH expression. Statistical significance from the mock infected cells is indicated with asterisks and WR-ΔE3L serves as a positive control for the assay. (*** $p < 0.001$; **** $p < 0.0001$)

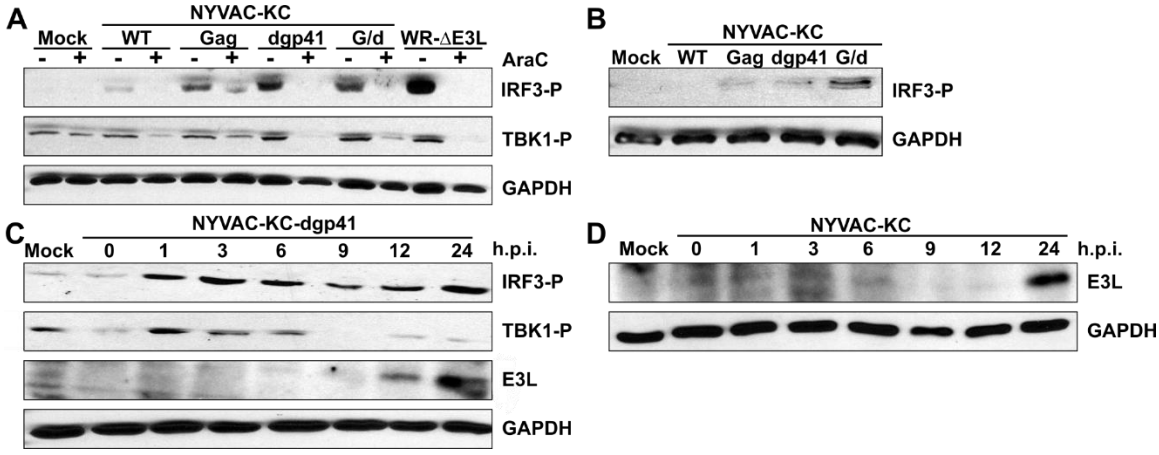

Figure 22 - IRF3 Activation Requires DNA Replication and Persists Through the Viral Life Cycle

THP-1 cells were infected with the indicated viruses at an MOI = 10 to match the NYVAC-KC-Gag/dgp41 (G/d) co-infection (MOI = 5 of each virus) and analyzed 18 hpi for phosphorylated IRF3 and TBK1, or GAPDH loading control. Cells were treated with 200 µg/mL AraC to inhibit DNA replication (A) or 100 µg/mL of rifampicin to inhibit viral morphogenesis (B). (C-D) THP-1 cells were infected in the presence of rifampicin and harvested at multiple time points to monitor viral replication using E3L for NYVAC-KC-dgp41 (C) and NYVAC-KC (D). The timeline for phosphorylation of IRF3 and TBK1 was also analyzed for NYVAC-KC-dgp41.

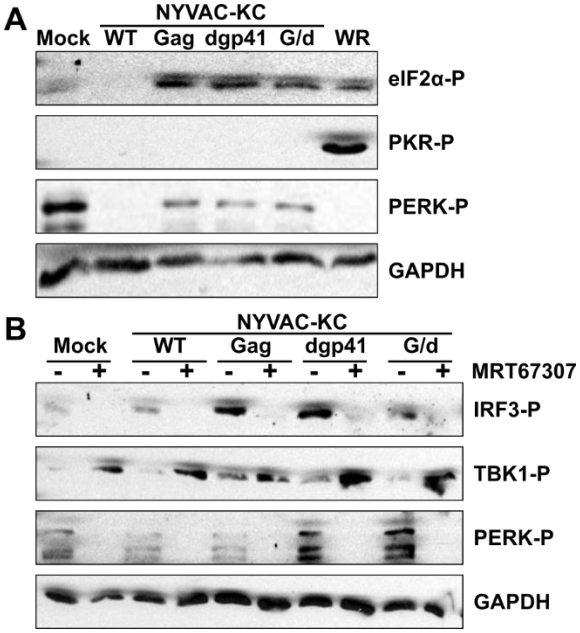

Figure 23 - NYVAC-KC Vectors Signal Through PERK and TBK1

(A) BSC-40 cells were infected with an MOI = 10 of the indicated viruses [MOI = 5 for each virus in NYVAC-KC-Gag/dgp41 (G/d) co-infection] and analyzed 18 hpi with the indicated antibodies. Two pathways for activation of eIF2α were analyzed: the ER stress PERK pathway and the dsRNA-sensing PKR pathway. WR expressing the coumermycin sensitivity gene, Gyrase-PKR, was used as a positive control for PKR activation. (B) THP-1 cells were infected as in (A) for 18 hours in the presence of 2 μM of a TBK1 inhibitor, MRT67307. IRF3, TBK1, and PERK phosphorylation was assessed. GAPDH expression is shown in both images as a loading control.

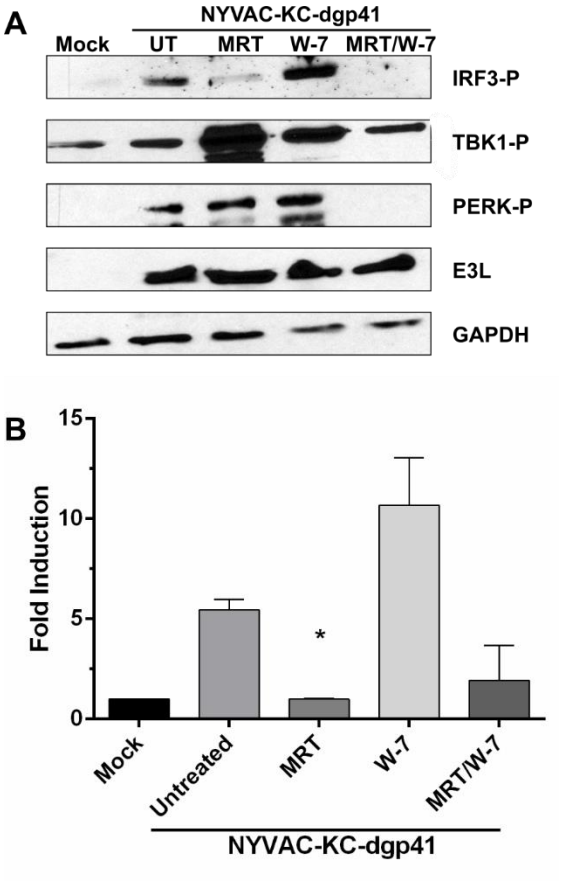

Figure 24 - Rescue of IRF3 Activation by Chemical Inhibitors

THP-1 cells were infected at an MOI = 5 with NYVAC-KC-dgp41 and either left untreated (UT) or were treated with the indicated inhibitor: 2 μM MRT67307 (MRT, TBK1 inhibitor), 10 μM W-7 (calmodulin antagonist), or both inhibitors (MRT/W-7). Cell lysates were analyzed 18 hpi for activation of IRF3, TBK1, and PERK (A) and IFN-β production via qRT-PCR (B). E3L is included as a control for equal viral infection and GAPDH is shown as a total loading control for western blots. RT-PCR data is normalized to GAPDH mRNA levels. Statistical significance from the untreated sample in (B) is indicated with an asterisk. (* $p < 0.01$)

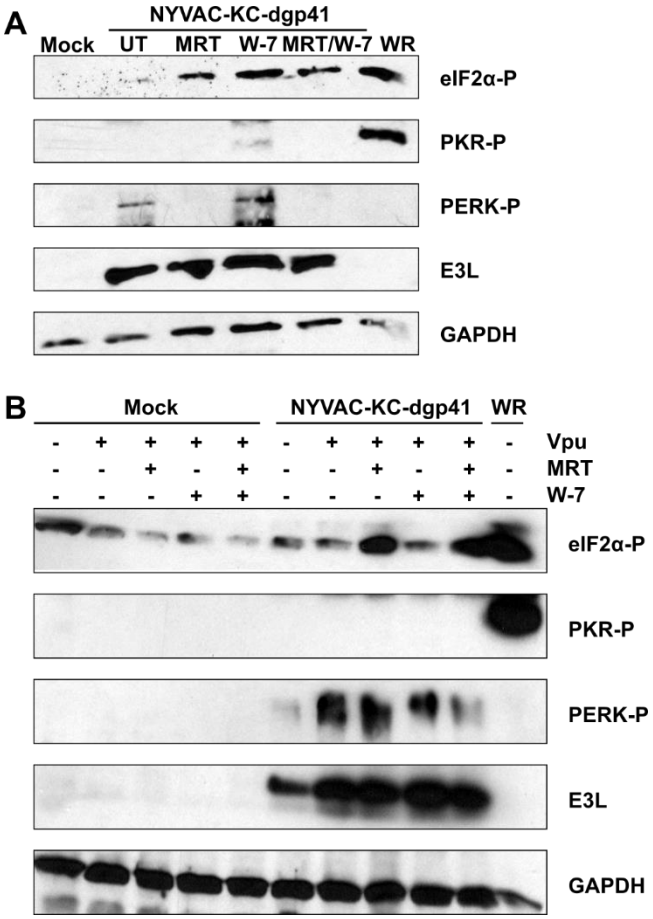

Figure 25 - Inhibition of ER Stress by Chemical Inhibitors and HIV-1 Vpu Expression

BSC-40 cells were infected at an MOI = 5 with NYVAC-KC-dgp41 or coumermycin treated WR expressing Gyrase-PKR (WR lane) as a PKR positive control. Cells were analyzed for activation of the indicated proteins, and E3L and GAPDH loading controls at 18 hpi. (A) Virally infected cells were left untreated (UT) or were treated with 2 μM MRT67307 (MRT), 10 μM W-7, or both inhibitors combined (MRT/W-7). (B) BSC-40 dishes were transfected with 500 ng/well of a Vpu expression vector then infected with viral vectors 24 hours later and treated with the indicated inhibitors at the same concentrations as in (A). Lysates were harvested 18 hours after viral infection.

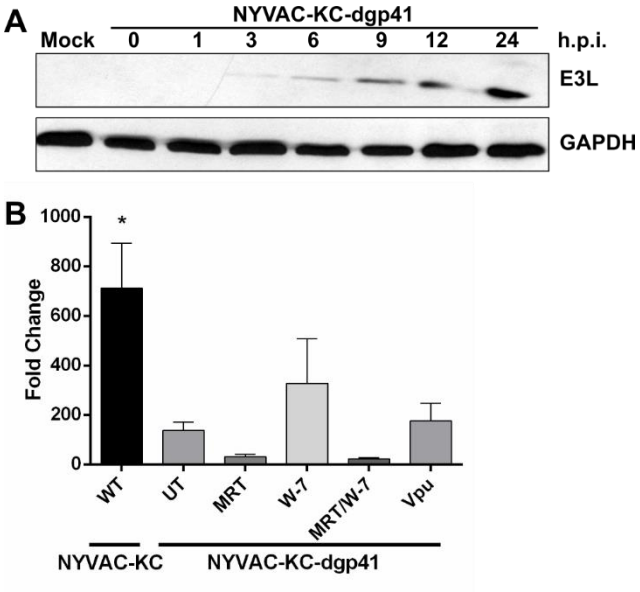

Figure 26 - Rescue of Viral Growth and Replication Kinetics

(A) BSC-40 cells were infected at an MOI = 5 with NYVAC-KC-dgp41 in the presence of 100 µg/mL rifampicin. Lysates were harvested at the indicated time points and assessed for E3L expression for viral replication kinetics using GAPDH as a loading control. (B) BSC-40 cells were infected for single-step growth curves at an MOI = 5 with NYVAC-KC wild-type (WT) or NYVAC-KC-dgp41 with or without inhibitors: untreated (UT), 2 µM MRT67307 (MRT), 10 µM W-7, both MRT67307 and W-7 (MRT/W-7), or transfected with a Vpu expression vector (Vpu). Cells were harvested at 0 and 24 hpi and titered in BSC-40s in duplicate. Fold change is calculated as the 24 hour titer divided by the input (0 hpi) titer. Statistical significance from the UT sample is indicated with an asterisk. (* $p < 0.05$)

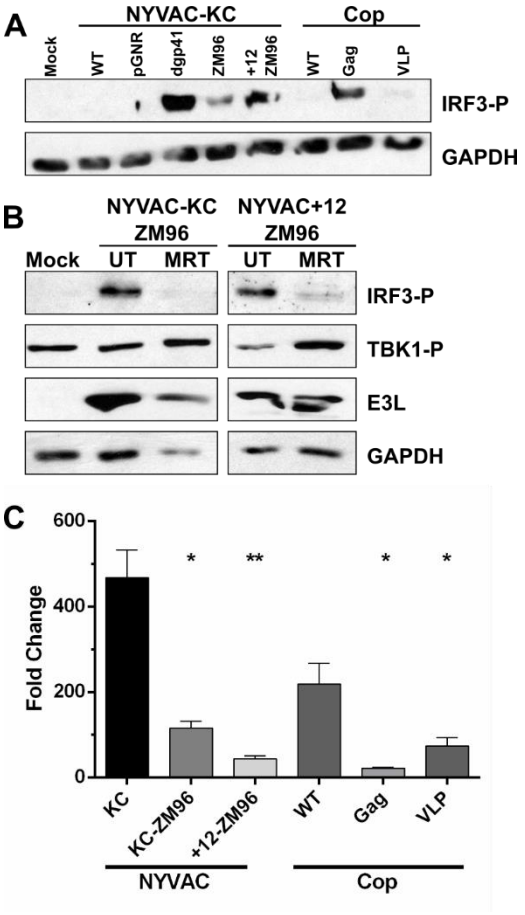

Figure 27 - Inhibition of IRF3 Activation by VACV Immune Modulators

(A) THP-1 cells were infected with the indicated viruses at an MOI = 5 for 18 hours. Cell lysates were analyzed for IRF3 phosphorylation. (B) THP-1 cells were infected at an MOI = 5 with NYVAC-KC-ZM96 or NYVAC+12-ZM96 for 18 hours with (MRT) or without (untreated, UT) the TBK1 inhibitor MRT67307. (C) Single-step growth curves in BSC-40 cells were harvested at 0 and 24 hpi in duplicate. The indicated viruses were used to infect cells at an MOI = 5. Cells were lysed and virus titer determined in BSC-40s. Fold change was calculated as the 24 hpi titer divided by the 0 hpi titer. Statistical significance from the respective wild-type (WT, i.e. no HIV-1 recombinant genes) is shown with asterisks. (* $p < 0.05$; ** $p < 0.01$)

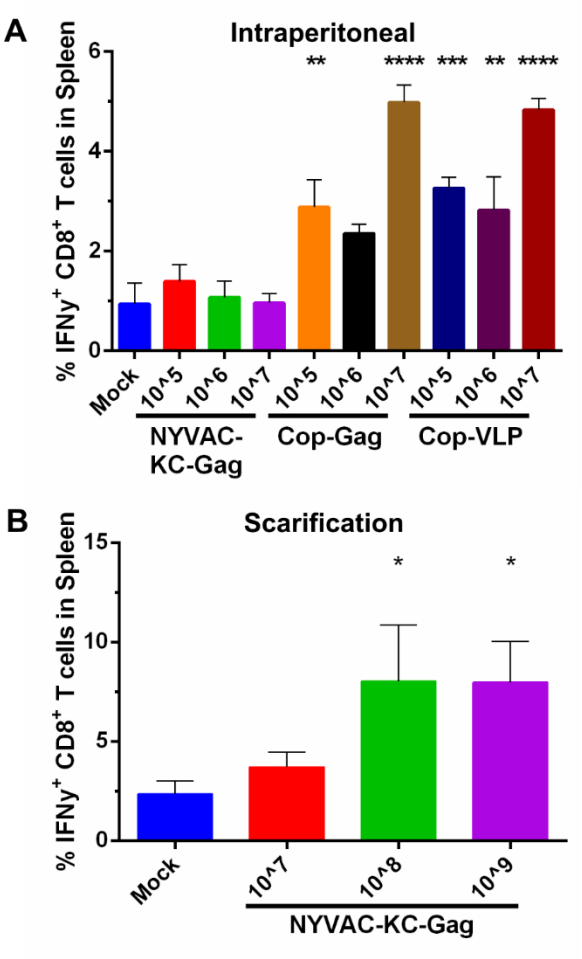

Figure 28 - Effect of Cytotoxicity Phenotype on Immunogenicity of Viral Vectors

Four- to six-week-old C57BL/6 mice were infected with increasing doses (pfu) of the NYVAC-KC-Gag (n = 3/dose), Cop-Gag (n = 4/dose), Cop-VLP (n = 4/dose) or mock infected (n = 3 for scarification, n = 5 for i.p.) either intraperitoneally (A) or via scarification (B). Peak Gag-specific CD8 T cell responses in the spleen were analyzed 7-10 dpi. Percent IFN-γ expressing $CD8^+$ T cells are shown with statistical significance from the mock infected group indicated by asterisks. (* $p < 0.05$; ** $p < 0.01$; *** $p < 0.001$; **** $p < 0.0001$)

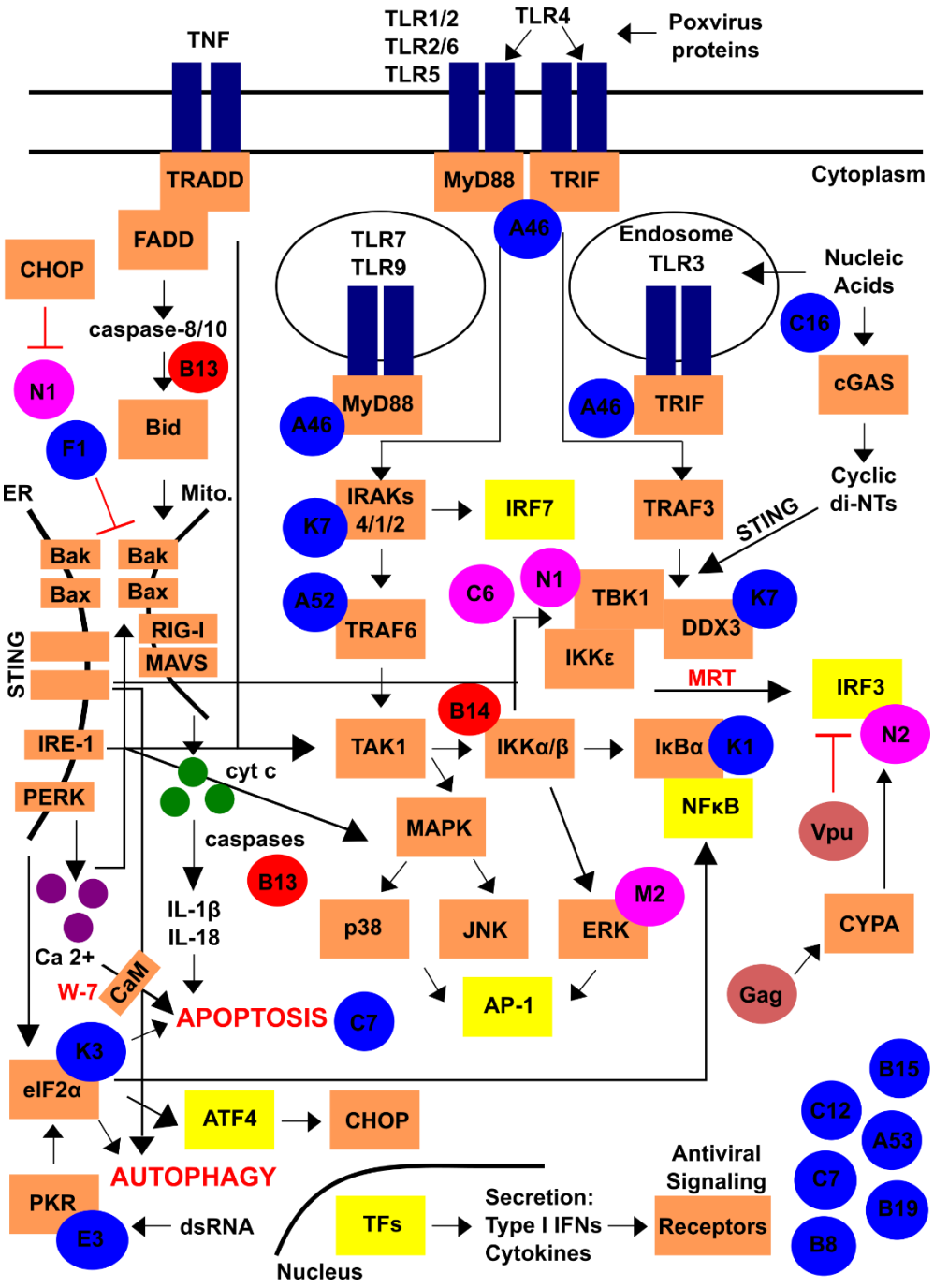

Figure 29 - NYVAC-KC Vector Inhibition of Signaling Pathways

The prominent signaling pathways are shown for stimulation of TLRs (navy blue), the TNF death receptor (navy blue), and ER stress activators (tan, shown on ER membrane), through their adaptor proteins (tan) culminating in the activation of one or more transcription factors (yellow). Encoded NYVAC-KC viral inhibitors are depicted as blue circles, additional genes in NYVAC+12 are shown in pink, and untested genes are shown in red. All viral proteins are shown at their point of inhibition. For reviews of the viral proteins and their effector functions, please see (Gonzalez and Esteban, 2010; Smith et al., 2013; Taylor and Barry, 2006). HIV-1 proteins are shown in burgundy at their points of interaction.

Chapter 5

A HETEROLOGOUS PRIME-BOOSTING STRATEGY WITH REPLICATING VACCINICA VIRUS VECTORS AND PLANT-PRODUCED HIV-1 GAG/DGP41 VIRUS-LIKE PARTICLES

Abstract

The past several decades have seen many HIV-1 vaccine clinical trials, testing various strategies, immunization regimens, and antigens. Still, more than 30 years after the discovery of HIV-1, only one such clinical trial has shown any, albeit modest, efficacy. The Phase III RV144 “Thai Trial” utilized a non-replicating canarypox viral vector and a gp120 protein boost to achieve approximately 30% efficacy, which waned over time. Despite the short-lived immune responses, this trial revived hope that a prophylactic HIV-1 vaccine was achievable. Here we built upon the Thai Trial strategy by developing a novel combination of a replicating, but highly attenuated Vaccinia virus vector, NYVAC-KC (Kibler et al., 2011), and plant-produced HIV-1 virus-like particles (VLPs). Both components contain the full-length Gag matrix and a truncated version of the transmembrane portion of the Envelope protein, denoted deconstructed-gp41 (dgp41). Gag is a desirable target for CD8 T cell responses while the membrane-anchored dgp41 presents the membrane proximal external region (MPER) with its conserved epitopes for broadly neutralizing antibodies such as 2F5, 4E10, and 10E8 in a conformation resembling the pre-fusion state. We tested different combinations of these components in C57BL/6 mice and showed that the group primed with NYVAC-KC vectors and boosted with both the viral vectors and plant-produced VLPs have the most robust Gag-specific CD8 T cell responses, at 12.7% of CD8 T cells expressing IFN-γ in response to stimulation with five Gag epitopes. The same immunization group elicited the best systemic and mucosal antibody responses to Gag and dgp41 with a bias towards IgG1.

Introduction

Despite the success of antiretroviral treatment, human immunodeficiency virus (HIV-1) still causes millions of new infections every year, primarily in regions of the world with limited access to healthcare, making the need for a vaccine more apparent every year. To date, even the

most successful HIV-1 vaccine clinical trial, the phase III Thai Trial (RV144) had only modest and short-lived efficacy, thus leaving room for improvement (Rerks-Ngarm et al., 2009). The Thai Trial used a non-replicating canarypox viral vector (ALVAC) carrying recombinant genes for Gag, Pol and the surface subunit of the envelope (Env) protein (gp120) followed by an AIDSVAX protein boost consisting of recombinant gp120 B/E produced in Chinese hamster ovary (CHO) cells. While ALVAC and AIDSVAX showed no protection when tested individually, their combination in RV144 was modestly protective and provided some valuable information on immune correlates of protection. The most direct immune correlates of protection pertained to antibody (Ab) responses against the V1-V2 loop of gp120 and revealed the importance of polyfunctional, non-neutralizing Abs (Chung et al., 2014; Haynes et al., 2012; Liao et al., 2013a; Yates et al., 2014). This short-lived humoral response faded over time and did not provide long-lasting protective advantage over the placebo arm (Yates et al., 2014). The results of the RV144 trial indicated the strength of a prime-boost approach integrating on a live vector with a subunit protein vaccine. However, the modest efficacy of the trial also suggests that the particular combination of the specific antigens chosen can be further optimized (Corey et al., 2015; Haynes et al., 2012; McMichael and Koff, 2014; Prentice et al., 2015; Yates et al., 2014).

Because of its surface exposure, its immunogenicity, and the critical roles it plays during target-cell infection, gp120 has been a natural target for vaccine development since the early days of HIV-1 research (Burton and Mascola, 2015; Mascola and Haynes, 2013). This, however, has proven to be far from straightforward, because gp120 also functions as a highly mutable decoy with most of its functionally important immunogenic sites conformationally occluded or shielded by glycans. In fact, monomeric preparations of gp120, as well as various preparations aimed at presentation of gp120 trimers, have repeatedly failed to induce protective immune responses in animal models or humans, with the sole and modest exception of the Thai Trial (Haynes et al., 2016; Jacob et al., 2015; McGuire et al., 2014; Moore et al., 2015).

In contrast, far fewer studies have examined gp41. It contains highly immunogenic determinants that induce production of Abs that are among the first to arise during acute HIV-1 infection but are of very limited protective value, showing little or no antiviral activities (Bonsignori

et al., 2012; Burton and Mascola, 2015; Liao et al., 2011). These immunodominant epitopes are located in a region of the protein spanning the two heptad repeat domains and in particular within the loop that connects them (Zolla-Pazner, 2004) and are exposed on the gp41 “stump” in its six-helical bundle conformation upon removal of the gp120 subunit (Burton and Mascola, 2015). Still, gp41 was found to be the target of a number of broadly neutralizing Abs (bnAbs) directed against conformational [35O22 binding at the gp41-gp120 interface, (Huang et al., 2014)] and linear epitopes [2F5, 4E10, Z13 and 10E8 that recognize closely situated sites within the membrane proximal external region, MPER, (Cardoso et al., 2005; Huang et al., 2012; Nelson et al., 2007; Parker et al., 2001)].

Beyond neutralization, anti-MPER Abs, including the above-mentioned bnAbs, were found to exhibit other potent anti-HIV-1 activities including transcytosis blockade (Matoba et al., 2008; Matoba et al., 2009; Matoba et al., 2004; Shen et al., 2010; Tudor et al., 2012), Ab-dependent cell-mediated cytotoxicity [ADCC, (Hessell et al., 2007; Tudor and Bomsel, 2011)], and curbing of dendritic cell-mediated trans-infection (Magerus-Chatinet et al., 2007; Sagar et al., 2012; Tudor et al., 2012). Moreover, passive immunization with these bnAbs provided impressive protection against mucosal transmission of a simian-HIV hybrid (SHIV) in the macaque model (Baba et al., 2000; Hessell et al., 2010; Klein et al., 2013b). Anti-MPER Abs with anti-viral activities were also described in mucosal secretions of highly-exposed but seronegative individuals (Devito et al., 2000a; Devito et al., 2000b; Kaul et al., 2001; Kaul et al., 1999; Pastori et al., 2000; Tudor et al., 2009). Lastly, anti-MPER Abs that were passively passed through breast milk from infected mothers to their uninfected babies were correlated with protection (Diomede et al., 2012; Pollara et al., 2015).

Despite their long-standing promise, anti-MPER bnAbs are naturally rare and are notoriously difficult to elicit. For example, less than 25% of HIV-1-infected patients develop broad and potent nAbs, which even if present require ~2-4 years to produce (Burton and Mascola, 2015; Haynes et al., 2016; Mascola and Haynes, 2013; Mascola and Montefiori, 2010). Several explanations have been suggested, including a lengthy maturation process involving many somatic mutations and extensive affinity maturation (Kepler et al., 2014; Klein et al., 2013a), and

clonal deletion of the B-cell lines secreting such bnAbs that were shown to be partially autoreactive (Verkoczy et al., 2011; Verkoczy et al., 2013; Verkoczy et al., 2010). Interestingly, many of the autoreactivity targets are lipids that can be found in both the plasma membrane of the host cell and in the viral envelope (Alam et al., 2007; Alam et al., 2009; Haynes et al., 2005; Irimia et al., 2016).

It is widely accepted that the membrane milieu of the MPER region plays a major role in the functional immunogenicity of gp41 (Alam et al., 2009; Chen et al., 2014). Both the metastable native conformation of the gp120-gp41 trimer and the highly stable post-fusion conformations do not expose the neutralizing epitopes (Buzon et al., 2010; Frey et al., 2010; Frey et al., 2008; Pancera et al., 2014), and fail to efficiently elicit bnAbs (Crooks et al., 2015; Davis et al., 2009; Decker et al., 2005; Labrijn et al., 2003; Sanders et al., 2015; Williams et al., 2015) or engage the germline B cell precursors for specific bnAbs (Hoot et al., 2013; Jardine et al., 2013; McGuire et al., 2014).

An effective MPER-based antigen therefore requires presentation of the MPER within a context of a membrane, and exposure of the region in a conformation mimicking the putative pre-fusion intermediate. For example, Bomsel and co-workers used a gp41 peptide (residues 649-684) spanning the MPER and part of the C-terminal heptad repeat to decorate liposomes ("virosome") and demonstrated the ability of the immunogen to elicit systemic and mucosal antibodies with transcytosis-blocking activity in humans (Leroux-Roels et al., 2013), and nonhuman primates that were thereafter protected against a mucosal SHIV challenge (Bomsel et al., 2011). Together, these results indicate a strong potential for this antigenic region to be used as a vaccine component when presented correctly on a membrane.

The laboratory of Tsafrir Mor previously developed an efficient production method for enveloped VLPs in the tobacco-relative *Nicotiana benthamiana*, consisting of Gag and deconstructed-gp41 (dgp41: MPER, transmembrane domain, and full-length cytoplasmic tail) (Kessans et al., 2013). Such VLPs display the MPER of gp41 without steric hindrance from gp120, without the immunodominant epitopes on both Env subunits, and with a higher antigen load per VLP than what exists in an HIV-1 virion (Kessans et al., 2016). A similar construct has

been shown to be a likely trimer with its bnAb epitopes exposed (Gong et al., 2015). When administered to mice, these VLPs elicit both serum IgG and mucosal IgA to Gag and dgp41 antigens (Kessans et al., 2016).

Live viral vectors are appealing as vaccine vehicles for the expression of HIV-1 antigens due to their proficiency for eliciting T cell responses. For example, a cytomegalovirus (CMV) vector was recently shown in nonhuman primates to clear an established SIV infection with dependency on CD8 T cells recognizing non-canonical epitopes on major histocompatibility complex (MHC) II instead of MHC I (Hansen et al., 2013a; Hansen et al., 2013b). Poxviruses also stand out amongst other viral vectors [see reviews (Gomez et al., 2012a; Jacobs et al., 2009; Pantaleo et al., 2010)], as attested by the Thai Trial that employed a canarypox-based vector and was the first and only HIV-1 vaccine clinical trial to show efficacy (Haynes et al., 2012; Rerks-Ngarm et al., 2009). The canarypox-based viral vector used in the trial, ALVAC, is not capable of replication in mammalian cells (Taylor and Paoletti, 1988; Taylor et al., 1988). Inability to replicate *in vivo* in humans makes the virus safer to use as a vaccine or a vaccine vector. However, it was hypothesized that replication could enhance immunogenicity by increasing antigen load as the virus replicates *in vivo*.

To test this hypothesis, a strategy was employed using a replicating vaccinia virus strain, NYVAC-KC. The virus was developed from the NYVAC strain, previously rendered replication incompetent in human cells by deletion of 18 open reading frames (ORFs) from the genome of Copenhagen (Cop), its parental strain (Tartaglia et al., 1992b). NYVAC-KC contains a re-insertion of two host-range genes, K1L and C7L, which allows the virus to replicate in human tissue, thus improving immunogenicity while remaining highly attenuated (Kibler et al., 2011; Quakkelaar et al., 2011).

In this study, we describe the development of replicating vaccinia virus vectors based on NYVAC-KC which express Gag and dgp41 as matching antigens to the plant-produced VLPs for prime/boosting purposes. It is shown that the viral vectors produce VLPs *in vitro*, and the viral vectors were tested in different combinations with plant-produced VLPs in mice. The animal study revealed that these two vaccine components work in concert to elicit Gag-specific CD8 T cell

responses and both systemic and mucosal antibodies to Gag and dgp41 peptides in the immunization group which most closely mimics the Thai Trial.

Materials and Methods

Cloning pGNR Plasmids for Virus Recombination

The Gag and dgp41 genes were cloned into the pGNR plasmid, which harbors a neoGFP selection cassette (neomycin resistance gene fused to GFP, known as pGNR) between homologous recombination arms for the vaccinia TK locus. Gag and dgp41 genes were amplified from pTM 488 (Gag) and pTM 602 (dgp41) [described in (Kessans et al., 2013)] into TOPO pCR-2.1 vectors (Invitrogen). Cloning was achieved using AccuStart Taq DNA polymerase HiFi PCR kit (Quanta Biosciences) with primers oTM 664 (5'- *ACTAGT*ATGGGAGCTAGAGCCTCT-3") and 665 (5'- *CCCGGG*TTATTGAGAGGAAG-3') for Gag and oTM 666 (5'- *ACTAGT*ATGGGATCTCAAACTCAACAA-3') and 667 (5'- *CCCGGG*TTATTGCAAAGCAG-3') for dgp41 for the addition of 5' flanking SpeI and 3' flanking XmaI sites, denoted in italics. Ligation reactions were electroporated into DH5α *Escherichia coli* and plated onto LB +ampicillin plates. Gene insertion was confirmed by colony PCR using GoTaq Green Master Mix (Promega). Plasmids were extracted using the E.Z.N.A. mini-prep kit (Omega) and sequences verified using backbone-specific primers M13-forward and M13-reverse. The TOPO plasmids were designated pTM 813 (Gag) and pTM 814 (dgp41). Both pTM 813, 814, and pGNR were digested with SpeI and XmaI (NEB) and fragments separated via gel electrophoresis and extracted using QIAquick Gel Extraction Kit (Qiagen), then ligated into the pGNR backbone using T4 DNA ligase (Promega). Ampicillin resistant DH5α *E. coli* colonies were screened by colony PCR and plasmids extracted as above. Sequences were confirmed with pGNR backbone-specific primers oTM 686 (5'- CCCACCCGCTTTTTATAGTAA-3') and 687 (5'- CGGTTTATCTAACGACACAACA-3'). Sequence-verified pGNR plasmids were named pTM 815 (Gag) and pTM 816 (dgp41).

Cell Lines and Viruses

BSC-40 cells were grown in DMEM (Corning Cellgro) with 5% FBS plus gentamycin and 2 mM L-glutamine. BHK-21 cells were grown in MEM (Corning Cellgro) with 5% FBS plus gentamycin. Generation of the parental vaccinia virus (VACV) strain NYVAC-KC was described previously (Kibler et al., 2011).

In vivo Recombination (IVR)

Simultaneous transfection/infection [*in vivo* recombination, IVR (Brandt and Jacobs, 2001; Kibler et al., 1997)] was performed with pTM 815 (Gag) and pTM 816 (dgp41) and NYVAC-KC to insert Gag and dgp41 into the vaccinia virus TK locus. 500 ng of plasmid DNA was transfected using Lipofectamine and Plus™ Reagent (Invitrogen) per manufacturer's protocol. This was immediately followed by infection with NYVAC-KC at an MOI = 0.01 in 35 mm^2 dishes of BSC-40 cells. Recombination was allowed to proceed for 24 hrs followed by addition of G418 antibiotic (500 µg/mL). Cells were harvested and lysed at 48 hours post infection (hpi). The IVR was used to infect 100 mm^2 dishes of BSC-40 cells for selection of individual antibiotic-resistant plaques for subsequent expression screening (note: a mutation in the GFP gene prevented use of fluorescent screening). This process was repeated for multiple rounds of antibiotic selection before a >98% pure virus was isolated as measured by immunoplaque assay.

Expression Screening

Individual antibiotic-resistant plaques were grown in 60 mm^2 dishes of BSC-40 cells to CPE and harvested in 1X SDS sample buffer [50 mM Tris-Cl pH 6.8, 2% SDS, 0.1% bromophenol blue, 10% glycerol, 100 mM β-mercaptoethanol, 1X protease inhibitor cocktail III (Research Products International Corp., Prospect, IL)], and then centrifuged through a QiaShredder (Qiagen) for NYVAC-KC-Gag plaques. For NYVAC-KC-dgp41, cells were lysed with RIPA lysis buffer [1% NP40, 0.1% SDS, 0.5% sodium deoxycholate, 1X protease inhibitor cocktail III, in 1X PBS without calcium or magnesium (Corning)]. RIPA lysates were mixed with an equal volume of 2X SDS sample buffer. Cell lysates were screened using SDS-PAGE as previously

described (Kessans et al., 2013). Briefly, boiled samples were run on 12% polyacrylamide gels under denaturing conditions, transferred to nitrocellulose membranes (Bio-Rad), and probed with either Gag or dgp41 antibodies and anti-rabbit or anti-human IgG-HRP, respectively. Proteins were detected via chemiluminescence (ImmunoCruz Luminol Reagent, Santa Cruz).

Immunoplaque Assays

Immunoplaque assays were performed in 6-well dishes by infecting BSC-40s with 50 pfu of individual plaques. Once plaques were visible, the cells were fixed with 1:1 acetone:methanol for 30 min at -20° C, washed with PBS, then incubated with anti-p24 Gag polyclonal rabbit serum or 2F5 (obtained through the NIH AIDS Reagent Program, Division of AIDS, NIAID, NIH: from Dr. Hermann Katinger) at 1:1000 in 3% FBS-PBS. Secondary biotinylated antibodies for anti-rabbit IgG or anti-human IgG from Vectastain ABC Kits (Vector Laboratories, Inc.) were used for detection with DAB peroxidase substrate (Vector Laboratories, Inc.) per manufacturer's protocol. After counting positive plaques, cells were stained with Coomassie blue dye to count the number of negative plaques. Percentages were calculated by dividing positive plaques by total plaques per well. The plaque with the highest percentage of positives was used for further purification until a plaque with >98% purity was identified and used to grow stocks.

Virus Stocks

The final NYVAC-KC-Gag and NYVAC-KC-dgp41 plaques with >98% purity determined by immunoplaque assay were grown to CPE in BHK-21 cells in a 60 mm^2 dish for the first passage (P1) stock. The P1 stock was titered in BSC-40s and used to infect five T150 flasks of BHK-21 cells at an MOI = 0.01 for the P2 stock. Cells were harvested at CPE, subjected to freeze-thaw and sonication, then cell lysates were placed on a 36% sucrose pad and centrifuged at 22,000 rpm for 80 min at 4° C with an SW28 rotor to pellet virions. Purified virions were resuspended in 10 mM Tris-HCl pH 9.0, their titer determined in BSC-40s, and were stored in aliquots at -80° C until further use.

Vaccinia in vitro VLP Production

BSC-40 cells seeded in 100 mm^2 dishes were infected at an MOI = 5. At 24 hpi, medium and cells were harvested and pelleted. Medium was subjected to 40% ammonium sulfate precipitation and resuspended in 1X PBS (140 mM NaCl, 2 mM KCl, 10 mM Na_2HPO_4, 1 mM KH_2PO_4, pH 7.4). Aliquots were boiled and analyzed by SDS-PAGE for presence of Gag and dgp41 as described above.

Expression in Plants of VLPs and their Purification

HIV-1 Gag/dgp41 VLPs were expressed and purified as previously described (Kessans et al., 2013). Briefly, Gag transgenic *N. benthamiana* plants were infiltrated with *Agrobacterium tumefaciens* harboring pTM 602 with the dgp41 gene and leaf tissue was harvested 4-6 days post infiltration (dpi). Leaf tissue was crushed in a blender in extraction buffer (25 mM sodium phosphate, 100 mM NaCl, 1 mM EDTA, 50 mM sodium ascorbate, 1 mM PMSF, pH 7.8). VLPs were precipitated with 40% ammonium sulfate and resuspended in 1X PBS (140 mM NaCl, 2 mM KCl, 10 mM Na_2HPO_4, 1 mM KH_2PO_4, pH 7.4), then purified via iodixanol density gradient centrifugation. The VLP-containing 20% iodixanol fraction was concentrated on a 300 kDa molecular weight cut-off membrane (Sartorius) and quantified via immunoblot for immunizations as described in (Kessans et al., 2016).

Antibodies

The following antibodies were used for the indicated assays: anti-p24 Gag polyclonal rabbit serum (Kessans et al., 2013); human anti-MPER 2F5 (AIDS Reagent Program and the kind gift of Morgane Bomsel); goat anti-human IgG-HRP (Sigma) for immunoblot; goat anti-rabbit IgG-HRP (Santa Cruz) for immunoblot; rabbit anti-human IgG-HRP (Santa Cruz) for ELISAs; rabbit anti-mouse IgG-HRP (Calbiochem) for ELISAs; mouse IgA-kappa (ICL Labs) for ELISAs; goat anti-mouse IgA (Sigma) for ELISAs.

Transmission Electron Microscopy (TEM)

BSC-40 cells grown in T75 flasks were infected at an MOI = 5 and harvested by trypsinization 24 hpi. Cells were pelleted between all wash steps at 700 x*g* for 5 min at 4° C until embedded in agarose prior to secondary fixation. Pelleted cells were washed twice in 1X PBS (140 mM NaCl, 2 mM KCl, 10 mM Na_2HPO_4, 1 mM KH_2PO_4, pH 7.4). For primary fixation, cells were placed in 2% glutaraldehyde in PBS for 15 min at room temperature followed by a second incubation with fresh fixative for 1 hour at 4° C. Fixed cells were resuspended in 1% agarose and washed three times in PBS for 30 min each at room temperature. Cells were then fixed with 1% osmium tetroxide in PBS for 1 hour at room temperature followed by four 15-minute washes in water. A 0.2% uranyl acetate solution in water was used to stain en bloc overnight at 4° C followed by three 15-minute washes in water. An ethanol series from 20% to 100% (anhydrous) was used for dehydration, increasing the ethanol concentration by 20% every 10 min with three incubations in anhydrous ethanol. Spurr's resin was gradually introduced through 4- to 8-hour incubations with 1:3, 1:1, and 3:1 ratios of resin:100% ethanol, followed by three 8 hour incubations in 100% resin. Cells were divided into several blocks of Spurr's resin and polymerized at 60° C for 36 hours. Sections were cut at 70 nm thick, and were placed on formvar-coated copper slot grids followed by post-stain treatment with 2% uranyl acetate and 3% Sato's lead citrate before imaging.

Mouse Immunizations

All animal experiments were done with approval from the Arizona State University Institutional Animal Care and Use Committee.

For the initial study (Experiment 1), six-week-old C57BL/6 mice (Jackson Laboratories) were split into five groups. Three groups (n = 5) received virus prime (VV) followed by two boosts of either mock (Group 1), VLP (Group 2), or VV+VLP (Group 3). Group 4 (n = 3) received no virus prime and two VLP boosts and Group 5 served as the naïve control (n = 1). NYVAC-KC-Gag and NYVAC-KC-dgp41 P2 stocks, each at a dose of 5 x 10^5 pfu, were mixed together for a total dose of 1 x 10^6 pfu per mouse. Virus immunizations prepared in Tris HCl pH 9.0 were injected

intramuscularly (i.m.) into the thigh. Plant-produced, gradient-purified VLPs were prepared in 1X PBS pH 7.4 with 2 µg p24 and 1.2 µg MPER and mixed with Ribi adjuvant (Sigma) per manufacturer's protocol to reach a final concentration of 2% oil [described previously in (Kessans et al., 2016)]. Mock mice were injected i.m. with Tris HCl pH 9.0 buffer in equivalent volumes. VACV and vehicle injections were delivered i.m. while VLPs were delivered intraperitoneally (i.p).

Subsequent experiments were designed in a similar manner, but with different groups for comparison. The second NYVAC-KC study (Experiment 2) separated six-week-old C57BL/6 mice into six groups. Five groups (n = 5) were primed with NYVAC-KC-Gag and dgp41 virus (VV) mixed equally for a total of 1 x 10^7 pfu prepared in 1X PBS and delivered either via scarification or i.m. Only one group (n = 5) was primed with VLPs. VLPs were delivered i.p. and prepared as described above, only the pTM 901 (Dual Gemini +p19) vector described in Chapter 2 was used to produce VLPs. These VLP injections contained 2 µg p24 and 5.5 µg MPER. Scarification groups were as follows: VV/VV, VV/VLP, VV/VV+VLP, and VLP/VV+VLPs. The two additional groups (n = 5) receiving virus via the i.m. route were VV/VV and VV/VV+VLPs. A seventh group (n = 5) received mock i.m. injections of PBS and was shared with the Cop-VLP study described below.

The third and final animal study (Experiment 3) was designed to compare the ability of a VACV vector simultaneously expressing Gag and dgp41 to boost and/or prime VLP Ab responses. This study utilized the Cop-VLP vector (abbreviated as Cop in figures shown here) that was described in Chapter 4. Cop-VLP was diluted in 1X PBS to administer 10^7 pfu i.m. VLPs generated with pTM 901 were prepared and delivered as described for Experiment 2. Four groups (n = 5/group) were assessed in this study: Cop/Cop, VLP/VLP, Cop/VLP, and VLP/Cop (where Cop = Cop-VLP).

Three immunizations were given to mice at days 0, 45, and 90. Serum, fecal, and vaginal lavage samples were collected as previously described (Kessans et al., 2016) every 2 weeks at days 0, 14, 28, 42, 56, 80, and at the endpoint of day 97 for analysis of Ab production. One week post the final boost (day 97), spleens were collected for analysis of CD8 T-cell responses as described below.

Animals were monitored every 2-3 days for weight loss and other signs of illness, as a measure of vector safety.

ELISA Detection of IgG and IgA

Antibody production was measured via ELISA as previously described (Kessans et al., 2016). Briefly, serum, fecal, and vaginal lavage samples were analyzed for IgG (serum) or IgA (mucosal sites) specific for Gag p24 or gp41 MPER regions. Samples were analyzed in threefold serial dilutions starting at 1:50, 1:2, and 1:5 for serum, fecal, and vaginal lavage samples, respectively. For mouse experiments where both vaginal IgG and IgA are assayed, lavage samples were initially tested at a 1:10 dilution. ELISAs were developed with either SIGMA*FAST*™ OPD (Sigma) and read at OD 490 nm (Experiment 1) or developed with 1-Step™ Ultra TMB-ELISA Substrate Solution (Thermo Scientific) and read at OD 450 nm (Experiments 2 and 3). Endpoint titers were calculated as the reciprocal of the dilution factor at which the OD was equal to background levels (OD < 0.1). IgG1 and IgG2a isotypes were detected with the same ELISA protocol, but with goat anti-mouse IgG1-HRP or goat anti-mouse IgG2a-HRP secondary antibodies (Santa Cruz Biotechnology) instead of total IgG. Purified mouse IgG1 kappa chain or mouse IgG2a kappa chain primary antibodies (Sigma) were used as controls.

For anti-VACV ELISAs, 96-well plates were coated with 10^7 pfu/well of sucrose-purified NYVAC-KC overnight at 37° C. Wells were fixed in 2% paraformaldehyde in 1X PBS for 10 min at 4° C to inactivate the virus. Wells were washed with buffer (150 mM NaCl, 0.5% Tween-20) then blocked with 5% non-fat milk in 1X PBST. Serum IgG was incubated in serial dilutions and detected as described for anti-p24 and anti-MPER ELISAs.

Intracellular Cytokine Staining and Flow Cytometry

Spleens were harvested in Hank's medium (Corning Cellgro) and cells were strained through a 0.7 µm filter for resuspension in complete RPMI [cRPMI: 10% FBS, penicillin (100 units/mL), streptomycin (100 µg/mL), 2 mM L-glutamine]. Red blood cells were lysed with ACK Lysing Buffer (Gibco) and splenocytes were resuspended in cRPMI at a concentration of 2 x 10^7

cells/mL. Cells were plated at 1 x 10^6 cells/well and incubated for 5 hours in the presence of GolgiPlug™ (BD Biosciences) and 50 µL of 1 µg/mL of one of five different immunodominant ZM96 Gag CD8 epitopes: LRSLYNTV (LRS8), VIPMFTAL (VIP8), AMQMLKDT (AMQ8), YSPVSILDI (YSP9), EVKNWMTDTL (EVK10) (synthesized by GenScript and resuspended according to manufacturer's protocol). For the second and third studies, splenocytes were incubated with 50 µL of a Gag peptide pool containing a total of 5 µg/mL of peptides (1 µg/mL of each peptide listed above).

Cells were stained with fluorescently conjugated antibodies: CD8-Pacific Blue or APC-Cy7, TNFα-FITC, and IFNγ-PE (all from BD Biosciences). Fixation and permeabilization was performed with a Cytofix/Cytoperm™ Kit (BD Biosciences) with final resuspension in FACS Buffer (1% FBS in 1X PBS). Samples were analyzed by flow cytometry on an LSR Fortessa. Data was analyzed using FlowJo Data Analysis Software (FlowJo, LLC; Ashland, OR).

Statistics

All statistical analyses were performed in GraphPad Prism Software (GraphPad Prism Software Inc.; La Jolla, CA). All data were analyzed using a one-way ANOVA multiple comparison with Dunn's post-test. Significance cut-off was defined as $p < 0.05$.

Results

Generation of Recombinant Vaccinia Virus Vectors

NYVAC-KC-Gag, NYVAC-KC-dgp41, Cop-Gag, and Cop-VLP viruses were generated through *in vitro* recombination (see Materials and Methods) (Figure 30A-B, Figure 31A). Each gene was under control of a synthetic early/late VACV promoter, ensuring the genes were expressed at all stages of viral replication to maximize antigen production. Second round individual plaques were screened for expression via immunoblot by probing for either Gag or dgp41 expression. Immunoplaque assays for either Gag or dgp41 were performed to identify the plaque with highest purity for further selection. This process was repeated until a plaque with >98% purity was identified and then used to grow a P2 stock. The final sucrose-pad purified P2

stock show Gag and dgp41 expression in BSC-40 cell lysates at the proper size for NYVAC-KC-Gag and NYVAC-KC-dgp41 (Figure 30C-D), and also for Cop-Gag and Cop-VLP (Figure 31B-C). It was noted during selection that viruses recombining with dgp41 plasmids had reduced plaque size and grew to much lower titers, suggesting that the HIV-1 gene makes the viral vector cytotoxic (discussed in Chapter 4).

Gag is known to be sufficient and necessary for HIV-1 VLP formation and budding into the medium (Garoff et al., 1998). To test whether BSC-40-infected cells support VLP formation and budding, culture medium was analyzed for the presence of Gag and dgp41. Indeed, Gag protein was detected in culture medium of cells either infected with NYVAC-KC-Gag or co-infected with NYVAC-KC-Gag and NYVAC-KC-dgp41 (Figure 30E, Lanes 2 and 4). In contrast, dgp41 was detected only in the medium from co-infected cells, not in medium from cells that were infected with NYVAC-KC-dgp41 alone (Figure 30E, Lane 4). The same results held true for Cop-Gag and Cop-VLP vectors. Gag was detectable in the medium for both vectors while dgp41 was only present in Cop-VLP when both proteins are co-expressed from the same genome (Figure 31D, Lane 4). This holds promise for *in vivo* production of dgp41-containing VLPs to enhance immunogenicity of the MPER.

NYVAC-KC-Gag/dgp41 Show Cytotoxicity and in vitro VLP Production

These results indicate that export of dgp41 to the medium depends on expression and export of Gag, suggesting that Gag VLPs and Gag/dgp41 VLPs are released, respectively, from cells that express Gag alone or co-express Gag and dgp41. We used TEM to test this possibility. BSC-40 cells that were infected (MOI = 5) with NYVAC-KC, NYVAC-KC-Gag, NYVAC-KC-dgp41, or co-infected with Gag/dgp4, were processed for TEM at 24 hpi.

In cells infected with the parental NYVAC-KC strain, viral replication factories are clearly visible and all stages of viral replication are easily identified (Figure 32A). Mature virions (indicated by white arrows) are seen both intracellularly (Figure 32A-1) and extracellularly (Figure 32A-2). Immature virions with and without incorporated genomes are also abundantly visible in this section (white and black triangles, respectively).

NYVAC-KC-Gag-, dgp41-, or co-infected cells have disorganized viral factories and mature viral particles are rare (Figure 32B-D). Many early crescent formations are visible (black arrow), along with what appears to be “unfilled” or empty virion shells (indicated by "E"). The rarity of mature virus particles corresponds well to the smaller plaques typical of these strains and their reduced titers, as noted above. Instead, these infected cells appear to have large protein aggregates or precipitates in their cytoplasm (“junk” indicated by "J"), mimicking a phenotype associated with palmitate deficiency (Greseth and Traktman, 2014). Additionally, NYVAC-KC-dgp41-infected cells demonstrate nuclear condensation (Figure 32C-2, “nucleus” indicated by "N"), a classic sign of apoptosis (Duprez et al., 2009). Furthermore, the mitochondria (indicated by "M") in NYVAC-KC-Gag- and NYVAC-KC-dgp41-infected cells appear to be malformed, potentially indicating loss of structural integrity, which can also indicate occurrence of apoptosis (Li and Dewson, 2015).This phenotype seems far more drastic than that of NYVAC-KC-infected cells.

Importantly, in cells that were infected with NYVAC-KC-Gag (Figure 32B-2) or co-infected with NYVAC-KC-Gag and NYVAC-KC-dgp41 (Figure 32D-2), particles of approximately 100 nm in diameter are seen budding at the cell surface (black stars). Based on their size and appearance, these particles are likely to be HIV-1 Gag or Gag/dgp41 particles budding out of the cell. This observation can explain the appearance of Gag and dgp41 in the media of these infected cells (Figure 30E).

Experiment 1: Mouse Immunizations

Six-week-old C57BL/6 mice were separated into five groups in order to assess different combinations of VACV and VLP immunization regimens (Figure 33A). Mice were given a total of three immunizations separated by 45 days to allow for memory responses to develop prior to boosting. Three groups (n = 5) were primed with the combination of NYVAC-KC-Gag and NYVAC-KC-dgp41 (denoted in all figures and text as VV), followed by two boosts with either vehicle (Group 1), VLPs alone (Group 2), or a combination of VV and VLPs (Group 3). A fourth

group (n = 3) received a mock (vehicle) prime followed by boosts with VLPs. The fifth group served as a naïve control (n = 1).

Monitoring of weight revealed that none of the mice in any group lost weight (data not shown). This indicates little to no pathogenicity of the virus and is consistent with previous virulence data for NYVAC-KC (Kibler et al., 2011) and general safety of the plant-derived VLPs (Kessans et al., 2016).

Serum IgG Responses to Gag and MPER

Antigen-specific serum IgG responses were measured by ELISA using p24 subunit or MPER peptide to detect Gag and dgp41 Ab responses, respectively. Throughout, OD 450 nm values for the lowest dilution tested (1:50) are shown both over time (Figure 33B-C) and for individual animals at the endpoint, Day 97 (Figure 34A). Additionally, endpoint titers were calculated for the final serum samples and are shown in Figure 35A as the reciprocal of the dilution where the OD fell below background levels (OD < 0.1).

Serum IgG responses against both p24 and MPER antigens remained undetectable in all groups until the first sample (Day 55) after the first boost. Titers increased gradually and were boosted after the final immunization with VLPs (Figure 33B-C), reaching significant levels at the endpoint analysis (Day 97) for both anti-p24 Gag and anti-MPER responses (Figure 34A). Endpoint Gag responses were highest in the group boosted with a combination of VV and VLPs (VV/VV+VLPs), while the group boosted with VLPs alone (VV/VLPs) also showed significant titers which were more variable responses among animals (Figure 35A). Anti-MPER serum IgG responses were lower than Gag titers but showed a similar trend, reaching significant levels in all groups receiving VLPs regardless of prime/boost regimen (Figure 34A). However, the endpoint titer calculations showed no difference between groups, consistent with low Ab responses (Figure 35A). It is interesting to note that plant-produced VLPs appear to be largely responsible for Ab stimulation because no detectable levels of antibodies were present in the first 45 days after a single dose of VV and only reached detectable levels after the second immunization in those groups that received VLPs.

Mucosal IgA Responses to Gag and MPER

Gastrointestinal IgA responses to the dgp41 (MPER) antigen (as determined by measuring the secreted Ab levels in fecal samples) were low but detectable (Figure 34B), whereas anti-MPER IgA levels in vaginal secretions were below our detection level irrespective of treatment (Figure 34C). Fecal anti-MPER IgAs were higher in groups that were immunized using the prime/boost VV/VLPs regimen than groups that were vaccinated with either VV or VLPs alone. Contrasting the two groups, those mice that were boosted with a combination of VV and VLPs exhibited marginally higher levels of fecal IgAs than those boosted with VLPs alone, but their fecal IgA levels were significantly higher than the group that was primed with VV only. Interestingly, levels of fecal and vaginal anti-p24 Gag IgAs were too low for detection in all groups. This contrasts sharply with the generally much higher titers of serum anti-p24 Gag IgGs as compared to serum anti-MPER IgGs.

IgG Isotyping

The two major IgG isotypes are IgG1 and IgG2a; the former is consistent with stimulation of a Th2 response for B cell activation, whereas the latter would be indicative of a Th1 response, which primarily results in inflammatory cytokine production and killing of intracellular pathogens (Snapper and Paul, 1987; Szabo et al., 2003). Our results so far indicate that the most important immunogens contributing to the elicitation of serum IgGs are the plant-derived VLPs. To further substantiate this conclusion, we determined the Ab isotypes contributing to this response, as protein-based vaccines (i.e. immune-complexes) usually elicit IgG1 (Martinez and Gordon, 2014; Mosser and Edwards, 2008).

To this end, serum samples from the endpoint for the two groups which showed the highest serum IgG responses (VV/VLP and VV/VV+VLP) were analyzed for their IgG isotype content by isotype-specific ELISA (Figure 35A and B, respectively). Both groups show high levels of antigen-specific (either anti-p24 or anti-MPER) IgG1, but levels of IgG2a were too low for detection, in agreement with our hypothesis and data shown in Chapter 3.

Anti-vector Antibody Responses

Having substantiated the contribution of the Gag/dgp41 VLPs for the elicitation of serum Ab responses against the two HIV-1 antigens, the question arose whether or not the viral vector induced production of anti-vector (i.e. anti-VV) serum Abs. Not surprisingly, mice belonging to Group 3 that received a total of three doses of VV (prime plus two boosts) showed significant levels of anti-VV serum IgG at the endpoint (Day 97, Figure 36). However, a single dose of VV at Day 0 was not enough to induce a potent anti-vector response (Group 1).

Gag-specific CD8 T Cell Responses

A major rationale to include Gag in an HIV-1 vaccine, especially a live-vectored one, is its excellent ability to induce cellular responses. To test induction of CD8 T cell responses, the ability of peptides corresponding to known Gag T-cell epitopes to stimulate proliferation of CD8 T-cells was tested among splenocytes obtained from vaccinated animals. One week after the final boost, splenocytes were harvested and stimulated with five CD8 ZM96 Gag peptides that were previously determined to be dominant in C57BL/6 mice (Chowell et al., 2015). Peptides were assessed individually in order to obtain a better resolution of their responses. CD8 T cells were analyzed for IFN-γ or TNF-α production in response to peptide stimulation using cytokine staining and flow cytometry. Little to no TNF-α production was seen in the flow cytometry analysis (data not shown); however, IFN-γ production was detectable in several groups. The group boosted with both VV and VLPs showed significant production of IFN-γ with two of the five Gag peptides, AMQ8 and EVK10, at 2.6 x 10^5 $CD8^+$ IFN-γ^+ T cells (3.5% of $CD8^+$ T cells) and 1.91 x 10^5 $CD8^+$ IFN-γ^+ T cells (2.4%), respectively (Figure 37A-B). The other three peptides, LRS8, VIP8, and YSP9 showed a similar trend as AMQ8 and EVK10 but with slightly lower responses of $CD8^+$ IFN-γ^+ T cells at 1.73 x 10^5 (2.4%), 1.61 x 10^5 (2.1%), and 1.67 x 10^5 cells (2.3%), respectively, but failed to reach significance (Figure 37C-E). When responses from all five peptides are added together, the VV/VV+VLPs group has a total CD8 Gag-specific mean response of 9.53 x 10^5 $CD8^+$ IFN-γ^+ T cells (12.7% of CD8 T cells, Figure 37F). The total Gag-specific CD8 responses of

the other groups show minute differences between groups at 8.0% in Tris/VLP, 5.6% in VV/VLP, and 4.2% in VV/Tris. This suggests that VLPs may be providing some component of the T cell response and potentially boosting the initial VV-primed T cell responses. Future experiments plan to distinguish the roles in these responses.

Experiment 2: VLPs used for Ab Priming and CD8 T Cell Boosting

The results of the initial NYVAC-KC experiment described above showed that the viral vectors were inefficient at inducing Ab responses (Figure 33), and mucosal responses were quite low (Figure 34). Furthermore, priming with protein-based vaccine components has been shown to induce Ab responses that are more protective than priming with a viral vector (Bessa et al., 2012; Link et al., 2012). Additionally, the groups in the initial study did not effectively assess whether VLPs were responsible for partially boosting the VV primed CD8 T cell responses (Figure 37). Therefore, a second experiment was devised to answer whether the VLPs could prime for higher Ab titers and boost VV primed CD8 T cell responses (Figure 38A).

Three groups of C57BL/6 mice (n = 5/group) were given VV prime at a higher dose (10^7 pfu) than the initial study (10^6 pfu) to increase responses, and the vector was administered via scarification (scar.) in an effort to improve Ab production at mucosal sites via access to Langerhans dendritic cells in the epidermis. These groups were boosted with either VV (Group 2-1), VLP (Group 2-2), or VV+VLP (Group 2-3). A fourth group received a VLP prime followed by VV+VLP boosting (VV given via scar., Group 2-4) to mimic the most successful group from Experiment 1 and to compare to a VV prime and VV+VLP boost (Group 2-3). Comparison between VV/VV and VV/VLP will permit analysis of the capacity of VLPs to successfully boost VV-primed CD8 T cell responses. The final two groups were given VV primes via the i.m. route and boosted with either VV alone (Group 2-5) or VV+VLPs (Group 2-6) to compare any difference in viral delivery route on T cell and Ab responses.

VLPs Prime Ab Responses More Efficiently than VV

Consistent with Experiment 1, the group receiving VLP priming (purple triangles) was the only group to have detectable Ab responses to both Gag (Figure 38B) and dgp41 (Figure 38C) prior to the first boost at Day 45. And this group had consistently higher serum IgG levels throughout the course of the experiment, therefore confirming that VLPs are primarily responsible for the Ab responses. However, groups primed with VV and then subsequently boosted with VLPs or VV+VLPs maintain a steadier OD_{450} after boosting when comparing Gag-specific serum IgG (Figure 38B). Furthermore, administering the VV via scarification actually appears to diminish the serum IgG responses, because groups primed with VV and boosted with either VLPs alone (red squares) or VV+VLPs (green triangles) display lower OD 450 nm upon boosting than those receiving VV i.m. (black circles, Figure 38B-C). Overall, responses to MPER were exceedingly transient compared to Gag serum IgG (Figure 38B-C). Though the group primed with VLPs had the highest detectable responses, all groups had detectable MPER-specific serum IgG at the endpoint, with the exception of the two VV/VV (scar. and i.m.). Thus, further implicating that the NYVAC-KC vectors do not elicit strong Ab responses when administered alone, but are capable of maintaining steadier levels of Gag-specific serum IgG upon boosting with VV+VLPs (black circles/green triangles, Figure 38B).

Furthermore, ELISA data from endpoint serum samples show that the only groups achieving a 100% responses rate (5/5 mice) for both Gag (Figure 39A & C) and MPER (Figure 39B & D) responses are those groups which primed with VLPs or VV (i.m.) and boosted with VV+VLPs (purple triangles/black circles). However, VV scarification prime followed by VLPs alone (red squares) or VV+VLPs (green triangles) was still able to achieve an 80% response rate for Gag (Figure 39A & C) and 100% for MPER (Figure 39B & D). Interestingly, though the OD values show that the scarification viral administration may reduce responses (Figure 39A-B), all responding groups achieved similar endpoint titers for both Gag (Figure 39C) and MPER (Figure 39D).

Mucosal Responses for Fecal IgA and Vaginal IgA/IgG

Endpoint (Day 97) fecal samples were analyzed for Gag- (left) and MPER- (right) specific IgA, and vaginal lavage samples were assessed for both antigen-specific IgA and IgG (Figure 40). Administering NYVAC-KC vectors via scarification did not improve the ability to elicit mucosal responses at any site measured. No detectable responses were achieved above mock background levels for either vaginal IgA (Figure 40C-D) or IgG (Figure 40E-F) for either Gag or MPER; thus re-affirming the results of Experiment 1 (Figure 34C). The only case where any group reached a higher mean OD_{450} was VV/VV+VLPs (i.m.) for MPER-specific fecal IgA (black circles, Figure 40B), however, this difference was not statistically significant. Interestingly, this is the same group which had significant MPER-specific fecal IgA in Experiment 1 (Figure 34B). No Gag-specific fecal IgA was detected in this study (Figure 40A), also aligning with results in Experiment 1. Therefore, there was no significant advantage to changing viral administration route, dose, or VLP expression vector in eliciting Ab responses at mucosal sites.

Gag-specific CD8 T Cell Responses are Improved with Scarification and VLP Boosting

One week after the final boost, Gag-specific CD8 T cell responses in the spleen were assessed using a peptide pool of five immunodominant ZM96 Gag epitopes for C57BL/6 mice (Figure 41). CD8 T cell populations were analyzed via flow cytometry for TNF-α and IFN-γ expression, and results are shown as the percentage of all CD8 T cells which are expressing one or both cytokines analyzed.

VLPs are capable of significantly boosting VV-primed T cell responses, noting that VV/VV (blue) achieved 3.1% cytokine-expressing Gag-specific CD8 T cells, and VV/VLP (red) reached 5.7%. Interestingly, the VV/VLP group had the highest CD8 T cell responses overall (5.7% of CD8 T cells) when scarification is used for the virus prime. After a scarification virus prime, boosting with VLPs alone (red) actually induced higher CD8 responses than boosting with both VV+VLPs (green), thus contrasting with the results of the Experiment 1. However, the second highest Gag-specific CD8 T cell responses were achieved by priming with VLPs and boosting with VV+VLPs (purple), reaching 4.5% Gag-specific CD8 T cells. There is no difference between

VV/VV and VV/VV+VLPs for either the i.m. or scarification route. However, scarification achieve slightly higher CD8 T cell responses at 3.1% and 2.7% for VV/VV and VV/VV+VLPs, respectively, compared with 1.8% Gag-specific CD8 T cells for both VV/VV and VV/VV+VLPs when administered via the i.m. route. Though this contrasts with the previous study, it is possible that the increase in dose also increased the anti-vector response, thus resulting in an overall reduction in Gag-specific CD8 T cells.

Experiment 3: In vivo VLP Production by Cop-VLP to Enhance Vector-induced Ab Responses

Several studies have shown that the MPER of gp41 must be in the context of a membrane to elicit bnAbs, and these responses are regulated by immune tolerance due to the self-reactivity of the bnAbs elicited by this region (Haynes et al., 2005; Haynes et al., 2016; Verkoczy et al., 2011; Verkoczy et al., 2013; Verkoczy et al., 2010; Williams et al., 2015; Zhang et al., 2016). Therefore, to enhance the immunogenicity of dgp41, a vector was generated which co-expresses both Gag and dgp41 from the TK locus (Figure 31), as described above. Furthermore, due to toxicity of Gag and dgp41, described above and in Chapter 4, the only VACV strain in which both proteins were successfully introduced was Cop, the parental strain of NYVAC, thus generating Cop-VLP (i.e. co-expressing Gag/dgp41). This vector releases Gag/dgp41 VLPs in the medium of infected cells (Figure 31D), and since both proteins are present within the same viral genome, this permits VLP production *in vivo* without the need for viral co-infection to occur as with the NYVAC-KC-Gag and dgp41 vectors. Additionally, as shown in Experiments 1 and 2, NYVAC-KC-Gag and dgp41 administered together in a mixture do not induce Ab responses in the absence of VLP injections. Therefore, a third experiment (Experiment 3) was designed to assess whether Cop-VLP can effectively prime and/or boost VLP-induced Ab responses.

Four- to six-week-old C57BL/6 mice (Jackson laboratories) were divided into four immunization groups and one mock group (n = 5/group, Figure 42A). The mock group received PBS i.m. injections and was shared with Experiment 2. Two groups received Cop-VLP (referred to as Cop in figures for brevity) priming with 10^7 pfu delivered via i.m. This dose was chosen due to the results of the dose-response experiment in Chapter 4 (Figure 28A). One group was boost

with Cop-VLP and the other with VLPs. VLP injections were prepared in PBS with Ribi adjuvant and administered i.p. The last two groups were both primed with VLPs and either boosted with VLPs or Cop-VLP. Comparison between groups will allow determination of the ability of *in vivo* vectored VLP production to both prime and boost Ab responses and whether it can achieve or surpass the high Ab titers known to be induced with the plant-produced VLPs alone (Kessans et al., 2016).

Cop-VLP Efficiently Primes Ab Responses

Serum IgG was monitored by ELISA at two week intervals for both Gag (Figure 42A) and MPER (Figure 42B). The OD_{450} is shown over the entire course of the experiment for both antigens and revealed that VLP priming induces much higher levels of Gag and MPER-specific responses, achieving a 100% response rate after a single dose (green and orange lines, Figure 42B-C). On the contrary, only one of ten mice receiving Cop-VLP prime responded after a single dose, and only 20% responded (1/5 mice) after three doses at the endpoint for the Cop/Cop group. The Cop/Cop group was the only immunization regimen which did not achieve a 100% response rate after all three doses. This could suggest one of two things, either the dose is not sufficient to induce Ab responses when the virus is administered i.m., or the parental Cop virus has multiple immune modulators which are suppressing the Ab responses. Interestingly, Cop-VLP did show efficient boosting of VLP-primed Gag responses, which continued to increase between the two boosts (orange line) as opposed to the decrease generally seen beyond two weeks post-boost with VLP immunizations (green line, Figure 42B). Consistent with this, the group primed with Cop-VLP and boosted with VLPs (Cop/VLP) sustained steadier levels of Gag-specific serum IgG between the two boosts as well (purple line, Figure 42B).

Furthermore, when looking at only the Day 97 serum IgG responses for Gag (Figure 43A) and MPER (Figure 43B), there is a general trend that groups boosted with VLPs achieve higher Ab levels than those boosted with Cop-VLP. However, while the VLP/Cop group reached OD levels similar to that of the VLP boosted groups, analysis of the endpoint titers for this group revealed that the Ab titers were in fact more similar to the Cop/Cop group for both Gag (Figure

43C) and MPER (Figure 43D). Interestingly, Cop-VLP priming was able to achieve Ab titers on-par with those of three VLP immunizations for both antigens (Figure 43C-D). Therefore, based on the actual endpoint titers, Cop-VLP can prime antigen-specific serum IgG just as effectively as VLPs, though it is not as effective when used to boost VLP-induced Ab responses. Taken together, these results suggest that the best responses are achievable with heterologous prime-boosting.

Mucosal Responses to Gag and MPER for Cop-VLP Vectors

Day 97 endpoint samples were analyzed for IgA and both fecal and vaginal sites in addition to IgG in vaginal lavages (Figure 44). Data is shown as the raw ELISA OD 450 nm values for all samples. Endpoint samples were assessed for fecal IgA to Gag (Figure 44A) and MPER (Figure 44B). Only one mouse had detectable Gag-specific IgA, and was surprisingly part of the Cop/Cop group which had lower serum IgG titers; however, this was a different mouse than the Gag-specific serum IgG responder in this group. Overall, mucosal responses to MPER were very low in fecal samples, however, the VLP/VLP group achieved a higher mean OD_{450} than the mock group, though this was not statistically significant.

Vaginal lavage samples had undetectable IgA for both Gag (Figure 44C) and MPER (Figure 44D). Responses to MPER were also low for vaginal IgG (Figure 44F). However, Gag-specific IgG was detectable in vaginal lavage samples with all groups achieving a higher mean than the mock (Figure 44E). For Gag-specific vaginal IgG, the VLP/VLP group achieved the highest mean. Unfortunately, results for individual mice within each group were too variable to detect statistical significance.

VLPs Induce the Highest Gag-specific CD8 T Cell Responses

One week after the final boost, Gag-specific CD8 T cell responses were assessed as described for Experiment 2 with a Gag peptide pool used for stimulation. The CD8 T cell population was analyzed for TNF-α and IFN-γ cytokine expressing and results are expressed as the percent of CD8 T cells expressing one or both cytokines (Figure 45). Results revealed that

the VLP/VLP group had the highest Gag-specific CD8 T cell responses, at 2.7%. All groups either boosted or primed with Cop-VLP did not achieve significantly higher responses than the mock background level. Therefore, it is likely that the Cop virus has genes which suppress the immune response that are deleted in the NYVAC-KC vector, thus accounting for its enhanced immunogenicity.

Discussion

The RV144 Thai Trial demonstrated the strength of prime/boost vaccination approach by effectively combining two components that were previously shown to be ineffective on their own: a live (albeit non-replicating) canarypox viral vector (ALVAC) and a soluble protein boost (AIDSVAX). The low efficacy of the trial left much to be desired for widespread use as a vaccine while providing the conceptual basis for further improvement (Rerks-Ngarm et al., 2009). The vaccine design strategy presented here makes use of replicating, but highly attenuated, vaccinia virus NYVAC-KC and plant-produced HIV-1 Gag/dgp41 VLPs.

Our approach reflects two hypotheses. First, it is suggested that in addition to their excellent facility in eliciting T cell responses, replicating vectors are expected to increase antigen load, resulting in improved immunogenicity. Second we propose that VLPs would improve presentation of relevant neutralizing determinants to the immune system.

Live recombinant vectors based on viruses belonging to a wide range of families such as adenoviridae, poxviridae, and herpesviridae have been previously tested for their immunogenicity (Buchbinder et al., 2008; Hansen et al., 2013a; Huang et al., 2015; Rerks-Ngarm et al., 2009; Tartaglia et al., 1992a). Considering the relative success of ALVAC within the context of RV144, this study and others have decided to focus on poxviruses [see reviews (Gomez et al., 2012a; Jacobs et al., 2009; Pantaleo et al., 2010)]. ALVAC is based on canarypox, which like other avipoxviruses is naturally attenuated in humans due to its restricted replication in non-avian cells (Taylor and Paoletti, 1988; Taylor et al., 1988), accounting for ALVAC's high safety profile (Corey et al., 2001; Nitayaphan et al., 2004). Similarly, when developing vaccinia-based vaccine vectors, efforts were initially focused on strains that are non-replicating in human cells (e.g. MVA and

NYVAC), due to safety concerns over potential complications with VACV infection in immune-compromised individuals.

NYVAC was originally designed as a highly attenuated vaccine vector by specifically deleting 18 open reading frames from its parental strain (Cop), thus preventing its replication in humans (Tartaglia et al., 1992b). NYVAC has been tested as an HIV-1 vaccine vector and was shown to induce robust, polyfunctional CD4 and CD8 T cell responses to Env and Gag-Pol-Nef (GPN) antigens in vaccinated individuals (Harari et al., 2008; Harari et al., 2012). Because mucosal immune responses are thought to be particularly important in protection against HIV-1, it was significant to note that such responses could be detected in the gut of NYVAC-immunized patients (Perreau et al., 2011).

More recently, intensive research led to partial uncoupling of attenuation and replication in NYVAC-based vectors showing enhanced immunogenicity without compromising their safety. Specifically, re-insertion of two host-range genes yielded NYVAC-KC. This strain is capable of replicating in human cells and displays enhanced immune activation, yet remains highly attenuated in a mouse model of pathogenesis (Kibler et al., 2011; Quakkelaar et al., 2011), thus giving this particular vector many desirable traits of a vaccine vector and was chosen for use in the work presented here.

A large focus of HIV-1 vaccine research is the envelope protein (Env/gp120), and variations thereof. However, gp120 is not highly conserved, and many critical neutralization targets are hidden or are only exposed upon conformational change during viral entry, thus limiting the effectiveness of any nAb response to this antigen (Decker et al., 2005; Labrijn et al., 2003; Pancera et al., 2014). Protein engineering has attempted to resolve many of these issues, including the design of SOSIP trimeric gp140 variants of Env to make a more structurally accurate target necessary for eliciting specific types of nAbs, including a design to specifically target nAb germline B cells (Billington et al., 2007; Du et al., 2009; Jardine et al., 2013; Sellhorn et al., 2012; Wan et al., 2009). Unfortunately, to date, no successful clinical trials incorporating an engineered gp140 antigen have been conducted. The HIV-1 membrane protein gp41 contains the bnAb target known as the MPER. This region requires the context of a membrane in order to elicit

the partially auto-reactive bnAbs found in HIV-infected patients (Haynes et al., 2005; Verkoczy et al., 2013; Verkoczy et al., 2010; Zhang et al., 2016). In an effort to achieve such responses in vaccination platforms, VLPs offer desirable qualities of enveloped, native virion structure for displaying this important neutralization target.

VLPs are safe, yet immunogenic, components of several vaccines and candidate vaccines for multiple infectious diseases [for a review see (Kushnir et al., 2012)]. The potential for success of VLP-based vaccines is indicated by the widespread use of the human papillomavirus (HPV) vaccines Gardasil® (Merck & Co., 2006) and Cervarix® (GlaxoSmithKline, 2014). To date, many plant-produced vaccines have been tested in animal studies for immunogenicity for both human and veterinary diseases (Rybicki, 2010; Scotti and Rybicki, 2013). The plant-produced HIV-1 VLPs described here have the advantage of displaying the MPER of gp41 in the native context of a Gag matrix, providing an immunogenic platform for humoral responses to both antigens (Kessans et al., 2013; Kessans et al., 2016). Additionally, HIV-1 VLPs have been shown to boost T cell responses primed by viral vectors (Pillay et al., 2010). CD8 T cell responses, often targeting the Gag protein, are known to be associated with reduced viral load, making this a key target for protective T cell immunity (Jiao et al., 2006; Kiepiela et al., 2007; Koup et al., 1994; Mudd et al., 2012; Stephenson et al., 2012).

Data presented here shows that infecting susceptible cells with NYVAC-KC-Gag with or without NYVAC-KC-dgp41 releases, respectively, ~100 nm Gag or Gag/dgp41 VLPs into the extracellular medium (Figure 30E). Such particles can be seen by TEM budding out of the cell (Figure 32B-2 and D-2). Interestingly, dgp41 is detected in the medium only when co-expressed with Gag (Figure 30E), a result compatible with the notion the two proteins assemble at the plasma membranes of cells in culture to form VLPs. Although HIV-1 VLPs produced by other VACV-based vectors were previously shown to elicit both humoral and cellular immunity (Chen et al., 2005; Goepfert et al., 2011), in the experiments presented here, no Abs were detectable in any group until after the first plant-derived VLP immunization (Figure 33B-C, Figure 38B-C). Among several potential explanations, the simplest one is that production of Gag/dgp41 VLPs *in vivo* necessitates co-infection of the same cell by the two viruses; this is achievable under cell

culture conditions where high MOI can be ensured, but is unlikely to occur in an animal. In an effort to accomplish *in vivo* formation of Gag/dgp41 VLPs launched from a VACV vector, the NYVAC parental strain, Cop, was engineered to co-express both proteins from the TK locus of a single recombinant virus, denoted Cop-VLP (Figure 31A). Infection with Cop-VLP showed a similar release of Gag/dgp41 into the growth medium, yet does not require co-infection of two viruses, making this a promising vector for *in vivo* studies (Figure 31D). Indeed, Cop-VLP was able to both prime and, to a lesser extent, boost plant-produced VLP-induced Ab responses (Figure 42B-C, Figure 43C-D). However, this vector worked best in a heterologous prime/boost system, because three doses of Cop-VLP resulted in a 20% response rate with low Ab titers (Figure 43).

Another possible reason for the limited functionality of the NYVAC-KC vectors is the poor replication and/or spread in mice, potentially due to the cytotoxicity represented by protein precipitates in the cytoplasm and nuclear condensation in NYVAC-KC-Gag-, dgp41- or co-infected cells (Figure 32B-D, and Chapter 3). The toxicity seen with TEM strongly correlates to reduced plaque sizes and lower viral titers noted during viral selection (see Chapter 4). Gp41 is known to have a toxic cytoplasmic tail (Micoli et al., 2006; Postler and Desrosiers, 2013), and it is possible that this is responsible for the toxic effects seen in Figure 32. The cytotoxicity of full-length gp160 has largely limited the use of gp41 in vaccine candidates despite the appealing, highly conserved target region of the MPER. Additionally, this is consistent with published data that NYVAC expressing HIV-1 Gag-Pol-Nef induces extensive apoptosis (Gomez et al., 2007). Currently, attempts to resolve this issue are being pursued through other VACV strains which are capable of limiting the toxic effects of the gp41 cytoplasmic tail in an effort to make it easier to produce vaccine candidates with full-length gp160 in its native, structurally accurate conformation (see Chapter 4).

Despite the poor priming capacity of the VV in terms of eliciting Ab responses against Gag and gp41, upon boosting with plant-derived VLPs at Day 45, Ab production spiked with another increase after the final immunization at Day 97 (Figure 33B-C, Figure 38B-C). Endpoint anti-p24 Ab titers reached significant levels for serum IgG in the group boosted with just VLPs or

the combination of VV+VLPs (Figure 35A), and all groups boosted with any combination of VV and VLPs (Groups 2-4) reached significance for MPER-specific serum IgG (Figure 34A). As noted above, due to the lack of detectable Abs prior to boosting with VLPs, it seems that the plant-produced VLPs are largely responsible for boosting the Ab responses following sub-responsive priming. This was confirmed with Experiment 2, where the only group with detectable Ab responses to either Gag or dgp41 prior to boosting was the group primed with VLPs (Figure 38B-C). However, priming with VV (i.m.) and boosting with VV+VLPs resulted in Ab titers which were just as robust as when priming with VLPs and administering the same boost (Figure 39C-D). Though again, the viral vector appears to have little influence on the titer because the VV/VLP group reached similar Ab levels as those boosted with VV+VLPs (Figure 39). The main advantage with VV prime and including VV in the boost appears to be in the steadiness of the Ab responses over time (Figure 38B-C). It is clear that those groups do not experience a rapid decline in Ab responses beyond 14 dpi, thus implicating that the viral vector is somehow sustaining these responses (Figure 38B-C). These results were further corroborated with Cop-VLP inducing a similar phenomenon in which the heterologous prime/boost groups maintain a steady state of Abs over time compared to the VLP/VLP group (Figure 42B-C). However, in this instance, VLP/Cop immunization resulted in much lower titers than the opposite Cop/VLP regimen (Figure 43C-D). For Experiment 1, in the groups with the highest responses, these Abs were shown to be entirely IgG1 with no detectable IgG2a (Figure 35B-C). This agrees with data presented in Chapter 3 showing that plant-produced HIV-1 VLPs stimulate a predominant Th2 response through activation of M2b macrophages, thus inducing strong B cell Ab production.

In the initial study (Experiment 1), Gag-specific CD8 T cell responses were highest in the group boosted with VV+VLPs (Group 3), reaching 12.7% of CD8 T cells expressing IFN-γ in response to the five Gag peptides (Figure 37). When a higher dose was employed in Experiment 2, the Gag-specific T cell responses actually declined from the initial study, indicated anti-vector responses may have been too high to allow substantial Gag-specific responses to develop (Figure 41). However, the use of scarification revealed that VV/VLP and VV/VV+VLPs induced the highest Gag-specific CD8 T cell responses, at 5.7% and 4.5%, respectively (Figure 41).

Interestingly, the use of scarification appeared to reduce the ability of VLPs to boost Ab responses (VV/VLPs, VV/VV+VLPs scar., Figure 38B-C). It is possible that sedation of the mice is largely responsible for the more limited Ab responses seen with scarification than with i.m. delivery, though by the endpoint, titers between these groups achieved highly similar levels (Figure 39C-D). Furthermore, VLPs were able to substantially boost VV-primed CD8 T cell responses (compare scar. VV/VV and VV/VLPs, Figure 41), and the Cop-VLP experiment showed VLPs alone can elicit up to 2.7% Gag-specific CD8 T cells (Figure 45). Cop-VLP administration with or without VLPs induced very low Gag-specific CD8 responses (< 2%) and were not significantly higher than background levels (Figure 45). It is likely that the immune modulators present in Cop that were deleted during the generation of NYVAC are primarily responsible for evading detection, thus limiting its use a vaccine vector. Therefore, a heterologous prime/boost system with NYVAC-KC vectors and plant-produced VLPs achieved almost twice the CD8 T cell response of VV or VLPs alone, and serves as further support for the use of both vaccine components in an immunization regimen.

While a non-replicating vector was not included in this study, these responses are higher than MVA-induced Gag-specific CD8 T cells (< 0.5%) in humans after two doses (Keefer et al., 2011). Additionally, results here show higher Gag-specific CD8 T cell responses than seen in mice after DNA-NYVAC or DNA-MVA prime-boost regimen which elicit < 2% GPN/Env-specific CD8 T cells (< 0.5% Gag specific) and 12-15% GPN/Env-specific CD8 T cells (5.5% Gag-specific), respectively (Garcia-Arriaza et al., 2013; Gomez et al., 2012b). Taken together, this may suggest that replication plays a role in increasing T cell responses. Results from NYVAC HIV-1 vaccines have shown proficiency for eliciting polyfunctional T cell responses (i.e. antigen-specific T cells expressing multiple cytokines) which are primarily effector memory T cells (Garcia-Arriaza et al., 2011; Gomez et al., 2012b; Harari et al., 2008; Harari et al., 2012). This is important to explore in future experiments involving replicating vectors such as NYVAC-KC due to the association of polyfunctional T cells in the periphery with prevention of HIV-1 infection (Betts et al., 2006). Additionally, it is important to note than when Env is included in the MVA or NYVAC vector, T cell responses are skewed to be primarily Env-specific with minimal Gag recognition

(Garcia-Arriaza et al., 2013; Garcia et al., 2011; Gomez et al., 2012b; Harari et al., 2008; Harari et al., 2012; Mooij et al., 2009). Env-specific cytotoxic T lymphocyte (CTL) responses were not protective in clinical trials nor correlated with improved disease in natural infection (McMichael and Koff, 2014), while Gag-specific responses have been correlated with improved CD4 count and reduced viral load (Brander and Walker, 1999; Jiao et al., 2006; Kiepiela et al., 2007; Koup et al., 1994; Ogg et al., 1998; Stephenson et al., 2012) and have epitopes which are less prone to CTL escape (Goulder and Watkins, 2004).

Here it was shown that the combination of NYVAC-KC-Gag/dgp41 replicating vaccinia virus vectors are immunogenic in mice and elicit the best responses when administered together in a regimen closely mimicking the RV144 clinical trial (VV/VV+VLPs). The NYVAC-KC vector is a replicating, but safe, live viral vector with which we can induce higher Gag-specific CD8 T cell responses than with non-replicating poxviral vaccine vectors. Plant-produced VLPs show proficiency for eliciting high Ab titers and may boost T cell responses primed by the NYVAC-KC vectors, though this is the subject of future studies. These vaccine candidates show promise as a cost-effective, scalable vaccine production platform to take forward in an effort to build upon the known success of the RV144 clinical trial to find the elusive HIV-1 vaccine.

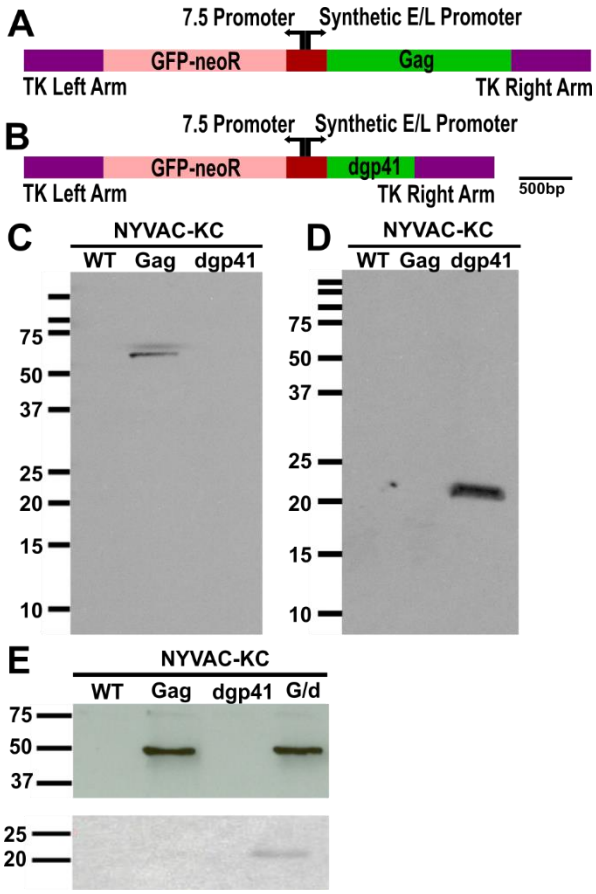

Figure 30 - Generation of Recombinant NYVAC-KC Viruses

Plasmids were cloned to contain either full-length HIV-1 Gag (A) or dgp41 (B) as pTM 815 and 816, respectively. The genes are located between homologous recombination arms for the VACV TK locus under the control of a synthetic early/late (E/L) promoter. Also included is the neomycin resistance gene fused to GFP (GFP-neoR). (C and D) SDS-PAGE shows full-length Gag (C) or dgp41 (D) expression in BSC-40's of NYVAC-KC-Gag (Lane 2) and dgp41 (Lane 3) from the final P2 virus stock used in animal experiments. Parental NYVAC-KC shows no expression of either protein (Lane 1). (E) SDS-PAGE of ammonium sulfate precipitations from media of BSC-40 cells infected with: NYVAC-KC (WT, Lane 1), Gag (Lane 2), dgp41 (Lane 3), or a co-infection of Gag/dgp41 viruses (G/d, Lane 4). Samples were tested for both Gag (top) and dgp41 (bottom) expression.

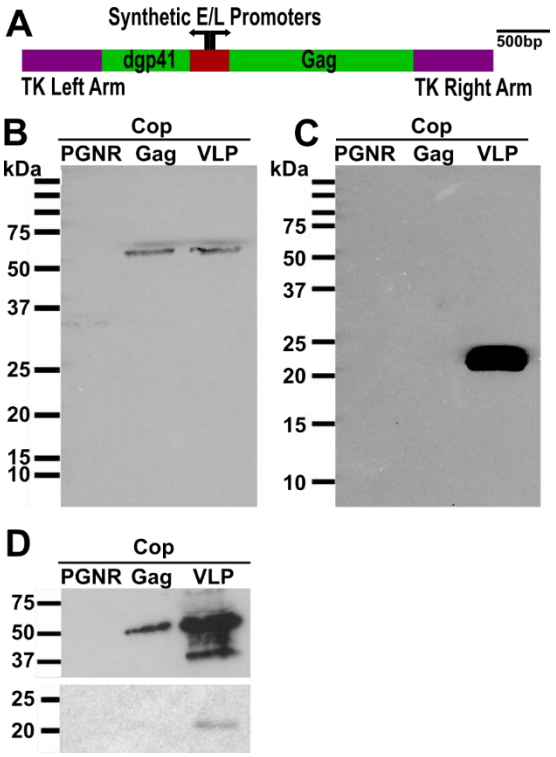

Figure 31 - Generation of Recombinant Cop Viral Vectors

A plasmid was cloned to co-express full-length HIV-1 Gag and dgp41 for insertion into the TK locus (A). Coumermycin selection was used to generate Cop-Gag with pTM 815 and Cop-VLP with pTK-Gag/dgp41 from the parental Cop-PGNR (Gyrase-PKR, neomycin resistance). Expression in BSC-40s is shown for both Gag (B) and dgp41 (C). (D) VLP release into the media is also shown for both Cop vectors for Gag (top) and dgp41 (bottom). Immunoblots were performed after ammonium sulfate precipitation of cellular growth medium of BSC-40s infected with the indicated vectors.

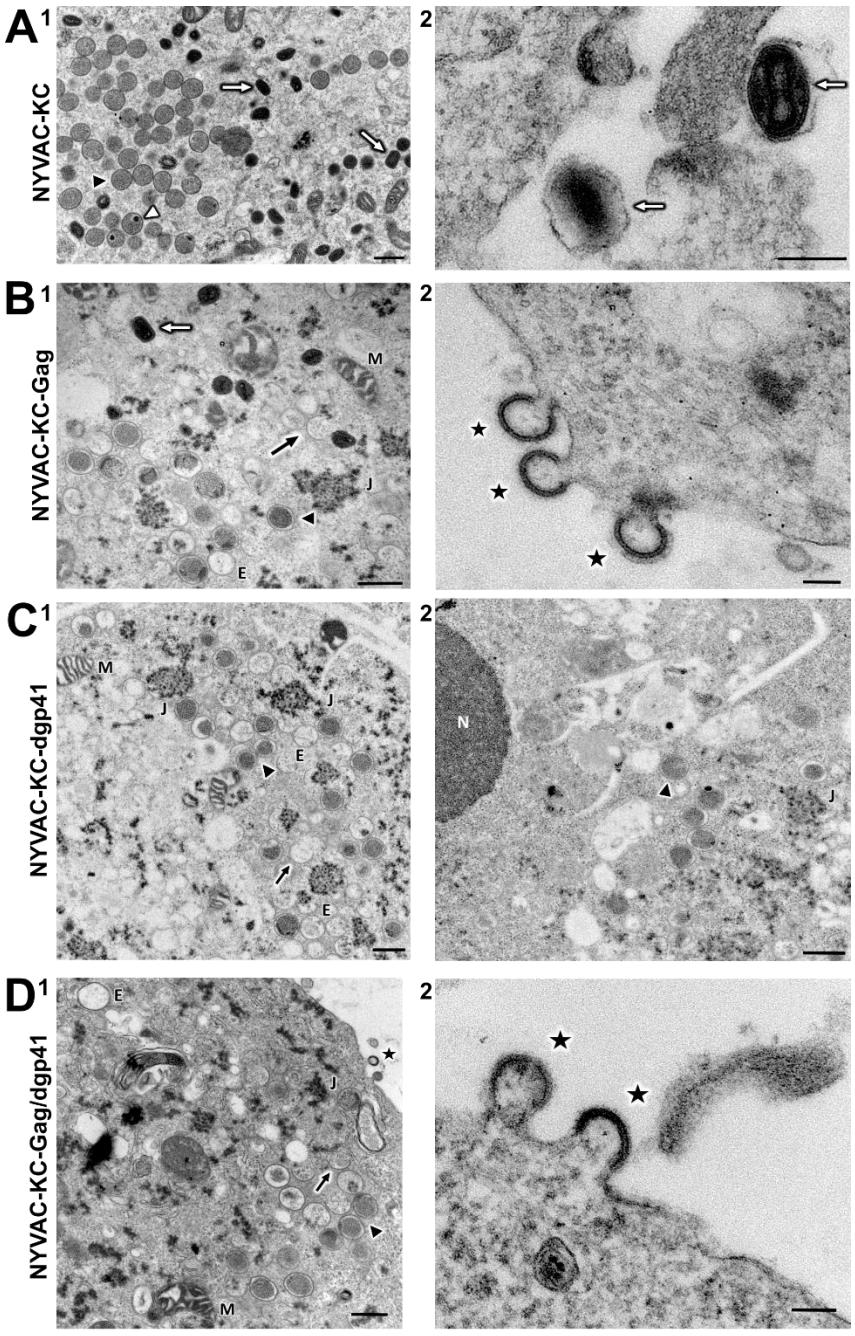

Figure 32 - Electron Microscopy of NYVAC-KC Infected BSC-40s

BSC-40 cells were infected at an MOI of 5 and harvested 24 hpi and prepared for transmission electron microscopy. Cells were infected with either NYVAC-KC (A), NYVAC-KC-Gag (B), NYVAC-KC-dgp41 (C), or a co-infection with an MOI of 5 for each NYVAC-KC-Gag and NYVAC-KC-dgp41 (D). All stages of VACV replication are present: mature virions (white arrow), immature virions (black triangle), immature virions with genome incorporated (white triangle), crescent formation (black arrow), and 'unfilled/empty' virions (E). Budding HIV-1 Gag VLPs (black star) are also seen in those cells infected with NYVAC-KC-Gag. In certain infections, an accumulation of cytoplasmic 'junk' (J) is visible. Other cellular features: mitochondria (M), nucleus (N). Scale bar: 500 nm for all images, except (B-2) and (D-2) images are 100 nm for HIV-1 VLPs.

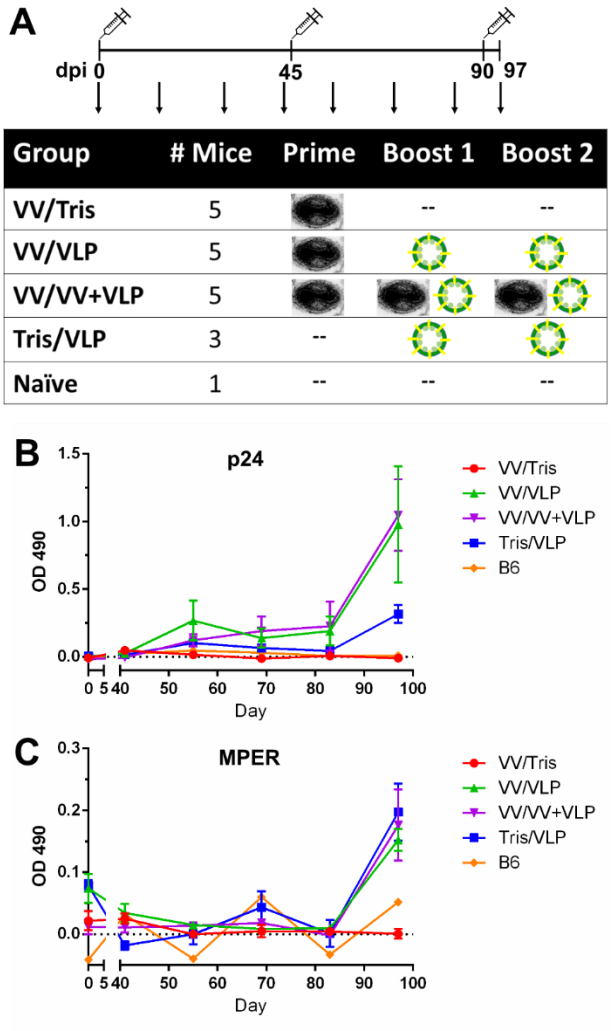

Figure 33 – Experiment 1: Mouse Immunization Schedule for NYVAC-KC Vectors

(A) Six-week-old C57BL/6 mice were immunized at days 0, 45, and 90 with different combinations of recombinant vaccinia virus and plant-produced HIV-1 VLPs, represented as an image of a poxvirus or green-enveloped particles, respectively. Vaccinia virus doses (VV) consisted of 1 x 10^6 pfu of equally mixed NYVAC-KC-Gag and NYVAC-KC-dgp41 delivered i.m. while plant-produced VLPs were mixed with Ribi adjuvant and delivered i.p. with 2 µg p24 and 1.2 µg MPER. Serum, fecal, and vaginal lavage samples were collected once every 2 weeks (indicated by arrows). Serum samples were analyzed for antigen-specific IgG to p24 Gag (B), or the MPER region of dgp41 (C), shown over the length of the experiment as the ELISA OD 490 nm for the 1:50 dilution (lowest tested).

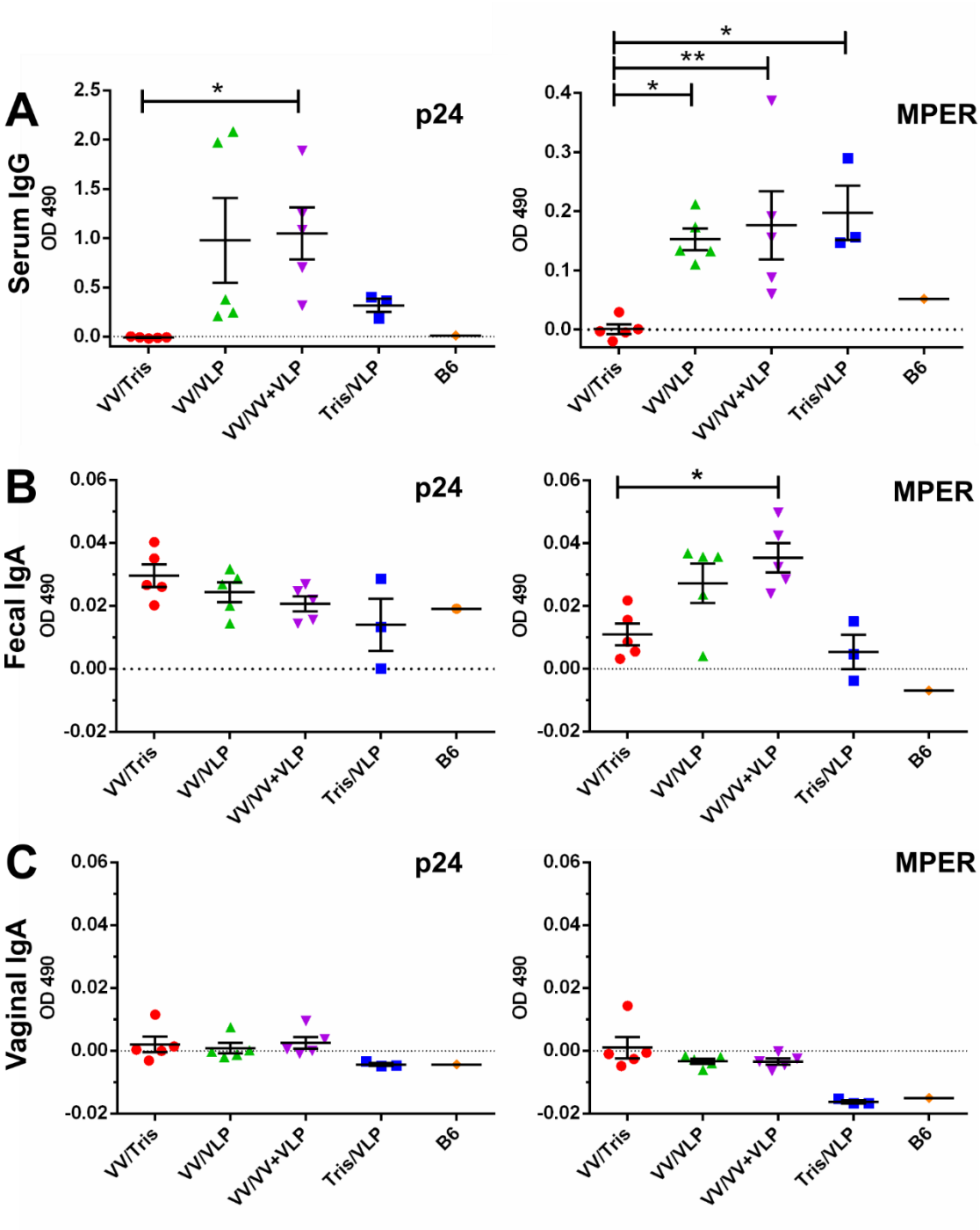

Figure 34 – Experiment 1: Systemic and Mucosal Ab Production with NYVAC-KC Vectors

Endpoint (Day 97) samples were analyzed for serum IgG (A), and mucosal IgA in fecal (B) and vaginal lavage (C) samples. Data is shown for both p24-specific (left) and MPER-specific (right) antibodies. Raw OD 490 nm values are shown for the lowest dilution factor tested (1:50). Statistically significant differences ($p < 0.05$) are indicated with an asterisk (*). Each marker represents a single animal.

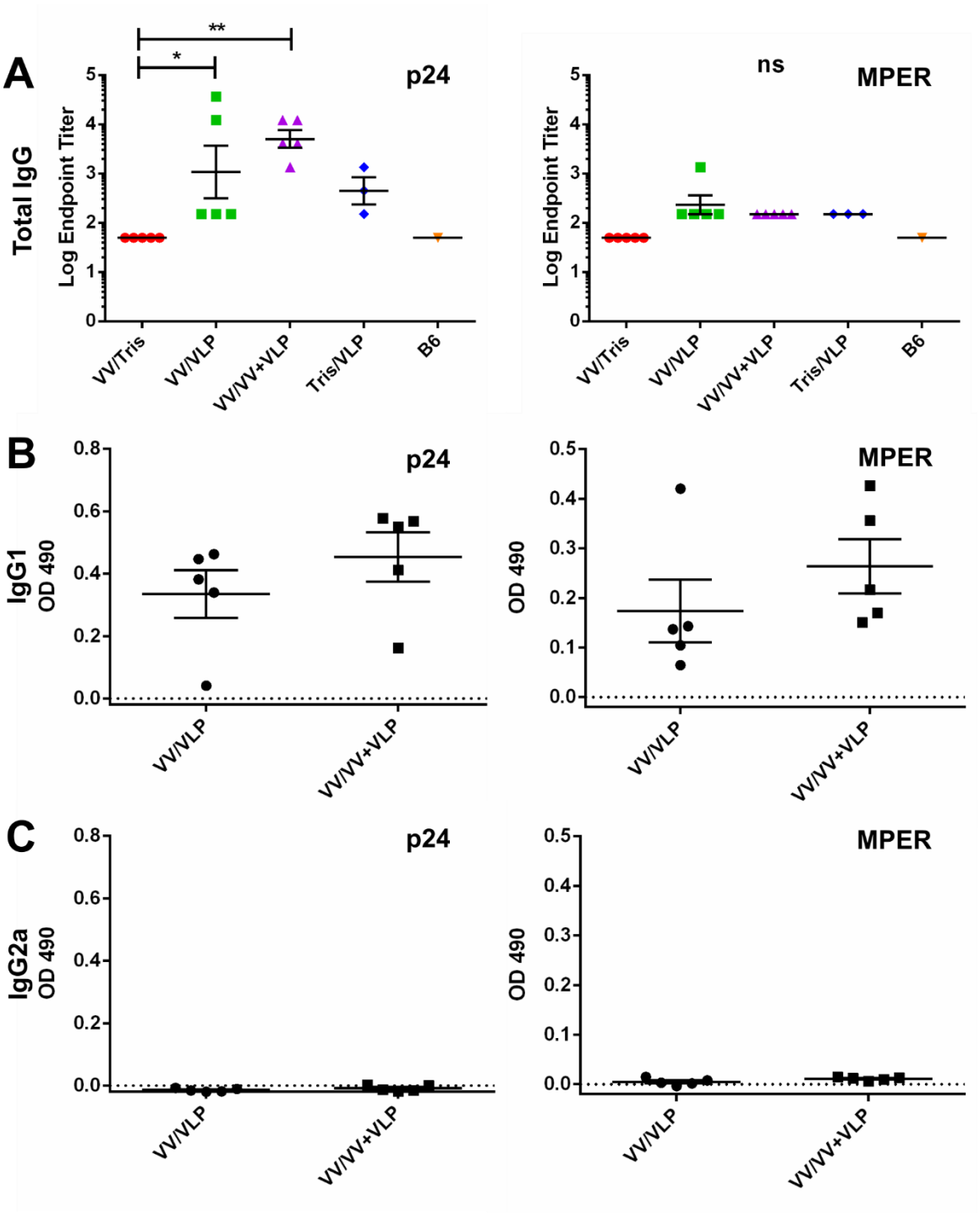

Figure 35 - Experiment 1: Endpoint Serum IgG Titers and Isotyping

(A) Endpoint titers were calculated as the reciprocal of the dilution factor that had background level of OD 490 nm (< 0.1). Isotypes were determined by ELISA for antigen-specific IgG1 (B) or IgG2a (C) for both p24 (left) and MPER (right) serum IgG. OD 490 nm readings are shown and clearly indicate a bias towards IgG1 production for both groups. Only endpoint (Day 97) serum samples were tested for these two groups because they had the highest responses.

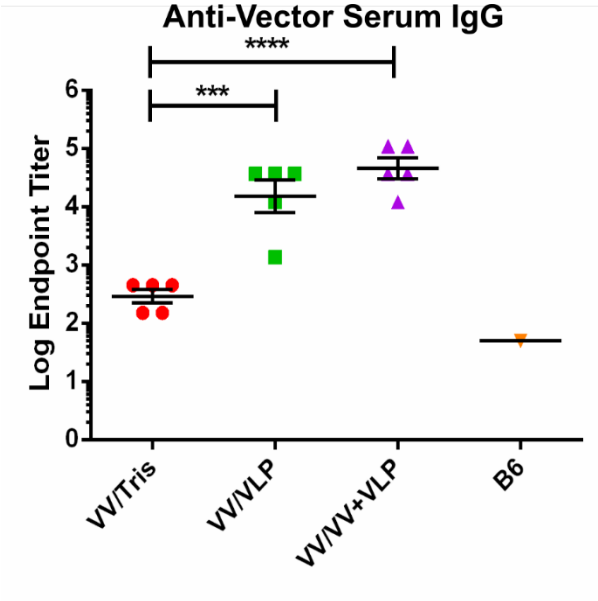

Figure 36 - Experiment 1: Anti-VACV Responses in Serum at Endpoint

Day 97 endpoint serum was analyzed by ELISA for anti-vector responses with endpoint titers calculated as for Gag and dgp41-specific serum IgG. The group which received a total of 3 doses of NYVAC-KC vectors shows significantly higher titers of VV-specific antibodies compared with any other group (purple triangles). (*** $p < 0.001$; **** $p < 0.0001$)

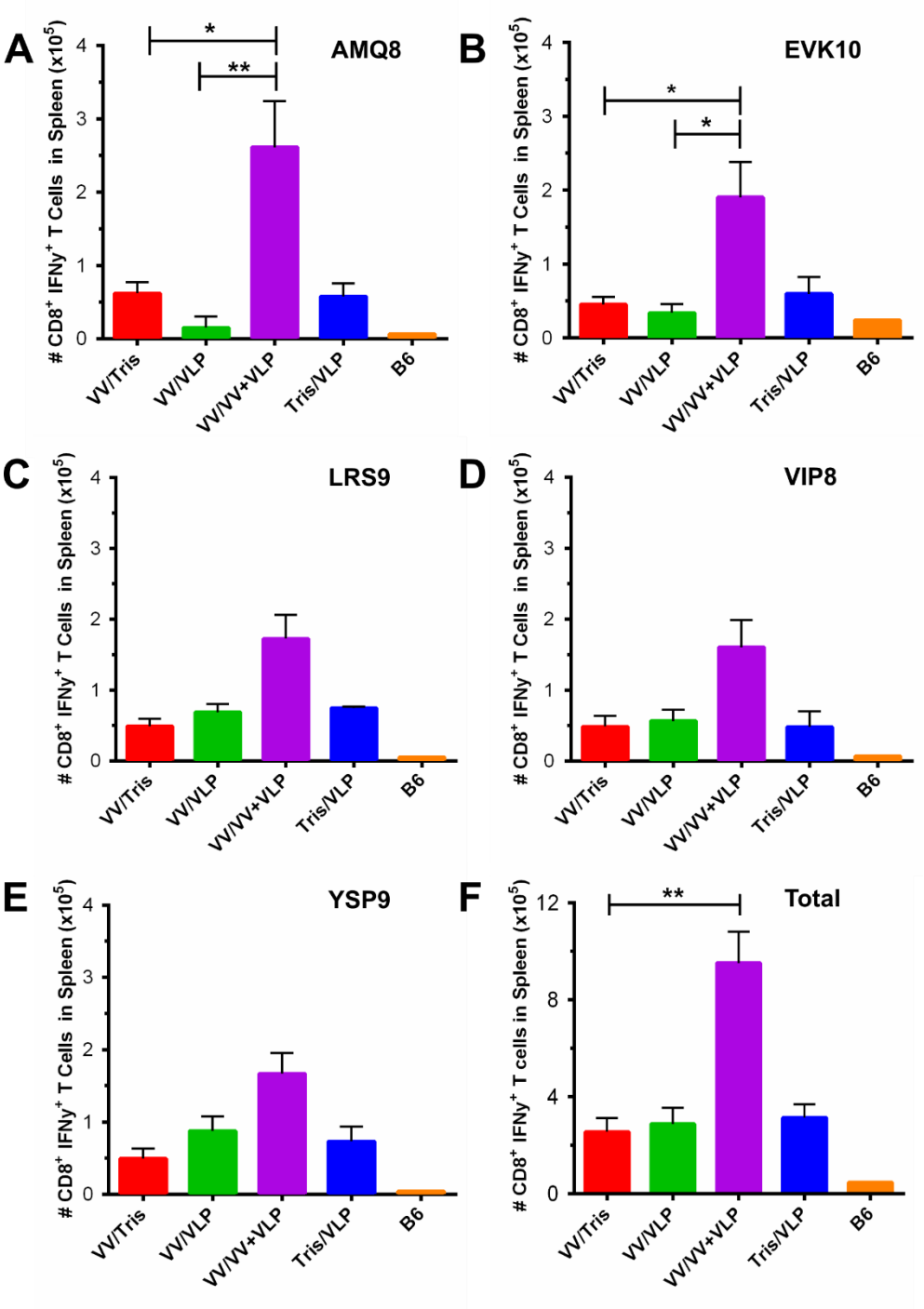

Figure 37 - Experiment 1: Gag-specific CD8 T Cell Responses

One week after the final immunization, peak CD8 T cell responses were measured by intracellular cytokine staining and flow cytometry for 5 immunodominant ZM96 Gag epitopes: AMQ8 (A), EVK10 (B), LRS8 (C), VIP8 (D), and YSP8 (E). Number of IFN-γ$^+$ CD8$^+$ T cells in the spleen is shown for each peptide individually and the total response in the spleen (F) was calculated by adding the individual responses together for each group. The group boosted with VV and VLPs (purple) was significantly higher than the VV/Tris group (red) for two peptides and the overall response. (* $p < 0.05$; ** $p < 0.01$)

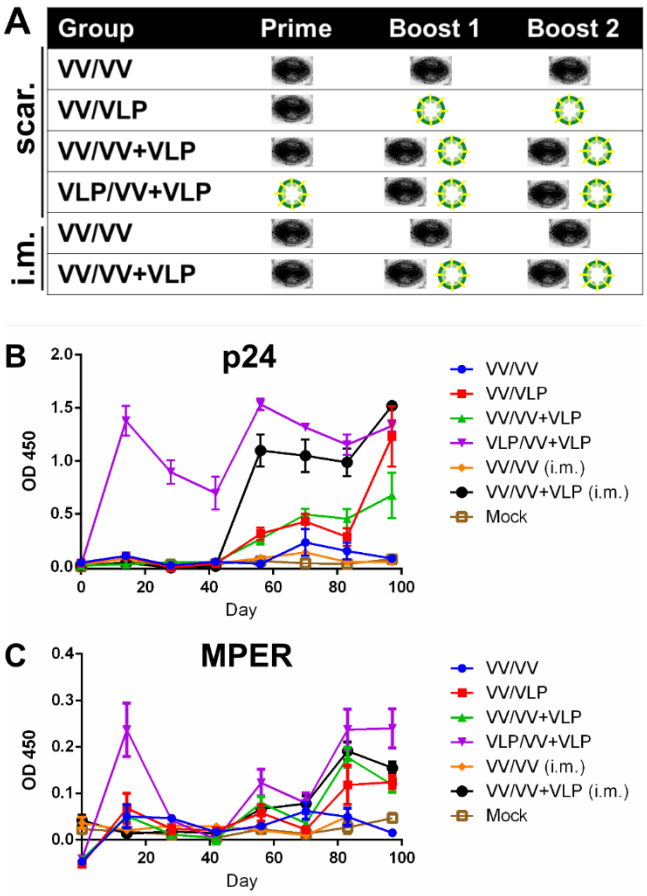

Figure 38 - Experiment 2: Mouse Immunization Schedule and Serum IgG Over Time

(A) Four- to six-week-old C57BL/6 mice (n = 5/group) were immunized at days 0, 45, and 90 with 10^7 pfu of mixed NYVAC-KC-Gag and dgp41 vectors either via scarification (scar.) or i.m. VLPs were mixed with Ribi adjuvant and delivered i.p. The mock group received i.m. injections of PBS and was shared with Experiment 3. Serum IgG specific for p24 Gag (B) or the MPER of dgp41 (C) are shown as OD 450 nm at 2 week intervals.

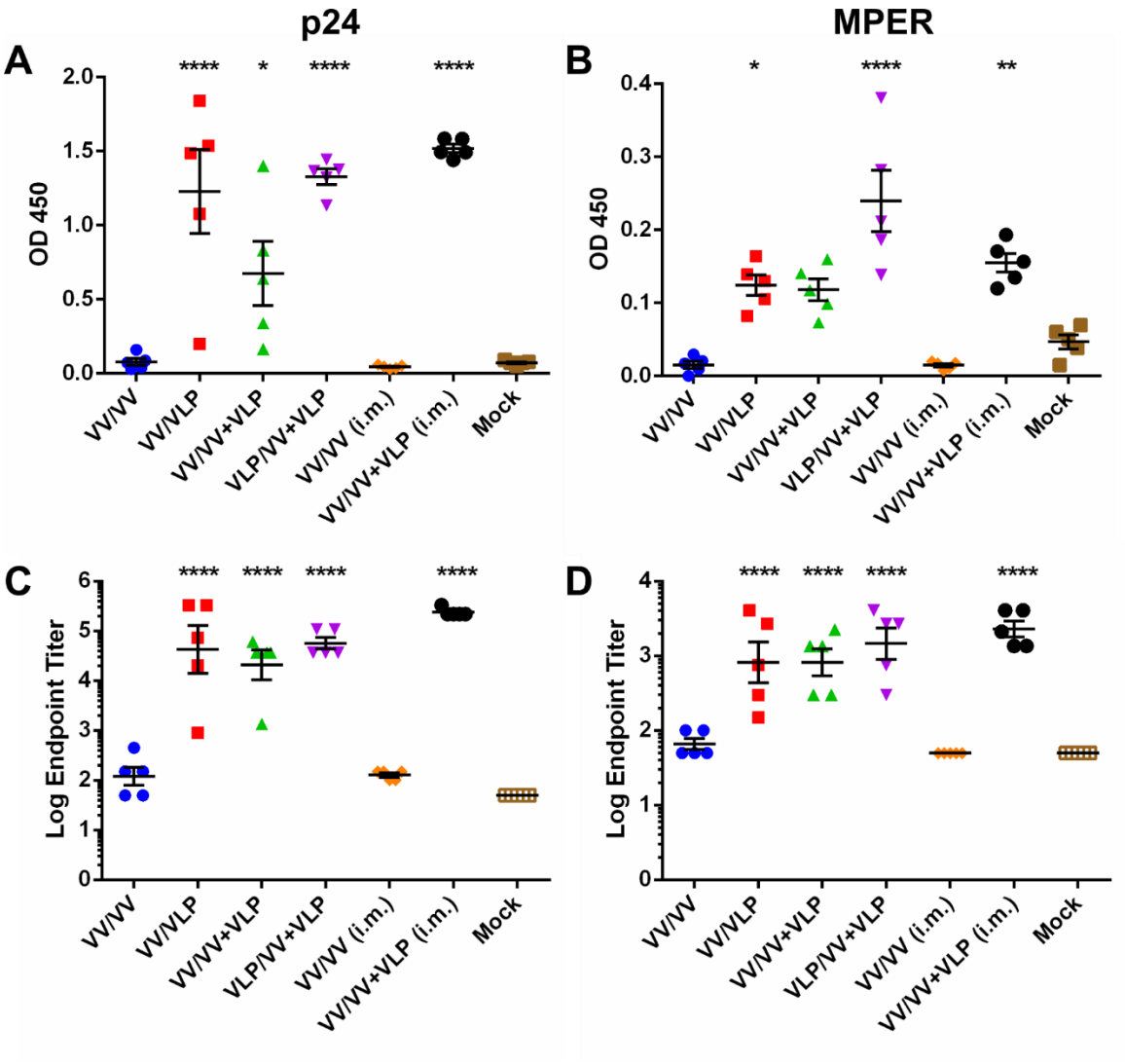

Figure 39 - Experiment 2: Endpoint Serum IgG Responses for Gag and MPER

Endpoint (Day 97) serum samples were analyzed for p24 Gag (left) or MPER (right) specific IgG. The raw ELISA OD 450 nm data is shown for both p24 (A) and MPER (B). Endpoint titers were calculated from this data as the reciprocal of the first dilution at which the OD 450 nm falls below background levels (OD < 0.1). Endpoint titers were log-transformed and are shown for both p24 (C) and MPER (D). Statistical significance is indicated with an asterisk. (* $p < 0.05$; ** $p < 0.01$; **** $p < 0.0001$)

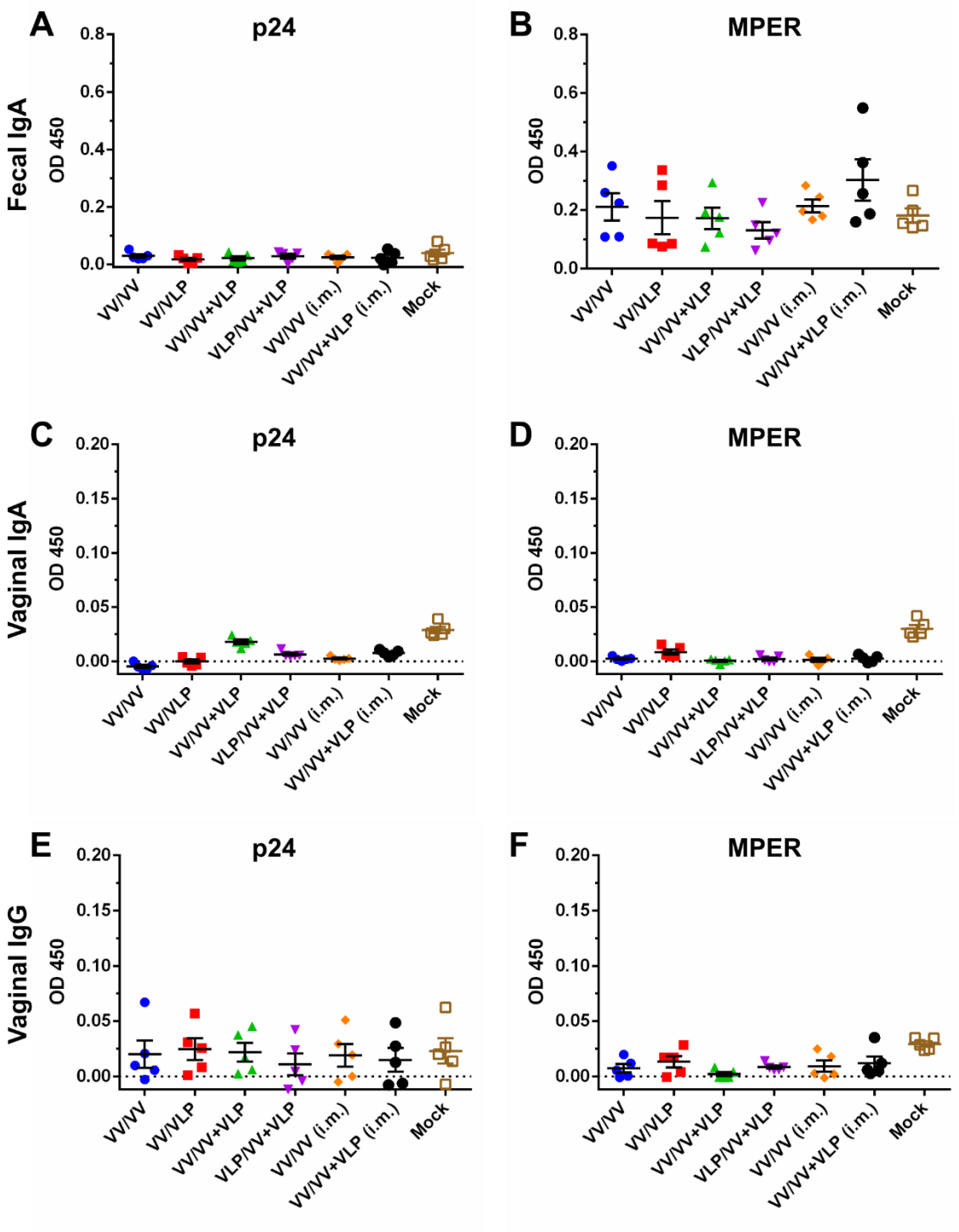

Figure 40 - Experiment 2: Mucosal Responses for Gag and MPER

Endpoint (Day 97) fecal samples were analyzed for antigen-specific IgA and vaginal lavage samples were analyzed for both antigen-specific IgA and IgG. All ELISA data is shown as the raw OD 450 nm value. Each data point represents a single animal. Fecal IgA is shown for both p24 Gag (A) and MPER (B). Vaginal lavage samples were assessed for p24-specfic IgA (C) and IgG (E) and MPER-specific IgA (D) and IgG (F). No statistical significance was found.

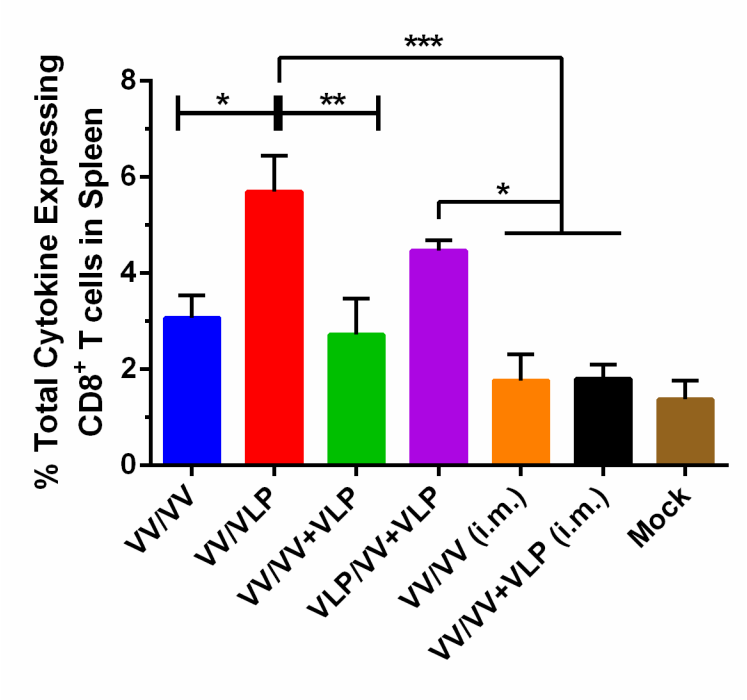

Figure 41 - Experiment 2: Gag-specific CD8 Responses in the Spleen

One-week after the final boost, Gag-specific CD8 responses were measured by incubating splenocytes with a peptide pool consisting of five immunodominant Gag peptides followed by intracellular cytokine staining for TNF-α and IFN-γ. Total cytokine expressing CD8 T cells (i.e. expressing one or both cytokines) are shown as the percent of all CD8 T cells. Statistical significance between groups is indicated with an asterisk. (* $p < 0.05$; ** $p < 0.01$; *** $p < 0.001$)

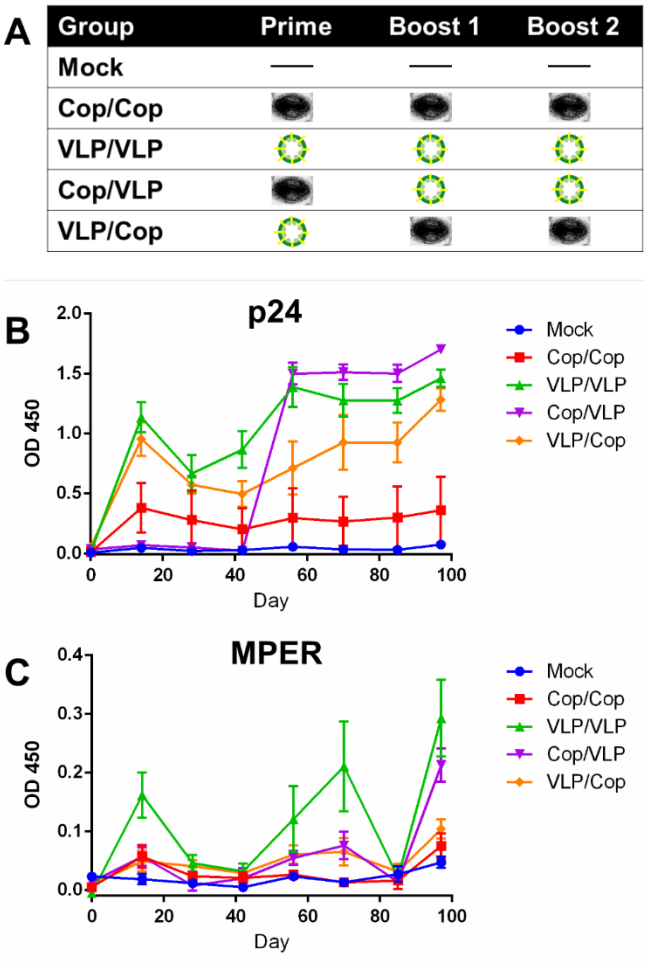

Figure 42 - Experiment 3: Mouse Immunization Regimens and Antigen-specific Serum IgG Over Time

(A) Four- to six-week-old C57BL/6 mice were immunized with the indicated regimens. Cop-VLP (shown as Cop) was administered at 10^7 pfu via the i.m. route. VLPs were prepared in Ribi adjuvant and delivered i.p. Antigen-specific serum IgG was analyzed every two weeks for p24 Gag (B) or MPER (C) responses. Data is shown as the raw OD 450 nm at each time point.

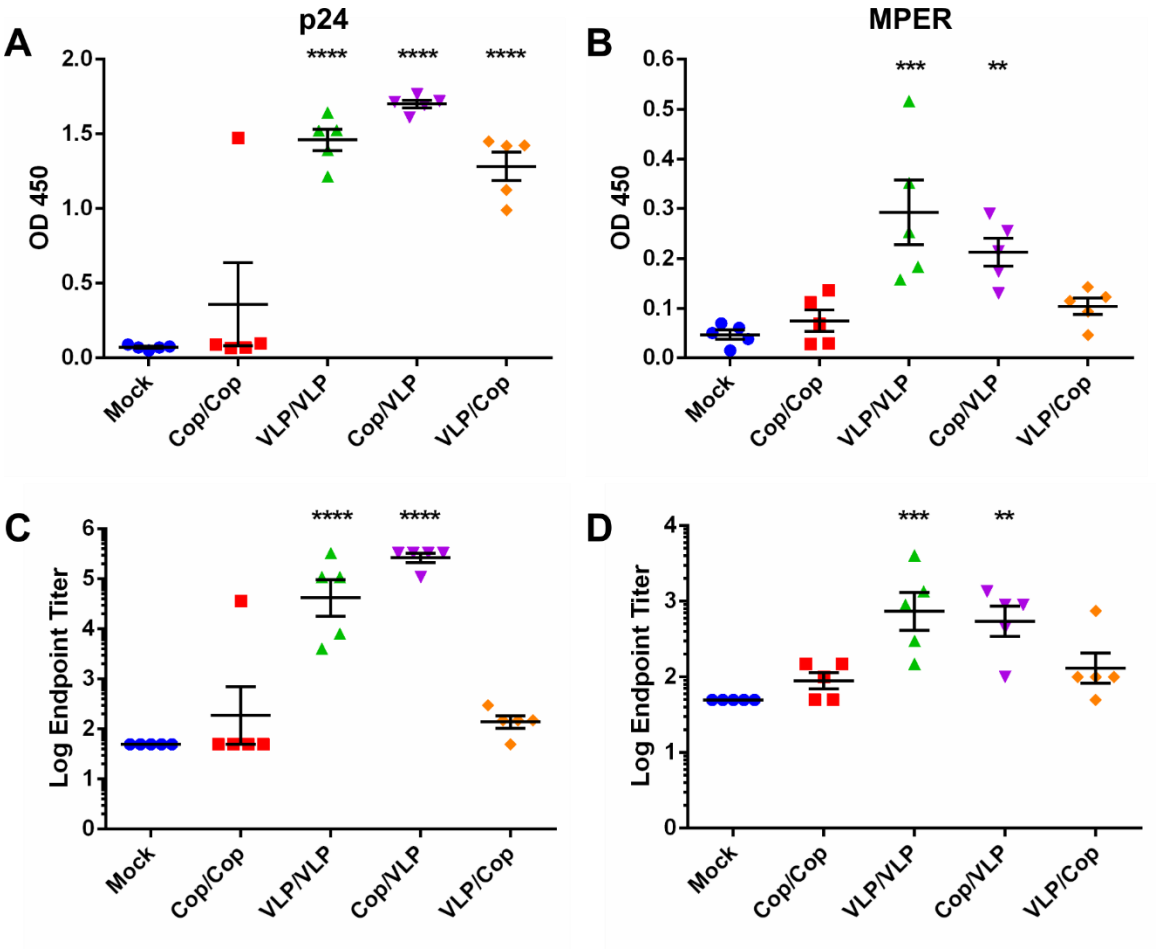

Figure 43 - Experiment 3: Endpoint Serum IgG Responses to Gag and MPER

Endpoint (Day 97) serum samples were analyzed for p24 Gag- (left) or MPER-specific (right) IgG responses. Raw ELISA OD 450 nm data is shown for both p24 (A) and MPER (B). Endpoint titers were calculated from OD 450 nm values as the reciprocal of the first dilution factor where the OD fell below background levels (OD < 0.1). The log of the endpoint titer is shown for p24 (C) and MPER (D) serum IgG responses. Statistical significance is indicated with asterisks. (** $p < 0.01$; *** $p < 0.001$; **** $p < 0.0001$)

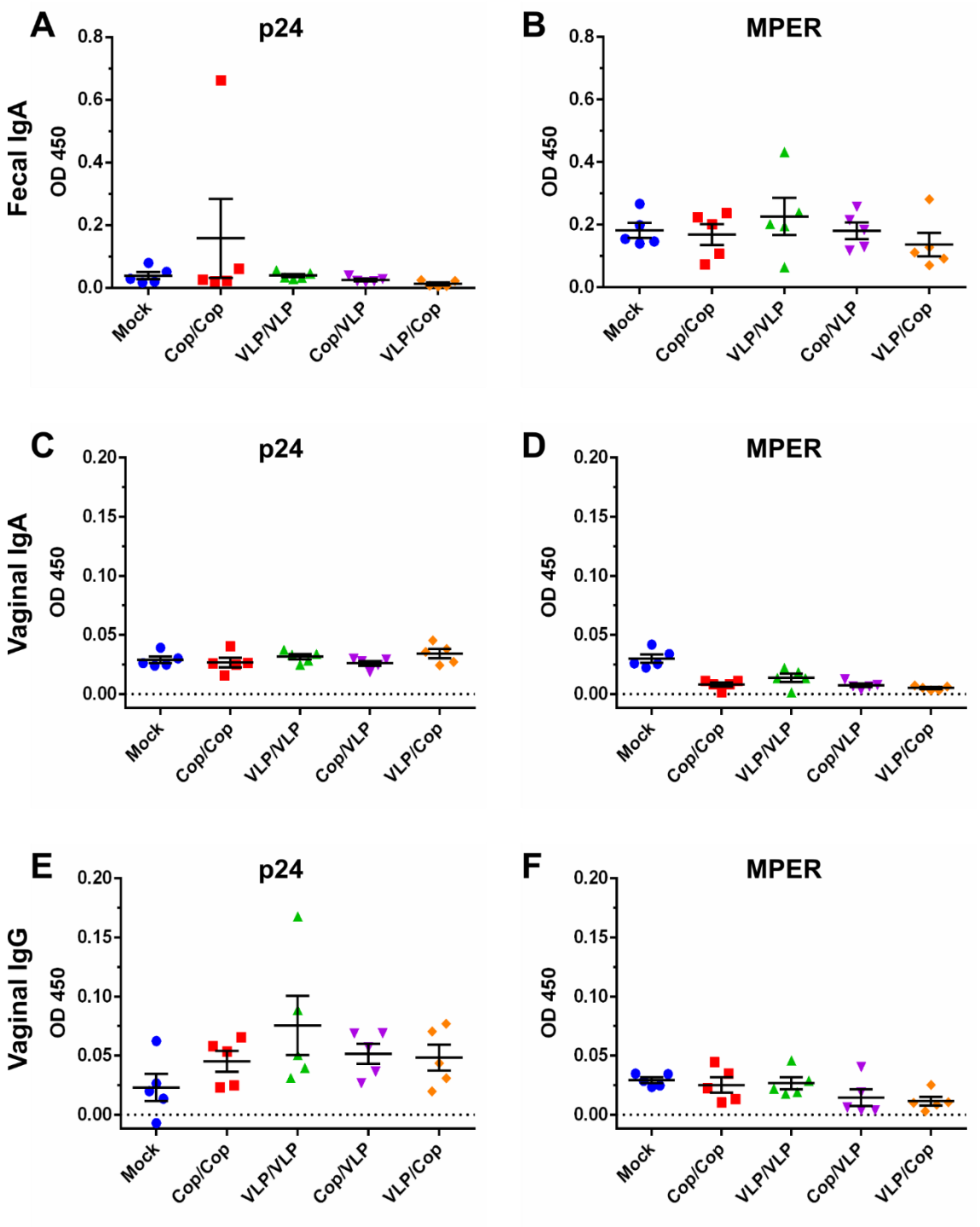

Figure 44 - Experiment 3: Mucosal Responses to Gag and MPER for Cop Vectors

Endpoint (Day 97) fecal samples were assessed for antigen-specific IgA and vaginal lavage samples were analyzed for both antigen-specific IgA and IgG. All data is shown as the raw OD 450 nm values. Each data point represents a single animal. Fecal IgA to both p24 Gag (A) and MPER (B) are shown. Vaginal lavage samples were assessed for p24 Gag-specific IgA (C) and IgG (E) and for MPER-specific IgA (D) and IgG (F). No statistical significance was observed.

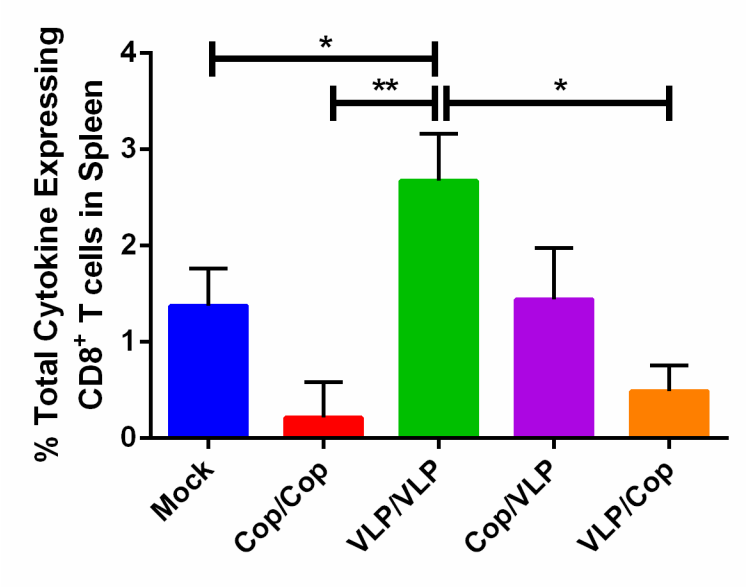

Figure 45 - Experiment 3: Gag-specific CD8 T Cell Responses in the Spleen

One week after the final boost, CD8 T cell responses to Gag were analyzed by incubating splenocytes with a pool of five immunodominant Gag epitopes followed by intracellular cytokine staining for TNF-α and IFN-γ. Total cytokine expressing Gag-specific CD8 T cells (i.e. expressing one or both cytokines) is shown as the percentage of all CD8 T cells in the spleen. Statistical significance between groups is indicated by an asterisk. (* $p < 0.05$; ** $p < 0.01$)

Chapter 6

SUMMARY AND OUTLOOK

The HIV-1 pandemic is a steep burden on society, economically and socially. The millions of new infections each year are disproportionately affecting populations that do not have the infrastructure to properly curb the spread and help those already infected. In the absence of a vaccine, antiretroviral therapy has proven to be the most powerful, yet temporary solution, and treatments are expensive and lifelong. The modest 31% efficacy of the RV144 trial revived hope that an HIV-1 vaccine is achievable (Rerks-Ngarm et al., 2009). The combination of a non-replicating canarypox vector with rgp120 boosting led many others to pursue other poxvirus vectors that were designed to be safe, yet highly immunogenic (Esteban, 2014; Gomez et al., 2012a; Pantaleo et al., 2010). NYVAC represents one of these vectors, and it has shown much success in preliminary phase I/II clinical trials (Table 2). However, NYVAC is non-replicating, and it has been hypothesized that replication-competent viral vectors will enhance immunogenicity through increased antigen presentation and immune activation (Parks et al., 2013). Indeed, the only study in which a vaccine was able to clear an established SIV infection used a replication-competent CMV vector (Hansen et al., 2013a), and this was shown to act through non-canonical MHC II antigen presentation to CD8 T cells (Hansen et al., 2013b). Thus, re-insertion of two genes into NYVAC generated NYVAC-KC, which is proposed as a replicating, immunogenic, and highly attenuated HIV-1 vaccine candidate (Kibler et al., 2011; Quakkelaar et al., 2011).

To further enhance immunogenicity, NYVAC-KC was used in conjunction with plant-produced HIV-1 Gag/dgp41 VLPs to replace the rgp120 used in RV144. These VLPs were previously shown to be immunogenic in mice and are capable of eliciting mucosal responses (Kessans et al., 2016). VLPs represent large immune complexes with high antigen density, as a safe alternative to attenuated HIV-1 vaccines and a more structurally accurate presentation of viral proteins than the soluble gp120 used in RV144, which has since been shown to not engage germline B cell precursors to bnAb lineages (Hoot et al., 2013; McGuire et al., 2014). The HIV-1 transmembrane protein gp41 is proposed here as a more highly conserved target than gp120

(Modrow et al., 1987), which contains the bnAb target MPER (Huang et al., 2012; Purtscher et al., 1994; Zwick et al., 2001). It has been suggested that bnAbs to the MPER are difficult to elicit due to their partial autoreactivity resulting in immune tolerance (Alam et al., 2007; Alam et al., 2009; Haynes et al., 2005; Haynes et al., 2016; Verkoczy et al., 2011; Verkoczy et al., 2013; Verkoczy et al., 2010; Zhang et al., 2016), in addition to the high affinity maturation and somatic mutations found in these B cell lineages (Kepler et al., 2014; Klein et al., 2013a; Liao et al., 2011; Mascola and Haynes, 2013). Therefore, a strong immunogen presenting MPER in the context of a membrane will likely be required in order to effectively elicit prolonged Ab responses that could lead to bnAbs. In studies presented here, NYVAC-KC vectors were successfully used in combination with Gag/dgp41 VLPs to elicit high titer Ab responses and CD8 T cell responses. Furthermore, the interaction of VLPs with the innate immune system was successfully characterized in addition to developing production methods in which the amount of MPER associated with Gag VLPs is increased to provide a higher antigen density.

Other groups have previously expressed full-length p55 Gag in *N. benthamiana* with low yield [44 µg/kg FW, (Meyers et al., 2008)], though this can be substantially increased when expressed in chloroplasts [over 500 mg/kg FW, (Scotti et al., 2009)]. Here efforts achieved enhanced cytoplasmic expression of p55 Gag VLPs, up to 1 mg/kg FW, using either transgenic plants or transient expression with Gemini vectors co-expressing dgp41 and a gene silencing suppressor protein. However, the most promising outcome from comparing different expression vectors was that the ratio of MPER:p24 can be substantially increased when co-expressing Gag and dgp41 transiently with a Dual Gemini +p19 vector. A molar ratio ranging from 1.7-11.8 MPER:p24 Gag, thus achieving the goal of increasing the available antigenic spikes for MPER. VLPs produced with this vector produced 1-2 log higher Ab titers than those produced with the TMV-based vector in our final vaccination studies when immunizations are standardized based on the amount of p24 Gag (compare Experiment 1 with Experiments 2 and 3 in Chapter 5). Future studies will determine whether this increased antigenic sites have any effect on neutralization capacity.

Additionally, plant-produced VLPs were shown to induce Ab responses through a TLR-dependent pathway that results in a Th2-biased response through a $CD11b^+$ population, at least partially consisting of M2b alternatively activated macrophages. Surprisingly, VLP stimulation of all TLRs was detectable, and *ex vivo* experiments with splenocytes from TICAM-/- and MyD88-/- mice suggest that both adaptor proteins are involved in the observed activation. Thus, based on known signaling pathways (Kawai and Akira, 2010; Takeda et al., 2003), TLR4 is likely the primary target of the VLPs, and implicates *A. tumefaciens*-derived LPS as the primary PAMP; however, this has yet to be determined in TLR4-/- mice or LPS-deficient VLPs and/or *A. tumefaciens*. Nucleic acids were also detectable encapsulated within the VLPs, confirming previous reports of Gag VLPs non-specifically incorporating host mRNA (Valley-Omar et al., 2011). It would be interesting to determine whether these RNA species are derived from the plant or the viral expression vector, because Gag VLPs from uninfiltrated plants did not stimulate the nucleic acid TLRs. Future studies should also address whether the RNA remains functional in mammalian cells (i.e. whether translation can occur), and delineate whether the VLPs are being endocytosed and autophagocytosed to deliver the nucleic acids to the endosomal TLRs.

Furthermore, an interesting characteristic of both DC and macrophage activation was the up-regulation of CD40 induced by the VLPs. CD40 is a main co-stimulatory molecule for DC and macrophage regulation of the T cell response (Grewal and Flavell, 1998; Quezada et al., 2004; Schonbeck and Libby, 2001; Summers deLuca and Gommerman, 2012). In binding to CD40L, APCs can initiate a Th1 response to initiate CD8 T cells or a Th2 response for B cell activation through differential cytokine secretion (Mosmann and Coffman, 1989). Soluble CD40L has been used in multiple vaccination studies (Hanks et al., 2005; Lefrancois et al., 2000), including as a type of adjuvant for an HIV-1 poxvirus vaccine (Gomez et al., 2009), to efficiently enhance immunogenicity. Future studies should delineate whether the observed CD40 up-regulation is required for VLP-induced Ab production and CD8 T cell responses.

Interestingly, the VLPs bias the immune response toward Th2, thus potently activating B cells to produce IgG1, as shown in Chapter 3. However, despite the clear Th2 bias in B cell responses, CD8 responses primed by NYVAC-KC vectors were effectively boosted by VLPs

alone, and these were more robust than boosting with NYVAC-KC (Chapter 5, Experiment 2). These characteristics indicate an inherent adjuvancy for the plant-produced VLPs that has not been previously described. Though baculovirus (Buonaguro et al., 2008) and yeast (Tsunetsugu-Yokota et al., 2003) based Gag VLPs have reported innate immune activation, only the latter was traceable to TLR2 stimulation. TLR-based adjuvants are of increasing interest for use in vaccines due to the immunological link between TLR activation and adaptive responses (Akira et al., 2001; Hjelm et al., 2014; Nagpal et al., 2015; Nemazee et al., 2006; Pasare and Medzhitov, 2004; Pasare and Medzhitov, 2005; Schnare et al., 2001; Steinhagen et al., 2011; van Duin et al., 2006). B cells can even be activated in a T-independent manner when binding an antigen while receiving signals from TLRs (Pasare and Medzhitov, 2005). These data suggest that adjuvants and antigens could be strategically matched for tailoring the immune response toward Th1 or Th2 based on the needs of the vaccine. For HIV-1, both potent CD8 T cell and B cell responses will likely be required for long-lived protection, thus the VLPs should be adjuvanted to enhance Th1 responses in an effort to further improve Gag-specific CD8 T cell frequency. Furthermore, a Th2 response results in IgG1, IgG3, and IgG4 isotype switching, but not IgG2a (Fujieda et al., 1995). Based on the comparison between VAX003 and RV144, it is now known that excessive protein boosting can lead to conversion of IgG3 protective Abs toward IgG4 inhibitory responses (Chung et al., 2014). Data here indicated strong bias toward IgG1, per the Th2 response, however, future isotyping should be pursued to characterize the difference in the heterologous prime/boosting regimens on the ratio of IgG3 to IgG4, in addition to determining Ab effector functions and neutralization capacity.

Vaccination studies with the NYVAC-KC vectors revealed that high doses of NYVAC-KC are necessary to induce higher CD8 T cell responses, and that the vectors alone are not good inducers of Ab responses. It is possible that some of this is due to the toxicity to infected cells and the viral vector. The observed toxicity seems to be a result of ER stress from recombinant protein expression and resulting activation of a TBK1-dependent IRF3 pathway. Interestingly, though inhibition of TBK1 abrogates IRF3/IFN-β and PERK signaling, this was unable to rescue viral growth and eIF2α phosphorylation. There are many upstream kinases for eIF2α (de Haro et al.,

1996; Donnelly et al., 2013), thus, it appears there may be redundant pathways involved in inhibiting NYVAC-KC replication when expressing HIV-1 antigens. Furthermore, addition of 10 extra genes in NYVAC-KC (NYVAC+12), including the TBK1 inhibitor C6L (Unterholzner et al., 2011), did not rescue IRF3 phosphorylation. Even Cop-Gag, which contains all genes missing from NYVAC-KC, still displayed IRF3 activation, though this vector was able to induce more potent CD8 T cell responses to Gag at lower doses than NYVAC-KC-Gag. Therefore, while C6L may not be sufficient to rescue IRF3 *in vitro*, NYVAC+12-ZM96 CD8 T cell responses should be directly compared to NYVAC-KC-Gag in a dose response experiment in order to assess the significance of this gene *in vivo*. Others have demonstrated that deletion of C6L from MVA actually enhances immunogenicity (Garcia-Arriaza et al., 2013; Garcia-Arriaza et al., 2011), however, MVA and NYVAC have different genetic deletions, thus the interaction of C6L with immunogenicity of NYVAC-KC should be assessed.

Two genes outside of the K1L to C7L fragment which may be involved in the reduced viral titers for NYVAC-KC-Gag and dgp41 could be B13R and B14R. B13R is an inhibitor of caspase-dependent apoptosis (Dobbelstein and Shenk, 1996; Kettle et al., 1997), while B14R is an inhibitor of NFκB, but not apoptosis (Chen et al., 2008; Graham et al., 2008). Specifically, B14R is of great interest due to its ability to bind to and inhibit IKKα/β and NEMO (Chen et al., 2008), which have been shown to regulate TBK1/IRF3 activation in TNF death receptor and TLR signaling cascades (Clark et al., 2011). The same study also demonstrated a direct interaction between TBK1 and NEMO (Clark et al., 2011), thus the absence of B14R may be the primary reason why the K1L-C7L gene fragment did not rescue signaling. This could further explain why MRT inhibition of TBK1/IRF3, but not IKKα/β regulation of NFκB, results in inability to rescue growth. Future work should include genetic knockouts for TBK1/IRF3 in addition to NFκB and up-stream kinases, especially STING, to delineate the exact pathway activated here. STING is a primary target, because it is involved in inflammasome activation through RIG-I/MAVS at the mitochondria interface, interacts with the secretory pathway from the ER for potential regulation of ER stress through calcium flux, and its ability to stimulate both NFκB and TBK1/IRF3 signaling

pathways (Ishikawa and Barber, 2008), thereby connecting STING to PERK, caspase activation (B13R function), and transcription factor regulation (B14R function).

The final vaccination trials with NYVAC-KC and plant-produced VLPs revealed that VLPs are the primary inducer of Ab responses, but viral vectors can prime and boost VLP-induced B cells responses. In contrast to a single dose of Cop-VLP, Abs could be detected, though the repetitive high dose seemed to decrease Gag-specific CD8 T cell responses compared to a single dose. Thus, the genes deleted from Cop to make NYVAC-KC seem to greatly alter immunogenicity and further support the use of NYVAC-KC as a vaccine vector. Additionally, a VLP prime is supported by reports that VLPs and not soluble antigen are capable of inducing follicular transport of antigen by DCs to enhance presentation to B cells (Bessa et al., 2012; Link et al., 2012), and that NYVAC is a more efficient boosting component than priming immunization (Bart et al., 2014). VLP priming should be directly compared to the common DNA priming used in the EuroVacc NYVAC phase I/II trials to determine whether the stronger Ab prime by VLPs could greatly enhance immunogenicity. Furthermore, an intriguing result showed that heterologous prime/boosting actually seemed to induce a more steady-state Ab response upon boosting than when VLPs were used alone. Similar recent studies using NYVAC and a gp120 boost have shown greatly enhance T cell and Ab responses, as described here (Asbach et al., 2016; Garcia-Arriaza et al., 2015; Hulot et al., 2015; Mooij et al., 2015). Some of these studies even used GPN VLPs with gp140 spikes (Garcia-Arriaza et al., 2015; Perdiguero et al., 2015). Such vectors would be interesting to pursue to determine the effect on the neutralization profile induced by an Env spike lacking a gp41 cytoplasmic tail (CTT), as others have reported significant morphological changes to gp120 when altering the CTT of gp41 (Durham et al., 2012; Kalia et al., 2005; Vzorov et al., 2016). Based on all of the studies above and results described throughout, it is proposed that VLPs should serve as the prime followed by a viral vector plus protein boost to elicit high titer, steady release Ab responses and to elicit more potent CD8 T cell responses than a viral vector prime.

Overall, this dissertation supports the heterologous prime/boost system of plant VLPs and NYVAC-KC HIV-1 vectors as a safe, immunogenic vaccine candidate with unique properties

for high density of MPER antigen on the surface of VLPs, unique innate immune stimulation, and ability to induce robust Ab and CD8 T cell responses. Results described here spawned the pursuit of similar strategies for emerging infectious diseases, including Ebola and Zika vaccines. Zika is an especially intriguing prospect because VACV has been used to produce VLPs *in vivo* for a Zika relative, Japenese encephalitis virus (JEV), which were shown to be protective in mice (Kanesa-thasan et al., 2000; Konishi et al., 1992). Ebola is an interesting concept as well because passive immunization with ZMapp, a plant-produced cocktail of monoclonal Abs, was protective in non-human primates and aided treatment efforts in the recent Ebola outbreak (Qiu et al., 2014). Others have also shown that Ebola VLPs are protective in non-human primates (Warfield et al., 2015), suggesting that the strong Ab induction of VLPs represents desirable platform for an Ebola vaccine. The ability of poxvirus vectors to elicit Ab responses is becoming an increasing focus point for vector research (Draper et al., 2013), thus, enhancing the Ab production by NYVAC-KC would provide a further boost to a heterologous vaccine, and identifying the genes responsible for the *in vitro* and *in vivo* attenuation of NYVAC-KC HIV-1 antigen-expressing vectors should a priority. Thus, NYVAC-KC and plant-produced VLPs have a promising future not only for HIV-1 vaccines, but for many other emerging infectious diseases which require rapid, large-scale production of attenuated, but highly immunogenic constituents capable of inducing potent Ab and T cell responses.

REFERENCES

Abe, T., Harashima, A., Xia, T., Konno, H., Konno, K., Morales, A., Ahn, J., Gutman, D. and Barber, G.N. (2013) STING recognition of cytoplasmic DNA instigates cellular defense. *Molecular Cell* **50**, 5-15.

Aderem, A. (2003) Phagocytosis and the Inflammatory Response. *The Journal of Infectious Diseases* **187**, S340-345.

Akira, S., Takeda, K. and Kaisho, T. (2001) Toll-like receptors: critical proteins linking innate and acquired immunity. *Nature Immunology* **2**, 675-680.

Akira, S., Uematsu, S. and Takeuchi, O. (2006) Pathogen recognition and innate immunity. *Cell* **124**, 783-801.

Alam, S.M., McAdams, M., Boren, D., Rak, M., Scearce, R.M., Gao, F., Camacho, Z.T., Gewirth, D., Kelsoe, G., Chen, P. and Haynes, B.F. (2007) The Role of Antibody Polyspecificity and Lipid Reactivity in Binding of Broadly Neutralizing Anti-HIV-1 Envelope Human Monoclonal Antibodies 2F5 and 4E10 to Glycoprotein 41 Membrane Proximal Envelope Epitopes. *The Journal of Immunology* **178**, 4424-4435.

Alam, S.M., Morelli, M., Dennison, S.M., Liao, H.X., Zhang, R., Xia, S.M., Rits-Volloch, S., Sun, L., Harrison, S.C., Haynes, B.F. and Chen, B. (2009) Role of HIV membrane in neutralization by two broadly neutralizing antibodies. *Proceedings of the National Academy of Sciences of the United States of America* **106**, 20234-20239.

Archin, N.M., Liberty, A.L., Kashuba, A.D., Choudhary, S.K., Kuruc, J.D., Crooks, A.M., Parker, D.C., Anderson, E.M., Kearney, M.F., Strain, M.C., Richman, D.D., Hudgens, M.G., Bosch, R.J., Coffin, J.M., Eron, J.J., Hazuda, D.J. and Margolis, D.M. (2012) Administration of vorinostat disrupts HIV-1 latency in patients on antiretroviral therapy. *Nature* **487**, 482-485.

Aregger, M., Borah, B.K., Seguin, J., Rajeswaran, R., Gubaeva, E.G., Zvereva, A.S., Windels, D., Vazquez, F., Blevins, T., Farinelli, L. and Pooggin, M.M. (2012) Primary and secondary siRNAs in geminivirus-induced gene silencing. *PLoS Pathogens* **8**, e1002941.

Arfi, Z.A., Hellwig, S., Drossard, J., Fischer, R. and Buyel, J.F. (2016) Polyclonal antibodies for specific detection of tobacco host cell proteins can be efficiently generated following RuBisCO depletion and the removal of endotoxins. *Biotechnology Journal* **11**, 507-518.

Asbach, B., Kliche, A., Kostler, J., Perdiguero, B., Esteban, M., Jacobs, B.L., Montefiori, D.C., LaBranche, C.C., Yates, N.L., Tomaras, G.D., Ferrari, G., Foulds, K.E., Roederer, M., Landucci, G., Forthal, D.N., Seaman, M.S., Hawkins, N., Self, S.G., Sato, A., Gottardo, R., Phogat, S., Tartaglia, J., Barnett, S.W., Burke, B., Cristillo, A.D., Weiss, D.E., Francis, J., Galmin, L., Ding, S., Heeney, J.L., Pantaleo, G. and Wagner, R. (2016) Potential To Streamline Heterologous DNA Prime and NYVAC/Protein Boost HIV Vaccine Regimens in Rhesus Macaques by Employing Improved Antigens. *Journal of virology* **90**, 4133-4149.

Baba, T.W., Liska, V., Hofmann-Lehmann, R., Vlasak, J., Xu, W., Ayehunie, S., Cavacini, L.A., Posner, M.R., Katinger, H., Stiegler, G., Bernacky, B.J., Rizvi, T.A., Schmidt, R., Hill, L.R., Keeling, M.E., Lu, Y., Wright, J.E., Chou, T.-C. and Ruprecht, R.M. (2000) Human neutralizing monoclonal antibodies of the IgG1 subtype protect against mucosal simian-human immunodeficiency virus infection. *Nature Medicine* **6**, 200-206.

Bai, Y., Qian, C., Qian, L., Ma, F., Hou, J., Chen, Y., Wang, Q. and Cao, X. (2012) Integrin CD11b negatively regulates TLR9-triggered dendritic cell cross-priming by upregulating microRNA-146a. *The Journal of Immunology* **188**, 5293-5302.

Banchereau, J. and Steinman, R. (1998) Dendritic cells and the control of immunity. *Nature* **392**, 245-252.

Barre-Sinoussi, F., Chermann, J., Rey, F., Nugeyre, M., Chamaret, S., Gruest, J., Dauguet, C., Axler-Blin, C., Vezinet-Brun, F., Rouzioux, C., Rozenbaum, W. and Montagnier, L. (1983) Isolation of a T-Lymphotropic Retrovirus from a Patient at Risk for Acquired Immune Deficiency Syndrome (AIDS). *Science* **220**, 868-871.

Bart, P.A., Goodall, R., Barber, T., Harari, A., Guimaraes-Walker, A., Khonkarly, M., Sheppard, N.C., Bangala, Y., Frachette, M.J., Wagner, R., Liljestrom, P., Kraehenbuhl, J.P., Girard, M., Goudsmit, J., Esteban, M., Heeney, J., Sattentau, Q., McCormack, S., Babiker, A., Pantaleo, G., Weber, J. and EuroVacc, C. (2008) EV01: a phase I trial in healthy HIV negative volunteers to evaluate a clade C HIV vaccine, NYVAC-C undertaken by the EuroVacc Consortium. *Vaccine* **26**, 3153-3161.

Bart, P.A., Huang, Y., Karuna, S.T., Chappuis, S., Gaillard, J., Kochar, N., Shen, X., Allen, M.A., Ding, S., Hural, J., Liao, H.X., Haynes, B.F., Graham, B.S., Gilbert, P.B., McElrath, M.J., Montefiori, D.C., Tomaras, G.D., Pantaleo, G. and Frahm, N. (2014) HIV-specific humoral responses benefit from stronger prime in phase Ib clinical trial. *The Journal of Clinical Investigation* **124**, 4843-4856.

Barth, H., Ulsenheimer, A., Pape, G., Diepolder, H., Hoffmann, M., Neumarin-Haefelin, C., Thimme, R., Henneke, P., Klein, R., Paranhos-Baccala, G., Depla, E., Liang, T., Blum, H. and Baumert, T. (2005) Uptake and presentation of hepatitis C virus-like particles by human dendritic cells. *Blood* **205**, 3605-3614.

Beattie, E., Tartaglia, J. and Paoletti, E. (1991) Vaccinia Virus-Encoded eIF-2α Homolog Abrogates the Antiviral Effect of Interferon. *Virology* **183**, 419-422.

Benlahrech, A., Harris, J., Meiser, A., Papagatsias, T., Hornig, J., Hayes, P., Lieber, A., Athanasopoulos, T., Bachy, V., Csomor, E., Daniels, R., Fisher, K., Gotch, F., Seymour, L., Logan, K., Barbagallo, R., Klavinskis, L., Dickson, G. and Patterson, S. (2009) Adenovirus vector vaccination induces expansion of memory CD4 T cells with a mucosal homing phenotype that are readily susceptible to HIV-1. *Proceedings of the National Academy of Sciences of the United States of America* **106**, 19940-19945.

Berges, C., Naujokat, C., Tinapp, S., Wieczorek, H., Hoh, A., Sadeghi, M., Opelz, G. and Daniel, V. (2005) A cell line model for the differentiation of human dendritic cells. *Biochemical and Biophysical Research Communications* **333**, 896-907.

Bessa, J., Jegerlehner, A., Hinton, H.J., Pumpens, P., Saudan, P., Schneider, P. and Bachmann, M.F. (2009) Alveolar macrophages and lung dendritic cells sense RNA and drive mucosal IgA responses. *The Journal of Immunology* **183**, 3788-3799.

Bessa, J., Zabel, F., Link, A., Jegerlehner, A., Hinton, H., Schmitz, N., Bauer, M., Kundig, T.M., Saudan, P. and Bachmann, M.F. (2012) Low-affinity B cells transport viral particles from the lung to the spleen to initiate antibody responses. *Proceedings of the National Academy of Sciences of the United States of America* **109**, 20566-20571.

Bettigole, S.E. and Glimcher, L.H. (2015) Endoplasmic reticulum stress in immunity. *Annual Review of Immunology* **33**, 107-138.

Betts, M.R., Nason, M.C., West, S.M., De Rosa, S.C., Migueles, S.A., Abraham, J., Lederman, M.M., Benito, J.M., Goepfert, P.A., Connors, M., Roederer, M. and Koup, R.A. (2006) HIV nonprogressors preferentially maintain highly functional HIV-specific CD8+ T cells. *Blood* **107**, 4781-4789.

Billington, J., Hickling, T.P., Munro, G.H., Halai, C., Chung, R., Dodson, G.G. and Daniels, R.S. (2007) Stability of a receptor-binding active human immunodeficiency virus type 1 recombinant gp140 trimer conferred by intermonomer disulfide bonding of the V3 loop: differential effects of protein disulfide isomerase on CD4 and coreceptor binding. *Journal of virology* **81**, 4604-4614.

Bomsel, M., Tudor, D., Drillet, A.S., Alfsen, A., Ganor, Y., Roger, M.G., Mouz, N., Amacker, M., Chalifour, A., Diomede, L., Devillier, G., Cong, Z., Wei, Q., Gao, H., Qin, C., Yang, G.B., Zurbriggen, R., Lopalco, L. and Fleury, S. (2011) Immunization with HIV-1 gp41 Subunit Virosomes Induces Mucosal Antibodies Protecting Nonhuman Primates against Vaginal SHIV Challenges. *Immunity* **34**, 269-280.

Bonsignori, M., Alam, S.M., Liao, H.X., Verkoczy, L., Tomaras, G.D., Haynes, B.F. and Moody, M.A. (2012) HIV-1 antibodies from infection and vaccination: insights for guiding vaccine design. *Trends in microbiology* **20**, 532-539.

Boutwell, C.L., Rowley, C.F. and Essex, M. (2009) Reduced viral replication capacity of human immunodeficiency virus type 1 subtype C caused by cytotoxic-T-lymphocyte escape mutations in HLA-B57 epitopes of capsid protein. *Journal of virology* **83**, 2460-2468.

Bowie, A., Kiss-Toth, E., Symons, J.A., Smith, G.L., Dower, S.K. and O'Neill, L.A. (2000) A46R and A52R from vaccinia virus are antagonists of host IL-1 and toll-like receptor signaling. *Proceedings of the National Academy of Sciences of the United States of America* **97**, 10162-10167.

Boyce, M. and Yuan, J. (2006) Cellular response to endoplasmic reticulum stress: a matter of life or death. *Cell Death and Differentiation* **13**, 363-373.

Brander, C. and Walker, B.D. (1999) T lymphocyte responses in HIV-1 infection: implications for vaccine development. *Current opinion in immunology* **11**, 451-459.

Brandt, T.A. and Jacobs, B.L. (2001) Both carboxy- and amino-terminal domains of the vaccinia virus interferon resistance gene, E3L, are required for pathogenesis in a mouse model. *Journal of virology* **75**, 850-856.

Bridge, S., Sharpe, S., Dennis, M., Dowall, S., Getty, B., Anson, D., Skinner, M., Stewart, J. and Blanchard, T. (2011) Heterologous prime-boost immunisation of Chinese cynomolgus macaques using DNA and recombinant poxvirus vectors expressing HIV-1 virus-like particles. *Virology Journal* **8**, 429.

Briggs, J.A. and Krausslich, H.G. (2011) The molecular architecture of HIV. *Journal of Molecular Biology* **410**, 491-500.

Buchbinder, S.P., Mehrotra, D.V., Duerr, A., Fitzgerald, D.W., Mogg, R., Li, D., Gilbert, P.B., Lama, J.R., Marmor, M., del Rio, C., McElrath, M.J., Casimiro, D.R., Gottesdiener, K.M., Chodakewitz, J.A., Corey, L. and Robertson, M.N. (2008) Efficacy assessment of a cell-mediated immunity HIV-1 vaccine (the Step Study): a double-blind, randomised, placebo-controlled, test-of-concept trial. *The Lancet* **372**, 1881-1893.

Buonaguro, L., Tornesello, M.L., Gallo, R.C., Marincola, F.M., Lewis, G.K. and Buonaguro, F.M. (2008) Th2 Polarization in Peripheral Blood Mononuclear Cells from Human Immunodeficiency Virus (HIV)-Infected Subjects, as Activated by HIV Virus-Like Particles. *Journal of virology* **83**, 304-313.

Buonaguro, L., Tornesello, M.L., Tagliamonte, M., Gallo, R.C., Wang, L.X., Kamin-Lewis, R., Abdelwahab, S., Lewis, G.K. and Buonaguro, F.M. (2006) Baculovirus-derived human immunodeficiency virus type 1 virus-like particles activate dendritic cells and induce ex vivo T-cell responses. *Journal of virology* **80**, 9134-9143.

Burdette, D.L. and Vance, R.E. (2013) STING and the innate immune response to nucleic acids in the cytosol. *Nature Immunology* **14**, 19-26.

Burton, D.R. and Mascola, J.R. (2015) Antibody responses to envelope glycoproteins in HIV-1 infection. *Nature Immunology* **16**, 571-576.

Buyel, J.F. and Fischer, R. (2014) Generic chromatography-based purification strategies accelerate the development of downstream processes for biopharmaceutical proteins produced in plants. *Biotechnology Journal* **9**, 566-577.

Buyel, J.F., Woo, J.A., Cramer, S.M. and Fischer, R. (2013) The use of quantitative structure-activity relationship models to develop optimized processes for the removal of tobacco host cell proteins during biopharmaceutical production. *Journal of Chromatography A* **1322**, 18-28.

Buzon, V., Natrajan, G., Schibli, D., Campelo, F., Kozlov, M.M. and Weissenhorn, W. (2010) Crystal structure of HIV-1 gp41 including both fusion peptide and membrane proximal external regions. *PLoS Pathogens* **6**, e1000880.

Cardoso, R.M., Zwick, M.B., Stanfield, R.L., Kunert, R., Binley, J.M., Katinger, H., Burton, D.R. and Wilson, I.A. (2005) Broadly neutralizing anti-HIV antibody 4E10 recognizes a helical conformation of a highly conserved fusion-associated motif in gp41. *Immunity* **22**, 163-173.

Carroll, K., Elroy-Stein, O., Moss, B. and Jagus, R. (1993) Recombinant Vaccinia Virus K3L Gene Product Prevents Activation of Double-stranded RNA-dependent, Initiation Factor 2α-specific Protein Kinases. *The Journal of Biological Chemistry* **268**, 12837-12842.

Chakrabarti, A., Chen, A.W. and Varner, J.D. (2011) A review of the mammalian unfolded protein response. *Biotechnology and bioengineering* **108**, 2777-2793.

Chen, J., Frey, G., Peng, H., Rits-Volloch, S., Garrity, J., Seaman, M.S. and Chen, B. (2014) Mechanism of HIV-1 neutralization by antibodies targeting a membrane-proximal region of gp41. *Journal of virology* **88**, 1249-1258.

Chen, Q. and Lai, H. (2013) Plant-derived virus-like particles as vaccines. *Human vaccines & immunotherapeutics* **9**, 26-49.

Chen, R.A.-J., Ryzhakov, G., Cooray, S., Randow, F. and Smith, G.L. (2008) Inhibition of IκB kinase by vaccinia virus virulence factor B14. *PLoS Pathogens* **4**, e22.

Chen, X., Rock, M.T., Hammonds, J., Tartaglia, J., Shintani, A., Currier, J., Slike, B., Crowe, J.E., Jr., Marovich, M. and Spearman, P. (2005) Pseudovirion particle production by live poxvirus human immunodeficiency virus vaccine vector enhances humoral and cellular immune responses. *Journal of virology* **79**, 5537-5547.

Chesnokova, O., Coutinho, J., Khan, I., Mikhail, M. and Kado, C. (1997) Characterization of flagella genes of *Agrobacterium tumefaciens*, and the effect of a bald strain on virulence. *Molecular Microbiology* **23**, 579-590.

Cho, H.Y., Choi, E.K., Lee, S.W., Kim, K.H., Park, S.J., Lee, C.K. and Lee, S.W. (2011) All-trans retinoic acid induces TLR-5 expression and cell differentiation and promotes flagellin-mediated cell functions in human THP-1 cells. *Immunology Letters* **136**, 97-107.

Chowell, D., Krishna, S., Becker, P.D., Cocita, C., Shu, J., Tan, X., Greenberg, P.D., Klavinskis, L.S., Blattman, J.N. and Anderson, K.S. (2015) TCR contact residue hydrophobicity is a hallmark of immunogenic CD8+ T cell epitopes. *Proceedings of the National Academy of Sciences of the United States of America* **112**, E1754–E1762.

Chun, T.-W., Stuyver, L., Mizell, S.B., Ehler, L.A., Mican, J.A.M., Baseler, M., Lloyd, A.L., Nowak, M.A. and Fauci, A.S. (1997) Presence of an inducible HIV-1 latent reservoir during highly active antiretroviral therapy. *Proceedings of the National Academy of Sciences of the United States of America* **94**, 13193-13197.

Chung, A.W., Ghebremichael, M., Robinson, H., Brown, E., Choi, I., Lane, S., Dugast, A., Schoen, M.K., Rolland, M., Suscovich, T.J., Mahan, A.E., Liao, L., Streeck, H., Andrews, C., Rerks-Ngarm, S., Nitayaphan, S., de Souza, M.S., Kaewkungwal, J., Pitisuttithum, P., Francis, D., Michael, N.L., Kim, J.H., Bailey-Kellogg, C., Ackerman, M.E. and Alter, G. (2014) Polyfunctional Fc-effector profiles mediated by IgG subclass selection distinguish RV144 and VAX003 vaccines. *Science Translational Medicine* **6**, 228ra238.

Čiplys, E., Samuel, D., Juozapaitis, M., Sasnauskas, K. and Slibinskas, R. (2011) Overexpression of human virus glycoprotein precursors induces cytosolic unfolded protein response in *Saccharomyces cerevisiae*. *Microbial Cell Factories* **10**, 37.

Clark, K., Peggie, M., Plater, L., Sorcek, R.J., Young, E.R., Madwed, J.B., Hough, J., McIver, E.G. and Cohen, P. (2011) Novel cross-talk within the IKK family controls innate immunity. *Biochemical Journal* **434**, 93-104.

Clavel , F. and Hance , A.J. (2004) HIV Drug Resistance. *New England Journal of Medicine* **350**, 1023-1035.

Corey, L., Gilbert, P.B., Tomaras, G.D., Haynes, B.F., Pantaleo, G. and Fauci, A.S. (2015) Immune correlates of vaccine protection against HIV-1 acquisition. *Science translational medicine* **7**, 310rv317.

Corey, L., Mulligan, M., Goepfert, P., Sabbaj, S., Clements-Mann, M.L., Harrow, C., Schwartz, D., Dolin, R., Evans, T., Keefer, M.C., Belshe, R., Gorse, G., Frey, S., McElrath, J., Graham, B., Write, P., Spearman, P., Weinhold, K., Montefiori, D., Greenberg, M., Klein, M., El Habib, R., Excler, J.L., Duliege, A.-M., Stablein, D., Wolff, M., Smith, C., Grabowsky, M., Savarese, B. and Walker, M.C. (2001) Cellular and Humoral Immune Responses to a Canarypox Vaccine Containing Human Immunodeficiency Virus Type 1 Env, Gag, and Pro in Combination with RGP120. *The Journal of Infectious Diseases* **183**, 563-570.

Crooks, E.T., Tong, T., Chakrabarti, B., Narayan, K., Georgiev, I.S., Menis, S., Huang, X., Kulp, D., Osawa, K., Muranaka, J., Stewart-Jones, G., Destefano, J., O'Dell, S., LaBranche, C., Robinson, J.E., Montefiori, D.C., McKee, K., Du, S.X., Doria-Rose, N., Kwong, P.D., Mascola, J.R., Zhu, P., Schief, W.R., Wyatt, R.T., Whalen, R.G. and Binley, J.M. (2015) Vaccine-Elicited Tier 2 HIV-1 Neutralizing Antibodies Bind to Quaternary Epitopes Involving Glycan-Deficient Patches Proximal to the CD4 Binding Site. *PLoS Pathogens* **11**, e1004932.

Dai, P., Wang, W., Cao, H., Avogadri, F., Dai, L., Drexler, I., Joyce, J.A., Li, X.D., Chen, Z., Merghoub, T., Shuman, S. and Deng, L. (2014) Modified vaccinia virus Ankara triggers type I IFN production in murine conventional dendritic cells via a cGAS/STING-mediated cytosolic DNA-sensing pathway. *PLoS Pathogens* **10**, e1003989.

Daigneault, M., Preston, J.A., Marriott, H.M., Whyte, M.K. and Dockrell, D.H. (2010) The identification of markers of macrophage differentiation in PMA-stimulated THP-1 cells and monocyte-derived macrophages. *PloS one* **5**, e8668.

Daniell, H., Singh, N.D., Mason, H. and Streatfield, S.J. (2009) Plant-made vaccine antigens and biopharmaceuticals. *Trends in Plant Science* **14**, 669-679.

Davis, K.L., Gray, E.S., Moore, P.L., Decker, J.M., Salomon, A., Montefiori, D.C., Graham, B.S., Keefer, M.C., Pinter, A., Morris, L., Hahn, B.H. and Shaw, G.M. (2009) High titer HIV-1 V3-specific antibodies with broad reactivity but low neutralizing potency in acute infection and following vaccination. *Virology* **387**, 414-426.

de Haro, C., Mendez, R. and Santoyo, J. (1996) The eIF-2α kinases and the control of protein synthesis. *The FASEB Journal* **10**, 1378-1387.

Decker, J.M., Bibollet-Ruche, F., Wei, X., Wang, S., Levy, D.N., Wang, W., Delaporte, E., Peeters, M., Derdeyn, C.A., Allen, S., Hunter, E., Saag, M.S., Hoxie, J.A., Hahn, B.H., Kwong, P.D., Robinson, J.E. and Shaw, G.M. (2005) Antigenic conservation and immunogenicity of the HIV coreceptor binding site. *The Journal of experimental medicine* **201**, 1407-1419.

Deeks, S.G. and Walker, B.D. (2007) Human immunodeficiency virus controllers: mechanisms of durable virus control in the absence of antiretroviral therapy. *Immunity* **27**, 406-416.

Delaloye, J., Filali-Mouhim, A., Cameron, M.J., Haddad, E.K., Harari, A., Goulet, J.P., Gomez, C.E., Perdiguero, B., Esteban, M., Pantaleo, G., Roger, T., Sekaly, R.P. and Calandra, T. (2015) Interleukin-1- and type I interferon-dependent enhanced immunogenicity of an NYVAC-HIV-1 Env-Gag-Pol-Nef vaccine vector with dual deletions of type I and type II interferon-binding proteins. *Journal of virology* **89**, 3819-3832.

Delaloye, J., Roger, T., Steiner-Tardivel, Q.G., Le Roy, D., Knaup Reymond, M., Akira, S., Petrilli, V., Gomez, C.E., Perdiguero, B., Tschopp, J., Pantaleo, G., Esteban, M. and Calandra, T. (2009) Innate immune sensing of modified vaccinia virus Ankara (MVA) is mediated by TLR2-TLR6, MDA-5 and the NALP3 inflammasome. *PLoS Pathogens* **5**, e1000480.

Deml, L., Speth, C., Dierich, M.P., Wolf, H. and Wagner, R. (2005) Recombinant HIV-1 Pr55gag virus-like particles: potent stimulators of innate and acquired immune responses. *Molecular Immunology* **42**, 259-277.

Devito, C., Broliden, K., Kaul, R., Svensson, L., Johansen, K., Kiama, P., Kimani, J., Lopalco, L., Piconi, S., Bwayo, J.J., Plummer, F., Clerici, M. and Hinkula, J. (2000a) Mucosal and Plasma IgA from HIV-1-Exposed Uninfected Individuals Inhibit HIV-1 Transcytosis Across Human Epithelial Cells. *The Journal of Immunology* **165**, 5170-5176.

Devito, C., Hinkula, J., Kaul, R., Lopalco, L., Bwayo, J.J., Plummer, F., Clerici, M. and Broliden, K. (2000b) Mucosal and plasma IgA from HIV-exposed seronegative individuals neutralize a primary HIV-1 isolate. *AIDS* **14**, 1917-1920.

Diomede, L., Nyoka, S., Pastori, C., Scotti, L., Zambon, A., Sherman, G., Gray, C.M., Sarzotti-Kelsoe, M. and Lopalco, L. (2012) Passively Transmitted gp41 Antibodies in Babies Born from HIV-1 Subtype C-Seropositive Women: Correlation between Fine Specificity and Protection. *Journal of virology* **86**, 4129-4138.

DiPerna, G., Stack, J., Bowie, A.G., Boyd, A., Kotwal, G., Zhang, Z., Arvikar, S., Latz, E., Fitzgerald, K.A. and Marshall, W.L. (2004) Poxvirus protein N1L targets the I-kappaB kinase complex, inhibits signaling to NF-kappaB by the tumor necrosis factor superfamily of receptors, and inhibits NF-kappaB and IRF3 signaling by toll-like receptors. *The Journal of Biological Chemistry* **279**, 36570-36578.

Dobbelstein, M. and Shenk, T. (1996) Protection against apoptosis by the vaccinia virus SPI-2 (B13R) gene product. *Journal of virology* **70**, 6479-6485.

Doehle, B.P., Chang, K., Fleming, L., McNevin, J., Hladik, F., McElrath, M.J. and Gale, M., Jr. (2012a) Vpu-deficient HIV strains stimulate innate immune signaling responses in target cells. *Journal of virology* **86**, 8499-8506.

Doehle, B.P., Chang, K., Rustagi, A., McNevin, J., McElrath, M.J. and Gale, M., Jr. (2012b) Vpu mediates depletion of interferon regulatory factor 3 during HIV infection by a lysosome-dependent mechanism. *Journal of virology* **86**, 8367-8374.

Donnelly, N., Gorman, A.M., Gupta, S. and Samali, A. (2013) The eIF2α kinases: their structures and functions. *Cell and Molecular Life Sciences* **70**, 3493-3511.

Draper, S.J., Cottingham, M.G. and Gilbert, S.C. (2013) Utilizing poxviral vectored vaccines for antibody induction-progress and prospects. *Vaccine* **31**, 4223-4230.

Du, S.X., Idiart, R.J., Mariano, E.B., Chen, H., Jiang, P., Xu, L., Ostrow, K.M., Wrin, T., Phung, P., Binley, J.M., Petropoulos, C.J., Ballantyne, J.A. and Whalen, R.G. (2009) Effect of trimerization motifs on quaternary structure, antigenicity, and immunogenicity of a noncleavable HIV-1 gp140 envelope glycoprotein. *Virology* **395**, 33-44.

Du, Z., Treiber, D., McCoy, R.E., Miller, A.K., Han, M., He, F., Domnitz, S., Heath, C. and Reddy, P. (2013) Non-invasive UPR monitoring system and its applications in CHO production cultures. *Biotechnology and bioengineering* **110**, 2184-2194.

Duprez, L., Wirawan, E., Berghe, T.V. and Vandenabeele, P. (2009) Major cell death pathways at a glance. *Microbes and Infection* **11**, 1050-1062.

Durham, N.D., Yewdall, A.W., Chen, P., Lee, R., Zony, C., Robinson, J.E. and Chen, B.K. (2012) Neutralization resistance of virological synapse-mediated HIV-1 Infection is regulated by the gp41 cytoplasmic tail. *Journal of virology* **86**, 7484-7495.

Ebina, H., Misawa, N., Kanemura, Y. and Koyanagi, Y. (2013) Harnessing the CRISPR/Cas9 system to disrupt latent HIV-1 provirus. *Scientific Reports* **3**, 2510.

Egelkrout, E., Rajan, V. and Howard, J.A. (2012) Overproduction of recombinant proteins in plants. *Plant Science* **184**, 83-101.

Engelman, A. and Cherepanov, P. (2012) The structural biology of HIV-1: mechanistic and therapeutic insights. *Nature Reviews Microbiology* **10**, 279-290.

Erridge, C. (2011a) The capacity of foodstuffs to induce innate immune activation of human monocytes in vitro is dependent on food content of stimulants of Toll-like receptors 2 and 4. *British Journal of Nutrition* **105**, 15-23.

Erridge, C. (2011b) Stimulants of Toll-like receptor (TLR)-2 and TLR-4 are abundant in certain minimally-processed vegetables. *Food and Chemical Toxicology* **49**, 1464-1467.

Esteban, M. (2014) Attenuated poxvirus vectors MVA and NYVAC as promising vaccine cadidates against HIV/AIDS. *Human Vaccines* **5**, 867-871.

Fan, S. and Edgington, T. (1991) Coupling of the Adhesive Receptor CD11b/CD18 to Functional Enhancement of Effector Macrophage Tissue Factor Response. *Journal of Clinical Investigation* **87**, 50-57.

Fang, Z.Y., Limbach, K., Tartaglia, J., Hammonds, J., Chen, X. and Spearman, P. (2001) Expression of vaccinia E3L and K3L genes by a novel recombinant canarypox HIV vaccine vector enhances HIV-1 pseudovirion production and inhibits apoptosis in human cells. *Virology* **291**, 272-284.

Feinberg, M.B. and Ahmed, R. (2012) Born this way? Understanding the immunological basis of effective HIV control. *Nature Immunology* **13**, 632-634.

Feller, U., Anders, I. and Mae, T. (2008) Rubiscolytics: fate of Rubisco after its enzymatic function in a cell is terminated. *Journal of Experimental Botany* **59**, 1615-1624.

Feng, G., Goodridge, H., Harnett, M., Wei, X., Nikolaev, A., Higson, A. and Liew, F. (1999) Extracellular Signal-Related Kinase (ERK) and p38 Mitogen-Activated Protein (MAP) Kinases Differentially Regulate the Lipopolysaccharide-Mediated Induction of Inducible Nitric Oxide Synthase and IL-12 in Macrophages: *Leishmania* Phosphoglycans Subvert Macrophage IL-12 Production by Targeting ERK MAP Kinase. *The Journal of Immunology* **163**, 6403-6412.

Ferguson, B.J., Benfield, C.T., Ren, H., Lee, V.H., Frazer, G.L., Strnadova, P., Sumner, R.P. and Smith, G.L. (2013) Vaccinia virus protein N2 is a nuclear IRF3 inhibitor that promotes virulence. *Journal of General Virology* **94**, 2070-2081.

Finzi, D., Hermankova, M., Pierson, T., Carruth, L.M., Buck, C., Chaisson, R.E., Quinn, T.C., Chadwick, K., Margolick, J., Brookmeyer, R., Gallant, J., Markowitz, M., Ho, D.D., Richman, D.D. and Siliciano, R.F. (1997) Identification of a Reservoir for HIV-1 in Patients on Highly Active Antiretroviral Therapy. *Science* **278**, 1295-1300.

Fischer, R., Schillberg, S., Hellwig, S., Twyman, R.M. and Drossard, J. (2012) GMP issues for recombinant plant-derived pharmaceutical proteins. *Biotechnology Advances* **30**, 434-439.

Flynn, N.M., Forthal, D.N., Harro, C.D., Judson, F.N., Mayer, K.H., Para, M.F., rgp, H.I.V.V.S.G. and The rgp, H.I.V.V.S.G. (2005) Placebo-Controlled Phase 3 Trial of a Recombinant Glycoprotein 120 Vaccine to Prevent HIV-1 Infection. *The Journal of Infectious Diseases* **191**, 654-665.

Frey, G., Chen, J., Rits-Volloch, S., Freeman, M.M., Zolla-Pazner, S. and Chen, B. (2010) Distinct conformational states of HIV-1 gp41 are recognized by neutralizing and non-neutralizing antibodies. *Nature structural & molecular biology* **17**, 1486-1491.

Frey, G., Peng, H., Rits-Volloch, S., Morelli, M., Cheng, Y. and Chen, B. (2008) A fusion-intermediate state of HIV-1 gp41 targeted by broadly neutralizing antibodies. *Proceedings of the National Academy of Sciences of the United States of America* **105**, 3739-3744.

Friedl, P., den Boer, A.T. and Gunzer, M. (2005) Tuning immune responses: diversity and adaptation of the immunological synapse. *Nature Reviews Immunology* **5**, 532-545.

Fujieda, S., Zhang, K. and Saxon, A. (1995) IL-4 plus CD40 monoclonal antibody induces human B cells gamma subclass-specific isotype switch: switching to gamma 1, gamma 3, and gamma 4, but not gamma 2. *The Journal of Immunology* **155**, 2318-2328.

Furth, J. and Cohen, S. (1968) Inhibition of mammalian DNA polymerase by the 5′-triphosphate of 1-β-d-arabinofuranosylcytosine and the 5′-triphosphate of 9-β-d-arabinofuranosyladenine. *Cancer Research* **28**, 2061-2067.

Garabagi, F., Gilbert, E., Loos, A., McLean, M.D. and Hall, J.C. (2012) Utility of the P19 suppressor of gene-silencing protein for production of therapeutic antibodies in Nicotiana expression hosts. *Plant biotechnology journal* **10**, 1118-1128.

Garcia-Arriaza, J., Arnaez, P., Gomez, C.E., Sorzano, C.O. and Esteban, M. (2013) Improving Adaptive and Memory Immune Responses of an HIV/AIDS Vaccine Candidate MVA-B by Deletion of Vaccinia Virus Genes (C6L and K7R) Blocking Interferon Signaling Pathways. *PloS one* **8**, e66894.

Garcia-Arriaza, J., Najera, J.L., Gomez, C.E., Tewabe, N., Sorzano, C.O., Calandra, T., Roger, T. and Esteban, M. (2011) A candidate HIV/AIDS vaccine (MVA-B) lacking vaccinia virus gene C6L enhances memory HIV-1-specific T-cell responses. *PloS one* **6**, e24244.

Garcia-Arriaza, J., Perdiguero, B., Heeney, J., Seaman, M., Montefiori, D.C., Labranche, C., Yates, N.L., Shen, X., Tomaras, G.D., Ferrari, G., Foulds, K.E., McDermott, A., Kao, S.F., Roederer, M., Hawkins, N., Self, S., Yao, J., Farrell, P., Phogat, S., Tartaglia, J., Barnett, S.W., Burke, B., Cristillo, A., Weiss, D., Lee, C., Kibler, K., Jacobs, B., Asbach, B., Wagner, R., Ding, S., Pantaleo, G. and Esteban, M. (2015) Head-to-Head Comparison of Poxvirus NYVAC and ALVAC Vectors Expressing Identical HIV-1 Clade C Immunogens in Prime-Boost Combination with Env Protein in Nonhuman Primates. *Journal of virology* **89**, 8525-8539.

Garcia, F., Bernaldo de Quiros, J.C., Gomez, C.E., Perdiguero, B., Najera, J.L., Jimenez, V., Garcia-Arriaza, J., Guardo, A.C., Perez, I., Diaz-Brito, V., Conde, M.S., Gonzalez, N., Alvarez, A., Alcami, J., Jimenez, J.L., Pich, J., Arnaiz, J.A., Maleno, M.J., Leon, A., Munoz-Fernandez, M.A., Liljestrom, P., Weber, J., Pantaleo, G., Gatell, J.M., Plana, M. and Esteban, M. (2011) Safety and immunogenicity of a modified pox vector-based HIV/AIDS vaccine candidate expressing Env, Gag, Pol and Nef proteins of HIV-1 subtype B (MVA-B) in healthy HIV-1-uninfected volunteers: A phase I clinical trial (RISVAC02). *Vaccine* **29**, 8309-8316.

Gardby, E., Chen, X.-J. and Lycke, N. (2000) Impaired CD40-Signaling in CD19-Deficient Mice Selectively Affects Th2-Dependent Isotype Switching. *Scandanavian Journal of Immunology* **53**, 13-23.

Garoff, H., Hewson, R. and Opstelten, D.E. (1998) Virus Maturation by Budding. *Microbiology and Molecular Biology Reviews* **62**, 1171-1190.

Gavin, A., Hoebe, K., Duong, B., Ota, T., Martin, C., Beutler, B. and Nemazee, D. (2006) Adjuvant-enhanced antibody responses occur without Toll-like receptor signaling. *Science* **314**, 1936-1938.

Gilbert, P.B., Peterson, M.L., Follmann, D., Hudgens, M.G., Francis, D.P., Gurwith, M., Heyward, W.L., Jobes, D.V., Popovic, V. and Self, S.G. (2005) Correlation between immunologic responses to a recombinant glycoprotein 120 vaccine and incidence of HIV-1 infection in a phase 3 HIV-1 preventive vaccine trial. *The Journal of Infectious Diseases* **191**, 666-677.

GlaxoSmithKline, I. (2014) Product Monograph - Cervarix.

Gleba, Y., Klimyuk, V. and Marillonnet, S. (2005) Magnifection--a new platform for expressing recombinant vaccines in plants. *Vaccine* **23**, 2042-2048.

Goepfert, P.A., Elizaga, M.L., Sato, A., Qin, L., Cardinali, M., Hay, C.M., Hural, J., DeRosa, S.C., DeFawe, O.D., Tomaras, G.D., Montefiori, D.C., Xu, Y., Lai, L., Kalams, S.A., Baden, L.R., Frey, S.E., Blattner, W.A., Wyatt, L.S., Moss, B., Robinson, H.L., National Institute of, A. and Infectious Diseases, H.I.V.V.T.N. (2011) Phase 1 safety and immunogenicity testing of DNA and recombinant modified vaccinia Ankara vaccines expressing HIV-1 virus-like particles. *The Journal of Infectious Diseases* **203**, 610-619.

Gomez, C.E., Najera, J.L., Jimenez, E.P., Jimenez, V., Wagner, R., Graf, M., Frachette, M.J., Liljestrom, P., Pantaleo, G. and Esteban, M. (2007) Head-to-head comparison on the immunogenicity of two HIV/AIDS vaccine candidates based on the attenuated poxvirus strains MVA and NYVAC co-expressing in a single locus the HIV-1BX08 gp120 and HIV-1(IIIB) Gag-Pol-Nef proteins of clade B. *Vaccine* **25**, 2863-2885.

Gomez, C.E., Najera, J.L., Sanchez, R., Jimenez, V. and Esteban, M. (2009) Multimeric soluble CD40 ligand (sCD40L) efficiently enhances HIV specific cellular immune responses during DNA prime and boost with attenuated poxvirus vectors MVA and NYVAC expressing HIV antigens. *Vaccine* **27**, 3165-3174.

Gomez, C.E., Perdiguero, B., Garcia-Arriaza, J. and Esteban, M. (2012a) Poxvirus vectors as HIV/AIDS vaccines in humans. *Human vaccines & immunotherapeutics* **8**, 1192-1207.

Gomez, C.E., Perdiguero, B., Najera, J.L., Sorzano, C.O., Jimenez, V., Gonzalez-Sanz, R. and Esteban, M. (2012b) Removal of vaccinia virus genes that block interferon type I and II pathways improves adaptive and memory responses of the HIV/AIDS vaccine candidate NYVAC-C in mice. *Journal of virology* **86**, 5026-5038.

Gong, Z., Martin-Garcia, J.M., Daskalova, S.M., Craciunescu, F.M., Song, L., Dorner, K., Hansen, D.T., Yang, J.H., LaBaer, J., Hogue, B.G., Mor, T.S. and Fromme, P. (2015) Biophysical Characterization of a Vaccine Candidate against HIV-1: The Transmembrane and Membrane Proximal Domains of HIV-1 gp41 as a Maltose Binding Protein Fusion. *PloS one* **10**, e0136507.

Gonzalez, J.M. and Esteban, M. (2010) A poxvirus Bcl-2-like gene family involved in regulation of host immune response: sequence similarity and evolutionary history. *Virology Journal* **7**, 59.

Gordon, S. (2003) Alternative activation of macrophages. *Nature Reviews Immunology* **3**, 23-35.

Goulder, P.J. and Watkins, D.I. (2004) HIV and SIV CTL escape: implications for vaccine design. *Nature Reviews Immunology* **4**, 630-640.

Graham, S.C., Bahar, M.W., Cooray, S., Chen, R.A., Whalen, D.M., Abrescia, N.G., Alderton, D., Owens, R.J., Stuart, D.I., Smith, G.L. and Grimes, J.M. (2008) Vaccinia virus proteins A52 and B14 Share a Bcl-2-like fold but have evolved to inhibit NF-kappaB rather than apoptosis. *PLoS Pathogens* **4**, e1000128.

Greenough, T.C., Cunningham, C.K., Muresan, P., McManus, M., Persaud, D., Fenton, T., Barker, P., Gaur, A., Panicali, D., Sullivan, J.L., Luzuriaga, K. and Pediatric, A.C.T.G.P.T. (2008) Safety and immunogenicity of recombinant poxvirus HIV-1 vaccines in young adults on highly active antiretroviral therapy. *Vaccine* **26**, 6883-6893.

Greseth, M.D. and Traktman, P. (2014) De novo fatty acid biosynthesis contributes significantly to establishment of a bioenergetically favorable environment for vaccinia virus infection. *PLoS Pathogens* **10**, e1004021.

Grewal, I. and Flavell, R.A. (1998) CD40 and CD154 in Cell-Mediated Immunity. *Annual Reviews of Immunology* **16**, 111-135.

Guerra, S., Lopez-Fernandez, L.A., Pascual-Montano, A., Najera, J.L., Zaballos, A. and Esteban, M. (2006) Host response to the attenuated poxvirus vector NYVAC: upregulation of apoptotic genes and NF-kappaB-responsive genes in infected HeLa cells. *Journal of virology* **80**, 985-998.

Guerra, S., Najera, J.L., Gonzalez, J.M., Lopez-Fernandez, L.A., Climent, N., Gatell, J.M., Gallart, T. and Esteban, M. (2007) Distinct gene expression profiling after infection of immature human monocyte-derived dendritic cells by the attenuated poxvirus vectors MVA and NYVAC. *Journal of virology* **81**, 8707-8721.

Gutierrez, C. (1999) Geminivirus DNA replication. *Cellular and Molecular Life Sciences* **56**, 313-329.

Hammer, S.M., Sobieszczyk, M.E., Janes, H., Karuna, S.T., Mulligan, M.J., Grove, D., Koblin, B.A., Buchbinder, S.P., Keefer, M.C., Tomaras, G.D., Frahm, N., Hural, J., Anude, C., Graham, B.S., Enama, M.E., Adams, E., DeJesus, E., Novak, R.M., Frank, I., Bentley, C., Ramirez, S., Fu, R., Koup, R.A., Mascola, J.R., Nabel, G.J., Montefiori, D.C., Kublin, J., McElrath, M.J., Corey, L., Gilbert, P.B. and Team, H.S. (2013) Efficacy trial of a DNA/rAd5 HIV-1 preventive vaccine. *The New England Journal of Medicine* **369**, 2083-2092.

Han, C., Jin, J., Xu, S., Liu, H., Li, N. and Cao, X. (2010) Integrin CD11b negatively regulates TLR-triggered inflammatory responses by activating Syk and promoting degradation of MyD88 and TRIF via Cbl-b. *Nature Immunology* **11**, 734-742.

Hanks, B.A., Jiang, J., Singh, R.A., Song, W., Barry, M., Huls, M.H., Slawin, K.M. and Spencer, D.M. (2005) Re-engineered CD40 receptor enables potent pharmacological activation of dendritic-cell cancer vaccines in vivo. *Nature Medicine* **11**, 130-137.

Hansen, S.G., Piatak, M., Jr., Ventura, A.B., Hughes, C.M., Gilbride, R.M., Ford, J.C., Oswald, K., Shoemaker, R., Li, Y., Lewis, M.S., Gilliam, A.N., Xu, G., Whizin, N., Burwitz, B.J., Planer, S.L., Turner, J.M., Legasse, A.W., Axthelm, M.K., Nelson, J.A., Fruh, K., Sacha, J.B., Estes, J.D., Keele, B.F., Edlefsen, P.T., Lifson, J.D. and Picker, L.J. (2013a) Immune clearance of highly pathogenic SIV infection. *Nature* **502**, 100-104.

Hansen, S.G., Sacha, J.B., Hughes, C.M., Ford, J.C., Burwitz, B.J., Scholz, I., Gilbride, R.M., Lewis, M.S., Gilliam, A.N., Ventura, A.B., Malouli, D., Xu, G., Richards, R., Whizin, N., Reed, J.S., Hammond, K.B., Fischer, M., Turner, J.M., Legasse, A.W., Axthelm, M.K., Edlefsen, P.T., Nelson, J.A., Lifson, J.D., Fruh, K. and Picker, L.J. (2013b) Cytomegalovirus vectors violate CD8+ T cell epitope recognition paradigms. *Science* **340**, 1237874.

Harari, A., Bart, P.A., Stohr, W., Tapia, G., Garcia, M., Medjitna-Rais, E., Burnet, S., Cellerai, C., Erlwein, O., Barber, T., Moog, C., Liljestrom, P., Wagner, R., Wolf, H., Kraehenbuhl, J.P., Esteban, M., Heeney, J., Frachette, M.J., Tartaglia, J., McCormack, S., Babiker, A., Weber, J. and Pantaleo, G. (2008) An HIV-1 clade C DNA prime, NYVAC boost vaccine regimen induces reliable, polyfunctional, and long-lasting T cell responses. *The Journal of experimental medicine* **205**, 63-77.

Harari, A., Rozot, V., Cavassini, M., Bellutti Enders, F., Vigano, S., Tapia, G., Castro, E., Burnet, S., Lange, J., Moog, C., Garin, D., Costagliola, D., Autran, B., Pantaleo, G. and Bart, P.A. (2012) NYVAC immunization induces polyfunctional HIV-specific T-cell responses in chronically-infected, ART-treated HIV patients. *European Journal of Immunology* **42**, 3038-3048.

Harding, H., Novoa, I., Zhang, Y., Zeng, H., Wek, R., Schapira, M. and Ron, D. (2000) Regulated Translation Initiation Controls Stress-Induced Gene Expression in Mammalian Cells. *Molecular Cell* **6**, 1099-1108.

Hasbold, J., Hong, J., Kehry, M. and Hodgkin, P.D. (1999) Integrating Signals from IFN-y and IL-4 by B Cells: Positive and Negative Effects on CD40 Ligand-Induced Proliferation, Survival, and Division-Linked Isotype Switching to IgG1, IgE, and IgG2a. *The Journal of Immunology* **163**, 4175-4181.

Haynes, B.F., Fleming, J., St Clair, E.W., Katinger, H., Stiegler, G., Kunert, R., Robinson, J., Scearce, R.M., Plonk, K., Staats, H.F., Ortel, T.L., Liao, H.X. and Alam, S.M. (2005) Cardiolipin polyspecific autoreactivity in two broadly neutralizing HIV-1 antibodies. *Science* **308**, 1906-1908.

Haynes, B.F., Gilbert, P.B., McElrath, J., Zolla-Pazner, S., Tomaras, G.D., Alam, S.M., Evans, D.T., Montefiori, D.C., Karnasuta, C., Sutthent, R., Liao, H.X., DeVico, A.L., Lewis, G.K., Williams, C., Pinter, A., Fong, Y., Janes, H., DeCamp, A., Huang, Y., Rao, M., Billings, E., Karasavvas, N., Robb, M.L., Ngauy, V., De Souza, M.S., Paris, R., Ferrari, G., Bailer, R.T., Soderberg, K.A., Andrews, C., Berman, P.W., Frahm, N., De Rosa, S.C., Alpert, M.D., Yates, N.L., Shen, X., Koup, R.A., Pitisuttihum, P., Kaewkungwal, J., Nitayaphan, S., Rerks-Ngarm, S., Michael, N.L. and Kim, J.H. (2012) Immune-correlates analysis of an HIV-1 vaccine efficacy trial. *The New England Journal of Medicine* **366**, 1275-1286.

Haynes, B.F., Shaw, G.M., Korber, B., Kelsoe, G., Sodroski, J., Hahn, B.H., Borrow, P. and McMichael, A.J. (2016) HIV-Host Interactions: Implications for Vaccine Design. *Cell Host & Microbe* **19**, 292-303.

Hel, Z., Nacsa, J., Tsai, W.-P., Thornton, A., Giuliani, L., Tartaglia, J. and Franchini, G. (2002) Equivalent Immunogenicity of the Highly Attenuated Poxvirus-Based ALVAC-SIV and NYVAC-SIV Vaccine Candidates in SIVmac251-Infected Macaques. *Virology* **304**, 125-134.

Hessell, A.J., Hangartner, L., Hunter, M., Havenith, C.E., Beurskens, F.J., Bakker, J.M., Lanigan, C.M., Landucci, G., Forthal, D.N., Parren, P.W., Marx, P.A. and Burton, D.R. (2007) Fc receptor but not complement binding is important in antibody protection against HIV. *Nature* **449**, 101-104.

Hessell, A.J., Rakasz, E.G., Tehrani, D.M., Huber, M., Weisgrau, K.L., Landucci, G., Forthal, D.N., Koff, W.C., Poignard, P., Watkins, D.I. and Burton, D.R. (2010) Broadly Neutralizing Monoclonal Antibodies 2F5 and 4E10 Directed against the Human Immunodeficiency Virus Type 1 gp41 Membrane-Proximal External Region Protect against Mucosal Challenge by Simian-Human Immunodeficiency Virus SHIV(Ba-L). *Journal of virology* **84**, 1302-1313.

Hetz, C. (2012) The unfolded protein response: controlling cell fate decisions under ER stress and beyond. *Nature Reviews Molecular Cell Biology* **13**, 89-102.

Hjelm, B.E., Kilbourne, J. and Herbst-Kralovetz, M.M. (2014) TLR7 and 9 agonists are highly effective mucosal adjuvants for norovirus virus-like particle vaccines. *Human vaccines & immunotherapeutics* **10**, 410-416.

Hoebe, K., Janssen, E.M., Kim, S.O., Alexopoulou, L., Flavell, R.A., Han, J. and Beutler, B. (2003) Upregulation of costimulatory molecules induced by lipopolysaccharide and double-stranded RNA occurs by Trif-dependent and Trif-independent pathways. *Nature Immunology* **4**, 1223-1229.

Hoebe, K., Janssenn, E. and Beutler, B. (2004) The interface between innate and adaptive immunity. *Nature Immunology* **5**, 971-974.

Holcik, M. and Sonenberg, N. (2005) Translational control in stress and apoptosis. *Nature Reviews Molecular Cell Biology* **6**, 318-327.

Hoot, S., McGuire, A.T., Cohen, K.W., Strong, R.K., Hangartner, L., Klein, F., Diskin, R., Scheid, J.F., Sather, D.N., Burton, D.R. and Stamatatos, L. (2013) Recombinant HIV envelope proteins fail to engage germline versions of anti-CD4bs bNAbs. *PLoS Pathogens* **9**, e1003106.

Horn, M.E., Pappu, K.M., Bailey, M.R., Clough, R.C., Barker, M., Jilka, J.M., Howard, J.A. and Streatfield, S.J. (2003) Advantageous features of plant-based systems for the development of HIV vaccines. *Journal of Drug Targeting* **11**, 539-545.

Hotter, D., Kirchhoff, F. and Sauter, D. (2013) HIV-1 Vpu does not degrade interferon regulatory factor 3. *Journal of virology* **87**, 7160-7165.

Hou, P., Chen, S., Wang, S., Yu, X., Chen, Y., Jiang, M., Zhuang, K., Ho, W., Hou, W., Huang, J. and Guo, D. (2015) Genome editing of CXCR4 by CRISPR/cas9 confers cells resistant to HIV-1 infection. *Scientific Reports* **5**, 15577.

Huang, J., Kang, B.H., Pancera, M., Lee, J.H., Tong, T., Feng, Y., Imamichi, H., Georgiev, I.S., Chuang, G.Y., Druz, A., Doria-Rose, N.A., Laub, L., Sliepen, K., van Gils, M.J., de la Pena, A.T., Derking, R., Klasse, P.J., Migueles, S.A., Bailer, R.T., Alam, M., Pugach, P., Haynes, B.F., Wyatt, R.T., Sanders, R.W., Binley, J.M., Ward, A.B., Mascola, J.R., Kwong, P.D. and Connors, M. (2014) Broad and potent HIV-1 neutralization by a human antibody that binds the gp41-gp120 interface. *Nature* **515**, 138-142.

Huang, J., Ofek, G., Laub, L., Louder, M.K., Doria-Rose, N.A., Longo, N.S., Imamichi, H., Bailer, R.T., Chakrabarti, B., Sharma, S.K., Alam, S.M., Wang, T., Yang, Y., Zhang, B., Migueles, S.A., Wyatt, R., Haynes, B.F., Kwong, P.D., Mascola, J.R. and Connors, M. (2012) Broad and potent neutralization of HIV-1 by a gp41-specific human antibody. *Nature* **491**, 406-412.

Huang, Y., Follmann, D., Nason, M., Zhang, L., Huang, Y., Mehrotra, D.V., Moodie, Z., Metch, B., Janes, H., Keefer, M.C., Churchyard, G., Robb, M.L., Fast, P.E., Duerr, A., McElrath, M.J., Corey, L., Mascola, J.R., Graham, B.S., Sobieszczyk, M.E., Kublin, J.G., Robertson, M., Hammer, S.M., Gray, G.E., Buchbinder, S.P. and Gilbert, P.B. (2015) Effect of rAd5-Vector HIV-1 Preventive Vaccines on HIV-1 Acquisition: A Participant-Level Meta-Analysis of Randomized Trials. *PloS one* **10**, e0136626.

Huang, Z., Chen, Q., Hjelm, B., Arntzen, C. and Mason, H. (2009) A DNA replicon system for rapid high-level production of virus-like particles in plants. *Biotechnology and bioengineering* **103**, 706-714.

Huang, Z., LePore, K., Elkin, G., Thanavala, Y. and Mason, H.S. (2008) High-yield rapid production of hepatitis B surface antigen in plant leaf by a viral expression system. *Plant biotechnology journal* **6**, 202-209.

Hulot, S.L., Korber, B., Giorgi, E.E., Vandergrift, N., Saunders, K.O., Balachandran, H., Mach, L.V., Lifton, M.A., Pantaleo, G., Tartaglia, J., Phogat, S., Jacobs, B., Kibler, K., Perdiguero, B., Gomez, C.E., Esteban, M., Rosati, M., Felber, B.K., Pavlakis, G.N., Parks, R., Lloyd, K., Sutherland, L., Scearce, R., Letvin, N.L., Seaman, M.S., Alam, S.M., Montefiori, D., Liao, H.X., Haynes, B.F. and Santra, S. (2015) Comparison of Immunogenicity in Rhesus Macaques of Transmitted-Founder, HIV-1 Group M Consensus, and Trivalent Mosaic Envelope Vaccines Formulated as a DNA Prime, NYVAC, and Envelope Protein Boost. *Journal of virology* **89**, 6462-6480.

Huppa, J.B. and Davis, M.M. (2003) T-cell-antigen recognition and the immunological synapse. *Nature Reviews Immunology* **3**, 973-983.

Hussain, H., Maldonado-Agurto, R. and Dickson, A.J. (2014) The endoplasmic reticulum and unfolded protein response in the control of mammalian recombinant protein production. *Biotechnology Letters* **36**, 1581-1593.

Hutnick, N.A., Carnathan, D.G., Dubey, S.A., Makedonas, G., Cox, K.S., Kierstead, L., Ratcliffe, S.J., Robertson, M.N., Casimiro, D.R., Ertl, H.C. and Betts, M.R. (2009) Baseline Ad5 serostatus does not predict Ad5 HIV vaccine-induced expansion of adenovirus-specific CD4+ T cells. *Nature Medicine* **15**, 876-878.

Hütter , G., Nowak , D., Mossner , M., Ganepola , S., Müßig , A., Allers , K., Schneider , T., Hofmann , J., Kücherer , C., Blau , O., Blau , I.W., Hofmann , W.K. and Thiel , E. (2009) Long-Term Control of HIV by CCR5 Delta32/Delta32 Stem-Cell Transplantation. *The New England Journal of Medicine* **360**, 692-698.

Irimia, A., Sarkar, A., Stanfield, R.L. and Wilson, I.A. (2016) Crystallographic Identification of Lipid as an Integral Component of the Epitope of HIV Broadly Neutralizing Antibody 4E10. *Immunity* **44**, 21-31.

Ishikawa, H. and Barber, G.N. (2008) STING is an endoplasmic reticulum adaptor that facilitates innate immune signalling. *Nature* **455**, 674-678.

Ishikawa, H., Ma, Z. and Barber, G.N. (2009) STING regulates intracellular DNA-mediated, type I interferon-dependent innate immunity. *Nature* **461**, 788-792.

Iwasaki, A. and Medzhitov, R. (2015) Control of adaptive immunity by the innate immune system. *Nature Immunology* **16**, 343-353.

Jabara, H.H., Weng, Y., Sannikova, T. and Geha, R.S. (2009) TRAF2 and TRAF3 independently mediate Ig class switching driven by CD40. *International Immunology* **21**, 477-488.

Jacob, R.A., Moyo, T., Schomaker, M., Abrahams, F., Grau Pujol, B. and Dorfman, J.R. (2015) Anti-V3/Glycan and Anti-MPER Neutralizing Antibodies, but Not Anti-V2/Glycan Site Antibodies, Are Strongly Associated with Greater Anti-HIV-1 Neutralization Breadth and Potency. *Journal of virology* **89**, 5264-5275.

Jacob, S.S., Cherian, S., Sumithra, T.G., Raina, O.K. and Sankar, M. (2013) Edible vaccines against veterinary parasitic diseases--current status and future prospects. *Vaccine* **31**, 1879-1885.

Jacobs, B.L., Langland, J.O., Kibler, K.V., Denzler, K.L., White, S.D., Holechek, S.A., Wong, S., Huynh, T. and Baskin, C.R. (2009) Vaccinia virus vaccines: past, present and future. *Antiviral Research* **84**, 1-13.

Janeway, C.A., Jr. and Medzhitov, R. (2002) Innate immune recognition. *Annual Reviews of Immunology* **20**, 197-216.

Jankovic, D., Kullberg, M., Hieny, S., Caspar, P., Collazo, C. and Sher, A. (2002) In the Absence of IL-12, CD4+ T Cell Responses to Intracellular Pathogens Fail to Default to a Th2 Pattern and Are Host Protective in an IL-10-/- Setting. *Immunity* **16**, 429-439.

Janssens, S., Pulendran, B. and Lambrecht, B.N. (2014) Emerging functions of the unfolded protein response in immunity. *Nature Immunology* **15**, 910-919.

Jardine, J., Julien, J.P., Menis, S., Ota, T., Kalyuzhniy, O., McGuire, A., Sok, D., Huang, P.S., MacPherson, S., Jones, M., Nieusma, T., Mathison, J., Baker, D., Ward, A.B., Burton, D.R., Stamatatos, L., Nemazee, D., Wilson, I.A. and Schief, W.R. (2013) Rational HIV immunogen design to target specific germline B cell receptors. *Science* **340**, 711-716.

Jardine, J.G., Ota, T., Sok, D., Pauthner, M., Kulp, D.W., Kalyuzhniy, O., Skog, P.D., Thinnes, T.C., Bhullar, D. and Briney, B. (2015) Priming a broadly neutralizing antibody response to HIV-1 using a germline-targeting immunogen. *Science* **349**, 156-161.

Jiao, Y., Xie, J., T., L., Han, Y., Qiu, Z., Zuo, L. and Wang, A. (2006) Correlation Between Gag-Specific CD8 T-Cell Responses, Viral Load, and CD4 Count in HIV-1 Infection is Dependent on Disease Status. *Journal of Acquired Immune Deficiency Syndrome* **42**, 263-268.

Kaisho, T., Hoshino, K., Iwabe, T., Takeuchi, O., Yasui, T. and Akira, S. (2002) Endotoxin can induce MyD88-deficient dendritic cells to support Th2 cell differentiation. *International Immunology* **14**, 695-700.

Kaisho, T., Takeuchi, O., Kawai, T., Hoshino, K. and Akira, S. (2001) Endotoxin-Induced Maturation of MyD88-Deficient Dendritic Cells. *The Journal of Immunology* **166**, 5688-5694.

Kalia, V., Sarkar, S., Gupta, P. and Montelaro, R.C. (2005) Antibody neutralization escape mediated by point mutations in the intracytoplasmic tail of human immunodeficiency virus type 1 gp41. *Journal of virology* **79**, 2097-2107.

Kanesa-thasan, N., Smucny, J.J., Hoke, C.H., Marks, D.H., Konishi, E., Kurane, I., Tang, D.B., Vaughn, D.W., Mason, P.W. and Shope, R.E. (2000) Safety and immunogenicity of NYVAC-JEV and ALVAC-JEV attenuated recombinant Japanese encephalitis virus—poxvirus vaccines in vaccinia-nonimmune and vaccinia-immune humans. *Vaccine* **19**, 483-491.

Kataru, R.P., Jung, K., Jang, C., Yang, H., Schwendener, R.A., Baik, J.E., Han, S.H., Alitalo, K. and Koh, G.Y. (2009) Critical role of CD11b+ macrophages and VEGF in inflammatory lymphangiogenesis, antigen clearance, and inflammation resolution. *Blood* **113**, 5650-5659.

Kaul, R., Plummer, F., Clerici, M., Bomsel, M., Lopalco, L. and Broliden, K. (2001) Mucosal IgA in exposed, uninfected subjects: evidence for a role in protection against HIV infection. *AIDS* **15**, 431-432.

Kaul, R., Trabattoni, D., Bwayo, J.J., Arienti, D., Zagliani, A., Mwangi, F.M., Kariuki, C., Ngugi, E.N., MacDonald, K.S., Ball, T.B., Clerici, M. and Plummer, F.A. (1999) HIV-1-specific mucosal IgA in a cohort of HIV-1-resistant Kenyan sex workers. *AIDS* **13**, 23-29.

Kawai, T., Adachi, O., Ogawa, T., Takeda, K. and Akira, S. (1999) Unresponsiveness of MyD88-Deficient Mice to Endotoxin. *Immunity* **11**, 115-122.

Kawai, T. and Akira, S. (2007) Antiviral signaling through pattern recognition receptors. *The Journal of Biochemistry* **141**, 137-145.

Kawai, T. and Akira, S. (2010) The role of pattern-recognition receptors in innate immunity: update on Toll-like receptors. *Nature Immunology* **11**, 373-384.

Keefer, M.C., Frey, S.E., Elizaga, M., Metch, B., De Rosa, S.C., Barroso, P.F., Tomaras, G., Cardinali, M., Goepfert, P., Kalichman, A., Philippon, V., McElrath, M.J., Jin, X., Ferrari, G., Defawe, O.D., Mazzara, G.P., Montefiori, D., Pensiero, M., Panicali, D.L., Corey, L. and Network, N.H.V.T. (2011) A phase I trial of preventive HIV vaccination with heterologous poxviral-vectors containing matching HIV-1 inserts in healthy HIV-uninfected subjects. *Vaccine* **29**, 1948-1958.

Kelleher, A.D., Long, C., Holmes, E.C., Allen, R.L., Wilson, J., Conlon, C., Workman, C., Shaunak, S., Olson, K. and Goulder, P. (2001) Clustered mutations in HIV-1 gag are consistently required for escape from HLA-B27–restricted cytotoxic T lymphocyte responses. *The Journal of experimental medicine* **193**, 375-386.

Kepler, T.B., Liao, H.X., Alam, S.M., Bhaskarabhatla, R., Zhang, R., Yandava, C., Stewart, S., Anasti, K., Kelsoe, G., Parks, R., Lloyd, K.E., Stolarchuk, C., Pritchett, J., Solomon, E., Friberg, E., Morris, L., Karim, S.S., Cohen, M.S., Walter, E., Moody, M.A., Wu, X., Altae-Tran, H.R., Georgiev, I.S., Kwong, P.D., Boyd, S.D., Fire, A.Z., Mascola, J.R. and Haynes, B.F. (2014) Immunoglobulin gene insertions and deletions in the affinity maturation of HIV-1 broadly reactive neutralizing antibodies. *Cell Host & Microbe* **16**, 304-313.

Kessans, S.A., Linhart, M.D., Matoba, N. and Mor, T. (2013) Biological and biochemical characterization of HIV-1 Gag/dgp41 virus-like particles expressed in Nicotiana benthamiana. *Plant biotechnology journal* **11**, 681-690.

Kessans, S.A., Linhart, M.D., Meador, L.R., Kilbourne, J., Hogue, B.G., Fromme, P., Matoba, N. and Mor, T.S. (2016) Immunological Characterization of Plant-Based HIV-1 Gag/Dgp41 Virus-Like Particles. *PloS one* **11**, e0151842.

Kettle, S., Alcam, A., Khanna, A., Ehret, R., Jassoy, C. and Smith, G.L. (1997) Vaccinia virus serpin B13R (SPI-2) inhibits interleukin-1beta-converting enzyme and protects virus-infected cells from TNF-and Fas-mediated apoptosis, but does not prevent IL-1beta-induced fever. *Journal of General Virology* **78**, 677-685.

Kibler, K.V., Gomez, C.E., Perdiguero, B., Wong, S., Huynh, T., Holechek, S., Arndt, W., Jimenez, V., Gonzalez-Sanz, R., Denzler, K., Haddad, E.K., Wagner, R., Sekaly, R.P., Tartaglia, J., Pantaleo, G., Jacobs, B.L. and Esteban, M. (2011) Improved NYVAC-Based vaccine vectors. *PloS one* **6**, e25674.

Kibler, K.V., Shors, T., Perkins, K., Zeman, C., MP, B., Biesterfeldt, J., Langland, J.O. and Jacobs, B.L. (1997) Double-Stranded RNA Is a Trigger for Apoptosis in Vaccinia Virus-Infected Cells. *Journal of virology* **71**, 1992-2003.

Kiepiela, P., Ngumbela, K., Thobakgale, C., Ramduth, D., Honeyborne, I., Moodley, E., Reddy, S., de Pierres, C., Mncube, Z., Mkhwanazi, N., Bishop, K., van der Stok, M., Nair, K., Khan, N., Crawford, H., Payne, R., Leslie, A., Prado, J., Prendergast, A., Frater, J., McCarthy, N., Brander, C., Learn, G.H., Nickle, D., Rousseau, C., Coovadia, H., Mullins, J.I., Heckerman, D., Walker, B.D. and Goulder, P. (2007) CD8+ T-cell responses to different HIV proteins have discordant associations with viral load. *Nature Medicine* **13**, 46-53.

Kim, D., Kim, T.H., Wu, G., Park, B.K., Ha, J.H., Kim, Y.S., Lee, K., Lee, Y. and Kwon, H.J. (2016) Extracellular Release of CD11b by TLR9 Stimulation in Macrophages. *PloS one* **11**, e0150677.

Kim, K.E., Koh, Y.J., Jeon, B.H., Jang, C., Han, J., Kataru, R.P., Schwendener, R.A., Kim, J.M. and Koh, G.Y. (2009) Role of CD11b+ macrophages in intraperitoneal lipopolysaccharide-induced aberrant lymphangiogenesis and lymphatic function in the diaphragm. *The American Journal of Pathology* **175**, 1733-1745.

Klein, F., Diskin, R., Scheid, J.F., Gaebler, C., Mouquet, H., Georgiev, I.S., Pancera, M., Zhou, T., Incesu, R.B., Fu, B.Z., Gnanapragasam, P.N., Oliveira, T.Y., Seaman, M.S., Kwong, P.D., Bjorkman, P.J. and Nussenzweig, M.C. (2013a) Somatic mutations of the immunoglobulin framework are generally required for broad and potent HIV-1 neutralization. *Cell* **153**, 126-138.

Klein, F., Mouquet, H., Dosenovic, P., Scheid, J.F., Scharf, L. and Nussenzweig, M.C. (2013b) Antibodies in HIV-1 vaccine development and therapy. *Science* **341**, 1199-1204.

Kloverpris, H.N., Payne, R.P., Sacha, J.B., Rasaiyaah, J.T., Chen, F., Takiguchi, M., Yang, O.O., Towers, G.J., Goulder, P. and Prado, J.G. (2013) Early antigen presentation of protective HIV-1 KF11Gag and KK10Gag epitopes from incoming viral particles facilitates rapid recognition of infected cells by specific CD8+ T cells. *Journal of virology* **87**, 2628-2638.

Kollar, P., Barta, T., Keltosova, S., Trnova, P., Muller Zavalova, V., Smejkal, K., Hosek, J., Fedr, R., Soucek, K. and Hampl, A. (2015) Flavonoid 4'-O-Methylkuwanon E from Morus alba Induces the Differentiation of THP-1 Human Leukemia Cells. *Evidence-Based Complementary Alternative Medicine* **2015**, 251895.

Komegae, E.N., Grund, L.Z., Lopes-Ferreira, M. and Lima, C. (2013) TLR2, TLR4 and the MyD88 signaling are crucial for the in vivo generation and the longevity of long-lived antibody-secreting cells. *PloS one* **8**, e71185.

Konishi, E., Pincus, S., Paoletti, E., Shope, R.E., Burrage, T. and Mason, P.W. (1992) Mice Immunized with a Subviral Particle Containing the Japanese Encephalitis Virus prM/M and E Proteins Are Protected from Lethal JEV Infection. *Virology* **188**, 714-720.

Koup, R.A., Safrit, J.T., Cao, Y., Andrews, C.A., McLeod, G., Borkowsky, W., Farthing, C. and Ho, D.D. (1994) Temporal Association of Cellular Immune Responses with the Initial Control of Viremia in Primary Human Immunodeficiency Virus Type 1 Syndrome. *Journal of virology* **68**, 4650-4655.

Kouroku, Y., Fujita, E., Tanida, I., Ueno, T., Isoai, A., Kumagai, H., Ogawa, S., Kaufman, R.J., Kominami, E. and Momoi, T. (2007) ER stress (PERK/eIF2alpha phosphorylation) mediates the polyglutamine-induced LC3 conversion, an essential step for autophagy formation. *Cell Death Differ* **14**, 230-239.

Kushnir, N., Streatfield, S.J. and Yusibov, V. (2012) Virus-like particles as a highly efficient vaccine platform: diversity of targets and production systems and advances in clinical development. *Vaccine* **31**, 58-83.

Kuwata, T., Kaori, T., Enomoto, I., Yoshimura, K. and Matsushita, S. (2013) Increased infectivity in human cells and resistance to antibody-mediated neutralization by truncation of the SIV gp41 cytoplasmic tail. *Frontiers in Microbiology* **4**, 117.

Labrijn, A.F., Poignard, P., Raja, A., Zwick, M.B., Delgado, K., Franti, M., Binley, J., Vivona, V., Grundner, C., Huang, C.C., Venturi, M., Petropoulos, C.J., Wrin, T., Dimitrov, D.S., Robinson, J., Kwong, P.D., Wyatt, R.T., Sodroski, J. and Burton, D.R. (2003) Access of Antibody Molecules to the Conserved Coreceptor Binding Site on Glycoprotein gp120 Is Sterically Restricted on Primary Human Immunodeficiency Virus Type 1. *Journal of virology* **77**, 10557-10565.

Lacasse, P., Denis, J., Lapointe, R., Leclerc, D. and Lamarre, A. (2008) Novel plant virus-based vaccine induces protective cytotoxic T-lymphocyte-mediated antiviral immunity through dendritic cell maturation. *Journal of virology* **82**, 785-794.

Lahaye, X., Satoh, T., Gentili, M., Cerboni, S., Conrad, C., Hurbain, I., El Marjou, A., Lacabaratz, C., Lelievre, J.D. and Manel, N. (2013) The capsids of HIV-1 and HIV-2 determine immune detection of the viral cDNA by the innate sensor cGAS in dendritic cells. *Immunity* **39**, 1132-1142.

Langland, J.O. and Jacobs, B.L. (2004) Inhibition of PKR by vaccinia virus: role of the N- and C-terminal domains of E3L. *Virology* **324**, 419-429.

Langland, J.O., Kash, J.C., Carter, V., Thomas, M.J., Katze, M.G. and Jacobs, B.L. (2006) Suppression of proinflammatory signal transduction and gene expression by the dual nucleic acid binding domains of the vaccinia virus E3L proteins. *Journal of virology* **80**, 10083-10095.

Lefrancois, L., Altman, J.D., Williams, K. and Olson, S. (2000) Soluble Antigen and CD40 Triggering Are Sufficient to Induce Primary and Memory Cytotoxic T Cells. *The Journal of Immunology* **164**, 725-732.

Lenz, P., Day, P., Pang, Y., Frye, S., Jensen, P., Lowy, D.R. and Schiller, J.T. (2001) Papillomavirus-Like Particles Induce Acute Activation of Dendritic Cells. *The Journal of Immunology* **166**, 5346-5355.

Leroux-Roels, G., Maes, C., Clement, F., van Engelenburg, F., van den Dobbelsteen, M., Adler, M., Amacker, M., Lopalco, L., Bomsel, M., Chalifour, A. and Fleury, S. (2013) Randomized Phase I: Safety, Immunogenicity and Mucosal Antiviral Activity in Young Healthy Women Vaccinated with HIV-1 Gp41 P1 Peptide on Virosomes. *PloS one* **8**, e55438.

Levitz, S.M. and Golenbock, D.T. (2012) Beyond empiricism: informing vaccine development through innate immunity research. *Cell* **148**, 1284-1292.

Li, M.X. and Dewson, G. (2015) Mitochondria and apoptosis: emerging concepts. *F1000Prime Reports* **7**, 42.

Liao, H.X., Bonsignori, M., Alam, S.M., McLellan, J.S., Tomaras, G.D., Moody, M.A., Kozink, D.M., Hwang, K.K., Chen, X., Tsao, C.Y., Liu, P., Lu, X., Parks, R.J., Montefiori, D.C., Ferrari, G., Pollara, J., Rao, M., Peachman, K.K., Santra, S., Letvin, N.L., Karasavvas, N., Yang, Z.Y., Dai, K., Pancera, M., Gorman, J., Wiehe, K., Nicely, N.I., Rerks-Ngarm, S., Nitayaphan, S., Kaewkungwal, J., Pitisuttithum, P., Tartaglia, J., Sinangil, F., Kim, J.H., Michael, N.L., Kepler, T.B., Kwong, P.D., Mascola, J.R., Nabel, G.J., Pinter, A., Zolla-Pazner, S. and Haynes, B.F. (2013a) Vaccine induction of antibodies against a structurally heterogeneous site of immune pressure within HIV-1 envelope protein variable regions 1 and 2. *Immunity* **38**, 176-186.

Liao, H.X., Chen, X., Munshaw, S., Zhang, R., Marshall, D.J., Vandergrift, N., Whitesides, J.F., Lu, X., Yu, J.S., Hwang, K.K., Gao, F., Markowitz, M., Heath, S.L., Bar, K.J., Goepfert, P.A., Montefiori, D.C., Shaw, G.C., Alam, S.M., Margolis, D.M., Denny, T.N., Boyd, S.D., Marshal, E., Egholm, M., Simen, B.B., Hanczaruk, B., Fire, A.Z., Voss, G., Kelsoe, G., Tomaras, G.D., Moody, M.A., Kepler, T.B. and Haynes, B.F. (2011) Initial antibodies binding to HIV-1 gp41 in acutely infected subjects are polyreactive and highly mutated. *The Journal of experimental medicine* **208**, 2237-2249.

Liao, H.X., Lynch, R., Zhou, T., Gao, F., Alam, S.M., Boyd, S.D., Fire, A.Z., Roskin, K.M., Schramm, C.A., Zhang, Z., Zhu, J., Shapiro, L., Program, N.C.S., Mullikin, J.C., Gnanakaran, S., Hraber, P., Wiehe, K., Kelsoe, G., Yang, G., Xia, S.M., Montefiori, D.C., Parks, R., Lloyd, K.E., Scearce, R.M., Soderberg, K.A., Cohen, M., Kamanga, G., Louder, M.K., Tran, L.M., Chen, Y., Cai, F., Chen, S., Moquin, S., Du, X., Joyce, M.G., Srivatsan, S., Zhang, B., Zheng, A., Shaw, G.M., Hahn, B.H., Kepler, T.B., Korber, B.T., Kwong, P.D., Mascola, J.R. and Haynes, B.F. (2013b) Co-evolution of a broadly neutralizing HIV-1 antibody and founder virus. *Nature* **496**, 469-476.

Liew, P.S. and Hair-Bejo, M. (2015) Farming of Plant-Based Veterinary Vaccines and Their Applications for Disease Prevention in Animals. *Advances in Virology* **2015**, 936940.

Lin, L., Finak, G., Ushey, K., Seshadri, C., Hawn, T.R., Frahm, N., Scriba, T.J., Mahomed, H., Hanekom, W., Bart, P.A., Pantaleo, G., Tomaras, G.D., Rerks-Ngarm, S., Kaewkungwal, J., Nitayaphan, S., Pitisuttithum, P., Michael, N.L., Kim, J.H., Robb, M.L., O'Connell, R.J., Karasavvas, N., Gilbert, P., S, C.D.R., McElrath, M.J. and Gottardo, R. (2015) COMPASS identifies T-cell subsets correlated with clinical outcomes. *Nature Biotechnology* **33**, 610-616.

Ling, G.S., Bennett, J., Woollard, K.J., Szajna, M., Fossati-Jimack, L., Taylor, P.R., Scott, D., Franzoso, G., Cook, H.T. and Botto, M. (2014) Integrin CD11b positively regulates TLR4-induced signalling pathways in dendritic cells but not in macrophages. *Nature Communications* **5**, 3039.

Link, A., Zabel, F., Schnetzler, Y., Titz, A., Brombacher, F. and Bachmann, M.F. (2012) Innate immunity mediates follicular transport of particulate but not soluble protein antigen. *The Journal of Immunology* **188**, 3724-3733.

Liu, Y.P., Zeng, L., Tian, A., Bomkamp, A., Rivera, D., Gutman, D., Barber, G.N., Olson, J.K. and Smith, J.A. (2012) Endoplasmic reticulum stress regulates the innate immunity critical transcription factor IRF3. *The Journal of Immunology* **189**, 4630-4639.

Liu, Z., Wang, S., Zhang, Q., Tian, M., Hou, J., Wang, R., Liu, C., Ji, X., Liu, Y. and Shao, Y. (2013) Deletion of C7L and K1L genes leads to significantly decreased virulence of recombinant vaccinia virus TianTan. *PloS one* **8**, e68115.

Lundgren, J.D., Babiker, A.G., Gordin, F., Emery, S., Grund, B., Sharma, S., Avihingsanon, A., Cooper, D.A., Fatkenheuer, G., Llibre, J.M., Molina, J.M., Munderi, P., Schechter, M., Wood, R., Klingman, K.L., Collins, S., Lane, H.C., Phillips, A.N. and Neaton, J.D. (2015) Initiation of Antiretroviral Therapy in Early Asymptomatic HIV Infection. *The New England Journal of Medicine* **373**, 795-807.

Ma, J.K., Chikwamba, R., Sparrow, P., Fischer, R., Mahoney, R. and Twyman, R.M. (2005) Plant-derived pharmaceuticals--the road forward. *Trends in Plant Science* **10**, 580-585.

Macen, J.L., Garner, R.S., Musy, P.Y., Brooks, M.A., Turner, P.C., Moyer, R.W., McFadden, G. and Bleackley, R.C. (1996) Differential inhibition of the Fas- and granule-mediated cytolysis pathways by the orthopoxvirus cytokine response modifier A/SPI-2 and SPI-1 protein. *Proceedings of the National Academy of Sciences of the United States of America* **93**, 9108-9113.

Maclean, J., Koekemoer, M., Olivier, A.J., Stewart, D., Hitzeroth, II, Rademacher, T., Fischer, R., Williamson, A.L. and Rybicki, E.P. (2007) Optimization of human papillomavirus type 16 (HPV-16) L1 expression in plants: comparison of the suitability of different HPV-16 L1 gene variants and different cell-compartment localization. *Journal of General Virology* **88**, 1460-1469.

Magerus-Chatinet, A., Yu, H., Garcia, S., Ducloux, E., Terris, B. and Bomsel, M. (2007) Galactosyl ceramide expressed on dendritic cells can mediate HIV-1 transfer from monocyte derived dendritic cells to autologous T cells. *Virology* **362**, 67-74.

Manel, N., Hogstad, B., Wang, Y., Levy, D.E., Unutmaz, D. and Littman, D.R. (2010) A cryptic sensor for HIV-1 activates antiviral innate immunity in dendritic cells. *Nature* **467**, 214-217.

Manganaro, L., de Castro, E., Maestre, A.M., Olivieri, K., Garcia-Sastre, A., Fernandez-Sesma, A. and Simon, V. (2015) HIV Vpu Interferes with NF-kappaB Activity but Not with Interferon Regulatory Factor 3. *Journal of virology* **89**, 9781-9790.

Marchi, S., Patergnani, S. and Pinton, P. (2014) The endoplasmic reticulum-mitochondria connection: one touch, multiple functions. *Biochimica et Biophysica Acta* **1837**, 461-469.

Marillonnet, S., Giritch, A., Gils, M., Kandzia, R., Klimyuk, V. and Gleba, Y. (2004) In planta engineering of viral RNA replicons: Efficient assembly by recombination of DNA modules deliveredy by Agrobacterium. *Proceedings of the National Academy of Sciences of the United States of America* **101**, 6852-6857.

Marillonnet, S., Thoeringer, C., Kandzia, R., Klimyuk, V. and Gleba, Y. (2005) Systemic Agrobacterium tumefaciens-mediated transfection of viral replicons for efficient transient expression in plants. *Nature Biotechnology* **23**, 718-723.

Martinez, F.O. and Gordon, S. (2014) The M1 and M2 paradigm of macrophage activation: time for reassessment. *F1000Prime Reports* **6**, 13.

Mascola, J.R. and Haynes, B.F. (2013) HIV-1 neutralizing antibodies: understanding nature's pathways. *Immunological Reviews* **254**, 225-244.

Mascola, J.R. and Montefiori, D.C. (2010) The role of antibodies in HIV vaccines. *Annual Review of Immunology* **28**, 413-444.

Mata-Haro, V., Cekic, C., Martin, M., Chilton, P., Casella, C. and Mitchell, T. (2007) The Vaccine Adjuvant Monophosphoryl Lipid A as a TRIF-Biased Agonist of TLR4. *Science* **316**, 1628-1632.

Matoba, N., Griffin, T.A., Mittman, M., Doran, J.D., Alfsen, A., Montefiori, D.C., Hanson, C.V., Bomsel, M. and Mor, T.S. (2008) Transcytosis-blocking Abs elicited by an oligomeric immunogen based on the membrane proximal region of HIV-1 gp41 target non-neutralizing epitopes. *Current HIV Research* **6**, 218-229.

Matoba, N., Kajiura, H., Cherni, I., Doran, J.D., Bomsel, M., Fujiyama, K. and Mor, T.S. (2009) Biochemical and immunological characterization of the plant-derived candidate human immunodeficiency virus type 1 mucosal vaccine CTB-MPR. *Plant biotechnology journal* **7**, 129-145.

Matoba, N., Magerus, A., Geyer, B.C., Zhang, Y., Muralidharan, M., Alfsen, A., Arntzen, C.J., Bomsel, M. and Mor, T.S. (2004) A mucosally targeted subunit vaccine candidate eliciting HIV-1 transcytosis-blocking Abs. *Proceedings of the National Academy of Sciences of the United States of America* **101**, 13584-13589.

Mattanovich, D., Gasser, B., Hohenblum, H. and Sauer, M. (2004) Stress in recombinant protein producing yeasts. *Journal of Biotechnology* **113**, 121-135.

McCormack, S., Stohr, W., Barber, T., Bart, P.A., Harari, A., Moog, C., Ciuffreda, D., Cellerai, C., Cowen, M., Gamboni, R., Burnet, S., Legg, K., Brodnicki, E., Wolf, H., Wagner, R., Heeney, J., Frachette, M.J., Tartaglia, J., Babiker, A., Pantaleo, G. and Weber, J. (2008) EV02: a Phase I trial to compare the safety and immunogenicity of HIV DNA-C prime-NYVAC-C boost to NYVAC-C alone. *Vaccine* **26**, 3162-3174.

McCurdy, L., Larkina, B., Martin, J. and Graham, B.S. (2004) Modified Vaccinia Ankara Potential in Alternative Smallpox Vaccine. *Clinical Infectious Diseases* **38**, 1749-1753.

McElrath, M.J., De Rosa, S.C., Moodie, Z., Dubey, S., Kierstead, L., Janes, H., Defawe, O.D., Carter, D.K., Hural, J. and Akondy, R. (2008) HIV-1 vaccine-induced immunity in the test-of-concept Step Study: a case–cohort analysis. *The Lancet* **372**, 1894-1905.

McGuire, A.T., Glenn, J.A., Lippy, A. and Stamatatos, L. (2014) Diverse recombinant HIV-1 Envs fail to activate B cells expressing the germline B cell receptors of the broadly neutralizing anti-HIV-1 antibodies PG9 and 447-52D. *Journal of virology* **88**, 2645-2657.

McHeyzer-Williams, M., McHeyzer-Williams, L., Panus, J., Bikah, G., Pogue-Caley, R., Driver, D. and Eisenbraun, M. (2000) Antigen-Specific Immunity. *Immunologic Research* **22**, 223-236.

McMichael, A.J. and Koff, W.C. (2014) Vaccines that stimulate T cell immunity to HIV-1: the next step. *Nature Immunology* **15**, 319-322.

Medzhitov, R. (2007) Recognition of microorganisms and activation of the immune response. *Nature* **449**, 819-826.

Meng, X., Jiang, C., Arsenio, J., Dick, K., Cao, J. and Xiang, Y. (2009) Vaccinia virus K1L and C7L inhibit antiviral activities induced by type I interferons. *Journal of virology* **83**, 10627-10636.

Merck & Co., I. (2006) Prescribing Information - Gardasil.

Meyers, A., Chakauya, E., Shephard, E., Tanzer, F.L., Maclean, J., Lynch, A., Williamson, A.L. and Rybicki, E.P. (2008) Expression of HIV-1 antigens in plants as potential subunit vaccines. *BMC Biotechnology* **8**, 53.

Micoli, K.J., Mamaeva, O., Piller, S.C., Barker, J.L., Pan, G., Hunter, E. and McDonald, J.M. (2006) Point mutations in the C-terminus of HIV-1 gp160 reduce apoptosis and calmodulin binding without affecting viral replication. *Virology* **344**, 468-479.

Migueles, S.A., Sabbaghian, M.S., Shupert, W.L., Bettinotti, M.P., Marincola, F.M., Martino, L., Hallahan, C.W., Selig, S.M., Schwartz, D., Sullivan, J. and Connors, M. (2000) HLA B*5701 is highly associated with restriction of virus replication in a subgroup of HIV-infected long term nonprogressors. *Proceedings of the National Academy of Sciences of the United States of America* **97**, 2709-2714.

Mitzel, D.N., Lowry, V., Shirali, A.C., Liu, Y. and Stout-Delgado, H.W. (2014) Age-enhanced endoplasmic reticulum stress contributes to increased Atg9A inhibition of STING-mediated IFN-beta production during Streptococcus pneumoniae infection. *The Journal of Immunology* **192**, 4273-4283.

Modrow, S., Hahn, B.H., Shaw, G.M., Gallo, R.C., Wong-Staal, F. and Wolf, H. (1987) Computer-assisted analysis of envelope protein sequences of seven human immunodeficiency virus isolates: prediction of antigenic epitopes in conserved and variable regions. *Journal of virology* **61**, 570-578.

Montero, M., van Houten, N.E., Wang, X. and Scott, J.K. (2008) The membrane-proximal external region of the human immunodeficiency virus type 1 envelope: dominant site of antibody neutralization and target for vaccine design. *Microbiology and Molecular Biology Reviews* **72**, 54-84, table of contents.

Mooij, P., Balla-Jhagjhoorsingh, S.S., Beenhakker, N., van Haaften, P., Baak, I., Nieuwenhuis, I.G., Heidari, S., Wolf, H., Frachette, M.J., Bieler, K., Sheppard, N., Harari, A., Bart, P.A., Liljestrom, P., Wagner, R., Pantaleo, G. and Heeney, J.L. (2009) Comparison of human and rhesus macaque T-cell responses elicited by boosting with NYVAC encoding human immunodeficiency virus type 1 clade C immunogens. *Journal of virology* **83**, 5881-5889.

Mooij, P., Balla-Jhagjhoorsingh, S.S., Koopman, G., Beenhakker, N., van Haaften, P., Baak, I., Nieuwenhuis, I.G., Kondova, I., Wagner, R., Wolf, H., Gomez, C.E., Najera, J.L., Jimenez, V., Esteban, M. and Heeney, J.L. (2008) Differential CD4+ versus CD8+ T-cell responses elicited by different poxvirus-based human immunodeficiency virus type 1 vaccine candidates provide comparable efficacies in primates. *Journal of virology* **82**, 2975-2988.

Mooij, P., Koopman, G., Drijfhout, J.W., Nieuwenhuis, I.G., Beenhakker, N., Koestler, J., Bogers, W.M., Wagner, R., Esteban, M. and Pantaleo, G. (2015) Synthetic long peptide booster immunization in rhesus macaques primed with replication-competent NYVAC-C-KC induces a balanced CD4/CD8 T-cell and antibody response against the conserved regions of HIV-1. *Journal of General Virology* **96**, 1478-1483.

Moore, P.L., Williamson, C. and Morris, L. (2015) Virological features associated with the development of broadly neutralizing antibodies to HIV-1. *Trends in microbiology* **23**, 204-211.

Mor, T.S., Moon, Y., Palmer, K.E. and Mason, H.S. (2003) Geminivirus vectors for high-level expression of foreign proteins in plant cells. *Biotechnology and bioengineering* **81**, 430-437.

Moscoso, C.G., Xing, L., Hui, J., Hu, J., Kalkhoran, M.B., Yenigun, O.M., Sun, Y., Paavolainen, L., Martin, L., Vahlne, A., Zambonelli, C., Barnett, S.W., Srivastava, I.K. and Cheng, R.H. (2014) Trimeric HIV Env provides epitope occlusion mediated by hypervariable loops. *Scientific Reports* **4**, 7025.

Mosmann, T. and Coffman, R. (1989) Th1 and Th2 Cells: Different Patterns of Lymphokine Secretion Lead to Different Functional Properties. *Annual Reviews of Immunology* **7**, 145-173.

Moss, B., Rosenblum, E. and Katz, E. (1969) Rifampicin: a Specific Inhibitor of Vaccinia Virus Assembly. *Nature* **224**, 1261-1264.

Mosser, D.M. (2003) The many faces of macrophage activation. *Journal of Leukocyte Biology* **73**, 209-212.

Mosser, D.M. and Edwards, J.P. (2008) Exploring the full spectrum of macrophage activation. *Nature Reviews Immunology* **8**, 958-969.

Mudd, P.A., Martins, M.A., Ericsen, A.J., Tully, D.C., Power, K.A., Bean, A.T., Piaskowski, S.M., Duan, L., Seese, A., Gladden, A.D., Weisgrau, K.L., Furlott, J.R., Kim, Y.I., Veloso de Santana, M.G., Rakasz, E., Capuano, S., 3rd, Wilson, N.A., Bonaldo, M.C., Galler, R., Allison, D.B., Piatak, M., Jr., Haase, A.T., Lifson, J.D., Allen, T.M. and Watkins, D.I. (2012) Vaccine-induced CD8+ T cells control AIDS virus replication. *Nature* **491**, 129-133.

Munro, J.B., Gorman, J., Ma, X., Zhou, Z., Arthos, J., Burton, D.R., Koff, W.C., Courter, J.R., Smith, A.B. and Kwong, P.D. (2014) Conformational dynamics of single HIV-1 envelope trimers on the surface of native virions. *Science* **346**, 759-763.

Murakami, T. and Freed, E.O. (2000) The long cytoplasmic tail of gp41 is required in a cell type-dependent manner for HIV-1 envelope glycoprotein incorporation into virions. *Proceedings of the National Academy of Sciences of the United States of America* **97**, 343-348.

Nagpal, G., Gupta, S., Chaudhary, K., Dhanda, S.K., Prakash, S. and Raghava, G.P. (2015) VaccineDA: Prediction, design and genome-wide screening of oligodeoxynucleotide-based vaccine adjuvants. *Scientific Reports* **5**, 12478.

Najera, J.L., Gomez, C.E., Domingo-Gil, E., Gherardi, M.M. and Esteban, M. (2006) Cellular and biochemical differences between two attenuated poxvirus vaccine candidates (MVA and NYVAC) and role of the C7L gene. *Journal of virology* **80**, 6033-6047.

Najera, J.L., Gomez, C.E., Garcia-Arriaza, J., Sorzano, C.O. and Esteban, M. (2010) Insertion of vaccinia virus C7L host range gene into NYVAC-B genome potentiates immune responses against HIV-1 antigens. *PloS one* **5**, e11406.

Nelson, J.D., Brunel, F.M., Jensen, R., Crooks, E.T., Cardoso, R.M.F., Wang, M., Hessell, A., Wilson, I.A., Binley, J.M., Dawson, P.E., Burton, D.R. and Zwick, M.B. (2007) An Affinity-Enhanced Neutralizing Antibody against the Membrane-Proximal External Region of Human Immunodeficiency Virus Type 1 gp41 Recognizes an Epitope between Those of 2F5 and 4E10. *Journal of virology* **81**, 4033-4043.

Nemazee, D., Gavin, A., Hoebe, K. and Beutler, B. (2006) Immunology: Toll-like receptors and antibody responses. *Nature* **441**, E4.

Newman, J.T., Sturgeon, T.J., Gupta, P. and Montelaro, R.C. (2007) Differential functional phenotypes of two primary HIV-1 strains resulting from homologous point mutations in the LLP domains of the envelope gp41 intracytoplasmic domain. *Virology* **367**, 102-116.

Nguyen, K.-L., Llano, M., Akari, H., Miyagi, E., Poeschla, E.M., Strebel, K. and Bour, S. (2004) Codon optimization of the HIV-1 vpu and vif genes stabilizes their mRNA and allows for highly efficient Rev-independent expression. *Virology* **319**, 163-175.

Nitayaphan, S., Pitisuttihum, P., Karnasuta, C., Eamsila, C., De Souza, M.S., Morgan, P., Polonis, V., Benenson, M., VanCott, T., Ratto-Kim, S., Kim, J.H., Thapinta, D., Garner, R., Bussaratid, V., Singharaj, P., el Habib, R., Gurunathan, S., Heyward, W., Birx, D.L., McNeil, J.G., Brown, A.E. and Group, T.A.V.E. (2004) Safety and Immunogenicity of an HIV Subtype B and E Prime-Boost Vaccine Combination in HIV-Negative Thai Adults. *The Journal of Infectious Diseases* **190**, 702-706.

Noad, R. and Roy, P. (2003) Virus-like particles as immunogens. *Trends in microbiology* **11**, 438-444.

O'Neill, L.A., Golenbock, D. and Bowie, A.G. (2013) The history of Toll-like receptors - redefining innate immunity. *Nature Reviews Immunology* **13**, 453-460.

Ogata, M., Hino, S., Saito, A., Morikawa, K., Kondo, S., Kanemoto, S., Murakami, T., Taniguchi, M., Tanii, I., Yoshinaga, K., Shiosaka, S., Hammarback, J.A., Urano, F. and Imaizumi, K. (2006) Autophagy is activated for cell survival after endoplasmic reticulum stress. *Mol Cell Biol* **26**, 9220-9231.

Ogg, G.S., Jin, X., Bonhoeffer, S., Dunbar, P.R., Nowak, M.A., Monard, S., Segal, J.P., Cao, Y., Rowland-Jones, S.L., Cerundolo, V., Hurley, A., Markowitz, M., Ho, D.D., Nixon, D.F. and McMichael, A.J. (1998) Quantitation of HIV-1 Specific Cytotoxic T Lymphocytes and Plasma Load of Viral RNA. *Science* **279**, 2103-2106.

Ohno, A., Maruyama, J., Nemoto, T., Arioka, M. and Kitamoto, K. (2011) A carrier fusion significantly induces unfolded protein response in heterologous protein production by Aspergillus oryzae. *Applied Microbiology and Biotechnology* **92**, 1197-1206.

Okada, T., Yoshida, H., Akazawa, R., Negishi, M. and Mori, K. (2002) Distinct roles of activating transcription factor 6 (ATF6) and double-stranded RNA-activated protein kinase-like endoplasmic reticulum kinase (PERK) in transcription during the mammalian unfolded protein response. *Biochemical Journal* **366**, 585-594.

Pancera, M., Zhou, T., Druz, A., Georgiev, I.S., Soto, C., Gorman, J., Huang, J., Acharya, P., Chuang, G.Y., Ofek, G., Stewart-Jones, G.B., Stuckey, J., Bailer, R.T., Joyce, M.G., Louder, M.K., Tumba, N., Yang, Y., Zhang, B., Cohen, M.S., Haynes, B.F., Mascola, J.R., Morris, L., Munro, J.B., Blanchard, S.C., Mothes, W., Connors, M. and Kwong, P.D. (2014) Structure and immune recognition of trimeric pre-fusion HIV-1 Env. *Nature* **514**, 455-461.

Pantaleo, G., Esteban, M., Jacobs, B.L. and Tartaglia, J. (2010) Poxvirus vector-based HIV vaccines. *Current Opinion in HIV and AIDS* **5**, 391-396.

Parent, L.J. and Gudleski, N. (2011) Beyond plasma membrane targeting: role of the MA domain of Gag in retroviral genome encapsidation. *Journal of Molecular Biology* **410**, 553-564.

Park, J.S., Svetkauskaite, D., He, Q., Kim, J.Y., Strassheim, D., Ishizaka, A. and Abraham, E. (2004) Involvement of toll-like receptors 2 and 4 in cellular activation by high mobility group box 1 protein. *The Journal of Biological Chemistry* **279**, 7370-7377.

Park, S.Y., Waheed, A.A., Zhang, Z.R., Freed, E.O. and Bonifacino, J.S. (2014) HIV-1 Vpu accessory protein induces caspase-mediated cleavage of IRF3 transcription factor. *The Journal of Biological Chemistry* **289**, 35102-35110.

Parker, C.E., Deterding, L.J., Hager-Braun, C., Binley, J.M., Schülke, N., Katinger, H., Moore, J.P. and Tomer, K.B. (2001) Fine Definition of the Epitope on the gp41 Glycoprotein of Human Immunodeficiency Virus Type 1 for the Neutralizing Monoclonal Antibody 2F5. *Journal of virology* **75**, 10906-10911.

Parks, C.L., Picker, L.J. and King, C.R. (2013) Development of replication-competent viral vectors for HIV vaccine delivery. *Current Opinion in HIV and AIDS* **8**, 402-411.

Pasare, C. and Medzhitov, R. (2004) Toll-dependent control mechanisms of CD4 T cell activation. *Immunity* **21**, 733-741.

Pasare, C. and Medzhitov, R. (2005) Control of B-cell responses by Toll-like receptors. *Nature* **438**, 364-368.

Pastori, C., Barassi, C., Piconi, S., Longhi, R., Villa, M.L., Siccardi, A.G., Clerici, M. and Lopalco, L. (2000) HIV neutralizing IgA in exposed seronegative subjects recognise an epitope within the gp41 coiled-coil pocket. *Journal of biological regulators and homeostatic agents* **14**, 15-21.

Payne, L. (1980) Significance of Extracellular Enveloped Virus in the *in vitro* and *in vivo* Dissemination of Vaccinia. *Journal of General Virology* **50**, 89-100.

Pejchal, R., Gach, J.S., Brunel, F.M., Cardoso, R.M., Stanfield, R.L., Dawson, P.E., Burton, D.R., Zwick, M.B. and Wilson, I.A. (2009) A conformational switch in human immunodeficiency virus gp41 revealed by the structures of overlapping epitopes recognized by neutralizing antibodies. *Journal of virology* **83**, 8451-8462.

Perdiguero, B., Gomez, C.E., Cepeda, V., Sanchez-Sampedro, L., Garcia-Arriaza, J., Mejias-Perez, E., Jimenez, V., Sanchez, C., Sorzano, C.O., Oliveros, J.C., Delaloye, J., Roger, T., Calandra, T., Asbach, B., Wagner, R., Kibler, K.V., Jacobs, B.L., Pantaleo, G. and Esteban, M. (2015) Virological and immunological characterization of novel NYVAC-based HIV/AIDS vaccine candidates expressing clade C trimeric soluble gp140(ZM96) and Gag(ZM96)-Pol-Nef(CN54) as virus-like particles. *Journal of virology* **89**, 970-988.

Perdiguero, B., Gomez, C.E., Di Pilato, M., Sorzano, C.O., Delaloye, J., Roger, T., Calandra, T., Pantaleo, G. and Esteban, M. (2013) Deletion of the vaccinia virus gene A46R, encoding for an inhibitor of TLR signalling, is an effective approach to enhance the immunogenicity in mice of the HIV/AIDS vaccine candidate NYVAC-C. *PloS one* **8**, e74831.

Perera, P.Y., Mayadas, T.N., Takeuchi, O., Akira, S., Zaks-Zilberman, M., Goyert, S.M. and Vogel, S.N. (2001) CD11b/CD18 Acts in Concert with CD14 and Toll-Like Receptor (TLR) 4 to Elicit Full Lipopolysaccharide and Taxol-Inducible Gene Expression. *The Journal of Immunology* **166**, 574-581.

Pereyra, F., Heckerman, D., Carlson, J.M., Kadie, C., Soghoian, D.Z., Karel, D., Goldenthal, A., Davis, O.B., DeZiel, C.E. and Lin, T. (2014) HIV control is mediated in part by CD8+ T-cell targeting of specific epitopes. *Journal of virology* **88**, 12937-12948.

Perreau, M., Welles, H.C., Harari, A., Hall, O., Martin, R., Maillard, M., Dorta, G., Bart, P.A., Kremer, E.J., Tartaglia, J., Wagner, R., Esteban, M., Levy, Y. and Pantaleo, G. (2011) DNA/NYVAC vaccine regimen induces HIV-specific CD4 and CD8 T-cell responses in intestinal mucosa. *Journal of virology* **85**, 9854-9862.

Persaud, D., Gay, H., Ziemniak, C., Chen, Y.H., Piatak, M., Jr., Chun, T.W., Strain, M., Richman, D. and Luzuriaga, K. (2013) Absence of detectable HIV-1 viremia after treatment cessation in an infant. *The New England Journal of Medicine* **369**, 1828-1835.

Petrasek, J., Iracheta-Vellve, A., Csak, T., Satishchandran, A., Kodys, K., Kurt-Jones, E., Fitzgerald, K. and Szabo, G. (2013) STING-IRF3 pathway links endoplasmic reticulum stress with hepatocyte apoptosis in early alcoholic liver disease. *Proceedings of the National Academy of Sciences of the United States of America* **110**, 16546-16540.

Petrizzo, A., Tornesello, M.L., Napolitano, M., D'Alessio, G., Salomone Megna, A., Dolcetti, R., De Re, V., Wang, E., Marincola, F.M., Buonaguro, F.M. and Buonaguro, L. (2012) Multiparametric analyses of human PBMCs loaded ex vivo with a candidate idiotype vaccine for HCV-related lymphoproliferative disorders. *PloS one* **7**, e44870.

Peyret, H. and Lomonossoff, G.P. (2013) The pEAQ vector series: the easy and quick way to produce recombinant proteins in plants. *Plant molecular biology* **83**, 51-58.

Pillay, S., Shephard, E.G., Meyers, A.E., Williamson, A.L. and Rybicki, E.P. (2010) HIV-1 sub-type C chimaeric VLPs boost cellular immune responses in mice. *Journal of Immune Based Therapies and Vaccines* **8**, 7.

Pinto, L.A., Castle, P.E., Roden, R.B., Harro, C.D., Lowy, D.R., Schiller, J.T., Wallace, D., Williams, M., Kopp, W., Frazer, I.H., Berzofsky, J.A. and Hildesheim, A. (2005) HPV-16 L1 VLP vaccine elicits a broad-spectrum of cytokine responses in whole blood. *Vaccine* **23**, 3555-3564.

Pitisuttithum, P., Gilbert, P., Gurwith, M., Heyward, W., Martin, M., van Griensven, F., Hu, D. and Tappero, J.W. (2006) Randomized, double-blind, placebo-controlled efficacy trial of a bivalent recombinant glycoprotein 120 HIV-1 vaccine among injection drug users in Bangkok, Thailand. *Journal of Infectious Diseases* **194**, 1661-1671.

Pollara, J., McGuire, E., Fouda, G.G., Rountree, W., Eudailey, J., Overman, R.G., Seaton, K.E., Deal, A., Edwards, R.W., Tegha, G., Kamwendo, D., Kumwenda, J., Nelson, J.A.E., Liao, H.-X., Brinkley, C., Denny, T.N., Ochsenbauer, C., Ellington, S., King, C.C., Jamieson, D.J., van der Horst, C., Kourtis, A.P., Tomaras, G.D., Ferrari, G. and Permar, S.R. (2015) Association of HIV-1 Envelope-Specific Breast Milk IgA Responses with Reduced Risk of Postnatal Mother-to-Child Transmission of HIV-1. *Journal of virology* **89**, 9952-9961.

Pone, E.J., Zhang, J., Mai, T., White, C.A., Li, G., Sakakura, J.K., Patel, P.J., Al-Qahtani, A., Zan, H., Xu, Z. and Casali, P. (2012) BCR-signalling synergizes with TLR-signalling for induction of AID and immunoglobulin class-switching through the non-canonical NF-kappaB pathway. *Nature Communications* **3**, 767.

Postler, T.S. and Desrosiers, R.C. (2013) The tale of the long tail: the cytoplasmic domain of HIV-1 gp41. *Journal of virology* **87**, 2-15.

Poteet, E., Lewis, P., Li, F., Zhang, S., Gu, J., Chen, C., Ho, S.O., Do, T., Chiang, S., Fujii, G. and Yao, Q. (2015) A Novel Prime and Boost Regimen of HIV Virus-Like Particles with TLR4 Adjuvant MPLA Induces Th1 Oriented Immune Responses against HIV. *PloS one* **10**, e0136862.

Prado, J.G., Honeyborne, I., Brierley, I., Puertas, M.C., Martinez-Picado, J. and Goulder, P.J. (2009) Functional consequences of human immunodeficiency virus escape from an HLA-B*13-restricted CD8+ T-cell epitope in p1 Gag protein. *Journal of virology* **83**, 1018-1025.

Precopio, M.L., Betts, M.R., Parrino, J., Price, D.A., Gostick, E., Ambrozak, D.R., Asher, T.E., Douek, D.C., Harari, A., Pantaleo, G., Bailer, R., Graham, B.S., Roederer, M. and Koup, R.A. (2007) Immunization with vaccinia virus induces polyfunctional and phenotypically distinctive CD8(+) T cell responses. *The Journal of experimental medicine* **204**, 1405-1416.

Prentice, H.A., Tomaras, G., Geraghty, D.E., Apps, R., Fong, Y., Ehrenberg, P.K., Rolland, M., Kijak, G.H., Krebs, S.J., Nelson, W., DeCamp, A., Shen, X., Yates, N.L., Zolla-Pazner, S., Nitayaphan, S., Rerks-Ngarm, S., Kaewkungwal, J., Pitisuttihum, P., Ferrari, G., McElrath, M.J., Montefiori, D., Bailer, R.T., Koup, R.A., O'Connell, R.J., Robb, M.L., Michael, N.L., Gilbert, P.B., Kim, J.H. and Thomas, R. (2015) HLA class II genes modulates vaccine-induced antibody responses to affect HIV-1 acquisition. *Science Translational Medicine* **7**, 296ra112.

Pulendran, B. and Ahmed, R. (2006) Translating innate immunity into immunological memory: implications for vaccine development. *Cell* **124**, 849-863.

Purtscher, M., Trkola, A., Gruber, G., Buchacher, A., Predl, R., Steindl, F., Tauer, C., Berger, R., Barrett, N., Jungbauer, A. and Katinger, H. (1994) A broadly neutralizing human monoclonal antibody against gp41 of Human Immunodeficiency Virus Type 1. *AIDS Research and Human Retroviruses* **10**, 1651-1658.

Pybus, L.P., Dean, G., West, N.R., Smith, A., Daramola, O., Field, R., Wilkinson, S.J. and James, D.C. (2014) Model-directed engineering of "difficult-to-express" monoclonal antibody production by Chinese hamster ovary cells. *Biotechnology and bioengineering* **111**, 372-385.

Qiu, X., Wong, G., Audet, J., Bello, A., Fernando, L., Alimonti, J.B., Fausther-Bovendo, H., Wei, H., Aviles, J., Hiatt, E., Johnson, A., Morton, J., Swope, K., Bohorov, O., Bohorova, N., Goodman, C., Kim, D., Pauly, M.H., Velasco, J., Pettitt, J., Olinger, G.G., Whaley, K., Xu, B., Strong, J.E., Zeitlin, L. and Kobinger, G.P. (2014) Reversion of advanced Ebola virus disease in nonhuman primates with ZMapp. *Nature* **514**, 47-53.

Quakkelaar, E.D., Redeker, A., Haddad, E.K., Harari, A., McCaughey, S.M., Duhen, T., Filali-Mouhim, A., Goulet, J.P., Loof, N.M., Ossendorp, F., Perdiguero, B., Heinen, P., Gomez, C.E., Kibler, K.V., Koelle, D.M., Sekaly, R.P., Sallusto, F., Lanzavecchia, A., Pantaleo, G., Esteban, M., Tartaglia, J., Jacobs, B.L. and Melief, C.J. (2011) Improved innate and adaptive immunostimulation by genetically modified HIV-1 protein expressing NYVAC vectors. *PloS one* **6**, e16819.

Quezada, S.A., Jarvinen, L.Z., Lind, E.F. and Noelle, R.J. (2004) CD40/CD154 interactions at the interface of tolerance and immunity. *Annual Review of Immunology* **22**, 307-328.

Raghunandan, R. (2011) Virus-like particles: innate immune stimulators. *Expert Review of Vaccines* **10**, 409-411.

Rainbolt, T.K., Saunders, J.M. and Wiseman, R.L. (2014) Stress-responsive regulation of mitochondria through the ER unfolded protein response. *Trends in Endocrinology and Metabolism* **25**, 528-537.

Rasaiyaah, J., Tan, C.P., Fletcher, A.J., Price, A.J., Blondeau, C., Hilditch, L., Jacques, D.A., Selwood, D.L., James, L.C., Noursadeghi, M. and Towers, G.J. (2013) HIV-1 evades innate immune recognition through specific cofactor recruitment. *Nature* **503**, 402-405.

Rasmussen, S.B., Horan, K.A., Holm, C.K., Stranks, A.J., Mettenleiter, T.C., Simon, A.K., Jensen, S.B., Rixon, F.J., He, B. and Paludan, S.R. (2011) Activation of autophagy by alpha-herpesviruses in myeloid cells is mediated by cytoplasmic viral DNA through a mechanism dependent on stimulator of IFN genes. *The Journal of Immunology* **187**, 5268-5276.

Re, F. and Strominger, J.L. (2001) Toll-like receptor 2 (TLR2) and TLR4 differentially activate human dendritic cells. *The Journal of Biological Chemistry* **276**, 37692-37699.

Rerks-Ngarm, S., Pitisuttihum, P., Nitayaphan, S., Kaewkungwal, J., Chiu, J., Paris, R., Premsri, N., Namwat, C., De Souza, M.S., Adams, E., Benenson, M., Gurunathan, S., Tartaglia, J., McNeil, J.G., Francis, D.P., Stablein, D., Birx, D.L., Chunsuttiwat, S., Khamboonruang, C., Thongcharoen, P., Robb, M.L., Michael, N.L., Kunasol, P. and Kim, J.H. (2009) Vaccination with ALVAC and AIDSVAX to prevent HIV-1 infection in Thailand. *The New England Journal of Medicine* **361**, 2210-2220.

Richard, K., Pierce, S. and Song, W. (2008) The agonists of TLR4 and 9 are sufficient to activate memory B cells to differentiate into plasma cells *in vitro* but not *in vivo*. *The Journal of Immunology* **181**, 1746-1752.

Rodriguez-Negrete, E.A., Carrillo-Tripp, J. and Rivera-Bustamante, R.F. (2009) RNA silencing against geminivirus: complementary action of posttranscriptional gene silencing and transcriptional gene silencing in host recovery. *Journal of virology* **83**, 1332-1340.

Ron, D. and Walter, P. (2007) Signal integration in the endoplasmic reticulum unfolded protein response. *Nature Reviews Molecular Cell Biology* **8**, 519-529.

Ronnelid, J., Tejde, A., Mathsson, L., Nilsson-Ekdahl, K. and Nilsson, B. (2003) Immune complexes from SLE sera induce IL10 production from normal peripheral blood mononuclear cells by an FcyRII dependent mechanism: implications for a possible vicious cycle maintaining B cell hyperactivity in SLE. *Annals of Rheumatic Diseases* **62**, 37-42.

Rosales-Mendoza, S., Rubio-Infante, N., Govea-Alonso, D.O. and Moreno-Fierros, L. (2012) Current status and perspectives of plant-based candidate vaccines against the human immunodeficiency virus (HIV). *Plant Cell Reports* **31**, 495-511.

Rosales-Mendoza, S., Rubio-Infante, N., Monreal-Escalante, E., Govea-Alonso, D.O., García-Hernández, A.L., Salazar-González, J.A., González-Ortega, O., Paz-Maldonado, L.M.T. and Moreno-Fierros, L. (2013) Chloroplast expression of an HIV envelop-derived multiepitope protein: towards a multivalent plant-based vaccine. *Plant Cell, Tissue and Organ Culture (PCTOC)* **116**, 111-123.

Rosmarin, A., Weil, S., Rosner, G., Griffin, J., Arnaout, M. and Tenen, D. (1989) Differential Expression of CD11b/CD18 (Mo1) and Myeloperoxidase Genes During Myeloid Differentiation. *Blood* **73**, 131-136.

Rybicki, E.P. (2009) Plant-produced vaccines: promise and reality. *Drug Discovery Today* **14**, 16-24.

Rybicki, E.P. (2010) Plant-made vaccines for humans and animals. *Plant biotechnology journal* **8**, 620-637.

Rybicki, E.P. (2014) Plant-based vacines against viruses. *Virology Journal* **11**.

Sagar, M., Akiyama, H., Etemad, B., Ramirez, N., Freitas, I. and Gummuluru, S. (2012) Transmembrane Domain Membrane Proximal External Region but Not Surface Unit-Directed Broadly Neutralizing HIV-1 Antibodies Can Restrict Dendritic Cell-Mediated HIV-1 Trans-infection. *J Infect Dis* **205**, 1248-1257.

Sainsbury, F., Thuenemann, E.C. and Lomonossoff, G.P. (2009) pEAQ: versatile expression vectors for easy and quick transient expression of heterologous proteins in plants. *Plant biotechnology journal* **7**, 682-693.

Saitoh, T., Fujita, N., Hayashi, T., Takahara, K., Satoh, T., Lee, H., Matsunaga, K., Kageyama, S., Omori, H., Noda, T., Yamamoto, N., Kawai, T., Ishii, K., Takeuchi, O., Yoshimori, T. and Akira, S. (2009) Atg9a controls dsDNA-driven dynamic translocation of STING and the innate immune response. *Proceedings of the National Academy of Sciences of the United States of America* **106**, 20842-20846.

Sakuragi, S., Goto, T., Sano, K. and Morikawa, Y. (2002) HIV type 1 Gag virus-like particle budding from spheroplasts of Saccharomyces cerevisiae. *Proceedings of the National Academy of Sciences of the United States of America* **99**, 7956-7961.

Sala, F., Rigano, M.M., Barbante, A., Basso, B., Walmsley, A.M. and Castiglione, S. (2003) Vaccine antigen production in transgenic plants: strategies, gene constructs and perspectives. *Vaccine* **21**, 803-808.

Sallusto, F. and Lanzavecchia, A. (1994) Efficient Presentation of Soluble Antigen by Cultured Human Dendritic Cells is Maintained by Granulocyte/Macrophage Colony-stimulating Factor Plus Interleukin 4 and Downregulated by Tumor Necrosis Factor alpha. *The Journal of Experimental Medicine* **179**, 1109-1118.

Sanchez-Sampedro, L., Mejias-Perez, E., CO, S.S., Najera, J.L. and Esteban, M. (2016) NYVAC vector modified by C7L viral gene insertion improves T cell immune responses and effectiveness against leishmaniasis. *Virus research* **220**, 1-11.

Sanders, R.W., van Gils, M.J., Derking, R., Sok, D., Ketas, T.J., Burger, J.A., Ozorowski, G., Cupo, A., Simonich, C., Goo, L., Arendt, H., Kim, H.J., Lee, J.H., Pugach, P., Williams, M., Debnath, G., Moldt, B., van Breemen, M.J., Isik, G., Medina-Ramirez, M., Back, J.W., Koff, W.C., Julien, J.P., Rakasz, E.G., Seaman, M.S., Guttman, M., Lee, K.K., Klasse, P.J., LaBranche, C., Schief, W.R., Wilson, I.A., Overbaugh, J., Burton, D.R., Ward, A.B., Montefiori, D.C., Dean, H. and Moore, J.P. (2015) HIV-1 VACCINES. HIV-1 neutralizing antibodies induced by native-like envelope trimers. *Science* **349**, aac4223.

Santos da Silva, E., Mulinge, M. and Bercoff, D. (2013) The frantic play of the concealed HIV envelope cytoplasmic tail. *Retrovirology* **10**, 54.

Sasaki, M., Uchiyama, J., Ishikawa, H., Matsushita, S., Kimura, G., Nomoto, K. and Koga, Y. (1996) Induction of Apoptosis by Calmodulin-Dependent Intracellular Ca+2 Elevation in CD4+ Cells Expressing gp160 of HIV. *Virology* **224**, 18-24.

Schnare, M., Barton, G.M., Holt, A.C., Takeda, K., Akira, S. and Medzhitov, R. (2001) Toll-like receptors control activation of adaptive immune responses. *Nat Immunol* **2**, 947-950.

Schneider, C.A., Rasband, W.S. and Eliceiri, K.W. (2012) NIH Image to ImageJ: 25 years of image analysis. *Nature Methods* **9**, 671-675.

Schneidewind, A., Brockman, M.A., Yang, R., Adam, R.I., Li, B., Le Gall, S., Rinaldo, C.R., Craggs, S.L., Allgaier, R.L., Power, K.A., Kuntzen, T., Tung, C.S., LaBute, M.X., Mueller, S.M., Harrer, T., McMichael, A.J., Goulder, P.J., Aiken, C., Brander, C., Kelleher, A.D. and Allen, T.M. (2007) Escape from the dominant HLA-B27-restricted cytotoxic T-lymphocyte response in Gag is associated with a dramatic reduction in human immunodeficiency virus type 1 replication. *Journal of virology* **81**, 12382-12393.

Schonbeck, U. and Libby, P. (2001) The CD40/CD154 receptor/ligand dyad. *Cellular and Molecular Life Sciences* **58**, 4-43.

Schroder, M. (2006) The Unfolded Protein Response. *Molecular Biotechnology* **34**, 279-290.

Schroder, M. and Kaufman, R.J. (2005) The mammalian unfolded protein response. *Annual Review of Biochemistry* **74**, 739-789.

Scotti, N., Alagna, F., Ferraiolo, E., Formisano, G., Sannino, L., Buonaguro, L., De Stradis, A., Vitale, A., Monti, L., Grillo, S., Buonaguro, F.M. and Cardi, T. (2009) High-level expression of the HIV-1 Pr55gag polyprotein in transgenic tobacco chloroplasts. *Planta* **229**, 1109-1122.

Scotti, N. and Rybicki, E.P. (2013) Virus-like particles produced in plants as potential vaccines. *Expert Review of Vaccines* **12**, 211-224.

Seemanpillai, M., Dry, I., Randles, J. and Rezaian, A. (2003) Transcriptional Silencing of Geminiviral Promoter-Driven Transgenes Following Homologous Virus Infection. *Molecular Plant-Microbe Interactions* **16**, 429-438.

Seet, B.T., Johnston, J.B., Brunetti, C.R., Barrett, J.W., Everett, H., Cameron, C., Sypula, J., Nazarian, S.H., Lucas, A. and McFadden, G. (2003) Poxviruses and immune evasion. *Annual Review of Immunology* **21**, 377-423.

Sellhorn, G., Kraft, Z., Caldwell, Z., Ellingson, K., Mineart, C., Seaman, M.S., Montefiori, D.C., Lagerquist, E. and Stamatatos, L. (2012) Engineering, expression, purification, and characterization of stable clade A/B recombinant soluble heterotrimeric gp140 proteins. *Journal of virology* **86**, 128-142.

Shen, R., Drelichman, E.R., Bimczok, D., Ochsenbauer, C., Kappes, J.C., Cannon, J.A., Tudor, D., Bomsel, M., Smythies, L.E. and Smith, P.D. (2010) GP41-specific antibody blocks cell-free HIV type 1 transcytosis through human rectal mucosa and model colonic epithelium. *The Journal of Immunology* **184**, 3648-3655.

Shisler, J.L. and Jin, X.L. (2004) The Vaccinia Virus K1L Gene Product Inhibits Host NF- B Activation by Preventing I B Degradation. *Journal of virology* **78**, 3553-3560.

Silhavy, D., Molnar, A., Lucioli, A., Szittya, G., Hornyik, C., Tavazza, M. and Burgyan, J. (2002) A viral protein suppresses RNA silencing and binds silencing-generated, 21- to 25-nucleotide double-stranded RNAs. *The EMBO Journal* **21**, 3070-3080.

Silipo, A., De Castro, C., Lanzetta, R., Molinario, A. and Parrilli, M. (2004) Full structural characterization of the lipid A components from the *Agrobacterium tumefaciens* strain C58 lipopolysaccharide fraction. *Glycobiology* **14**, 805-815.

Smith, G.L., Benfield, C.T., Maluquer de Motes, C., Mazzon, M., Ember, S.W., Ferguson, B.J. and Sumner, R.P. (2013) Vaccinia virus immune evasion: mechanisms, virulence and immunogenicity. *Journal of General Virology* **94**, 2367-2392.

Smith, G.L. and Law, M. (2004) The exit of vaccinia virus from infected cells. *Virus research* **106**, 189-197.

Smith, J.A. (2014) A new paradigm: innate immune sensing of viruses via the unfolded protein response. *Frontiers in Microbiology* **5**, 222.

Smith, V.P., Bryant, N.A. and Alcamí, A. (2000) Ectromelia, vaccinia and cowpox viruses encode secreted interleukin-18-binding proteins. *Journal of General Virology* **81**, 1223-1230.

Snapper, C.M. and Paul, W.E. (1987) Interferon-gamma and B Cell Stimulatory Factor-1 Reciprocally Regulate Ig Isotype Production. *Science* **236**, 944-947.

Speth, C., Bredl, S., Hagleitner, M., Wild, J., Dierich, M., Wolf, H., Schroeder, J., Wagner, R. and Deml, L. (2008) Human immunodeficiency virus type-1 (HIV-1) Pr55gag virus-like particles are potent activators of human monocytes. *Virology* **382**, 46-58.

Spok, A., Twyman, R.M., Fischer, R., Ma, J.K. and Sparrow, P.A. (2008) Evolution of a regulatory framework for pharmaceuticals derived from genetically modified plants. *Trends in Biotechnology* **26**, 506-517.

Spreitzer, R.J. and Salvucci, M.E. (2002) Rubisco: structure, regulatory interactions, and possibilities for a better enzyme. *Annual Review of Plant Biology* **53**, 449-475.

Spriggs, M.K., Hruby, D.E., Maliszewski, C.R., Pickup, D.J., Sims, J.E., Buller, R.M.L. and VanSlyke, J. (1992) Vaccinia and cowpox viruses encode a novel secreted interleukin-1-binding protein. *Cell* **71**, 145-152.

Steinhagen, F., Kinjo, T., Bode, C. and Klinman, D.M. (2011) TLR-based immune adjuvants. *Vaccine* **29**, 3341-3355.

Stephenson, K.E., Li, H., Walker, B.D., Michael, N.L. and Barouch, D.H. (2012) Gag-specific cellular immunity determines in vitro viral inhibition and in vivo virologic control following SIV challenges of vaccinated monkeys. *Retrovirology* **9**, P245.

Summers deLuca, L. and Gommerman, J.L. (2012) Fine-tuning of dendritic cell biology by the TNF superfamily. *Nature Reviews Immunology* **12**, 339-351.

Sun, W., Li, Y., Chen, L., Chen, H., You, F., Zhou, X., Zhou, Y., Zhai, Z., Chen, D. and Jiang, Z. (2009) ERIS, an endoplasmic reticulum IFN stimulator, activates innate immune signaling through dimerization. *Proceedings of the National Academy of Sciences of the United States of America* **106**, 8653-8658.

Symons, J.A., Alcamí, A. and Smith, G.L. (1995) Vaccinia virus encodes a soluble type I interferon receptor of novel structure and broad species specificity. *Cell* **81**, 551-560.

Szabo, S.J., Sullivan, B.M., Peng, S.L. and Glimcher, L.H. (2003) Molecular mechanisms regulating Th1 immune responses. *Annual Review of Immunology* **21**, 713-758.

Takeda, K. and Akira, S. (2004) TLR signaling pathways. *Seminars in Immunology* **16**, 3-9.

Takeda, K., Kaisho, T. and Akira, S. (2003) Toll-like receptors. *Annual Review of Immunology* **21**, 335-376.

Tanaka, Y. and Chen, Z.J. (2012) STING specifies IRF3 phosphorylation by TBK1 in the cytosolic DNA signaling pathway. *Science Signaling* **5**, ra20.

Tartaglia, J., Cox, W.I., Taylor, J., Perkus, M.E., Riviere, M., Meignier, B. and Paoletti, E. (1992a) Highly Attenuated Poxvirus Vectors. *AIDS Research and Human Retroviruses* **8**, 1445-1447.

Tartaglia, J., Perkus, M.E., Taylor, J., Norton, E.K., Audonnet, J.C., Cox, W.J., Davis, S.W., van der Hoeven, J., Meignier, B., Riviere, M., Languet, B. and Paoletti, E. (1992b) NYVAC: A highly attenuated strain of vaccinia virus. *Virology* **188**, 217-232.

Taylor, J. and Paoletti, E. (1988) Fowlpox virus as a vector in non-avian species. *Vaccine* **6**, 466-468.

Taylor, J., Weinberg, R., Languet, B., Desmettre, P. and Paoletti, E. (1988) Recombinant fowlpox virus inducing protective immunity in non-avian species. *Vaccine* **6**, 497-503.

Taylor, J.M. and Barry, M. (2006) Near death experiences: poxvirus regulation of apoptotic death. *Virology* **344**, 139-150.

Tebas, P., Stein, D., Tang, W.W., Frank, I., Wang, S.Q., Lee, G., Spratt, S.K., Surosky, R.T., Giedlin, M.A., Nichol, G., Holmes, M.C., Gregory, P.D., Ando, D.G., Kalos, M., Collman, R.G., Binder-Scholl, G., Plesa, G., Hwang, W.T., Levine, B.L. and June, C.H. (2014) Gene editing of CCR5 in autologous CD4 T cells of persons infected with HIV. *The New England Journal of Medicine* **370**, 901-910.

Teigler, J.E., Phogat, S., Franchini, G., Hirsch, V.M., Michael, N.L. and Barouch, D.H. (2014) The canarypox virus vector ALVAC induces distinct cytokine responses compared to the vaccinia virus-based vectors MVA and NYVAC in rhesus monkeys. *Journal of virology* **88**, 1809-1814.

Tripp, C., Beckerman, K. and Unanue, E. (1995) Immune Complexes Inhibit Antimicrobial Responses through Interleukin-10 Production: Effects in Severe Combined Immunodeficient Mice during *Listeria* Infection. *Journal of Clinical Investigation* **95**, 1628-1634.

Tsuchiya, S., Kobayashi, Y., Goto, Y., Okumura, H., Nakae, S., Konno, T. and Tada, K. (1982) Induction of Maturation in Cultured Human Monocytic Leukemia Cells by a Phorbol Diester. *Cancer Research* **42**, 1530-1535.

Tsunetsugu-Yokota, Y., Morikawa, Y., Isogai, M., Kawana-Tachikawa, A., Odawara, T., Nakamura, T., Grassi, F., Autran, B. and Iwamoto, A. (2003) Yeast-Derived Human Immunodeficiency Virus Type 1 p55gag Virus-Like Particles Activate Dendritic Cells (DCs) and Induce Perforin Expression in Gag-Specific CD8+ T Cells by Cross-Presentation of DCs. *Journal of virology* **77**, 10250-10259.

Tudor, D. and Bomsel, M. (2011) The broadly neutralizing HIV-1 IgG 2F5 elicits gp41-specific antibody-dependent cell cytotoxicity in a FcgammaRI-dependent manner. *AIDS* **25**, 751-759.

Tudor, D., Derrien, M., Diomede, L., Drillet, A.S., Houimel, M., Moog, C., Reynes, J.M., Lopalco, L. and Bomsel, M. (2009) HIV-1 gp41-specific monoclonal mucosal IgAs derived from highly exposed but IgG-seronegative individuals block HIV-1 epithelial transcytosis and neutralize CD4(+) cell infection: an IgA gene and functional analysis. *Mucosal Immunology* **2**, 412-426.

Tudor, D., Yu, H., Maupetit, J., Drillet, A.-S., Bouceba, T., Schwartz-Cornil, I., Lopalco, L., Tuffery, P. and Bomsel, M. (2012) Isotype modulates epitope specificity, affinity, and antiviral activities of anti–HIV-1 human broadly neutralizing 2F5 antibody. *Proceedings of the National Academy of Sciences of the United States of America* **109**, 12680-12685.

Unterholzner, L., Sumner, R.P., Baran, M., Ren, H., Mansur, D.S., Bourke, N.M., Randow, F., Smith, G.L. and Bowie, A.G. (2011) Vaccinia virus protein C6 is a virulence factor that binds TBK-1 adaptor proteins and inhibits activation of IRF3 and IRF7. *PLoS Pathogens* **7**, e1002247.

Valley-Omar, Z., Meyers, A., Shephard, E., Williamson, A.L. and Rybicki, E.P. (2011) Abrogation of contaminating RNA activity in HIV-1 Gag VLPs. *Virology Journal* **8**, 462.

van Duin, D., Medzhitov, R. and Shaw, A.C. (2006) Triggering TLR signaling in vaccination. *Trends in Immunology* **27**, 49-55.

Verardi, P.H., Jones, L.A., Aziz, F.H., Ahmad, S. and Yilma, T.D. (2001) Vaccinia virus vectors with an inactivated gamma interferon receptor homolog gene (B8R) are attenuated In vivo without a concomitant reduction in immunogenicity. *Journal of virology* **75**, 11-18.

Verardi, P.H., Titong, A. and Hagen, C.J. (2012) A vaccinia virus renaissance: new vaccine and immunotherapeutic uses after smallpox eradication. *Human vaccines & immunotherapeutics* **8**, 961-970.

Verkoczy, L., Chen, Y., Bouton-Verville, H., Zhang, J., Diaz, M., Hutchinson, J., Ouyang, Y.B., Alam, S.M., Holl, T.M., Hwang, K.K., Kelsoe, G. and Haynes, B.F. (2011) Rescue of HIV-1 broad neutralizing antibody-expressing B cells in 2F5 VH x VL knockin mice reveals multiple tolerance controls. *The Journal of Immunology* **187**, 3785-3797.

Verkoczy, L., Chen, Y., Zhang, J., Bouton-Verville, H., Newman, A., Lockwood, B., Scearce, R.M., Montefiori, D.C., Dennison, S.M., Xia, S.M., Hwang, K.K., Liao, H.X., Alam, S.M. and Haynes, B.F. (2013) Induction of HIV-1 broad neutralizing antibodies in 2F5 knock-in mice: selection against membrane proximal external region-associated autoreactivity limits T-dependent responses. *The Journal of Immunology* **191**, 2538-2550.

Verkoczy, L., Diaz, M., Holl, T.M., Ouyang, Y.B., Bouton-Verville, H., Alam, S.M., Liao, H.X., Kelsoe, G. and Haynes, B.F. (2010) Autoreactivity in an HIV-1 broadly reactive neutralizing antibody variable region heavy chain induces immunologic tolerance. *Proceedings of the National Academy of Sciences of the United States of America* **107**, 181-186.

Veyer, D.L., Maluquer de Motes, C., Sumner, R.P., Ludwig, L., Johnson, B.F. and Smith, G.L. (2014) Analysis of the anti-apoptotic activity of four vaccinia virus proteins demonstrates that B13 is the most potent inhibitor in isolation and during viral infection. *J Gen Virol* **95**, 2757-2768.

Voinnet, O., Rivas, S., Mestre, P. and Baulcombe, D. (2003) An enhanced transient expression system in plants based on suppression of gene silencing by the p19 protein of tomato bushy stunt virus. *The Plant Journal* **33**, 949-956.

Vzorov, A.N., Wang, L., Chen, J., Wang, B.Z. and Compans, R.W. (2016) Effects of modification of the HIV-1 Env cytoplasmic tail on immunogenicity of VLP vaccines. *Virology* **489**, 141-150.

Wan, Y., Liu, L., Wu, L., Huang, X., Ma, L. and Xu, J. (2009) Deglycosylation or Partial Removal of HIV-1 CN54 gp140 V1/V2 Domain Enhances Env-Specific T Cells. *AIDS Research and Human Retroviruses* **25**, 607-617.

Warfield, K.L., Dye, J.M., Wells, J.B., Unfer, R.C., Holtsberg, F.W., Shulenin, S., Vu, H., Swenson, D.L., Bavari, S. and Aman, M.J. (2015) Homologous and heterologous protection of nonhuman primates by Ebola and Sudan virus-like particles. *PloS one* **10**, e0118881.

Wehrle, P.F. (1980) A Reality in Our Time: Certification of the Global Eradication of Smallpox. *The Journal of Infectious Diseases* **142**, 636-638.

White, S.D., Conwell, K., Langland, J.O. and Jacobs, B.L. (2011) Use of a negative selectable marker for rapid selection of recombinant vaccinia virus. *Biotechniques* **50**, 303-309.

Whitney, J.B., Hill, A.L., Sanisetty, S., Penaloza-MacMaster, P., Liu, J., Shetty, M., Parenteau, L., Cabral, C., Shields, J., Blackmore, S., Smith, J.Y., Brinkman, A.L., Peter, L.E., Mathew, S.I., Smith, K.M., Borducchi, E.N., Rosenbloom, D.I., Lewis, M.G., Hattersley, J., Li, B., Hesselgesser, J., Geleziunas, R., Robb, M.L., Kim, J.H., Michael, N.L. and Barouch, D.H. (2014) Rapid seeding of the viral reservoir prior to SIV viraemia in rhesus monkeys. *Nature* **512**, 74-77.

Wilken, L.R. and Nikolov, Z.L. (2012) Recovery and purification of plant-made recombinant proteins. *Biotechnology Advances* **30**, 419-433.

Wilks, A.B., Christian, E.C., Seaman, M.S., Sircar, P., Carville, A., Gomez, C.E., Esteban, M., Pantaleo, G., Barouch, D.H., Letvin, N.L. and Permar, S.R. (2010) Robust vaccine-elicited cellular immune responses in breast milk following systemic simian immunodeficiency virus DNA prime and live virus vector boost vaccination of lactating rhesus monkeys. *The Journal of Immunology* **185**, 7097-7106.

Williams, W.B., Liao, H.X., Moody, M.A., Kepler, T.B., Alam, S.M., Gao, F., Wiehe, K., Trama, A.M., Jones, K., Zhang, R., Song, H., Marshall, D.J., Whitesides, J.F., Sawatzki, K., Hua, A., Liu, P., Tay, M.Z., Seaton, K.E., Shen, X., Foulger, A., Lloyd, K.E., Parks, R., Pollara, J., Ferrari, G., Yu, J.S., Vandergrift, N., Montefiori, D.C., Sobieszczyk, M.E., Hammer, S., Karuna, S., Gilbert, P., Grove, D., Grunenberg, N., McElrath, M.J., Mascola, J.R., Koup, R.A., Corey, L., Nabel, G.J., Morgan, C., Churchyard, G., Maenza, J., Keefer, M., Graham, B.S., Baden, L.R., Tomaras, G.D. and Haynes, B.F. (2015) HIV-1 VACCINES. Diversion of HIV-1 vaccine-induced immunity by gp41-microbiota cross-reactive antibodies. *Science* **349**, aab1253.

Winzler, C., Rovere, P., Rescigno, M., Granucci, F., Penna, G., Adorini, L., Zimmermann, V., Davoust, J. and Ricciardi-Castagnoli, P. (1997) Maturation Stages of Mouse Dendritic Cells in Growth Factor-dependent Long-Term Cultures. *The Journal of Experimental Medicine* **185**, 317-328.

Wong, J.K., Hezareh, M., Gunthard, H.F., Havlir, D.V., Ignacio, C.C., Spina, C.A. and Richman, D.D. (1997) Recovery of Replication-Competent HIV Despite Prolonged Suppression of Plasma Viremia. *Science* **278**, 1291-1295.

Wright, S., Levin, S., Jong, M., Chad, Z. and Kabbash, L. (1989) CR3 (CD11b/CD18) expresses one binding site for Arg-Gly-Asp-containing peptides and a second site for bacterial lipopolysaccharide. *The Journal of Experimental Medicine* **169**, 175-183.

Yan, M., Peng, J., Jabbar, I., Liu, X., Filgueira, L., Frazer, I.H. and Thomas, R. (2005) Activation of dendritic cells by human papillomavirus-like particles through TLR4 and NF-kB-mediated signalling, moderated by TGF-Beta. *Immunology and Cell Biology* **83**, 83-91.

Yang, R., Murillo, F.M., Cui, H., Blosser, R., Uematsu, S., Takeda, K., Akira, S., Viscidi, R.P. and Roden, R.B. (2004) Papillomavirus-like particles stimulate murine bone marrow-derived dendritic cells to produce alpha interferon and Th1 immune responses via MyD88. *Journal of virology* **78**, 11152-11160.

Yates, N.L., Liao, H.X., Fong, Y., deCamp, A., Vandergrift, N.A., Williams, W.T., Alam, S.M., Ferrari, G., Yang, Z., Seaton, K.E., Berman, P.W., Alpert, M.D., Evans, D.T., O'Connell, R.J., Francis, D., Sinangil, F., Lee, C., Nitayaphan, S., Rerks-Ngarm, S., Kaewkungwal, J., Pitisuttithum, P., Tartaglia, J., Pinter, A., Zolla-Pazner, S., Gilbert, P.B., Nabel, G.J., Michael, N.L., Kim, J.H., Montefiori, D.C., Haynes, B.F. and Tomaras, G.D. (2014) Vaccine-induced Env V1-V2 IgG3 correlates with lower HIV-1 infection risk and declines soon after vaccination. *Science Translational Medicine* **6**.

Ye, L., Wang, J., Beyer, A.I., Teque, F., Cradick, T.J., Qi, Z., Chang, J.C., Bao, G., Muench, M.O., Yu, J., Levy, J.A. and Kan, Y.W. (2014) Seamless modification of wild-type induced pluripotent stem cells to the natural CCR5Delta32 mutation confers resistance to HIV infection. *Proceedings of the National Academy of Sciences of the United States of America* **111**, 9591-9596.

Yildiz, I., Shukla, S. and Steinmetz, N.F. (2011) Applications of viral nanoparticles in medicine. *Current opinion in biotechnology* **22**, 901-908.

Yusibov, V., Streatfield, S.J. and Kushnir, N. (2014) Clinical development of plant-produced recombinant pharmaceuticals: Vaccines, antibodies and beyond. *Human Vaccines* **7**, 313-321.

Zak, D.E., Andersen-Nissen, E., Peterson, E.R., Sato, A., Hamilton, M.K., Borgerding, J., Krishnamurty, A.T., Chang, J.T., Adams, D.J., Hensley, T.R., Salter, A.I., Morgan, C.A., Duerr, A.C., De Rosa, S.C., Aderem, A. and McElrath, M.J. (2012) Merck Ad5/HIV induces broad innate immune activation that predicts CD8(+) T-cell responses but is attenuated by preexisting Ad5 immunity. *Proceedings of the National Academy of Sciences of the United States of America* **109**, E3503-3512.

Zhang, L., Chen, H., Brandizzi, F., Verchot, J. and Wang, A. (2015) The UPR branch IRE1-bZIP60 in plants plays an essential role in viral infection and is complementary to the only UPR pathway in yeast. *PLoS Genetics* **11**, e1005164.

Zhang, L. and Wang, A. (2012) Virus-induced ER stress and the unfolded protein response. *Frontiers in Plant Science* **3**, 293.

Zhang, R., Verkoczy, L., Wiehe, K., Alam, S.M., Nicely, N.I., Santra, S., Bradley, T., Pemble IV, C.W., Zhang, J., Gao, F., Montefiori, D., Bouton-Verville, H., Kelsoe, G., Larimore, K., Trama, A.M., Vandergrift, N.A., Tomaras, G., Kepler, T.B., Moody, M.A., Liao, H.X. and Haynes, B.F. (2016) Initiation of immune tolerance-controlled HIV-gp41 neutralizing B cell lineages. *Science Translational Medicine* **8**, 336ra362.

Zhao, W. (2013) Negative regulation of TBK1-mediated antiviral immunity. *FEBS Letters* **587**, 542-548.

Zhong, B., Yang, Y., Li, S., Wang, Y.Y., Li, Y., Diao, F., Lei, C., He, X., Zhang, L., Tien, P. and Shu, H.B. (2008) The adaptor protein MITA links virus-sensing receptors to IRF3 transcription factor activation. *Immunity* **29**, 538-550.

Zimran, A., Brill-Almon, E., Chertkoff, R., Petakov, M., Blanco-Favela, F., Munoz, E.T., Solorio-Meza, S.E., Arnato, D., Duran, G., Giona, F., Heitner, R., Rosenbaum, H., Giraldo, P., Mehta, A., Park, G., Phillips, M., Elstein, D., Altarescu, G., Szleifer, M., Hashmueli, S. and Aviezer, D. (2011) Pivotal trial with plant cell-expressed recombinant gucocerebrosidase taliglucerase alfa, a novel enzyme replacement therapy for Gaucher disease. *Blood* **118**, 5767-5773.

Zolla-Pazner, S. (2004) Identifying epitopes of HIV-1 that induce protective antibodies. *Nature Reviews Immunology* **4**, 199-210.

Zwick, M.B., Labrijn, A.F., Wang, M., Spenlehauer, C., Saphire, E.O., Binley, J.M., Moore, J.P., Stiegler, G., Katinger, H., Burton, D.R. and Parren, P.W. (2001) Broadly neutralizing antibodies targeted to the membrane-proximal external region of human immunodeficiency virus type 1 glycoprotein gp41. *Journal of virology* **75**, 10892-10905.

BIOSKETCH

Lydia Meador is the daughter of Greg and Judy Meador and the oldest of three girls. She is originally from Ponca City, OK but her love of science from a young age drove her to pursue higher education. Lydia graduated in 2011 from Oklahoma State University as a first-generation college student with two Bachelor's degrees in Botany and Microbiology/Molecular Genetics. During her time at OSU, her participation in research activities earned her multiple prestigious national awards, including the Young Botanist Award from the Botanical Society of America, and the Barry M. Goldwater Scholar Award. She also received the National Science Foundation Graduate Research Fellowship to fund her doctoral studies at Arizona State University. For her graduate studies, Lydia desired to combine her two degrees in Botany and Microbiology by joining a plant biotechnology group at ASU which uses plants to produce pharmaceuticals, including vaccines. She was able to achieve this goal by joining a collaborative HIV vaccine project with the labs of Tsafrir Mor and Bert Jacobs for her PhD work. Lydia has presented at multiple national and international conferences and mentored over a dozen undergraduate students during her time at ASU. During her PhD, Lydia also received two dissertation fellowships: the ASU Dissertation Fellowship and the Philanthropic Education Organization Scholar Award for women completing their PhD. After successfully defending her thesis, Lydia will be joining the lab of Karen Hastings at the University of Arizona College of Medicine in downtown Phoenix where she will expand her virology and plant biotechnology knowledge by studying T cell cancer immunology in melanoma. Eventually, Lydia hopes to pursue a career in vaccinology/immunology for emerging infectious diseases.